Volume 7, Issue 4, Autumn 2020

JARIE

# JOURNAL OF APPLIED RESEARCH ON INDUSTRIAL ENGINEERING

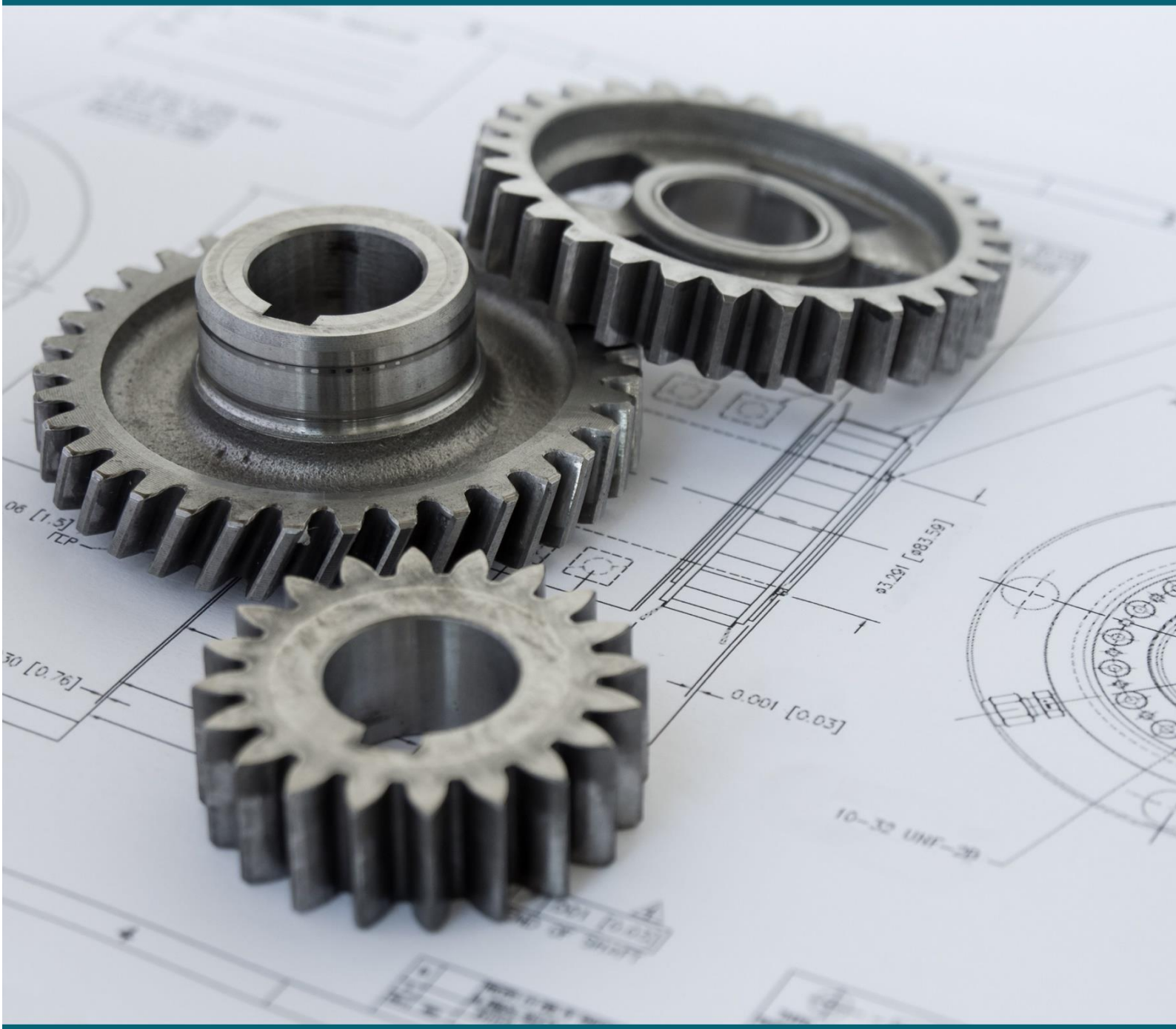

Print ISSN: 2538-5110
Online ISSN: 2676-6167
www. journal-aprie.com

Journal of Applied Research on Industrial Engineering
www.journal-aprie.com

Journal of Applied Research on Industrial Engineering

www.journal-aprie.com

JARIE

J. Appl. Res. Ind. Eng. Vol. 7, No. 4 (2020) 313–449.

# TABLE OF CONTENTS

Journal of Applied Research on Industrial Engineering
www.journal-aprie.com

# Modeling the Effects of Intellectual Capital Components on the Economic Competitiveness, and Assessing its Consequences Using a Fuzzy Cognitive Map

***Mohammad Hadi Zohdi[1], Morteza Shafiee[2,*], Fariborz Evazzadeh Fath[3]***

[1]*Department of Accounting and Management, Yasooj Branch, Islamic Azad University, Yasooj, Iran.*
[2]*Associate Professor of Department of Industrial Management, Faculty of Economic and Management, Shiraz Branch, Islamic Azad University, Shiraz, Iran.*
[3]*Department of Accounting, Gachsaran Branch, Islamic Azad University, Gachsaran, Iran.*

**PAPER INFO**

**Chronicle:**
*Received:18 August 2020*
*Reviewed:09 September 2020*
*Revised: 29 October 2020*
*Accepted: 26 November2020*

**Keywords:**
*Intellectual Capital.*
*Physical and Fiscal Capital.*
*Economic Competitiveness.*
*Fuzzy Cognitive Map.*

**ABSTRACT**

Despite its known importance, relatively few studies have focused on studying the effects of Intellectual Capital Components (ICC) on the economic competitiveness, determining related elements and relationships exists between them to assess its consequences. This study was designed to provide a comprehensive evaluation of the problem. After a literature review, fifteen related elements, obtained from the previous studies, were collected. A Fuzzy Cognitive Map (FCM) was used to determine the relations exists between the elements, where the opinions of fifteen experts were applied when making related decisions. Data were analyzed using statistical analysis. The results showed relations exist between all fifteen elements, where all of them were confirmed using FCM representation.

## 1. Introduction

Although it has been a symbol of power since the beginning of the industrial revolution, the physical and fiscal capital is currently facing upstaging [12]. Today, economists consider other factors that boost growth, development, and productivity, besides traditional manufacturing elements (including land, capital, and labor). Accumulation of physical capital is no longer considered as a criterion for economic growth and development, while sustainable economic growth can only be achieved relying on productivity and innovation and through effective management of tangible and invisible assets simultaneously [13]. In other words, firms have resources that are critical to achieving strong financial

Zohdi, M. H., Shafiee, M., & Evazzadeh Fath, F. (2020). Modeling the effects of intellectual capital components on the economic competitiveness, and assessing its consequences using a fuzzy cognitive map. *Journal of applied research on industrial engineering, 7*(4), 313-328.

* Corresponding author
E-mail address: ma.shafiee277@gmail.com

10.22105/jarie.2020.235457.1174

performance and competitive advantage. In the first group, there are tangible assets such as properties, machinery, and alternative physical technologies that can be traded easily on free markets. The second group includes invisible assets, all of them are valuable, scare, irreplaceable and strategic, with high potential for creating competitive advantage and superior financial performance [41]. The role and importance of physical assets are well documented, while invisible assets, especially intellectual capital, as strategic resources, are needed to be further explored, since the producing (manufacturing) and extending such resources is challenging and may create considerable value [28].

Extensive research has been conducted on the intellectual capital at organizations and confirming their importance. Bose showed that measuring performance at organizations using an intellectual capital approach improves the quality of user decisions, internal management, reporting to outside the organization, exchanging this capital within and outside the company, as well as accounting functionality [6]. Effective management of intellectual capital can create value to the business entity, and increase its competitive advantage. Ting and Lean [21] considered intellectual capital as the only source of competitive capacity in the business entity that could increase the enterprise's profit. The question arose is that which factors are affected by intellectual capital? Nematollahi [36] confirmed the effect that intellectual capital has on the relative efficiency of manufacturing cooperation. Ghasem Zadeh et al. [15] confirmed the role that intellectual capital and professional ethics plays on organizational learning capacity and knowledge sharing. According to the results of numerous studies, there is a positive relationship between intellectual capital and competitiveness (Rastogi [42], Vătămănescu et al. [54], Cherkesova et al. [8], and Zambon [57]). Though according to the literature review, intellectual capital has a significant impact on factors such as efficiency, effectiveness, organizational learning, knowledge sharing, and competitive ability, further research can provide different outcomes.

It should be considered that the results of each of these factors, which themselves are affected by intellectual capital, lead to other results and factors that can be investigated. Organizational competitiveness, for example, can have an impact on stock prices [40], organization assets [9], environmental performance [55], and accounting information [3]. Considering the number of factors affecting (are affected by) above-mentioned elements, there is a need to a perspective and thinking that can examine all these factors and their relationship simultaneously. The present study aims at investigating all the variables related to intellectual capital, especially the relationship exists between intellectual capital and competitive advantage in the organization, as well as evaluating related consequences.

The rest of this paper is structured as follows. The concept of intellectual capital and competitiveness are first discussed, and theoretical foundations and research backgrounds are then provided. The relationship between variables is determined using a Fuzzy Cognitive Map (FCM) and the initial model is presented. The relationship exists between the variables is obtained using data obtained from a researcher-made questionnaire and then is analyzed statistical tests. Finally, the model on the effects that intellectual capital components have on economic competitiveness, as well as assessing consequences is presented.

## 2. Theoretical Foundations and Research Background

### *2.1. Intellectual Capital*

Many definitions have been proposed for the concept of intellectual capital. John Kenneth Galbraith, who first proposed the term "intellectual capital" in 1969, argues that "intellectual capital is beyond a pure thinking" and includes the degree of intellectual measures [5]. Edvinsson and Malone [14] defined the "intellectual capital" as a gap exists between the book value and the company's market value. Kaplan et al. [25] argued that intellectual capital consists of invisible assets including human capital (e.g. skills and knowledge), information assets (e.g. databases, information systems, and technology infrastructures), and organizational capital (e.g. culture, leadership style and ability to share knowledge). Although there is no definite agreement on the definition of intellectual capital, some consensus exists on the main components of intellectual capital, including "human capital", "structural capital" and "customer (relational) capital" [43].

Human capital is the first and most important component of intellectual capital in most classifications. Its importance is mainly since it can't easily be copied by other companies and therefore gives a sustainable advantage to the organization. Also, there is no specific scope for the benefits and exploitation resulted from human capital. Human capital has significant advantages, but organizations can't ensure its long-term durability [30]. Organizations are therefore looking for a different kind of intellectual capital with more durability and higher ownership than human capital. It can be a structural capital that includes technologies, data networks, publications, and processes. Edwardson considered structural capital as a resource applied to support productivity, reduce risk and increase restructuring capacity [19].

Customer or relationship capital is another component of intellectual capital with considerable importance in organizations. Accordingly, considerable resources are used by business establishments to create value for customers aiming to benefit from related advantages [34].

### *2.2. Economic Competitiveness*

Economic competitiveness means the ability to achieve superiority in a competitive world, aiming to distinguish between an organization and others, from one or more point of view [20]. Economic competition brings competitive advantage, which includes a set of factors or capabilities and always provides the company with better performance [44]. Superiority is necessary for all areas covered by an organization, but in some financial organizations, having economic competitiveness gains more importance. Economic competitiveness can, therefore, be considered as the set of capabilities of an organization to have economic superiority to other organizations [56]. Different resources can be used in an organization to achieve economic competitiveness. More importantly, the lower accessibility of competitors to these resources, the greater the competitive advantage will be achieved [24]. Many researchers, therefore, consider intellectual capital as one of the most powerful sources for creating competitive advantage, where it is suggested to use competitive advantages of human, organization and cyberspace fields as well as the competitive advantage derived from customer or relationship capital, aiming to create economic competitiveness [7].

### *2.3. Fuzzy Cognitive Map (FCM)*

In recent years, fuzzy logic has gained wide acceptance in the field of accounting and business. This acceptance is due to the ability to management in situations of ambiguity and lack of consistency that does not exist within other approaches to dual value logic. In dual value logic, the proposition is true or false. Also, accounting has ambiguous in many important respects [23].

There are different techniques and methods for making multiple fuzzy criteria that have different advantages and disadvantages over each other. A supply chain is a series of organizations involved in the production and delivery of a product or service. This chain starts with raw material suppliers and continues to the end customer. Supply chain management is one of the effective and efficient approaches that reduces production costs and waiting time. This attitude facilitates the provision of better customer service and ensures the opportunity for effective monitoring of transportation systems, inventory, and distribution networks. In this way, the organization can exceed the expectations and demands of customers [51].

### *2.4. Research Background*

Extensive research has been conducted on intellectual capital in the organization, where, in most cases, intellectual capital includes human capital, structural capital, and customer or relationship capital [2]. In most researches, intellectual capital includes three aspects of human capital, structural capital and relationship capital, but the major differences are in the relationship exists between these three variables and others. The results of researches and the relationship between intellectual capital aspects and other variables are presented in *Table 1*.

***Table 1.*** *Aspects of intellectual capital according to research background.*

| **Author(s)** | **Related Concepts** |
|---|---|
| *Fuzzy logic in accounting and auditing.* | *[23]* |
| *Investigating the impact of intellectual capital on equity returns.* | *[29]* |
| *Product market competition.* | *[52]* |
| *Intellectual capital and productivity.* | *[39]* |
| *Human resource productivity.* | *[19]* |
| *Efficacy.* | *[43]* |
| *Competitive advantage and organizational innovation.* | *[32]* |
| *Organizational entrepreneurship.* | *[46]* |
| *Financial Performance.* | *[10]* |
| *Developing innovative products.* | *[16]* |
| *The influence of intellectual capital on the effectiveness of productive.* | *[36]* |
| *Market value, Return On Total Assets (ROA), assets turnover, Return On Equity Capital (ROEC).* | *[4]* |
| *Quality of financial information.* | *[11]* |
| *The relationship between intellectual capital and the performance.* | *[34]* |
| *The position of intellectual capital in the performance.* | *[49]* |
| *Earnings per share, ROEC rate, annual return.* | *[1]* |
| *Current and future financial performance.* | *[31]* |
| *Competitive advantage.* | *[18]* |
| *Measuring the competitive power of products.* | *[35]* |

As the *Table 1* shows, intellectual capital affects product market competition, organization's productivity, human resource productivity, efficiency, competitive advantage, entrepreneurship,

financial performance, products development, Return On Equity Capital (ROEC), Return On Total Assets (ROA), market value, quality of financial information, company's performance, earnings per share, annual returns and financial performance.

On the other hand, extensive research has been conducted on economic competitiveness (*Table 1*). The results confirm the relationship between variables and economic competitiveness. Mojtahed zadeh et al. [34] examined the relationship between competitiveness and product market competition and confirmed this relationship. Soltani et al. [50] examined the role of human resources in creating competitive advantage and identified human resources as one of the main sources in creating a sustainable and unique competitive advantage. Riasi [43] conducted a comprehensive study on the competitive advantage and found that performance (especially when reducing costs) could lead to a competitive advantage for the organization. Haji Hoseini and Norozade Moghadam [22] studied the effect of innovation and market orientation on business performance and competitive advantage in industrial companies and confirmed the relationship exists between these factors. Khazai et al. [27] confirmed the relationship exists between strategic entrepreneurship and competitive advantage. Saeidi et al. [47] also confirmed the relationship exists between financial performance and competitive advantage.

Khalique et al. [26] showed that human capital has a significant importance in intellectual capital. Dzenopoljac et al. [13] found that intellectual capital affects the organization's overall performance. Kianto [28] described intellectual capital as the most important asset in knowledge management, which can create value in the organization. Nimtrakoon [36] examined the relationship between intellectual capital, the market value of a company and the financial performance of the organization.

According to previous researches, there is a positive association between intellectual capital and economic competitiveness; these two concepts are also indirectly related by other variables. It's not possible to neglect the effect of other variables on the relationship exists between intellectual capital and competitiveness; therefore, we aim at examining the direct, indirect, and internal relationships of all variables with each other, based on the results of previous researches and using research and statistical methods.

Marzband [33], in study entitled "Precise Services and Supply Chain Prioritization in Manufacturing Companies Using Cost Analysis Provided in a Fuzzy Environment" in order to identify and prioritize the factors affecting the supply chain in manufacturing companies, using indicators such as cost, timely delivery and procurement time to evaluate the supply chain efficiency was considered. And performance evaluation was performed at the manufacturer level. Therefore, to evaluate the performance of the supply chain using the AHP integration approach and the DEA method approach in the fuzzy environment, the suppliers and suppliers of the manufacturing company were evaluated and ranked in terms of performance. Results lead to a competitive advantage and are more effective and decisive in the performance indicators of the organization, including earning more.

## 3. Research Methodology

This was an applied, fundamental and causal research aiming to examine the relationship exists between the variables of intellectual capital and economic competitiveness as well as all related variables. The participants were 15 specialists, including university professors and financial company executives. The statistical population in the other part of the study was employees of financial companies who were

studied for the quantitative analysis of data. A total of 800 employees were employed, while according to the Morgan table, a sample of 260 people is enough.

The FCM representation was used to obtain the desired model. In general, the relationship between the variables is determined by using the FCM's outputs, but in order to achieve better and more accurate results, based on the FCM results, a researcher-made questionnaire was prepared and distributed among participation after its validity and reliability were evaluated. The one-sample t-test value was determined using statistical methods, aiming to determine the relationship exists between variables. The conceptual model of research is presented in *Fig. 1*.

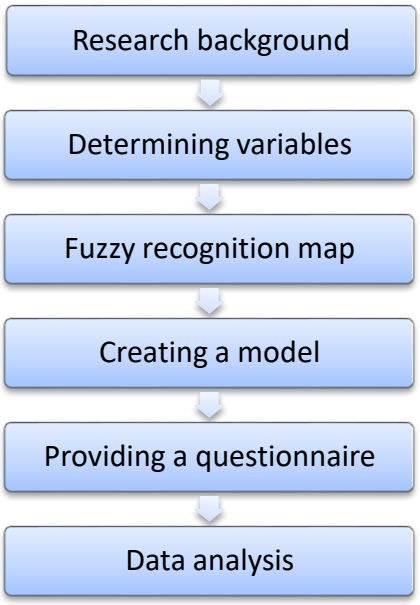


***Fig. 1.*** *The conceptual model of the research.*

### *3.1. Research Background and Variables Determination*

The research background was provided in intellectual capital, economic competitiveness and economic consequences. This section mainly focuses on identifying different aspects associated with the above-mentioned variables. Outputs of this section includes intellectual capital, economic competitiveness, product market competition, productivity, efficiency, organizational innovation, organizational entrepreneurship, financial performance, product development, market value, total assets, ROEC, quality of financial information, firm performance, earnings per share, ROA and annual returns.

### *3.2. Applied Algorithm*

Research algorithm is based on a fuzzy approach called Fuzzy Cognitive Map (the abbreviation is FCM obtained from initial letters). FCMs have gained considerable research interest due to their ability in representing structured knowledge and model complex systems in various fields. This growing interest led to the need for enhancement and making more reliable models that can better represent real situations that leads to our used algorithm, FCM method [45].

Fuzzy cognitive maps are signed fuzzy digraphs. They may look at first blush like Hasse diagrams, but they are not. Spreadsheets or tables are used to map FCMs into matrices for further computation. FCM is a technique used for causal knowledge acquisition and representation, it supports causal knowledge reasoning process and belong to the neuro-fuzzy system that aim at solving decision making problems, modeling and simulate complex systems [6]. Learning algorithms have been proposed for training and updating FCMs weights mostly based on ideas coming from the field of Artificial Neural Networks. Adaptation and learning methodologies used to adapt the FCM model and adjust its weights. Schneider and Hase [48], suggested the Differential Hebbian Learning (DHL) to train FCM. There have been proposed algorithms based on the initial Hebbian algorithm; other algorithms come from the field of genetic algorithms, swarm intelligence and evolutionary computation. Learning algorithms are used to overcome the shortcomings that the traditional FCM present i.e. decreasing the human intervention by suggested automated FCM candidates or by activating only the most relevant concepts every execution time; or by making models more transparent and dynamic [45].

### *3.3. Fuzzy Cognitive Map and Determining a Model*

FCM is a modeling methodology for complex decision-making systems that can describe a system's behavior based on its concepts. Each concept represents identity, a status, a variable, or a feature of the system. FCMs have applications in simulation, modeling of organizational strategies, supporting the formulation of strategic plans and analysis of failure situations, specifications, and requirements of urban design support systems, managing relations in the services provided by the airline companies and promoting the network's operation. A cognitive map is a diagram designed to express a person's cause and effect view of a particular field, as well as to analyze the effects of some items such as policies or business decisions in connection with the realization of specific goals [45].

The methodology developed by Rodriguez-Repiso et al. [45] uses four matrices including the initial matrix of success, the pseudo-successive fuzzy matrix, the matrix of the successful relationship power, and the final matrix of success for creating FCMs. The process of creating an FCM consists of five steps. In the first step, the initial matrix of success is formed. This contains an $n \times m$ matrix, where n is the number of key factors of success (also called the concepts or variables) and m is the number of people interviewed for data acquisition. Each element of the matrix reflects the importance that the individual "*j*" considers for a particular concept "*I*" on a particular scale; this can be different in different projects and even for different factors of a success in a project, because these results in the future will become a fuzzy set, with values between zero and one also between one. The fuzzy matrix of success is created in the next step, where numerical vectors *Vi* are transferred to fuzzy sets in which each element of the fuzzy set indicates the membership of each element *Oij* of vector *Vi* with the vector *Vi* itself. Numerical vectors with values between zero and one are converted into fuzzy sets.

The maximum value is determined in *Vi* and $Xi = 1$ is considered for it. Then the maximum value is determined in *Vi* and $Xi = 0$ is considered for it. The ratio of all elements of the vector *Vi* is determined from 0 to 1.

$$X_i(O_{ij}) = \frac{O_{ij} - \min(O_{ip})}{\mathrm{Max}\,(O_{ip}) - \min(O_{ip})}.$$

In the third step, the relationship matrix of the success power is created, which is an $n \times n$ matrix. Matrix rows and columns are key factors of success, and each element in the matrix indicates the relationship

between factors *I* and *j*. $S_{ij}$ can also gain values from -1 to +1. Each key factor of success is represented as a numerical vector Si, which contains the element n for any concept demonstrated on the map. There are three possible relationships between the two concepts of $S_{ij}$.

$S_{ij} > 0$ represents a direct (positive) causality between the concepts of i and j, where the increase in the value of the concept of *i* increases the value of the concept of *j*.

$S_{ij} < 0$ represents the inverse (negative) causality between the concepts of *i* and *j*, where the increase in the value of the concept of *i* leads to the decrease of the value of the concept of *j*.

$S_{ij} = 0$ shows that there is no relation between the concepts of *i* and *j*.

Before the next step, the duality of the relationships must be determined. The numerical vectors IMS and FZMS are converted to fuzzy sets. Given the *V1* and *V2* (vectors associated with factors 1 and 2) and *X1* (*Vj*) and *X2* (*Vj*) (degrees of membership j in vectors *V1* and *V2*), these vectors only have an increasing relationship (i.e. a direct relationship between concepts 1 and 2; $S_{ij} > 0$). If *X1* (Vj) is similar to *X2* (*Vj*) for all or most of the elements related to both vectors, and when vectors V1 and V2 exclusively have a decreasing relation with concepts 1 and 2, and if *X1* (*Vj*) is similar to (*1-X2 (Vj*)) for all or most of the elements related with both vectors, then *Sij<0*.

The proximity between the two vectors *V1* and *V2* must be determined in order to determine the relationship level. Calculating similarity between these two vectors indicates the power of the relationship between concepts 1 and 2 in relation to these two vectors, represented by the element *S12*, which is presented in the Strength of Relationship Matrix (SRMS). The proximity of the relationship between two distance-based vectors is based on the concept of the distance between vectors. The mathematical procedure for calculating the similarity between these two vectors is the approach presented by Schneider and Hase [48].

Different computational methods are needed for vectors having a direct relationship and vectors having an inverse relationship. If the vectors *V1* and *V2* are directly related, then the closest relationship between them for each j is achieved when *X1 (Vj) = X2 (Vj)*.

If *dj* is the distance between the elements *j* of vectors *V1* and *V2* (as follows):

$$d_j = \left|X_1(v_j) - X_2(v_j)\right|.$$

And if AD is the mean distance between vectors *V1* and *V2* (as follows),

$$AD = \frac{\sum|d_j|}{m}.$$

The proximity or similarity *S* between the two vectors is shown in this equation:

*S = 1- AD, S = 1* represents the complete similarity and *S = 0* indicates the maximum non-similarity.

If vectors *V1* and *V2* have an inverse relation, then the method for calculating the similarity between them is similar to that of the previous one, while in this case, the equation for calculating the distance between the corresponding elements is a reverse relation with vectors *V1* and *V2*.

$$D_j = \left|X_1(V_j) - (1 - x_2(V_j)\right|.$$

The remaining equations are similar to calculate the mean distance between the two vectors *AD* and their similarity *S*.

In this case, *S = 1* represents a complete reverse similarity, and *S = 0* indicates a complete inverse non-similarity between the two vectors.

The final success index is the next step. After completing the SRMS matrix, part of its data can be misleading. All key factors of success presented in the matrix are not related, and there is not always a causal relationship between them. An expert opinion is needed to analyze the data and transform SRMS into the final matrix of success, which only includes those numerical fuzzy elements that represent the causal relationships among the key factors of success. When analyzing data in an SRMS matrix, two vectors can be related intersecting. Vectors can represent close mathematical relations, however, logically, two indicators/concepts can be completely non-related. These unconventional relationships can be easily identified by experts.

The graphic representation of the FCM is the last step. The graphical representation of the final matrix of success as an FCM, draws out a targeted FCM for illustrating key factors of success. In the final display, each flash of factors *i* and *j* have a marked weight. This value represents the power of the positive or inverse relationship of causality between the two factors and the value contained in the final matrix of the success in row *i* and column *j* [38].

In the present study and according to the proposed method, 15 variables studied including product market competition, productivity, efficiency, organizational innovation, organizational entrepreneurship, financial performance, product development, market value, total assets, ROEC, quality of financial information, company's performance, earnings per share, ROA, and annual returns as intermediary variables between the two main variables "intellectual capital" and "competitiveness". In fact, the aim of using an FCM is to determine the relationship between these variables and the two main variables of the research. Note that intellectual capital and competitiveness are based on research hypotheses, while the other 15 variables are selected based on the research background. Fifteen specialists rated all 17 variables, where the importance of the existence of the variable in the intellectual capital-economic competitiveness relationship was determined from 0 to 100. The scoring results are presented in *Table 2*, where the columns represent the score of each specialist to each variable, while the rows represent the 17 variables, as follows:

1 = Intellectual capital; 2 = Economic competitiveness; 3 = Product competitiveness; 4 = Productivity; 5 = Efficiency; 6 = Organizational innovation; 7 = Organizational entrepreneurship; 8 = Financial performance; 9 = Product development; 10 = Market value; 11 = Total assets; 12 = ROEC; 13 = Quality of financial information; 14 = Company's performance; 15 = Earnings per share; 16 = ROEC rate; and 17 = Annual returns.

***Table 2.*** *Primary matrix.*

| | | | | | | | | | | | | | | | |
|---|---|---|---|---|---|---|---|---|---|---|---|---|---|---|---|
| 15 | 14 | 13 | 12 | 11 | 10 | 9 | 8 | 7 | 6 | 5 | 4 | 3 | 2 | 1 | |
| 60 | 80 | 80 | 90 | 70 | 80 | 90 | 80 | 90 | 90 | 40 | 60 | 80 | 50 | 95 | 1 |
| 100 | 100 | 100 | 100 | 100 | 100 | 100 | 100 | 100 | 100 | 100 | 100 | 100 | 100 | 100 | 2 |
| 60 | 40 | 70 | 60 | 60 | 80 | 80 | 60 | 80 | 50 | 80 | 60 | 80 | 60 | 80 | 3 |
| 70 | 50 | 80 | 80 | 80 | 60 | 40 | 80 | 60 | 80 | 60 | 70 | 60 | 80 | 30 | 4 |
| 80 | 80 | 90 | 60 | 60 | 70 | 60 | 60 | 70 | 60 | 70 | 80 | 70 | 60 | 60 | 5 |
| 90 | 80 | 40 | 70 | 80 | 80 | 80 | 70 | 80 | 80 | 80 | 90 | 80 | 70 | 70 | 6 |
| 40 | 60 | 50 | 80 | 60 | 90 | 80 | 80 | 90 | 60 | 90 | 60 | 90 | 80 | 40 | 7 |
| 100 | 90 | 100 | 90 | 90 | 90 | 100 | 90 | 100 | 90 | 90 | 90 | 100 | 90 | 100 | 8 |
| 50 | 80 | 80 | 90 | 70 | 40 | 60 | 90 | 40 | 80 | 50 | 80 | 80 | 90 | 50 | 9 |
| 80 | 60 | 60 | 40 | 80 | 50 | 80 | 40 | 80 | 60 | 80 | 60 | 60 | 40 | 80 | 10 |
| 60 | 70 | 80 | 90 | 90 | 80 | 10 | 50 | 60 | 70 | 40 | 70 | 80 | 30 | 60 | 11 |
| 80 | 80 | 60 | 40 | 40 | 80 | 80 | 80 | 70 | 80 | 80 | 80 | 60 | 60 | 80 | 12 |
| 60 | 60 | 70 | 80 | 50 | 60 | 60 | 60 | 80 | 90 | 60 | 80 | 70 | 70 | 60 | 13 |
| 70 | 70 | 80 | 60 | 80 | 80 | 70 | 80 | 90 | 80 | 70 | 60 | 80 | 40 | 70 | 14 |
| 80 | 80 | 90 | 70 | 90 | 60 | 80 | 60 | 40 | 40 | 80 | 70 | 90 | 50 | 80 | 15 |
| 90 | 90 | 40 | 80 | 40 | 70 | 80 | 70 | 50 | 70 | 90 | 80 | 40 | 80 | 90 | 16 |
| 40 | 40 | 80 | 90 | 80 | 80 | 60 | 80 | 80 | 80 | 40 | 90 | 90 | 60 | 40 | 17 |

In *Table 2*, the number 95 (expert 1; variable 1) means that expert 1 believes that intellectual capital has directly 95% effect on economic competitiveness.

The fuzzy matrix is then obtained. The lower limit of 20 and the upper limit of 90 are considered for responses, aiming to avoid responses from divergence, where all answers with a score equal to or lower than 20 are considered 0, while all answers equal or more than 90 are considered 1. In the next step, the power matrix of relations is obtained that illustrate the relationship of all 17 factors to each other. A focus group was created with 6 members to form the final matrix. The members of the group included university professors and specialists of economic competitiveness. According to their opinions, non-significant associations between factors were excluded and the casual orientation of relationships was determined. The results are presented in *Table 3*; the FCM diagram is shown in *Fig. 2*. According to the results, factors "ROEC" and "ROEC rate" have the same meaning and concept and therefore the factor "ROEC" was excluded. Also, the factors "financial performance" and "company's performance" were similar, due to the financial nature of the organization and so the factor "company's performance" was excluded. Other non-logical relationships were also excluded, according to experts.

***Table 3.*** *Matrix fuzzy cognitive map.*

| | 1 | 2 | 3 | 4 | 5 | 6 | 7 | 8 | 9 | 10 | 11 | 13 | 15 | 16 | 17 |
|---|---|---|---|---|---|---|---|---|---|---|---|---|---|---|---|
| 1 | | 4.64 | | 5.68 | 5.73 | 5.21 | 5.42 | 4.44 | | | | | | | |
| 2 | | | 6.19 | 6.32 | | | | 2.36 | 5.97 | 7.06 | 7.54 | 6.55 | 5.83 | | |
| 3 | | | | | | | | | | | | | | | |
| 4 | | | | | 4.91 | | | | | | | | | | |
| 5 | | | | | | | | | | | | | | | |
| 6 | | | | | | | | | 6.48 | | | | | | |
| 7 | | | | | | | | | 6.09 | | | | | | |
| 8 | | | | | | | | | | | | 6.55 | 5.83 | | |
| 9 | | | | | | | | | | 8.28 | 5.11 | | 5.51 | 7.51 | 4.54 |
| 10 | | | | | | | | | | | | | | | 6.88 |
| 11 | | | | | | | | | | | | | | | |
| 13 | | | | | | | | | | | | | | | |
| 15 | | | | | | | | | | | | | | 5.63 | |
| 16 | | | | | | | | | | | | | | | 8.68 |
| 17 | | | | | | | | | | | | | | | |

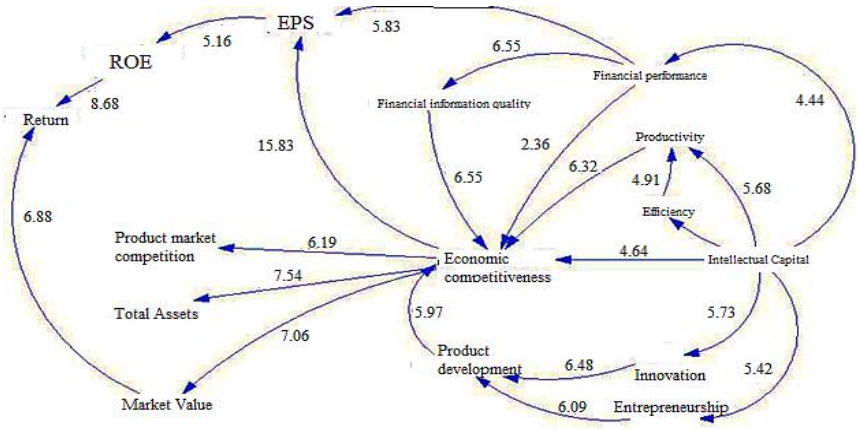


***Fig. 2.*** *A fuzzy cognitive map for intellectual capital, economic competitiveness and related variables.*

The model shows the relationship between intellectual capital and economic competitiveness variables and its value. Accordingly, intellectual capital affects economic competitiveness, innovation, entrepreneurship, efficiency, productivity, and financial performance. Economic competitiveness is also related to productivity, financial performance, quality of financial information, earnings per share, product market competition, total assets, market value, and product development. On the other hand, there is an indirect relationship between ROEC rate and annual returns with intellectual capital and economic competitiveness, where economic competition first influences market value and earnings per share, and then these two variables affect annual returns and ROEC, respectively. The model also shows the effect that ROEC rate has on annual returns.

### *3.4. Providing Questionnaire and Data Analysis*

Statistical tests were used for quantitative data analysis. Toward this end, a 21-items researcher-made questionnaire was designed based on the final model, where each item represents the relationship between the variables of the model and is designed based on the five-point Likert scale, ranging from very high to very low. For example, "intellectual capital affects the economic competitiveness" indicates the relationship between these two variables. The face and content validity of the questionnaire was evaluated using opinions from 6 experts in intellectual capital, economic competitiveness, and financial management, as well as by Cronbach's alpha (0.933). After approval, the questionnaires were distributed among 280 participants, of which 265 were completed that is, in fact, more than the minimum number (i.e. 260) required.

Sixty-five and thirty-five percent of respondents were male and female, respectively, most of them with a master's degree. Forty-eight percent were aged 36 and 45 years. In the next step, mean and the one-sample t-test were used for analyzing data obtained from questions. The fixed value in the one-sample t-test was 3 in the Likert scale. The results of each item are presented in *Table 4*.

***Table 4.*** *Mean and one-sample t-test results for each item.*

| No. | Question | Mean | t-value | Significance |
|---|---|---|---|---|
| **1** | *Intellectual capital affects economic competitiveness.* | *3.99* | *9.827* | *0.000* |
| **2** | *Intellectual capital affects efficiency.* | *3.83* | *7.365* | *0.000* |
| **3** | *Intellectual capital affects productivity.* | *3.83* | *7.799* | *0.000* |
| **4** | *Intellectual capital affects innovation.* | *3.85* | *8.017* | *0.000* |
| **5** | *Intellectual capital affects entrepreneurship.* | *3.92* | *8.897* | *0.000* |
| **6** | *Intellectual capital affects financial performance.* | *3.95* | *9.272* | *0.000* |
| **7** | *Efficiency affects productivity.* | *3.96* | *9.699* | *0.000* |
| **8** | *Productivity affects economic competitiveness.* | *3.62* | *5.314* | *0.000* |
| **9** | *Innovation affects product development.* | *4.06* | *11.095* | *0.000* |
| **10** | *Entrepreneurship affects product development.* | *3.96* | *9.528* | *0.000* |
| **11** | *Product development affects economic competitiveness.* | *4.08* | *11.493* | *0.000* |
| **12** | *Financial performance affects economic competitiveness.* | *3.64* | *5.574* | *0.000* |
| **13** | *Financial performance affects quality of financial information.* | *3.34* | *5.600* | *0.000* |
| **14** | *Quality of financial information affects economic competitiveness.* | *3.98* | *9.897* | *0.000* |
| **15** | *Financial performance affects earnings per share.* | *4.00* | *9.874* | *0.000* |
| **16** | *Economic competitiveness affects earnings per share.* | *3.76* | *6.980* | *0.000* |
| **17** | *Economic competitiveness affects product market competition.* | *3.77* | *7.259* | *0.000* |
| **18** | *Economic competitiveness affects total assets.* | *3.78* | *7.296* | *0.000* |
| **19** | *Economic competitiveness affects market value.* | *3.75* | *6.901* | *0.000* |
| **20** | *Market value affects annual return.* | *3.88* | *8.462* | *0.000* |
| **21** | *Earnings per share affects ROEC rate.* | *3.80* | *7.348* | *0.000* |
| **22** | *ROEC rate affects annual return.* | *3.81* | *7.356* | *0.000* |

According to *Table 4*, if the mean is higher than 3 and the significance value is less than 0.05, then it can be stated that the observed t is acceptable and, as a result, there is a single-variable relationship. Accordingly, it can be claimed that all relationships in the model are confirmed. On the other hand, based on the results, the highest mean obtained for the "the effect of product development on economic competitiveness", where it can be stated that product development has a significant effect on the economic competitiveness. Also, the mean value of the relationship between innovation and product development and the relationship between financial performance and earnings per share was higher than 4, and so these relationships are also significant. The lowest mean was obtained for the effect of financial performance on the quality of financial information, where this relationship is confirmed considering observed statistics, and, on the other hand, the effect that financial performance has on the quality of financial information is at the least level, given the lower mean value obtained than the other variables.

## 4. Conclusion and Suggestion

As the results confirm, there is a direct and nonlinear relationship between intellectual capital and economic competitiveness that is influenced by other factors. Creating economic competitiveness firstly leads to the establishment of some other variables and then affects them directly or indirectly. Intellectual capital affects economic competitiveness; it then affects total assets, product market competition, market value, and earnings per share. There is a correlation between the findings of this research and the results of researches conducted by Rastogi [42], Vătămănescu et al. [54], Cherkesova et al. [8] and Zambon [57], in terms of product market competition. Intellectual capital can also affect productivity, efficiency, financial performance, innovation, and entrepreneurship, where all these variables affect economic competitiveness. Nematollahi [37] emphasized the relationship between intellectual capital and efficiency. All of these eventually affect the annual ROEC. Taghavi and Alifarri [52], and Kiyamehr and Asgharzadeh [29] considered the direct relationship between intellectual capital

and ROEC. Yahyazadehfar et al. [54] confirmed the effect of intellectual capital on financial performance directly or indirectly; there is a correlation between these findings and the results of this research. Based on the FCM results, the highest and lowest impact was observed in the "relationship between economic competitiveness and earnings per share" and "the effect of financial performance on economic competitiveness", respectively. With one-sample t-test, the highest mean was observed for 11th items and the relationship between product development and economic competitiveness, while the lowest mean was observed for the item "financial performance affects the quality of financial information." According to employees' opinions, it can be claimed that the mean values of the relationship between "financial performance and earnings per share", "product development and economic competitiveness," as well as "innovation and product development" are higher 4, resulting in stronger effectiveness. In general, the effect that intellectual capital has on economic competitiveness can be confirmed, but the relation between these two variables is not simple and affected by other variables and the economic consequences. Also, according to experts, and considering the FCM results, the effect of intellectual capital on economic competitiveness, and the effect of other variables on annual returns are confirmed. Therefore, annual returns can be the most important and final economic consequence. The highest effectiveness was observed for intellectual capital, while the greatest effect is on economic competitiveness.

Scenarios can be presented based on the proposed model. For example, in a probable scenario, increased intellectual capital will lead to increased economic competitiveness, high economic competitiveness will lead to higher market value, and ultimately high market value will lead to an increase in annual returns. When using the results of this study, some considerations should be considered. The results obtained in this study are based on the results of research conducted in Iran. As a result, interpreting the results of this study should be based on observed variables. On the other hand, experts included managers and professors in financial management, while other experts have different opinions. Therefore, studying different scenarios by other researchers is recommended. It is also suggested the model be expanded using approaches such as system dynamics and using software such as Vensim PLE.

## References


[1] Abbasi, E., & Goldi, S. (2010). The Influences survey of the intellectual capital elements efficiency on the firms financial performance in Tehran stock exchange. *Accounting and auditing reviews, 17*(60), 57-74. (**In Persian**). https://acctgrev.ut.ac.ir/article_21209.html

[2] Ahmadian, H., & Ghorbani, R. (2013). Investigating the relationship between intellectual capital and organizational performance: a case study of the ministry of economic affairs and finance. *Economic journal, 13*(11), 111-130. (**In Persian**). http://ejip.ir/browse.php?a_id=679&sid=1&slc_lang=fa

[3] Amin, A., & Thrift, N. (2000). What kind of economic theory for what kind of economic geography? *Antipode, 32*(1), 4-9.

[4] Asadi, G. H., & Yokhneh Alghiaee, M. (2014). The impact of intellectual capital on financial performance of companies listed in TSE. *Empirical studies in financial accounting quarterly, 11*(41), 83-103. (**In Persian**). https://qjma.atu.ac.ir/article_1106.html?lang=en

[5] Bontis, N. (1998). Intellectual capital: an exploratory study that develops measures and models. *Management decision*, 36(2), 63-76.

[6] Bose, S., & Oh, K. B. (2004). Measuring strategic value-drivers for managing intellectual capital. *The learning organization, 11*(4/5), 347-356.

[7] Sparrow, P., Brewster, C., & Chung, C. (2016). *Globalizing human resource management*. Routledge.

[8] Cherkesova, E. Y., Breusova, E. A., Savchishkina, E. P., & Demidova, N. E. (2016). Competitiveness of the human capital as strategic resource of innovational economy functioning. *Journal of advanced research in law and economics, 7*(7 (21)), 1662-1667.

[9] Crouch, G. I., & Ritchie, J. B. (1999). Tourism, competitiveness, and societal prosperity. *Journal of business research, 44*(3), 137-152.

[10] Dastgir, M., Arab Salehi, M., Amin Jafari, R., & Akhlaghi, H. (2014). The effects of intellectual capital on the financial performance of corporate. *Financial accounting and audit research, 6*(21), 1-36. (**In Persian**). http://faar.iauctb.ac.ir/article_510521.html
[11] Dianati Deilami, D., & Ramezani, M. (2012). The impact of intellectual capital on the financial information quality for listed firms in Tehran stock exchange. *Knowledge of accounting and financial accounting, 1* (2), 50 -37. (**In Persian**). http://jmaak.srbiau.ac.ir/article_7322.html
[12] Zambon, S., & Dumay, J. (2016). A critical reflection on the future of intellectual capital: from reporting to disclosure. *Journal of intellectual capital, 17*(1), 168-184.
[13] Dzenopoljac, V., Yaacoub, C., Elkanj, N., & Bontis, N. (2017). Impact of intellectual capital on corporate performance: evidence from the Arab region. *Journal of intellectual capital, 18*(4), 884-903.
[14] Edvinsson, L., & Malone, M. (1997). *Intellectual capital: realizing your company's true value by finding its hidden brainpower*. Harper Business.
[15] Ghasem Zadeh, A., & Maleki, Sh., & Sharifi, L. (2016). The mediating effect of professional ethics on the relationship between intellectual capital, organizational learning and knowledge sharing. *Journal of medical education development, 9*(22), 76-88. (**In Persian**). http://zums.ac.ir/edujournal/article-1-575-fa.html
[16] Ghasemi Nejad, Y., & Salgi, M. (2014). Investigating the influence of intellectual capital on the development of innovative products (case study: one of the industrial defense research centers). *Strategic studies of Basij, 65*, 141-163. (**In Persian**). http://ensani.ir/fa/article/365659/%D8%A8%D8%B1%D8%B1%D8%B3%DB%8C-%D8%AA%D8%A3%D8%AB%DB%8C%D8%B1-%D8%B3%D8%B1%D9%85%D8%A7%DB%8C%D9%87-%D9%81%DA%A9%D8%B1%DB%8C-%D8%A8%D8%B1-%D8%AA%D9%88%D8%B3%D8%B9%D9%87-%D9%85%D8%AD%D8%B5%D9%88%D9%84%D8%A7%D8%AA-%D9%86%D9%88%D8%A2%D9%88%D8%B1%D8%A7%D9%86%D9%87-%D9%85%D9%88%D8%B1%D8%AF-%D9%85%D8%B7%D8%A7%D9%84%D8%B9%D9%87-%DB%8C%DA%A9%DB%8C-%D8%A7%D8%B2-%D9%85%D8%B1%D8%A7%DA%A9%D8%B2-%D8%AA%D8%AD%D9%82%DB%8C%D9%82%D8%A7%D8%AA%DB%8C-%D8%B5%D9%86%D8%B9%D8%AA%DB%8C-%D8%AF%D9%81%D8%A7%D8%B9%DB%8C-
[17] Ghiyasi, S., & Aminalroaya, E. (2016). Investigating the effects of social and intellectual capital on productivity of human resources. *Management studies in development and evolution, 25*(80), 183-209. (**In Persian**). https://jmsd.atu.ac.ir/article_4035.html
[18] Ghelich, B., KHodad, H., & Moshbaki, A. (2008). The role of intellectual capital in making competitive advantages. *Humanities teacher, 15*(3), 109-124. (**In Persian**). https://www.sid.ir/fa/journal/ViewPaper.aspx?id=81911
[19] Ghezel, A., Ramezan, M., & Zohdi, M. (2013). Provide a conceptual framework for measuring structural capital at a university. *Technology growth, 10*(37), 63-73. (**In Persian**). https://www.sid.ir/fa/journal/ViewPaper.aspx?id=217041
[20] Gupta, S., Malhotra, N. K., Czinkota, M., & Foroudi, P. (2016). Marketing innovation: a consequence of competitiveness. *Journal of business research, 69*(12), 5671-5681.
[21] Ting, I. W. K., & Lean, H. H. (2009). Intellectual capital performance of financial institutions in Malaysia. *Journal of intellectual capital, 10*(4), 588-599.
[22] Haji Hoseini, H., & Norozade Moghadam, E. (2014). The effect of innovation and market orientation on business performance and sustainable competitive advantage in industrial firms. *Industrial technology development, 23*, 21-29. (**In Persian**). http://jtd.iranjournals.ir/article_11903.html?lang=en
[23] Imeni, M. (2020). Fuzzy logic in accounting and auditing. *Journal of fuzzy extension and applications, 1*(1), 69-75.
[24] Ivanov, G., & Mayorova, E. (2015). Intangible assets and competitive advantage in retail: case study from Russia. *Asian social science, 11*(12), 38.
[25] Kaplan, R. S., Kaplan, R. E., Norton, D. P., Davenport, T. H., & Norton, D. P. (2004). *Strategy maps: converting intangible assets into tangible outcomes*. Harvard Business Press, Boston, MA.
[26] Khalique, M., Bontis, N., Bin Shaari, J. A. N., & Isa, A. H. M. (2015). Intellectual capital in small and medium enterprises in Pakistan. *Journal of intellectual capital, 16*(1), 224-238.
[27] Khazaei Pool, M., Zarei, H., Dehghan, M. S., & Karimi, A. H. (2012). Strategic entrepreneurship and competitive advantage. *National conference on entrepreneurship and management of knowledge-based businesses*. Babolsar. (**In Persian**). https://civilica.com/doc/174751/
[28] Lerro, A., Linzalone, R., Schiuma, G., Kianto, A., Ritala, P., Spender, J. C., & Vanhala, M. (2014). The interaction of intellectual capital assets and knowledge management practices in organizational value creation. *Journal of intellectual capital, 15*(3), 362-375.
[29] Kiamehr, A., Asgharzadeh, M. (2017). Investigating the impact of intellectual capital on return on equity of companies listed on the Tehran stock exchange. *The first conference on accounting, management and economics with a national economic dynamics approach*. Malayer. (**In Persian**). https://civilica.com/doc/660595/

[30] Kostopoulos, K. C., Bozionelos, N., & Syrigos, E. (2015). Ambidexterity and unit performance: Intellectual capital antecedents and cross-level moderating effects of human resource practices. *Human resource management*, *54*(S1), s111-s132.

[31] Namazi, M., & Ebrahimi, Sh. (2009). Investigating the effect of intellectual capital on current and future financial performance of listed companies in Tehran stock exchange. *Accounting research, 1*(4), 1-25. (**In Persian**). http://ensani.ir/fa/article/9731/%D8%A8%D8%B1%D8%B1%D8%B3%DB%8C-%D8%AA%D8%A7%D8%AB%DB%8C%D8%B1-%D8%B3%D8%B1%D9%85%D8%A7%DB%8C%D9%87-%D9%81%DA%A9%D8%B1%DB%8C-%D8%A8%D8%B1-%D8%B9%D9%85%D9%84%DA%A9%D8%B1%D8%AF-%D9%85%D8%A7%D9%84%DB%8C-%D8%AC%D8%A7%D8%B1%DB%8C-%D9%88-%D8%A2%DB%8C%D9%86%D8%AF%D9%87-%D8%B4%D8%B1%DA%A9%D8%AA-%D9%87%D8%A7%DB%8C-%D9%BE%D8%B0%DB%8C%D8%B1%D9%81%D8%AA%D9%87-%D8%B4%D8%AF%D9%87-%D8%AF%D8%B1-%D8%A8%D9%88%D8%B1%D8%B3-%D9%88-%D8%A7%D9%88%D8%B1%D8%A7%D9%82-%D8%A8%D9%87%D8%A7%D8%AF%D8%A7%D8%B1-%D8%AA%D9%87%D8%B1%D8%A7%D9%86

[32] Mahmoudi, M., & Kiyarazm, A. (2015). Investigating the relationship between intellectual capital components and drivers of organizational innovation. *Transformation management journal, 5*(19), 41-66. (**In Persian**). https://doi.org/10.22067/pmt.v7i14.44792

[33] Marzband, A. (2020). Precise services and supply chain prioritization in manufacturing companies using cost analysis provided in a fuzzy environment. *Journal of fuzzy extension and applications*, *1*(1), 42-59.

[34] Mojtahed Zadeh, V., Alavi, S. H., & Mahdi Zadeh, M. (2010). The relationship between intellectual capital (human, customer and structural) and the performance of the insurance industry (from the perspective of managers). *Accounting and auditing review*, *7*(17). (**In Persian**). http://ensani.ir/fa/article/219633/%D8%B1%D8%A7%D8%A8%D8%B7%D9%87-%D8%B3%D8%B1%D9%85%D8%A7%DB%8C%D9%87-%D9%81%DA%A9%D8%B1%DB%8C-%D8%A7%D9%86%D8%B3%D8%A7%D9%86%DB%8C-%D9%85%D8%B4%D8%AA%D8%B1%DB%8C-%D9%88-%D8%B3%D8%A7%D8%AE%D8%AA%D8%A7%D8%B1%DB%8C-%D9%88-%D8%B9%D9%85%D9%84%DA%A9%D8%B1%D8%AF-%D8%B5%D9%86%D8%B9%D8%AA-%D8%A8%DB%8C%D9%85%D9%87-%D8%A7%D8%B2-%D8%AF%DB%8C%D8%AF%DA%AF%D8%A7%D9%87-%D9%85%D8%AF%DB%8C%D8%B1%D8%A7%D9%86-

[35] Najarzadeh, R. (2007). Measuring the competitive power of products of Tabriz petrochemical complex in accession to WTO. *Business research journal, 11(43), 35-61*. (**In Persian**). https://www.sid.ir/fa/journal/ViewPaper.aspx?id=67605

[36] Nematollahi, Z., & Mohammad, D. (2013). An investigation of the intellectual capital effects on relative efficiency. *Asset managing & financing*, *2*(5), 51-74. (**In Persian**). https://amf.ui.ac.ir/article_19898.html?lang=en

[37] Nimtrakoon, S. (2015). The relationship between intellectual capital, firms' market value and financial performance. *Journal of intellectual capital, 16*(3), 587-618.

[38] Osoba, O. A., & Kosko, B. (2017). Fuzzy cognitive maps of public support for insurgency and terrorism. *The journal of defense modeling and simulation, 14*(1), 17-32.

[39] Ola, M., Haji Zade, H., & Saeidi, M. (2016). The relationships between intellectual capital and productivity in medicine corporates. *Financial accounting and auditing research, 8*(31), 73-91. (**In Persian**). http://faar.iauctb.ac.ir/article_526869.html

[40] Pan, Y., Wang, T. Y., & Weisbach, M. S. (2015). Learning about CEO ability and stock return volatility. *The review of financial studies*, *28*(6), 1623-1666.

[41] Pratheepkanth, P. (2018). Intellectual capital disclosure: a study of Australia and Sri Lanka. *World academy of science, engineering and technology, international journal of economics and management engineering*, *12*(3). Retrieved from https://publications.waset.org/abstracts/84015/intellectual-capital-disclosure-a-study-of-australia-and-sri-lanka

[42] Rastogi, P. N. (2000). Knowledge management and intellectual capital–the new virtuous reality of competitiveness. *Human systems management*, *19*(1), 39-48.

[43] Rahimi Rigi, Q., Kazemi Cheleh Gahi, R., Ghanbari Milasi, H., & Agham Mohammadpour, H. (2014). The influence of intellectual capital components on the effectiveness of shares accepted by Tehran stock exchange using the data envelopment analysis model. *International conference on accounting, economics and financial management.* (**In Persian**). https://civilica.com/doc/325355/

[44] Riasi, A. (2015). Competitive advantages of shadow banking industry: an analysis using Porter diamond model. *Business management and strategy*, *6*(2), 15-27.

[45] Rodriguez-Repiso, L., Setchi, R., & Salmeron, J. L. (2007). Modelling IT projects success with fuzzy cognitive maps. *Expert systems with applications*, *32*(2), 543-559.

[46] Safari, S., Shams, F., & Ahopay, M. (2014). The importance of intellectual capital and its elements in organizational entrepreneurship development. *Social development & Welfare planning, 12*(3), 3-25. (**In Persian**). https://qjsd.atu.ac.ir/article_685.html?lang=en

[47] Saeidi, S. P., Sofian, S., Saeidi, P., Saeidi, S. P., & Saaeidi, S. A. (2015). How does corporate social responsibility contribute to firm financial performance? The mediating role of competitive advantage, reputation, and customer satisfaction. *Journal of business research*, *68*(2), 341-350.

[48] Schneider, M., & Hase, F. (2009). Improving spectroscopic line parameters by means of atmospheric spectra: theory and example for water vapor and solar absorption spectra. *Journal of quantitative spectroscopy and radiative transfer, 110*(17), 1825-1839.

[49] Sepehrdoust, H. (2010). The position of intellectual capital in the performance of stock exchange companies. *Economic studies and policies*, *24*, 249-236. (**In Persian**). http://economic.mofidu.ac.ir/article_26194.html
[50] Soltani, M., Zare, A., Parniyankhoy, M. (2015). Analysis of human Resources's role in creating competitive advantage; use of VRIO model. *Organizational culture management*, *13*(2), 393-414. (**In Persian**). 10.22059/JOMC.2015.54107
[51] Shafi Salimi, P., & Edalatpanah, S. A. (2020). Supplier selection using fuzzy AHP method and D-Numbers. *Journal of fuzzy extension and applications*, *1*(1), 1-14.
[52] Jabbarzadeh Kongerloui, S., Naseri, G., Khadivi, S. H. (2017). The effect of intellectual capital on the relationship between business strategy adoption on product market competition and financial crisis in companies listed on the Tehran stock exchange. *7th national conference on accounting applications*. (**In Persian**). https://civilica.com/doc/807589/
[53] Seidi, H., & Heidari, A. (2013). The effect of intellectual capital on the financial performance of investment companies listed on the Tehran stock exchange. *11th national accounting conference of Iran*. Mashhad. (**In Persian**). https://civilica.com/doc/339849/
[54] Vătămănescu, E. M., Andrei, A. G., Dumitriu, D. L., & Leovaridis, C. (2016). Harnessing network-based intellectual capital in online academic networks. From the organizational policies and practices towards competitiveness. *Journal of knowledge management*, *20*(3), 594-619.
[55] Wagner, M., & Schaltegger, S. (2004). The effect of corporate environmental strategy choice and environmental performance on competitiveness and economic performance: an empirical study of EU manufacturing. *European management journal*, *22*(5), 557-572.
[56] Yahyazadehfar, M., Aghajani, H., & Yahyatabar, F. (2014). Investigation of the relationship between intellectual capital and companies' performance in Tehran stock exchange. *Financial research journal*, *16*(1), 181-199. (**In Persian**). https://jfr.ut.ac.ir/article_51847.html
[57] Zambon, S. (2004). Intangibles and intellectual capital: an overview of the reporting issues and some measurement models. In P. Bianchi (Ed.), *The economic importance of intangible assets* (pp. 153-183). Aldershot.
[58] Zoraki, Sh., & Nasab, A. (2017). An investigation of effective factors in the growth of the tourism with an emphasis on destination competitiveness (application of DPDM and GMM-Sys estimator). *Tourism planning and development*. (**In Persian**). https://dx.doi.org/10.22080/jtpd.2018.1765

Journal of Applied Research on Industrial Engineering
www.journal-aprie.com

# Stabilization of Low Plastic and High Plastic Clay Using Guar Gum Biopolymer

***Muhammad Ali Rehman*, Turab Jafri***
*Institute of Civil Engineering, National University of Sciences and Technology (NUST), Islamabad, Pakistan.*

**PAPER INFO**

**Chronicle:**
*Received: 05 July 2020*
*Reviewed: 30 August 2020*
*Revised: 04 October 2020*
*Accepted: 13 November 2020*

**Keywords:**
*Biopolymer.*
*Guar Gum.*
*Low Plastic Clay.*
*High Plastic Clay.*
*Soil Stabilization.*
*Compressive Strength.*
*CBR.*

**ABSTRACT**

In geotechnical engineering, soil stabilization provides practical and cost-effective solutions related to problematic soils. With the growing necessity for environmentally friendly and sustainable materials, researchers have been exploring alternative methods such as biological approaches for soil stabilization. Biopolymers are produced from living organisms and are considered to be environmentally friendly soil stabilizers. A detailed study on stabilization of soil using Guar gum biopolymer was carried out through intensive laboratory testing. For this purpose, low plastic (CL) and high plastic (CH) clays were treated with varying contents of Guar gum biopolymer (1%, 2%, 3% and 4%) by the weight of dry soil. The experimental program mainly focused on compaction characteristics, unconfined compressive strength, California Bearing Ratio (CBR) and swell potential tests. All the samples were prepared on dry mix basis. The UCS of cured and soaked samples was tested after 2, 7, 14, and 28 days of curing and soaking. Strengthening effect of Guar gum biopolymer was observed with the increasing biopolymer content and curing period. An increase of 182.64% and 243.30% was observed in the UCS of CL and CH respectively at the end of curing period using 2% biopolymer content. The results indicated a significant increase in the CBR of both CL and CH under soaked and unsoaked conditions. The incorporation of Guar gum biopolymer has shown significant improvement in geotechnical properties of low plastic and high plastic clays and can be adopted as a potentially sustainable soil stabilizer.

## 1. Introduction

Soil has a critical role in construction as it acts as ultimate load bearing material for structures such as buildings, roads, bridges etc. As a result of continuous construction and development works, the odds of availability of favorable soil at construction sites have decreased, which urges the engineers to utilize the land with unfavorable & problematic soil for the construction purposes. Clayey soils are expansive in nature as they tend to experience volumetric changes upon interaction with water. The swelling and shrinkage behavior of clayey soils instigates severe soil related problems. Improvement in soil

Rehman, M. A., & Jafri, T. (2020). Stabilization of low plastic and high plastic clay using guar gum biopolymer. *Journal of applied research on industrial engineering, 7*(4), 329-343.

* Corresponding author
E-mail address: ar.siddiqui@hotmail.com

10.22105/jarie.2020.247859.1195

properties has been an important consideration for engineers and researchers throughout the construction history. Soil stabilization is a process of modification of soil properties such as compaction, bearing capacity, strength, and swelling potential for improved engineering performance [1, 2]. Researchers have been examining a variety of soil stabilization practices such as compaction, drainage, pre-compression, consolidation, grouting, soil reinforcement, geotextiles, and chemical stabilizers [3]. The use of various soil stabilizers has been in practice such as cement, lime, gypsum, fly ash, rice husk ash, rubber wastes, bitumen, and slag [4]. Among these conventional additives, cement is one of the most abundantly used material for soil stabilization [5]. Cement has been identified as the leading source of carbon dioxide emission, causing approximately 5% of annual carbon dioxide production [6]. The excessive use of conventional soil stabilizers, such as cement, leads to serious environmental impacts. Keeping in view the environmental sustainability, researchers have been intensively studying alternative materials such as geosynthetics, geopolymers, biopolymers, synthetic polymers, bio-enzymes, and microbial injections to be used as stabilizers [7]. Biopolymers are produced by living organisms and are considered to be environmentally friendly and sustainable materials to be used as alternative soil stabilizers [8]. The use of biopolymers in not utterly new in the field of geotechnical engineering, as humans used various materials such as straw and sticky rice binders for soil improvement in the past [9]. Utilizing the biopolymers can help in improving the soil properties such as compressive strength, erosion control, reduction in permeability and vegetation suitability [10]. Biopolymers have shown the capability of being sustainable materials for the improvement of strength and stability of various soils and found to be advantageous over traditional stabilizers in terms of being environmentally friendly and effective at low concentrations [11]. Soils treated with biopolymers exhibit that small concentration of biopolymers mixed with soils result in higher compressive strength as compared to large amount of cement mixed with soil [9]. Biopolymers on interaction with fine soil particles form soil-biopolymer matrices having the strength mainly linked by hydrogen bonding, thus improving the overall compressive strength and resistance of soil [12]. Addition of biopolymers at low concentrations has been reported to improve compaction characteristics, compressive strength, CBR, swelling potential, permeability, collapsible potential, and shear parameters [13-16]. Due to the lack of biological approach for soil improvement in Pakistan, a biopolymer commonly known as Guar gum was selected as the soil stabilizing agent in this work. The addition of Guar gum to the soil has been reported to improve the compaction characteristics, compressive strength, CBR, resistance to wind erosion, dust resistance, water retention capacity, collapsible potential, surface strength and other mechanical properties of the soil [6, 13, 16, 17, 18]. In this study, the effects of Guar gum on low and high plastic clays has been investigated.

## 2. Materials

### *2.1. Soil*

Two types of soils, low plastic and high plastic clay, have been used in this study to investigate the effect of biopolymer on selected soil properties. The low plastic soil exhibiting swelling behavior used in this study was collected from Ballewala, Pakistan. Various studies have been conducted to control swelling and improve geotechnical properties such as compaction, compressive strength and CBR of Ballewala clay [19-22]. High plastic clay was prepared in the laboratory by mixing 25% bentonite with low plastic clay. Trial tests were conducted for the selection of suitable percentage of bentonite in order to prepare high plastic clay in laboratory. CL soil was mixed with 10%, 15%, 20%, and 25% bentonite and Atterberg Limits tests were conducted for each replacement. A significant change in liquid limit of the soil was observed at 25% bentonite mix, thus it was selected as the suitable percentage for preparing

CH samples in the laboratory. The geotechnical properties of low plastic and high plastic clays obtained through laboratory testing are shown in *Table1*.

***Table 1.*** *Properties of untreated CL and CH.*

| **Property** | **CL** | **CH** |
|---|---|---|
| *Passing Sieve # 200 (%)* | *94.42* | *97.09* |
| *Clay Fraction (%)* | *19* | *26* |
| *Liquid Limit, LL (%)* | *48* | *59* |
| *Plastic Limit, PL (%)* | *21* | *28* |
| *Plasticity Index, PI (%)* | *27* | *31* |
| *Specific Gravity (Gs)* | *2.67* | *2.69* |
| *AASHTO Classification* | *A-7-6* | *A-7-6* |
| *USCS Classification* | *CL* | *CH* |
| *MDD (kN/m$^3$)* | *17.80* | *17.50* |
| *OMC (%)* | *12.00* | *12.34* |
| *UCS (kPa)* | *170.53* | *211.44* |
| *Un-soaked CBR (%)* | *3.69* | *2.61* |
| *Soaked CBR (%)* | *2.12* | *1.36* |
| *Swell Potential (%)* | *5.89* | *7.83* |

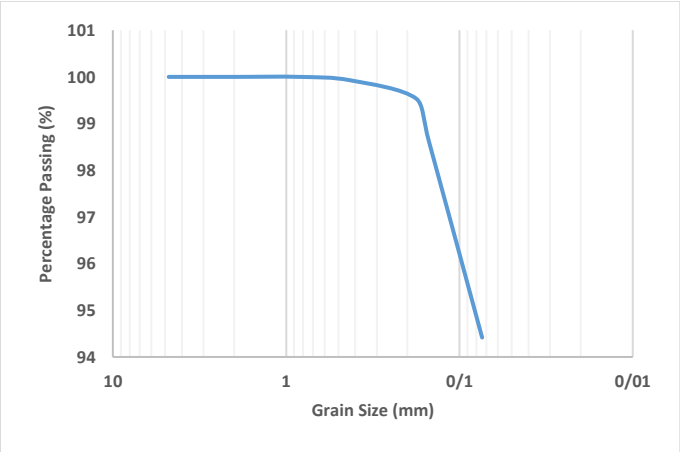


***Fig. 1.*** *Grain size distribution of CL.*

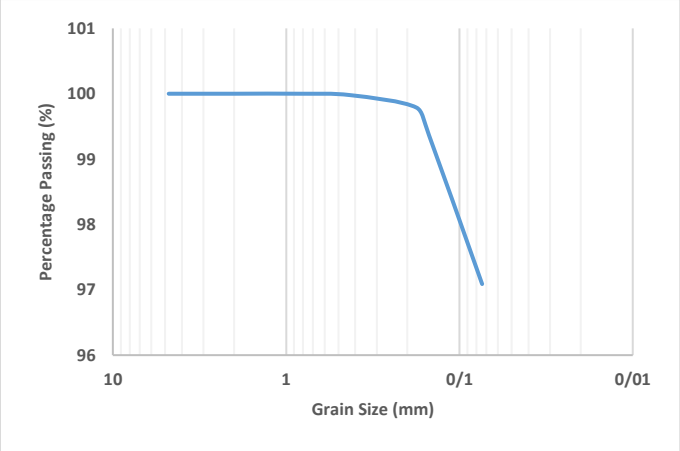


***Fig. 2.*** *Grain size distribution of CH.*

The bentonite used in this research to prepare high plastic clay in laboratory was obtained from Lahore, Pakistan. The chemical composition of industrial bentonite clay, known as Sodium Bentonite, is shown in *Table 2*.

***Table 2.*** *Chemical composition of bentonite clay.*

| Name | Formula | Percentage |
|---|---|---|
| *Silica* | $SiO_2$ | *50.0 to 65.0 %* |
| *Alumina* | $Al_2O_3$ | *15.0 to 25.0 %* |
| *Ferric Oxide* | $Fe_3O_3$ | *2.0 to 4.0 %* |
| *Magnesium Oxide* | $MgO$ | *3.0 to 6.0 %* |
| *Calcium Oxide* | $CaO$ | *0.50 to 2.0 %* |
| *Sodium Oxide* | $Na_2O$ | *0.50 to 5.0 %* |
| *Potassium Oxide* | $K_2O$ | *0.20 to 1.0 %* |
| *Titanium Oxide* | $TiO_2$ | *0.20 to 0.50 %* |

### *2.2. Biopolymer*

Guar (botanically known as Cyamopsis Tetragonoloba) is grown in arid and semi-arid regions of Punjab and Sind provinces of Pakistan and its seeds are locally processed in industries to form Guar gum in powdered form, as shown in *Fig. 3*.

The industrially produced Guar gum used in this research was obtained from Karachi, Pakistan. Guar gum comes from polysaccharide family of biopolymers which is mainly composed of sugars galactose and mannose. The basic structure of Guar gum consists of a linear chain of *β-1*, 4-linked mannose with *α-1*, 6-linked galactose residues [23], shown in *Fig. 4*. The galactose residues are linked with every second mannose in the chain, thus establishing short side branches [16]. Guar gum biopolymer through its hydroxyl groups (-OH) can form frequent hydrogen bonds, which further adds up to the strength of soil-biopolymer matrices [24].

***Fig. 3.*** *Guar gum powder.*

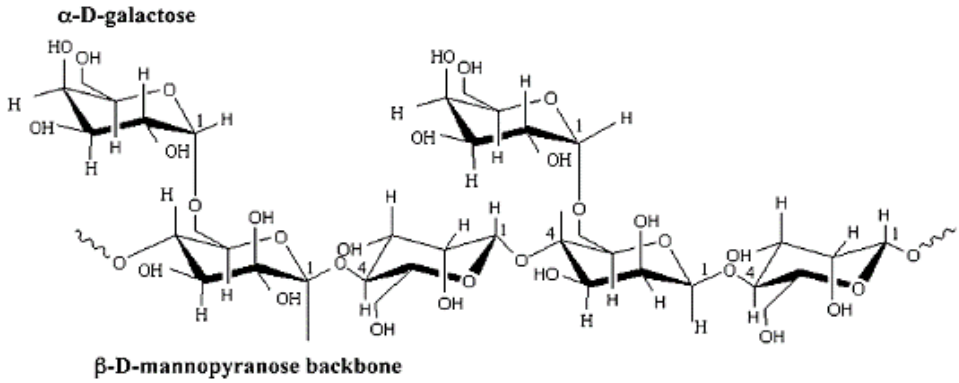


***Fig. 4.*** *Structure of Guar gum biopolymer [23].*

## 3. Experimental Procedure

The experimental program mainly focused on the compaction characteristics, Unconfined Compressive Strength (UCS), CBR and swell potential of the soil. In order to evaluate the effectiveness of Guar gum biopolymer on these soil properties, a number of laboratory tests were conducted which include modified proctor test, unconfined compressive strength test and CBR test. In order to perform UCS and CBR tests, the samples were prepared at Optimum Moisture Content (OMC) obtained from modified proctor tests. UCS was performed in both curing and soaking conditions for evaluating the effect of curing period on the development of strength. CBR tests were also conducted under unsoaked and soaked conditions. Swell potential of the soil was determined from soaked CBR samples.

### *3.1. Sample Preparation*

In light of the literature, dry mixing method was adopted for sample preparation [9, 13, 15, 17]. The Guar gum powder was thoroughly hand mixed with the soil and a predetermined amount of water was then added to the soil-biopolymer mixture to prepare the specimen for testing. In this study, different

quantities of Guar gum biopolymer were used with the soil according to its percentage by weight of dry soil sample. The mixing percentages are denoted in this study as BP-1, BP-2, BP-3, and BP-4 for 1%, 2%, 3% and 4% biopolymer content, respectively.

## 4. Results and Discussions

The selected properties of soil were evaluated for assessing the effectiveness of Guar gum at four different percentages of biopolymer: 1%, 2%, 3%, and 4%, by weight of dry soil. The main results of this study are discussed below.

### *4.1. Compaction Characteristics*

Compaction is a primary process in soil stabilization, in which a soil is compacted to a certain density after mixing the stabilizer. The attained density influences other soil properties such as bearing capacity, settlement, and shear strength. It is of prime importance to determine the compaction characteristics of soil mixed with varying percentages of biopolymer. The modified proctor test was performed using both low plastic and high plastic clays (CL and CH) mixed with each biopolymer percentage in order to determine the effect of Guar gum biopolymer on Maximum Dry Density (MDD) and OMC. The results for both the CL and CH soils are shown in *Fig. 5* and *Fig. 6*, respectively. The modified proctor test results for both CL and CH soils show an increasing trend in the MDD and corresponding OMC values for biopolymer content up to 2%. Guar gum biopolymer fills up the pore spaces in the soil and also bonds with the fine particles of clay, thus increasing the dry density of the soil. Upon further increase in biopolymer content, the MDD showed a decreasing trend but the corresponding OMC kept on increasing with the increase in biopolymer content. This can be attributed to highly viscous nature of Guar gum biopolymer, which changes the water absorption and specific gravity of the soil sample resulting in decrease in MDD at higher biopolymer content.

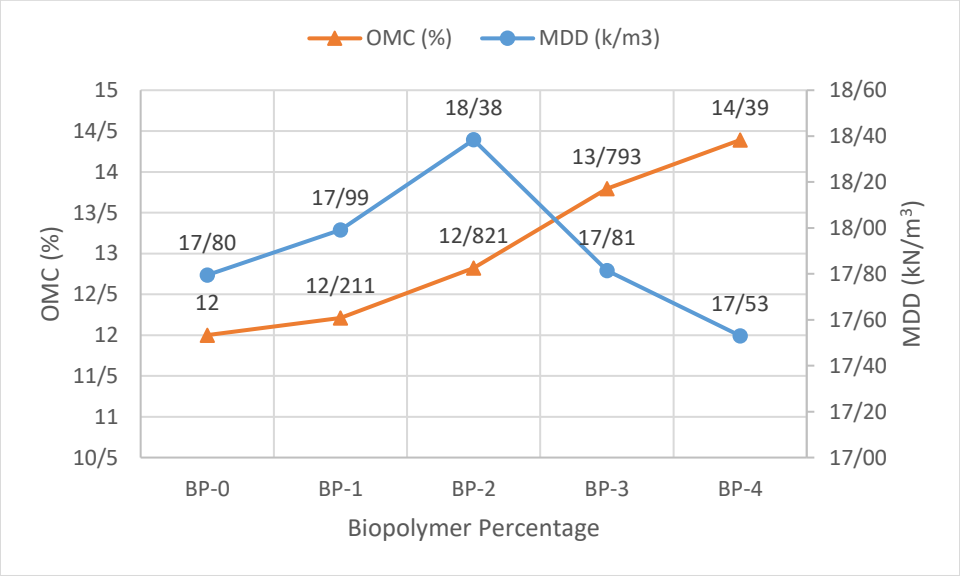


***Fig. 5.*** *Trend of OMC and MDD at different biopolymer percentages for CL.*

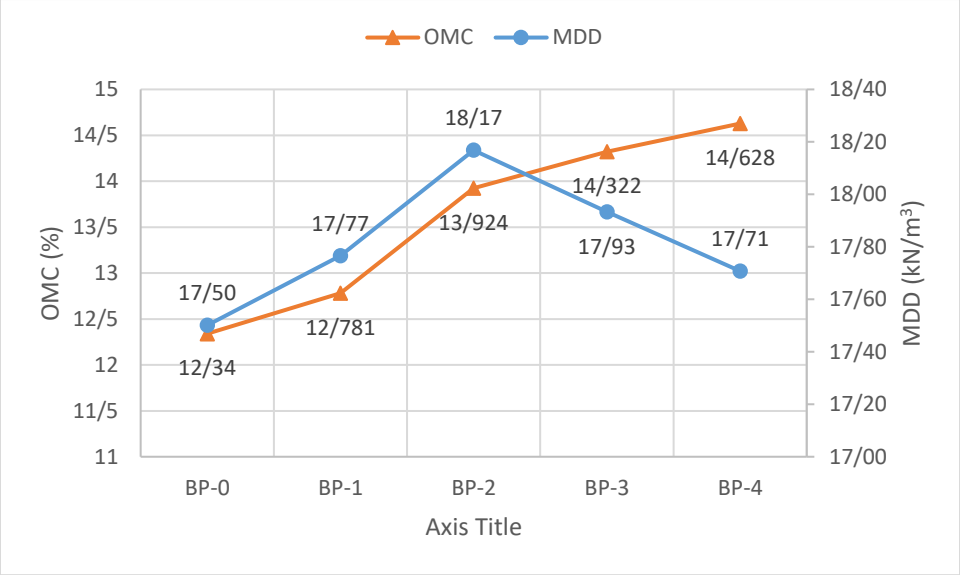


***Fig. 6.*** *Trend of OMC and MDD at different biopolymer percentages for CH.*

### *4.2. Unconfined Compressive Strength*

The unconfined compressive strength test was conducted using both CL and CH samples. The test specimens were prepared at MDD and OMC obtained from modified proctor test for different percentages of Guar gum biopolymer. The prepared specimens were wrapped in plastic sheet and left at room temperature for 24 hours before testing. *Fig. 7* shows the results of UCS tests for both the CL and CH soil specimens at different biopolymer percentages. For both soils, maximum values were observed at 2% biopolymer content. The effect of strength development with time was evaluated by curing the samples for 2, 7, 14, and 28 days in a thermostatically controlled oven. The prepared specimens were wrapped in plastic sheet and placed in oven at 40°C for desired curing period. The results of curing effect on strength of CL and CH soil samples are shown in *Fig. 8* and *Fig. 9*, respectively. For soaking test, the UCS cured samples were placed in desiccator for 48 hours. The soaking test signifies the strength of soil subjected to capillary rise of water. Biopolymers generally have high specific surfaces and upon interaction with fine particles of the soil, they form firm soil-biopolymer matrices.

Guar gum biopolymer have large hydroxyl groups which form a network of hydrogels between soil particles and free water linked by hydrogen bonds, thus contributing to the higher compressive strength of the soil [15, 25, 26]. The unconfined compressive strength of both CL and CH soil samples used in this study showed significant improvement according to both the curing period of soil-biopolymer mix and also the content of biopolymer. The maximum values were achieved at 2% biopolymer content. Upon further increase in Guar gum biopolymer content, a decrease in UCS values was observed for both CL and CH soils. It was also observed that the UCS of both soils attained maximum values after 28 days curing for all the biopolymer contents, among which the maximum value was obtained in BP-2 case. The UCS value of CL and CH soils increased from 170.53 kPa to 482 kPa and from 211.44 kPa to 725.88 kPa, respectively after 28 days of curing. It indicates an increase of 182.64% and 243.30% in unsoaked UCS of CL and CH, respectively.

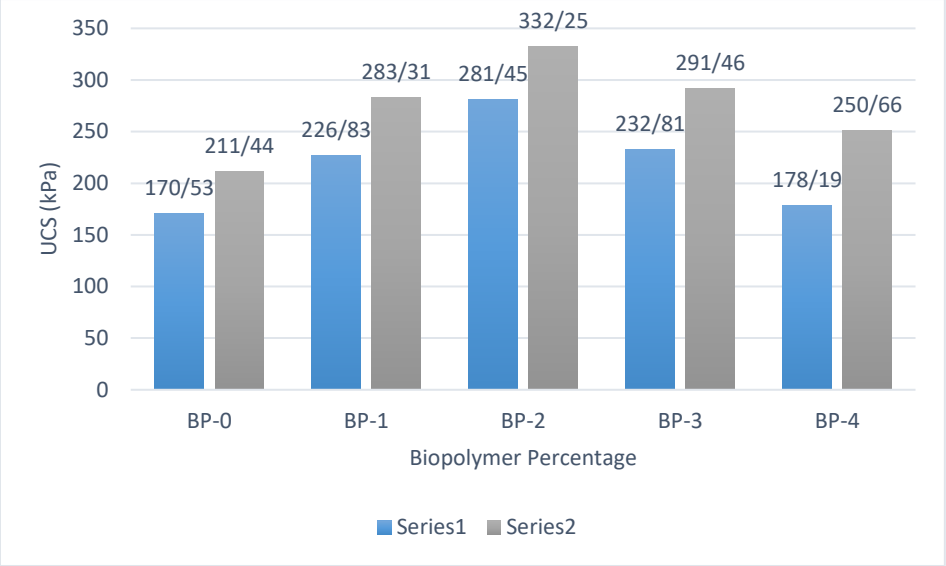


***Fig. 7.*** *UCS of uncured CL and CH samples at different biopolymer percentages.*

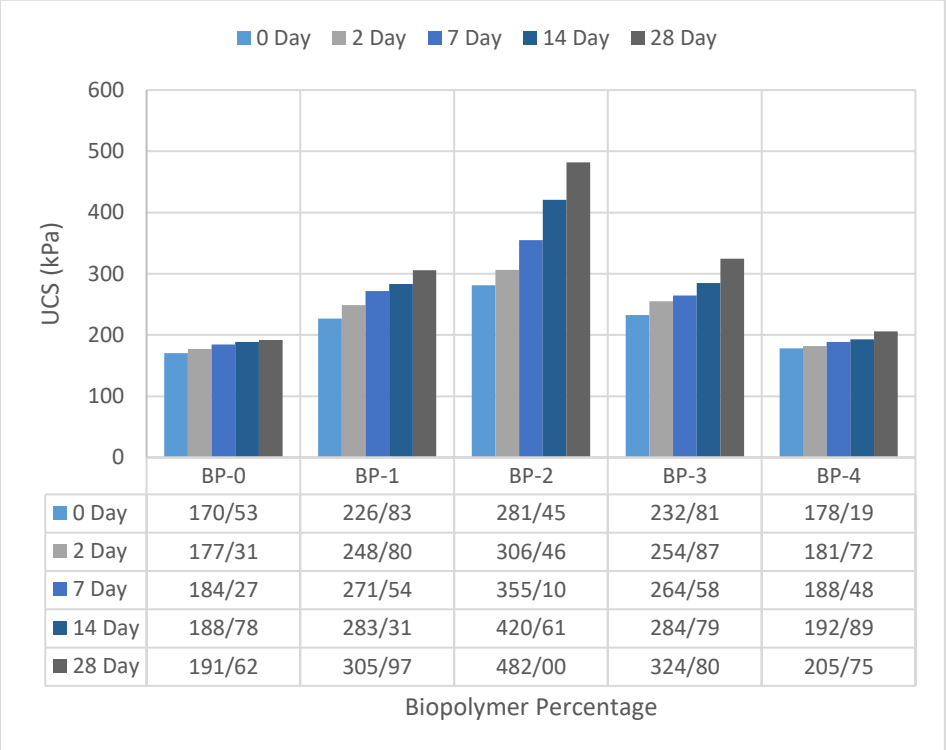


| | BP-0 | BP-1 | BP-2 | BP-3 | BP-4 |
|---|---|---|---|---|---|
| 0 Day | 170/53 | 226/83 | 281/45 | 232/81 | 178/19 |
| 2 Day | 177/31 | 248/80 | 306/46 | 254/87 | 181/72 |
| 7 Day | 184/27 | 271/54 | 355/10 | 264/58 | 188/48 |
| 14 Day | 188/78 | 283/31 | 420/61 | 284/79 | 192/89 |
| 28 Day | 191/62 | 305/97 | 482/00 | 324/80 | 205/75 |

***Fig. 8.*** *UCS of CL soil at different curing periods.*

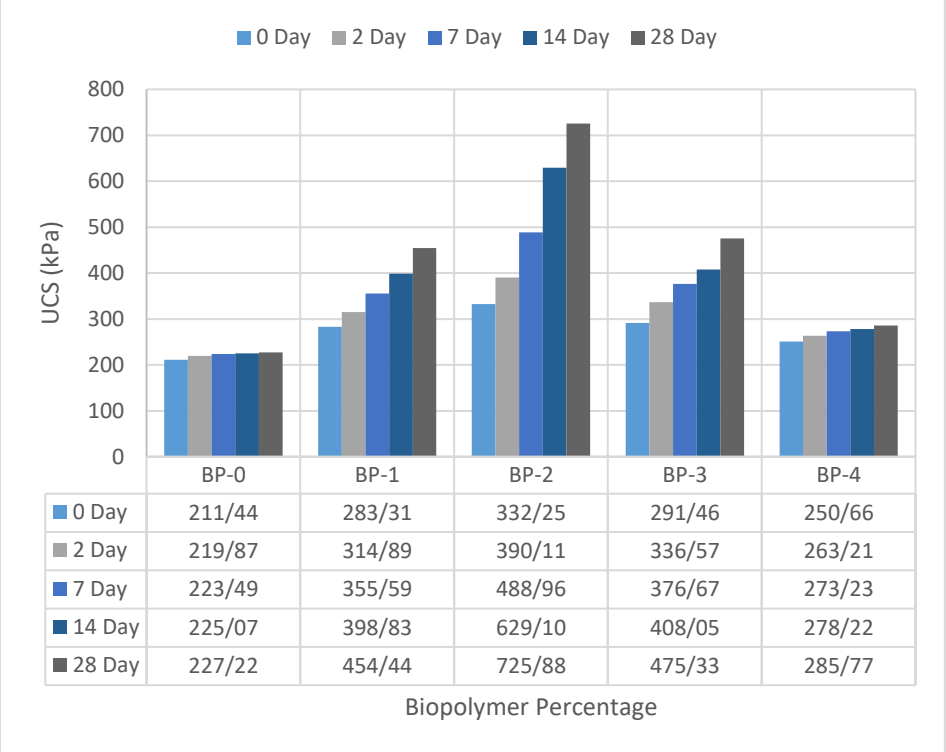


| | BP-0 | BP-1 | BP-2 | BP-3 | BP-4 |
|---|---|---|---|---|---|
| 0 Day | 211/44 | 283/31 | 332/25 | 291/46 | 250/66 |
| 2 Day | 219/87 | 314/89 | 390/11 | 336/57 | 263/21 |
| 7 Day | 223/49 | 355/59 | 488/96 | 376/67 | 273/23 |
| 14 Day | 225/07 | 398/83 | 629/10 | 408/05 | 278/22 |
| 28 Day | 227/22 | 454/44 | 725/88 | 475/33 | 285/77 |

***Fig. 9.*** *UCS of CH soil at different curing periods.*

In the presence of moisture, clays experience swelling and reduction in density, which results in the loss of strength. In order to replicate such conditions, soaking test on UCS samples was conducted. The results of soaked UCS samples at optimum biopolymer content for both CL and CH soils are shown in *Fig. 10* and *Fig. 11*, respectively. The results are shown for the optimum biopolymer content in the case of BP-2 since maximum strength was observed in this case, as shown in *Figs. 6 & 7*. The results indicate the loss of strength for both CL and CH samples due to soaking in all the cases of biopolymer content. In BP-2 case, the strength for CL sample dropped from 482 kPa to 385.64 kPa, while for CH sample the strength decreased from 725.88 kPa to 550.64 kPa. It indicates a decrease of 19.99% and 24.14% in soaked UCS of CL and CH, respectively.

Both CL and CH soils exhibited a loss in the strength due to the presence of moisture, although in comparison with the untreated soil samples, the biopolymer-soil mix has shown a significant strength under soaking conditions. At optimum biopolymer content, an improvement of 275.89% and 252.93% was observed in soaked UCS of CL and CH soils, respectively. The comparison of soaked UCS of untreated and treated soil samples is shown in *Fig. 12* and *Fig. 13*, respectively.

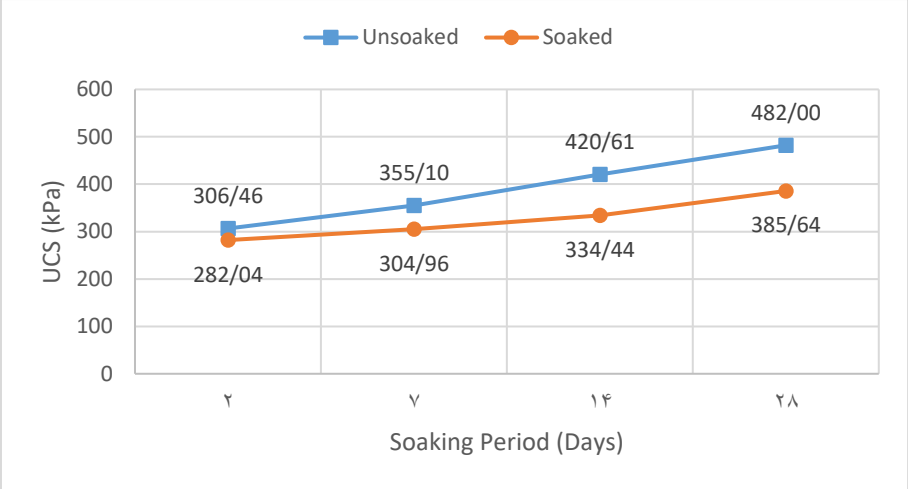


***Fig. 10.*** *Difference in UCS of CL soil according to soaking conditions.*

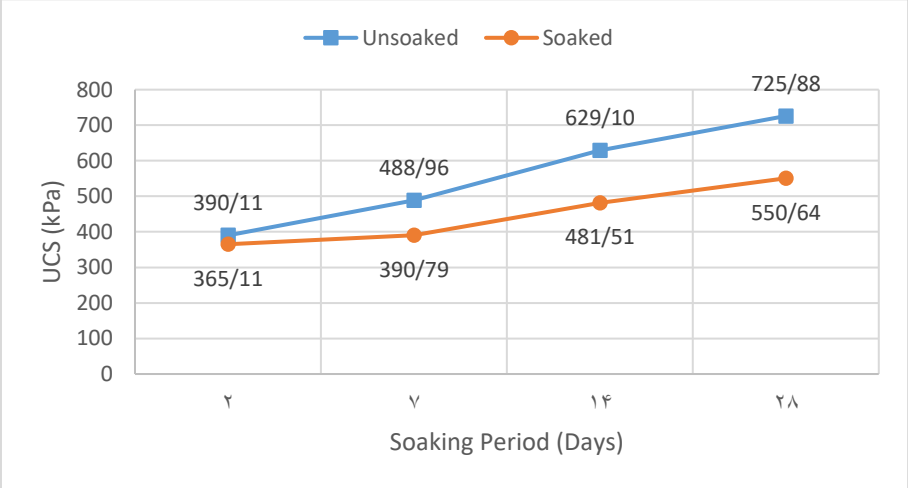


***Fig. 11.*** *Difference in UCS of CH soil according to soaking conditions.*

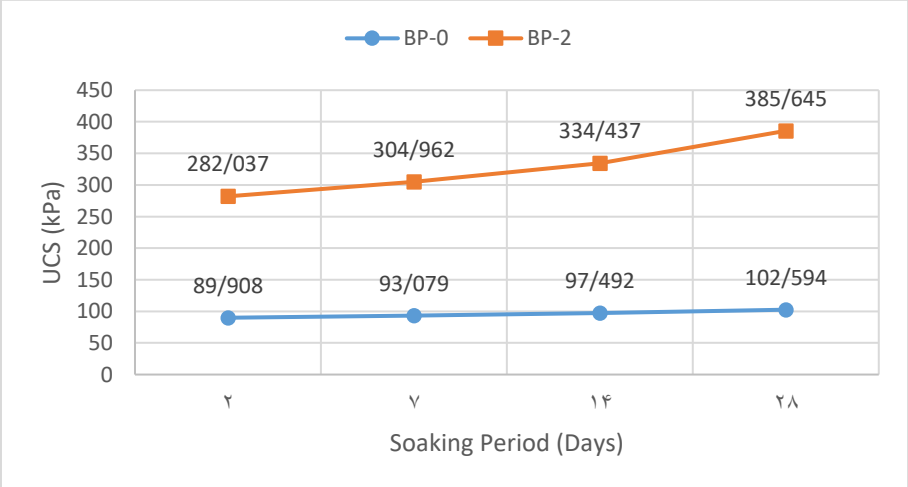


***Fig. 12.*** *Comparison of untreated and treated UCS of CL according to soaking conditions.*

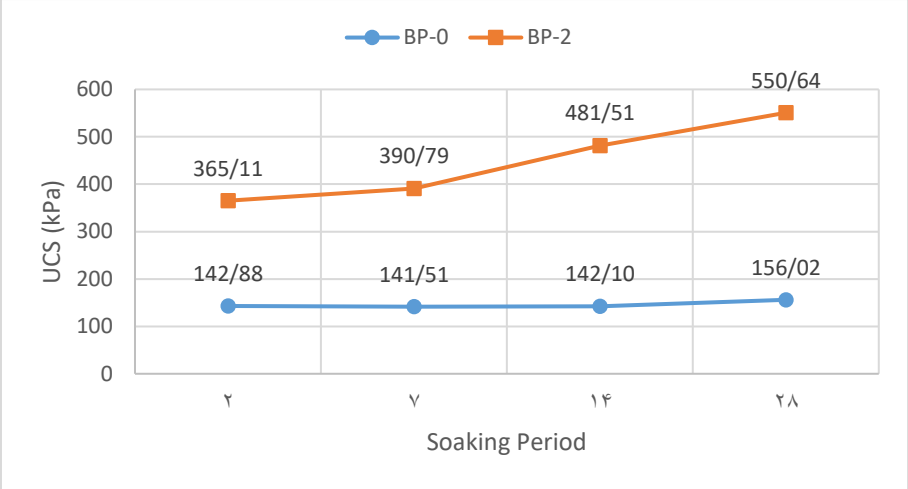


***Fig. 13.*** *Comparison of untreated and treated UCS of CH according to soaking conditions.*

### *4.3. California Bearing Ratio*

CBR value largely depends on the compaction characteristics of the soil. CBR samples were prepared at OMC obtained from modified proctor test for each biopolymer percentage. Both unsoaked and soaked CBR tests were carried out at all four percentages of biopolymer for both CL and CH soils. The results of CBR test for CL and CH soils are shown in *Fig. 14* and *Fig. 15*, respectively. It was observed from the results that the CBR value increased with increase in the biopolymer content up to 2%. Upon further increase in biopolymer content, a decrease in CBR of both CL and CH was observed under unsoaked and soaked conditions. The results indicate that the effect of Guar gum biopolymer was slightly more significant on the CBR value of CL soil as compared to that of CH soil since both the soaked and un-soaked CBR values in BP-2 case were slightly greater for CL soil.

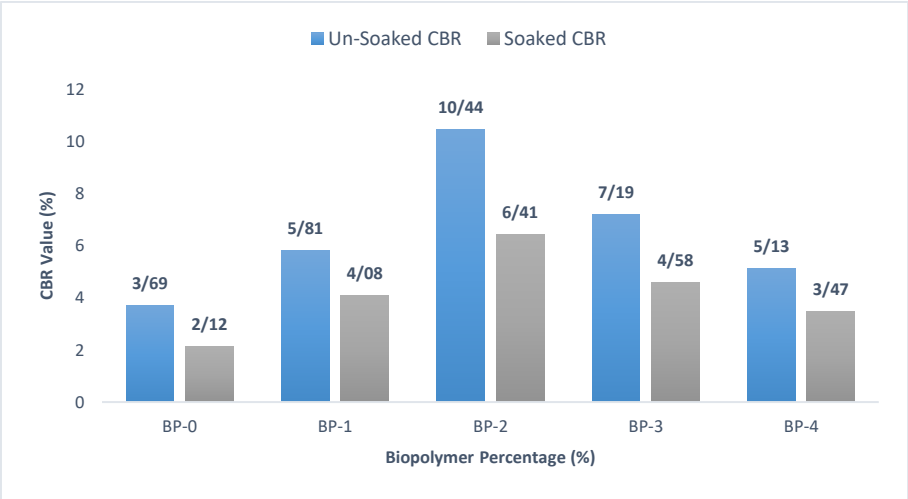


***Fig. 14.*** *Soaked and unsoaked CBR of CL at different biopolymer percentages.*

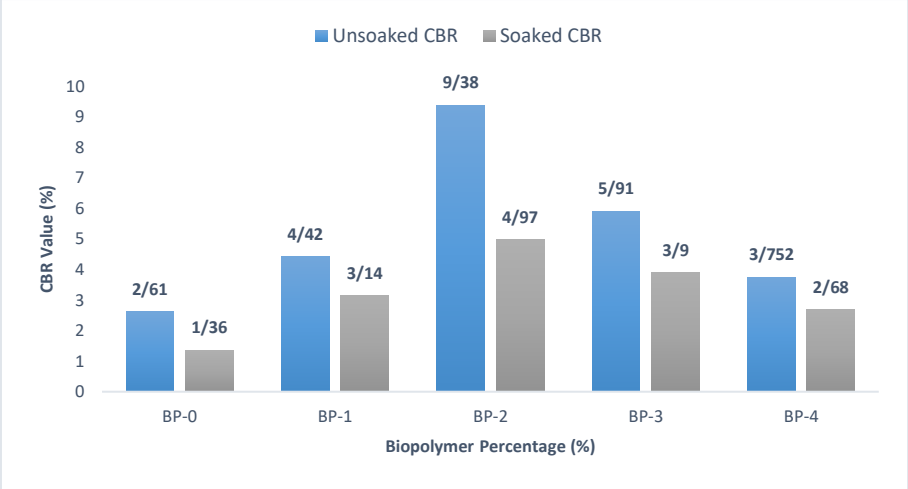


***Fig. 15.*** *Soaked and unsoaked CBR of CH at different biopolymer percentages.*

The combined results of CBR for CL and CH under soaked and unsoaked conditions are presented in *Fig. 16* for comparison of the effectiveness of Guar gum biopolymer on subgrade soil strength.

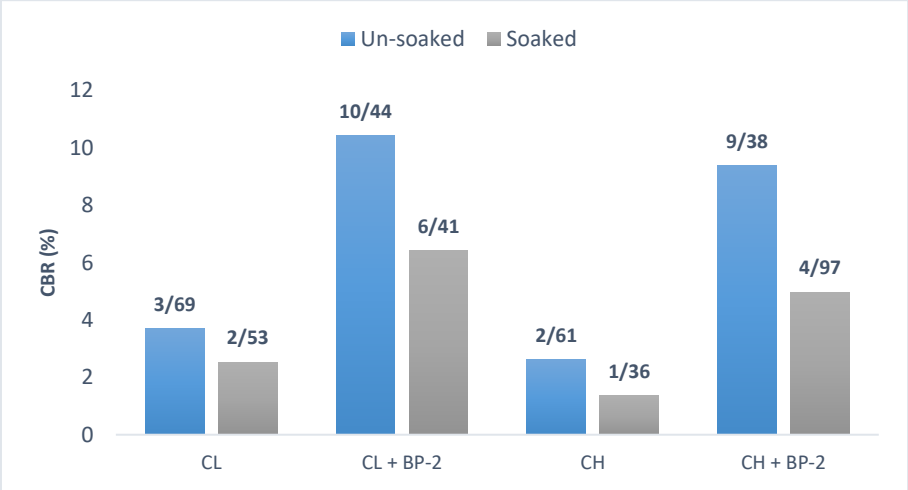


***Fig. 16.*** *Comparison of soaked unsoaked CBR of CL and CH at optimum BP content.*

### *4.4. Swell Potential*

Swell potential of both untreated and treated low plastic and high plastic soil samples was evaluated during the soaked CBR tests. The soaked CBR specimen was subjected to a 5 kg load and a dial gauge was attached to measure the change in the volume of soil specimen. The evaluation of treated soil specimen was carried out only at the optimum biopolymer content (BP-2 case) for both CL and CH. A significant reduction in the swelling potential of both CL and CH soils was observed according to the addition of optimum percentage of biopolymer. The results of swell potential for untreated and treated soil specimens are shown in *Fig. 17* for both CL and CH soils. As shown in *Figs. 16* & *17*, it was observed that CL soil exhibit better results after the addition of Gaur gum biopolymer.

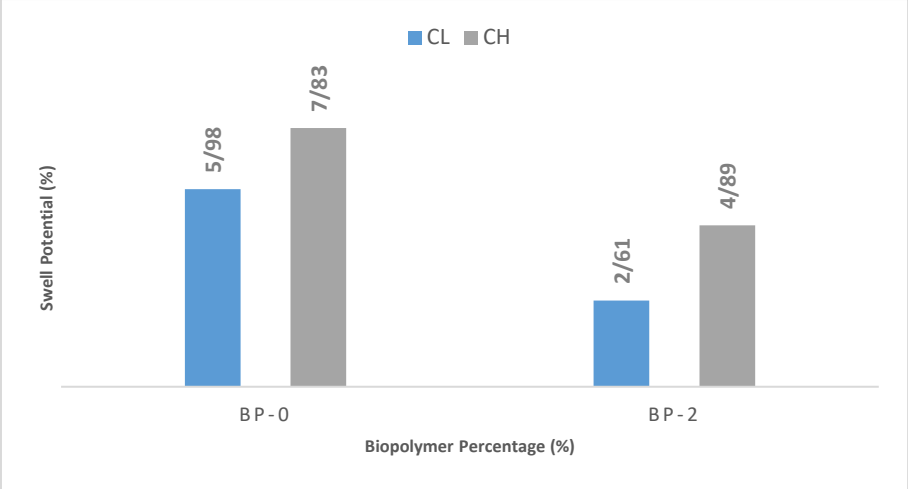


***Fig. 17.*** *Swell potential of CL and CH soils at optimum BP percentage.*

## 5. Conclusions

With recent developments in construction industry, the most vital aspects involved in selection of the material to be used as soil stabilizer became the environment friendliness and sustainability. This work was focused on the use of Guar gum biopolymer as an environmentally friendly material to improve the geotechnical properties of low plastic and high plastic clays. An elaborate study was conducted to investigate the effectiveness of Guar gum biopolymer as potential substitute to conventional soil stabilizers. The chosen soil parameters to evaluate the feasibility of Guar gum biopolymer included the compaction characteristics, unconfined compressive strength, CBR, and one-dimensional swell potential. Based on the experiments conducted in laboratory on both the low plastic (CL) and high plastic (CH) clays, following conclusions were drawn:

- The optimum amount of Guar gum biopolymer to be used with CL and CH soils was observed to be 2%, making it the optimum biopolymer content in this study.
- The MDD of CL and Ch increased from 17.80 kN/m$^3$ to 18.83 kN/m$^3$ and from 17.50 kN/m$^3$ to 18.17 kN/m$^3$, respectively.
- For CL soil, the UCS value increased from 170.53 kPa to 281.45 kPa at optimum biopolymer content, which further increased to 482 kPa after 28 days of curing indicating an increase of 182.64%.
- For CH, the UCS value climbed from 211.44 kPa to 332.25 kPa at optimum biopolymer content, which further increased to 725.88 kPa after 28 days of curing indicating an increase of 243.30%.
- The strengthening effect of Guar gum biopolymer depends not only on the biopolymer content but also on the curing time.
- Both CL and CH soil samples showed a decrease in strength due to the presence of moisture under soaked conditions.
- After soaking, the UCS of CL samples treated with BP decreased from 482 kPa to 385.64 kPa indicating a decrease of 19.99%.
- Similarly, UCS of CH samples treated with BP decreased from 725.88 kPa to 550.64 kPa indicating a decrease of 24.14%.
- As compared to untreated samples, the soaked UCS of treated CL and CH samples was improved by 275.89% and 252.93%, respectively.
- At optimum biopolymer content, the unsoaked and soaked CBR values of CL soil increased up to 182.93% and 202.36%, respectively.

- Similarly, the unsoaked and soaked CBR values of CH soil increased up to 259.39% and 265.44%, respectively by using optimum biopolymer content.
- The resistance to swell potential of CL and CH soil specimens was improved by 56.35% and 33.74%, respectively.

The results presented in this study indicate that the addition of Guar gum biopolymer at low percentages (1-3% by soil-weight) can significantly improve the geotechnical properties of such soils. This study will help increasing the confidence in using Guar gum biopolymer so that it can be effectively adopted as a potential soil stabilizer. Biopolymers are considered to be renewable materials, therefore utilizing biopolymers in stabilization techniques and construction can help in developing sustainable industry.

## Acknowledgment

The authors appreciate the valuable support and guidance of NICE (NUST) Islamabad for completion of the work and are also grateful to United gums Industries and Ittefaq Clay Tiles Industries for providing Guar gum Powder and Bentonite Clay required for laboratory experiments.

## References

[1] Lim, S. M., Wijeyesekera, D. C., Lim, A. J. M. S., & Bakar, I. B. H. (2014). Critical review of innovative soil road stabilization techniques. *International journal of engineering and advanced technology, bhopal*, *3*(5), 204-211.

[2] Kazemian, S., & Huat, B. B. (2010, December). Assessment of stabilization methods for soft soils by admixtures. *2010 international conference on science and social research (CSSR 2010)* (pp. 118-121). IEEE.

[3] Delatte, N. J. (2001). Lessons from Roman cement and concrete. *Journal of professional issues in engineering education and practice*, *127*(3), 109-115.

[4] Tingle, J. S., Newman, J. K., Larson, S. L., Weiss, C. A., & Rushing, J. F. (2007). Stabilization mechanisms of nontraditional additives. *Transportation research record*, *1989*(1), 59-67.

[5] Basu, D., Misra, A., & Puppala, A. J. (2015). Sustainability and geotechnical engineering: perspectives and review. *Canadian geotechnical journal*, *52*(1), 96-113.

[6] Chen, R., Lee, I., & Zhang, L. (2015). Biopolymer stabilization of mine tailings for dust control. *Journal of geotechnical and geoenvironmental engineering*, *141*(2), 04014100.

[7] Anjaneyappa, V., & Amarnath, M. S. (2011). Studies on soils treated with non-traditional stabilizer for pavements. *Indian Geotech J*, *41*(3), 162-167.

[8] Biju, M. S., & Arnepalli, D. N. (2019). Biopolymer-modified soil: prospects of a promising green technology. In *Geotechnical Characterisation and Geoenvironmental Engineering* (pp. 163-169). Springer, Singapore.

[9] Chang, I., Jeon, M., & Cho, G. C. (2015). Application of microbial biopolymers as an alternative construction binder for earth buildings in underdeveloped countries. *International journal of polymer science*. Doi: 10.1155/2015/326745

[10] Cole, D. M., Ringelberg, D. B., & Reynolds, C. M. (2012). Small-scale mechanical properties of biopolymers. *Journal of Geotechnical and Geoenvironmental engineering*, *138*(9), 1063-1074. Doi: doi:10.1061/(ASCE)GT.1943-5606.0000680

[11] Cho, G. C., & Chang, I. (2018, August). Cementless soil stabilizer–biopolymer. *Proceedings of the 2018 world congress on advances in civil, environmental, & materials research (ACEM18)* (pp. 27-31). Songdo Convensia, Incheon, Korea.

[12] Chang, I., Im, J., & Cho, G. C. (2016). Introduction of microbial biopolymers in soil treatment for future environmentally-friendly and sustainable geotechnical engineering. *Sustainability*, *8*(3), 251. Doi:10.3390/su8030251

[13] Vijayan, A., & Vijayan, V. (2018). Study on the strength characteristics of biopolymer on kaolinite clay. *International journal of research and scientific innovation*, *V*( XII), 68-71.

[14] Naveena, S. & Reddy, G. S. (2015). Strength characteristics of expansive soils using eco-friendly xanthan gum. *International journal of science and research*, *6*(6), 2443-2445.

[15] Cabalar, A. F., Awraheem, M. H., & Khalaf, M. M. (2018). Geotechnical properties of a low-plasticity clay with biopolymer. *Journal of materials in civil engineering*, *30*(8), 04018170.

[16] Ayeldeen, M., Negm, A., El-Sawwaf, M., & Kitazume, M. (2017). Enhancing mechanical behaviors of collapsible soil using two biopolymers. *Journal of rock mechanics and geotechnical engineering*, *9*(2), 329-339.

[17] Kullayappa, G. & Kumar, S. P. (2018). Experimental study by of soil mixed with guar gum a bio enzyme-(case study). *International research journal of engineering and technology*, 5(8),

[18] Muguda, S., Booth, S. J., Hughes, P. N., Augarde, C. E., Perlot, C., Bruno, A. W., & Gallipoli, D. (2017). Mechanical properties of biopolymer-stabilised soil-based construction materials. *Géotechnique letters*, *7*(4), 309-314.

[19] Mehmood, E., Ilyas, M., & Farooq, K. (2011). Effect of initial placement conditions on swelling characteristics of expansive soils. *Geo-Frontiers 2011: advances in geotechnical engineering* (pp. 2397-2403).

[20] Liaqat, N., Awan, N. B., Baig, M. F., Sami, M. F., Aalam, M., & Abbas, S. F. Influence of RHA on Engineering Properties of Medium Plastic Clay. *International journal of engineering research and technology (IJERT)*, *8*(10). DOI : http://dx.doi.org/10.17577/IJERTV8IS100101

[21] Khan, S. H. (2019). Use of gypsum and bagasse ash for stabilization of low plastic and high plastic clay. *Journal of applied research on industrial engineering*, *6*(3), 251-267.

[22] ur Rehman, Z., Khalid, U., Farooq, K., & Mujtaba, H. (2018). On yield stress of compacted clays. *International journal of geo-engineering*. https://doi.org/10.1186/s40703-018-0090-2

[23] Mudgil, D., Barak, S., & Khatkar, B. S. (2014). Guar gum: processing, properties and food applications—a review. *Journal of food science and technology*, *51*(3), 409-418.

[24] Patel, K. C. & Shah, A. J. (2016). Effect of guar and xanthan gum biopolymer on soil strengthening. *International journal for scientific research & development*, *4*(3), 280-283.

[25] Chudzikowski, R. J. (1971). Guar gum and its applications. *J Soc Cosmet Chem*, *22*(1), 43. 10.1016/j.ijbiomac.2016.04.001

[26] Chen, R., Zhang, L., & Budhu, M. (2013). Biopolymer stabilization of mine tailings. *Journal of geotechnical and geoenvironmental engineering*, *139*(10), 1802-1807.

Journal of Applied Research on Industrial Engineering
www.journal-aprie.com

# Optimization of Parameter Settings to Achieve Improved Tensile and Impact Strength of Bamboo Fibre Composites

***Okwuchi Smith Onyekwere[1,]*, Mobolaji Humphrey Oladeinde[2], Kindness Alfred Uyanga[3]***
[1]*Department of Mechanical Engineering, Faculty of Engineering, Federal University Wukari, Taraba State, Nigeria.*
[2]*Department of Production Engineering, Faculty of Engineering, University of Benin, Nigeria.*
[3]*School of Energy and Environment, City University of Hong Kong, Kowloon, Hong Kong.*

**PAPER INFO**

**Chronicle:**
*Received: 11 August 2020*
*Reviewed: 04 September 2020*
*Revised: 06 November 2020*
*Accepted: 03 December 2020*

**Keywords:**
*Taguchi Orthogonal Array.*
*Composite.*
*Optimization.*
*Fiber Modification.*
*Mercerized-Acetylated.*

**ABSTRACT**

There is great interest in application of natural fibres, such as bamboo fibre, as reinforcement in composite production. Herein, to achieve high performance under optimum process conditions, experimental design and optimization techniques are used to investigate the best parameter settings for processing bamboo fibre polyester composites. Single response optimization of the properties of bamboo fibre polyester composites using Taguchi orthogonal array, analysis of variance and Post hoc test was carried out. The test samples comprised of untreated, mercerized, acetylated and mercerized-acetylated bamboo fibre composites at fibre contents of 10, 20, 30, 40, and 50 wt %. All composite samples were fabricated using conventional hand lay-up process on randomly oriented long bamboo fibres. It was found that optimum parameter setting for impact strength was achieved at mercerization treatment and 30wt% fibre content with impact strength of 158.23 J/cm. For flexural strength, optimum parameter setting was found to be mercerization treatment at 50 wt % level of fibre content which resulted to flexural strength of 62.7 MPa. The optimum parameter setting for tensile strength is observed at mercerized-acetylation treatment at 50 wt% fibre content with tensile strength of 72.96 MPa. However, no significant difference, (P <.005) was observed in flexural strength, tensile strength and impact strength of mercerized and mercerized-acetylated fibre composites. This study established a research approach to improve bamboo fibre composite properties for more extended applications and to obtain optimal operating conditions by using optimization techniques. It will also serve as a guide for composite manufacturers on parameter settings selection.

## 1. Introduction

Natural fibres such as bamboo fibre are of interest in composite production due to their renewable and ecological characteristics amongst other properties [1-5]. One natural fibre with a lot of potentials in composite production is Bamboo fibre. It is considered a promising renewable resource in composite production because of its high growth rate, ease of processing, multiple application potentials and high specific strength [6-9]. Though suitable as an engineering material, further research is necessary to

Onyekwere, O. S., Oladeinde, M. H., & Uyanga, K. A. (2020). Optimization of parameter settings to achieve improved tensile and impact strength of bamboo fibre composites. *Journal of applied research on industrial engineering, 7*(4), 344-364.

* Corresponding author
E-mail address: smithonyekwere@gmail.com
10.22105/jarie.2020.257974.1207

improve bamboo properties for more extensive engineering applications [10, 11]. Besides, natural fibres differ in their chemical constituents and performance characteristics. Therefore, for each natural fibre and production process, there is need to obtain optimal parameter setting for improved composite properties. A possible research approach to improve bamboo fibre composite properties for more extended applications and to obtain optimal operating conditions is by using optimization techniques.

Thus, in this study Taguchi orthogonal array and analysis of variance were applied to determine the optimal parameter setting for improving tensile, flexural and impact strength of bamboo fibre/polyester composites. Applying design of experiment in production process can reduce production cost, time and result to products and processes with better function and high reliability [12-14]. It is anticipated that this study will provide a guide on factor setting for composite manufacturers.

## 2. Materials and Methods

### *2.1. Materials*

Bamboo fibres were obtained from sound bamboo culms in a forest in Aba. Unsaturated polyester resin (average molecular weight of 2200, boiling point of 154°C, specific density of 1.194 g/cm$^3$ and viscosity 0.24 Pa.s at 25$^0$C) was purchased from Zhejiang Tianhe Resin Company Limited, China and used as matrix. Methyl Ethyl Ketone Peroxide (MEKP) and cobalt naphthenate were purchased from CAMIC chemicals, Aba and used as accelerator and catalyst, respectively.

### *2.2. Bamboo Fibre Extraction*

Bamboo culms were split into strips of about 10 cm long and soaked in a solution containing 8% v/v sodium hypochlorite, 5% w/v sodium hydroxide and 0.5% w/v sodium chloride for 12 h at room temperature. Subsequently, to loosen the fibres, the bamboo strips were subjected to a pressure of 2 MPa in a hydraulic press. The fibres were extracted by manually scraping the pressed strips. Water was used to rinse the extracted fibres after which the fibres were dried in an oven at 60°C until a steady weight was obtained.

### *2.3. Experimental Design*

Two operating parameters–treatment at four levels and treatment at five levels, were selected to assess the compressive and impact strength of the composites. The factors and their levels are given in *Table 1*.

***Table 1.*** *Factors and level selection for composite formulation.*

| Factors | Level 1 | Level 2 | Level 3 | Level 4 | Level 5 |
|---|---|---|---|---|---|
| *Fibre content (PHR)* | *10* | *20* | *30* | *40* | *50* |
| *Surface modification* | *Crude* | *Mercerized* | *Acetylated* | *Mercerized-Acetylated* | - |

PHR = per hundred resins

Using Taguchi method, an L20-Othorgonal Array was selected for the study. *Table 2* contains the L20-OA design matrix generated by "Minitab" software.

***Table 2.*** *L20-OA design matrix for composite formulation.*

| Experiment Number | Treatment | Fibre Content |
|---|---|---|
| *1* | *1* | *1* |
| *2* | *1* | *2* |
| *3* | *1* | *3* |
| *4* | *1* | *4* |
| *5* | *1* | *5* |
| *6* | *2* | *1* |
| *7* | *2* | *2* |
| *8* | *2* | *3* |
| *9* | *2* | *4* |
| *10* | *2* | *5* |
| *11* | *3* | *1* |
| *12* | *3* | *2* |
| *13* | *3* | *3* |
| *14* | *3* | *4* |
| *15* | *3* | *5* |
| *16* | *4* | *1* |
| *17* | *4* | *2* |
| *18* | *4* | *3* |
| *19* | *4* | *4* |
| *20* | *4* | *5* |

The sequence for Taguchi optimization in this study is as follows:

- Select factors.
- Select Taguchi orthogonal array.
- Conduct experiments.
- Measure the responses.
- Analyze results (Signal-to-noise ratio): The desirable parameter settings are determined through analysis of the "Signal-to-Noise" (SN) ratio where factor levels that maximize the appropriate SN ratio are optimal. There are three standard types of SN ratios depending on the desired performance response [15-17]. The following equations were used for the SN analysis.

$$\text{Smaller the better} = -10\log\frac{1}{n}\sum y_i{}^2. \quad (1)$$

$$\text{Nominal the best} = 10\log\frac{\bar{Y}^2}{S^2}. \quad (2)$$

$$\text{Larger the better} = -10\log\frac{1}{n}\sum\left(\frac{1}{y_i{}^2}\right). \quad (3)$$

These SN ratios are derived from the quadratic loss function and the unit is decibel (dB).

### *2.4. Composite Formulation*

In composite production, polyester resins were used as matrix while bamboo fibres served as reinforcement. The bamboo fibre polyester composites were fabricated by conventional hand lay-up process followed by light compression moulding technique with five different fibre loading (10 wt, 20 wt, 30 wt, 40 wt and 50 wt Per Hundred Resins (PHR), which was coded as P1, P2, P3, P4, and P5 respectively). First, unsaturated polyester resin was mixed with 1wt% cobalt naphtenate accelerator and 1 wt% MEKP catalyst. Second, the fibres were placed in a mould and the resin mixture was poured evenly on the fibres and allowed to wet completely. Then, a load of 50 kg was applied over the mould for 12 h during the curing process of the composites. Third, the cast of composites were removed from the mould and post-curing was done at $80^0$C for 4 hours. Silicon spray was used as a releasing agent for easy removal of cured composite panels from the mould. Lastly, the samples of proper dimensions, according to ASTM standards, were cut out as test specimens from the sheet.

### *2.5. Chemical Modification of Fibres*

The fibres were subjected to mercerization, acetylation and mercerized-acetylation treatments and classified as mercized, acetylated and mercirized-acetylated, respectively. The untreated fibre samples were classified as crude.

#### *2.5.1. Mercerization treatment of fibre*

Alkali solution (8 wt% NaOH concentration) was prepared by diluting sodium hydroxide (NaOH) pellets in water. Bamboo fibres were immersed in the NaOH solutions for 60 min at $32^0$C [18]. Thereafter, the fibres were washed under running tap water until all traces of excess alkali were completely removed. Then, the fibres were oven dried to a constant weight at 60ºC until a constant weight was achieved. The dried fibres were storedin plastic bags to avoid exposure to moisture.

#### *2.5.2. Acetylation treatment of fibre*

Non-catalyzed room temperature acetylation method was employed [19]. 10 g of fibres, from each run in the experimental design, was soaked in a beaker containing 200 ml of 15% acetic acid for 50 min. The fibres were then transferred to a beaker containing 200 ml of 5% acetic anhydride for 30 min. The fibres were removed from acetic anhydride and washed with running water until acid-free and dried to a constant weight in an oven set at $80^0$C.

#### *2.5.3 Mercerized-acetylation treatment of fibre*

Bamboo fibres prepared using the mercerization method described in *Section 2.5.1* were subjected to acetylation treatment to produce mercerized-acetylated fibres.

### *2.6. Characterization of Bamboo Fibre Polyester Composites*

#### *2.6.1. Tensile test*

Tensile strength testing of all specimens was conducted according to ASTME 8 on 15 mm × 200 mm × 3 mm composite samples. The gauge length between the two clamps was set at 100 mm. Three identical tests specimen for each section thickness per sample were tested at room temperature with a strain/loading rate of 5 mm/min using a computerized Instron Testing Machine (Model 3369). The test piece which is of gauge length 100 mm was fixed at the edges of the upper and lower grip of the Instron testing machine tensile force applied until failure.Load displacement plots were obtained on an X–Y recorder and the testing machine displayed the ultimate tensile strength and yield strength.

#### *2.6.2. Flexural test*

Flexural test were performed using 3-point bending method according to ASTM D790-03. During flexural test, rectangular specimens having dimensions of 100 mm x 20 mm x 3 mm was lied on support spans in Instron Testing Machine (Model 3369) and a load of 5 KN was applied to the centre of the specimen by the loading nose of the Instron machine producing a three point bending at a crosshead speed of 5 mm/min, at a room temperature. The test was stopped when a specimen broke. In each case, three samples were tested and the average value was reported.

#### *2.6.3. Compressive test*

The compressive test was carried out in accordance with ASTM D 695-96. The specimens were cut to 25mm x 25mm x plate thickness and then ground with carbide sand paperto obtain a smooth surface. The test was carried out in an Instron testing machine (Model 3369) equipped with a 50 kN load cell and a compression test fixture. Samples were placed on the machine and pressure was applied continuously at the rate of 2 mm/min until the samples failed. Three replicates were tested.

#### *2.6.4. Impact strength test*

Impact testing was done according to ASTM/A29M-15. The tests were carried out using Izod Impact Testing method on Hounsfield Impact Testing Machine (Tensometer Ltd., Croydon, England) on 75 mm x 15 mm x 3 mm samples. The specimen was notched at an angle of 45º from 28 mm end length of 75 mm. The specimen was subjected to impact blow and the amount of impact energy absorbed by the specimen was read off on a calibrated scale attached to the machine as a measure of impact strength in Joules.

## 3. Results and Discussion

### *3.1. Tensile Strength*

The average tensile strength values measured from the experiment and their corresponding S/N ratios are listed in *Table 3*. The S/N ratios were calculated using *Eq. 3*. An $L_{20}$ orthogonal array was used to collect the experimental data. Column 2 and Column 3 were used to represent the two control factors. The first factor, which is the treatments, contains 4 levels which were denoted by 1-4 while the second factor, which is the fibre content, contains 5 levels which were denoted by 1–5. *Table 4* contain the S/N ratio values of tensile strength by factor level. The level with the highest signal-to-noise ratio value is

optimum level for the control factor. The results show that level 4 of treatment, which is mercerized-acetylation and level 5 of fibre content, which is P5 is the optimum factor combination for tensile strength of the composite. This corresponds to the main effect plot (See *Fig. 1*).

***Table 3.*** *Factor level, mean tensile strength and their corresponding signal-to-noise level of bamboo fibre polyester composites.*

| Exp. No. | Treatment | Fibre Content | Tensile Strength (Mpa) | S/N Ratio (dB) |
|---|---|---|---|---|
| *1* | *1* | *1* | *55.995* | *29.975* |
| *2* | *1* | *2* | *59.914* | *33.557* |
| *3* | *1* | *3* | *59.588* | *32.276* |
| *4* | *1* | *4* | *63.700* | *33.587* |
| *5* | *1* | *5* | *65.390* | *34.489* |
| *6* | *2* | *1* | *53.521* | *32.540* |
| *7* | *2* | *2* | *61.369* | *33.964* |
| *8* | *2* | *3* | *62.377* | *34.217* |
| *9* | *2* | *4* | *62.968* | *34.206* |
| *10* | *2* | *5* | *64.394* | *34.432* |
| *11* | *3* | *1* | *49.277* | *28.832* |
| *12* | *3* | *2* | *57.922* | *32.414* |
| *13* | *3* | *3* | *55.164* | *31.473* |
| *14* | *3* | *4* | *56.828* | *30.382* |
| *15* | *3* | *5* | *58.270* | *31.368* |
| *16* | *4* | *1* | *60.409* | *33.845* |
| *17* | *4* | *2* | *69.913* | *35.452* |
| *18* | *4* | *3* | *60.077* | *33.568* |
| *19* | *4* | *4* | *69.387* | *35.625* |
| *20* | *4* | *5* | *72.964* | *36.414* |

***Table 4.*** *Response for signal-to-noise ratios of tensile strength-larger is better.*

| Level | Treatment | Fibre Content |
|---|---|---|
| *1* | *32.78* | *31.30* |
| *2* | *33.87* | *33.85* |
| *3* | *30.89* | *32.88* |
| *4* | *34.98* | *33.45* |
| *5* | | *34.18* |
| *Delta* | *4.09* | *2.88* |
| *Rank* | *1* | *2* |

### *3.1.1. Main and interaction effect of treatment and fibre content on tensile strength*

*Fig.1* shows the main effects of treatment and fibre contents on tensile strength. The main effect of mercerized-acetylated bamboo fibres on tensile strength (*Fig. 1a*) has the highest values, followed by

that of mercerized fibre composites. Mercerized-acetylated fibre composite has the highest tensile strength with an average tensile strength of 66.5 MPa followed by mercerized fibre composites with average of 60.93 MPa for all levels of fibre content. Acetylated fibre composites show the lowest tensile strength among all treatments with an average of 55.49 MPa.

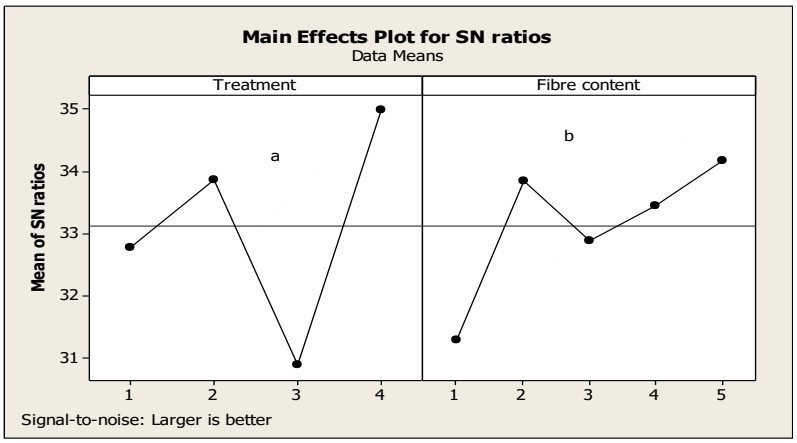


***Fig. 1.*** *Main effect plot for signal-to-noise ratio of treatment and fibre content on tensile strength.*

Similar observation was made by [20] on rice husk-oil palm fibre hybrid composite where mercerization showed the highest tensile strength (the authors did not analyse tensile strength of mercerized-acetylated fibre composites). Mercerization produces better effect as it increases surface roughness and decreases the surface polarity. During mercerization, NaOH cleans the fibres surface by removing impurities, waxes and part of the lignin as lignin acts as a cementing substance that holds the fibre together [21]. Partial removal of lignin causes some debonding of the fibrils which leads to exposure or protruding of some of them. Such protrusion will produce mechanical bonding of the fibres and consequently, improve fibre-matrix interaction resulting to improved properties of the composite [22-25]. Similar observations were also made by [26] on bamboo fibre epoxy composites, [27] on 5% (w/V) NaOH treated coir fibre polyester composite and [28] on sisal polyester composite. Acetylated fibre composites exhibited the lowest tensile strength. Acetylation probably causes agglomeration of the filler, weakening the interfacial regions and making them less resistance to crack propagation. However, mercerizing before acetylation improves the tensile properties of acetylated fibre composites as this method blends the advantages of mercerization and acetylation to yield excellent tensile properties.

As shown in *Fig. 1b*, the tensile strength increases with increase in fibre content in the composite. For mercerized and mercerized-acetylated fibre composites, there is a marginal reduction in tensile strength at fibre content P3. Rashed et al. [29] made similar observation on jute fibre reinforced polypropylene composite. The authors observed an increase in tensile strength with increase in fibre content up to 10% fibre content. The increase in tensile strength was attributed to the reinforcing effect of natural fibres. However, they attributed the reduction in strength to poor dispersion of fibres in polymer due to strong inter fibre hydrogen bonding which holds the fibres together. Girisha et al. [30] also reported similar results.

A slight decrease in tensile strength is observed at P3 with subsequent increase up to the maximum fibre content of P5 for crude, acetylation and mercerization-acetylation (*Fig. 1b*). Similar observation, where tensile strength decreases after an initial increase, with further increase at very high fibre content, has been made by previous researchers [31-33]. However, Figure 1b shows that mercerized fibre composite showed a steady increase in tensile strength up to the maximum fibre content of P5.Tensile strength of

72.96 MPa was obtained at the optimal parameter setting. The tensile strength is comparable to the result of previous studies Prasanna et al. [34] reported maximum tensile strength of 19.8 MPa on sisal fibre polyester composite; Hussain et al. [35] reported maximum tensile strength of 15.06 MPa on bamboo fibre polyester composite. Neslihan et al. [36] observed a tensile strength of 35 MPa on bamboo fibre epoxy composite. Shito et al. [37] observed tensile strength of 35.1 MPa on single bamboo fibres MAPP composite. Chukwudi et al. [38] observed a maximum tensile strength of 23.50 MPa on Rafia palm polyester composites. Maximum tensile strength of 2 MPa was observed by [39] on sisal polyester composites while maximum tensile strengths of 52 MPa on banana fabric polyester composite and 39 MPa on cotton fibre polyester composites was observed by [40] and [41]. The interaction plots of treatment and fibre content on tensile strength are illustrated in *Fig. 2*. No appreciable interaction was observed.

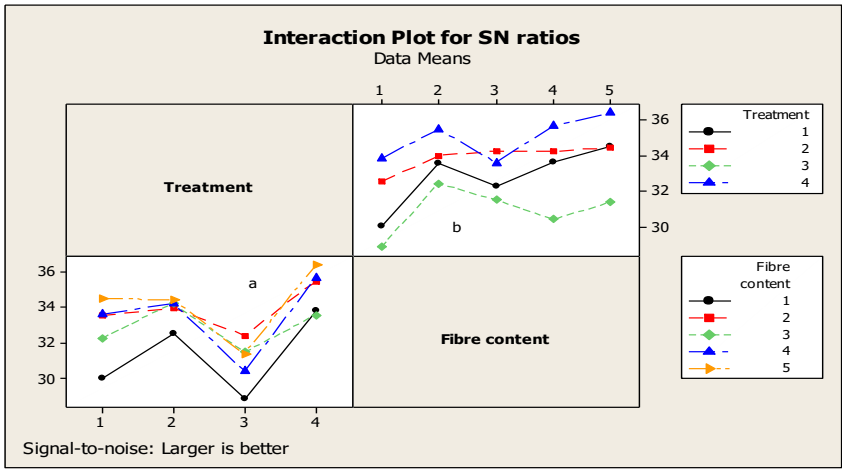


***Fig. 2.*** *Interaction plot for signal-to-noise ratio of treatment and fibre content on tensile strength.*

### *3.1.2. Analysis of variance and post hoc test for tensile strength*

The Analysis Of Variance (ANOVA), generated using Minitab 17 software, is shown in *Table 5*. ANOVA was conducted to determine if the differences in the main effect and interaction effects on tensile strength among the treatments and among the fibre contents are significant. *Table 5* shows a significant main effect of treatments on tensile strength, $F(3, 80) = 7.83$, $P < .001$ and also a significant main effect of fibre content on tensile strength, $F(4, 80) = 4.40$, $P = .003$. The interaction effect was not significant, $F(12, 80) = 0.28$, $P = .99$.

Test of equality of error variance was conducted to investigate if the error variance of the dependent variable is equal across the groups. The result of the test, shown in *Table 6*, indicates equal error variance. Thus, a post hoc test that assumes equal error variance was chosen for mean comparison, in this case, a Turkey HSD post hoc test. A post hoc test, shown in *Table 7* & *8* was carried out to determine the factor levels with significant mean difference in the group.

***Table 5.*** *Tests of between-subjects effects: dependent variable -tensile strength.*

| Source | Type III Sum of Squares | df | Mean Square | F | Sig. |
|---|---|---|---|---|---|
| *Corrected model* | *2824.954[a]* | *19* | *148.682* | *2.341* | *.007* |
| *Intercept* | *41889.979* | *1* | *41889.979* | *659.496* | *.000* |
| *Fibre content* | *1116.943* | *4* | *279.236* | *4.396* | *.003* |
| *Treatment* | *1491.341* | *3* | *497.114* | *7.826* | *.000* |
| *Fibre content * Treatment* | *216.669* | *12* | *18.056* | *.284* | *.990* |
| *Error* | *3811.088* | *60* | *63.518* | | |
| *Total* | *48526.020* | *80* | | | |
| *Corrected total* | *6636.041* | *79* | | | |

R Squared = .626 (Adjusted R Squared = .644)

***Table 6.*** *Levene's test of equality of error variances[a]: dependent variable-tensile strength.*

| F | df1 | df2 | Sig. |
|---|---|---|---|
| *1.119* | *19* | *60* | *.357* |

The fibre content P1 has significantly lower tensile strength than P2, P4, and P5 (*Table 7*). There is no significant difference in the tensile strengths among P2, P3, P4 and P5 fibre contents. This indicates that increasing the fibre content beyond P2 up to P5 has no significant impact on the tensile strength of bamboo fibre polyester composite. *Table 8* indicate that the tensile strength of mercerized-acetylated fibre composite is significantly higher than that of crude and acetylated composites. However, there is no significant mean difference in the tensile strength of mercerized-acetylated and mercerized composites.

***Table 7.*** *Turkey HSD multiple comparison of tensile strength among various fibre contents.*

| | P1 | P2 | P3 | P4 | P5 |
|---|---|---|---|---|---|
| **P1** | | *-8.2673** | *-5.2916* | *-8.7628** | *-10.7328** |
| **P2** | *8.2673** | | *2.9756* | *-.4956* | *-2.4655* |
| **P3** | *5.2916* | *-2.9756* | | *-3.4712* | *-5.4412* |
| **P4** | *8.7628** | *.4956* | *3.4712* | | *-1.9700* |
| **P5** | *10.7328** | *2.4655* | *5.4412* | *1.9700* | |

***Table 8.*** *Turkey HSD multiple comparison of tensile strength among various treatments.*

| | Crude | Mercerized | Acetylated | Mercerized-Acetylated |
|---|---|---|---|---|
| **Crude** | | *-1.7228* | *5.2258* | *-6.8640** |
| **Mercerized** | *1.7228* | | *6.9486** | *-5.1412* |
| **Acetylated** | *-5.2258* | *-6.9486** | | *-12.0898** |
| **Mercerized-Acetylated** | *6.8640** | *5.1412* | *12.0898** | |

Hence, the tensile strength results show that, (1) while the main effect of treatment and fibre content on tensile strength is significant, the interaction effects are not significant. The main effect of mercerized-acetylated bamboo fibres on tensile strength has the highest values for each fibre content level with the acetylated fibre composites showing the lowest tensile strength among all treatments and (2) the optimum parameter setting for tensile strength is observed at mercerized-acetylation treatment and P5 fibre content with tensile strength of 72.96 MPa. The posthoc test shows that the effect of mercerized-

acetylation on tensile strength of the fibre composites is significantly higher than that of untreated and acetylation. However, no significant difference is observed between the effect of mercerization and mercerized-acetylation on tensile strength of the fibre composites. The effect of P5 level of fibre contents on tensile strength is found to be significantly higher than P1. However, P5 level of fibre content is not significantly higher than P2, P3, and P4 levels of fibre contents.

### *3.2. Flexural Strength*

The average flexural strength values measured from the experiment and their corresponding S/N ratios are listed in *Table 9*. The S/N ratios were calculated using *Eq. 3*. *Table 10* gives the S/N ratio values of flexural strength by factor levels. The level with the highest signal-to-noise ratio value is optimum level for the control factor.

*Table 10* shows that level 2 and level 4 of treatment, which are mercerized and mercerized-acetylated, have almost the same highest S/N ratio value. Level 5 of fibre content, which is P5, have the highest S/N ratio in fibre content.

***Table 9.*** *Factor level, mean flexural strength and the corresponding signal-to-noise level of bamboo fibre polyester composites.*

| Exp. No. | Treatment | Fibre Content | Mean Flexural Strength (Mpa) | S/N Ratio (dB) |
|---|---|---|---|---|
| *1* | *1* | *1* | *3.997* | *9.402* |
| *2* | *1* | *2* | *15.668* | *23.213* |
| *3* | *1* | *3* | *21.804* | *26.124* |
| *4* | *1* | *4* | *42.949* | *32.222* |
| *5* | *1* | *5* | *54.565* | *34.588* |
| *6* | *2* | *1* | *10.156* | *19.715* |
| *7* | *2* | *2* | *18.448* | *24.851* |
| *8* | *2* | *3* | *24.461* | *27.716* |
| *9* | *2* | *4* | *32.277* | *29.969* |
| *10* | *2* | *5* | *62.696* | *35.705* |
| *11* | *3* | *1* | *9.697* | *18.616* |
| *12* | *3* | *2* | *29.969* | *28.973* |
| *13* | *3* | *3* | *20.185* | *25.878* |
| *14* | *3* | *4* | *11.893* | *21.139* |
| *15* | *3* | *5* | *37.945* | *31.339* |
| *16* | *4* | *1* | *17.237* | *24.335* |
| *17* | *4* | *2* | *28.311* | *28.167* |
| *18* | *4* | *3* | *33.037* | *30.146* |
| *19* | *4* | *4* | *18.988* | *25.103* |
| *20* | *4* | *5* | *37.235* | *30.928* |

***Table 10.*** *Response for signal to noise ratios: flexural strength.*

| Level | Treatment | Fibre Content |
|---|---|---|
| *1* | *25.11* | *18.02* |
| *2* | *27.59* | *26.30* |
| *3* | *25.19* | *27.47* |
| *4* | *27.54* | *27.11* |
| *5* | | *33.14* |
| *Delta* | *2.63* | *15.12* |
| *Rank* | *2* | *1* |

*3.2.1. Main and interaction effect of treatment and fibre content on flexural strength*

The main effect plot for S/N ratios of treatment and fibre contents on flexural strength is shown in *Fig. 3*. The main effect of mercerized and mercerized-acetylated bamboo fibres on flexural strength of the composite (*Fig. 3a*) have the highest values followed by that of crude fibre. Similar observation on alkaline treated fibre composite was made by [28]; the authors reported increase in flexural strength of alkaline treated sisal fibre/unsaturated polyester composite from 1 MPa in untreated fibre to 1.5 MPa in alkaline treated fibre. They attributed this to increase in fibre-matrix interaction due to removal of some portions of lignin, hemicelluloses and cellulose, resulting in increased surface area available for contact with the matrix. Shah et al. [39] also observed improvement in the flexural strength and modulus of alkaline treated (6% wt) woven banana fibre/unsaturated polyester composite over untreated fibre composite from 58 MPa to 64 MPa for flexural strength. They attributed the improvement to improved wetting of the treated fibre with the matrix. This results from removal of artificial and natural impurities and waxy substances from the fibre surface and imparting rougher surface to the fibre surface after mercerization which eventually results to better mechanical interlocking and improved interfacial adhesion. Other researchers also reported similar behaviour in; polyester resin reinforced with long and short hemp and kenaf fibre, wood flour–PP composite, coir-polyester composite; with about 22% increase in flexural strength from 38 – 49 MPa in untreated fibre to 49 to 56 MPa in alkaline treated fibre composites, kenaf epoxy composite [42-44].

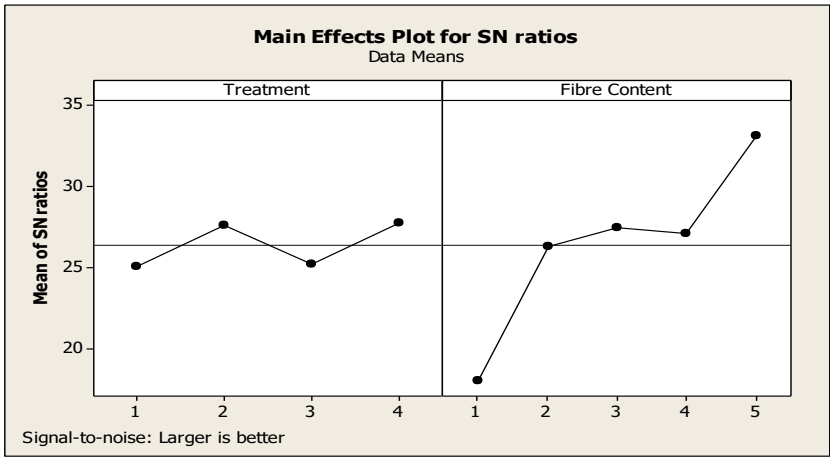


***Fig. 3.*** *Main effect plot for signal- to- noise ratio of treatment and fiber content on flexural strength*.

Acetylated fibre composites have the lowest flexural strength. Acetylation probably causes agglomeration of the filler, weakening the interfacial regions. Similar observation was made by kallakas et al. [41], the authors reported a decrease in flexural strength of uncatalyzed acetylated wood flour – PP composite over unmodified wood flour composite from 36.2 MPa to 33.4 MPa. They attributed this

to poor interfacial adhesion between the PP matrix and the acetylated wood flour. *Fig. 3b* shows that there is general increase in flexural strength with increase in fibre content. For all treatments, P1 has the lowest flexural strength while P5 has the highest. Krishnan et al. [44] reported similar finding of an increase in flexural strength with increase in fibre content of PP/Isora composite from 43.25 MPa in 5 wt% fibre content to 45.6 wt% in 15 wt% fibre composite. They attributed the increase to the nature of the natural fibre which acts as a rigid filler responsible for increasing the stiffness of the polymer matrix. Other researchers also found similar behaviour in; Grewia optival/PF composite, Habiscus Sabdarifa/UF Composite, Piassava fibre polystyrene composite, and cotton fibre reinforced isophthallic polyester composite [45-48].

The flexural strength at the optimum parameter setting is 62.7 MPa. The flexural strength is comparable to the results of previous studies where maximum flexural strength of 54.1 MPa and 56.78 MPa where obtained on Sisal fibre polyester composite and Sisal/bamboo hybrid polyester composites, respectively [34]. Maximum flexural strength of 38.98 MPa was reported for bamboo fibre polyester composites [35]. Maximum flexural strength of 70 MPa was reported on bamboo fibre epoxy composites [36]. Maximum flexural strength of 54.31 MPa was obtained by [27] on Coir polyester composite while [39] observed flexural strength of 64 MPa on woven Banana fabric polyester composites.

The interaction effect of treatment and fibre content on flexural strength is shown in *Fig. 4*. There is interaction among the various fibre treatments and levels of fibre content. At the low fibre content of P1, the crude fibre composite has the lowest flexural strength while mercerized-acetylated composite has the highest flexural strength but as the fibre content increases, the flexural strength of mercerized and crude fibre composite becomes higher.

It could be that acetylation reduces the protruding micro fibrils from the mercerized frayed fibres. However, increase in fibre content leads to increase in available micro fibrils and rough surface, in mercerized-acetylated fibre composites, to form an improved interlocking bond with the matrix.

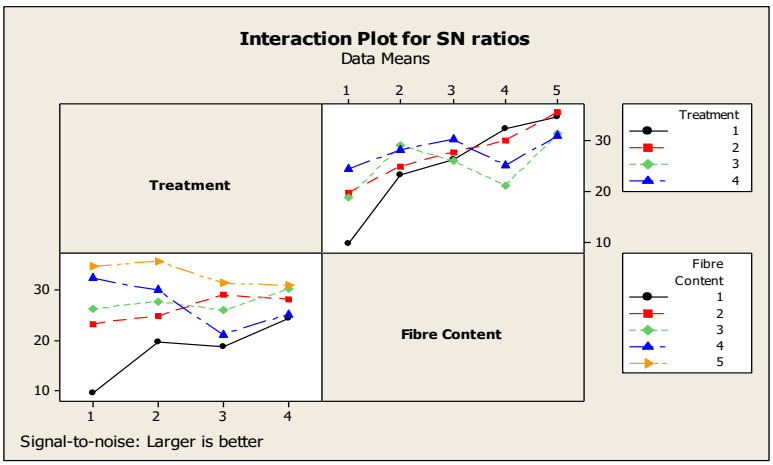


***Fig. 4.*** *Interaction plot for signal-to-noise ratio of treatment and fibre content on flexural strength.*

*3.2.2. Analysis of variance and post hoc test for flexural strength*

ANOVA generated using Minitab 17 software, is shown in *Table 11*. ANOVA was conducted to determine if the differences in the main effect and interaction effects on flexural strength among the treatments and among the fibre contents are significant. *Table 11* shows a significant main effect of treatments on flexural strength, $F\ (3, 80) = 6.54, P = .001$ and also a significant main effect of fibre content on flexural strength, $F\ (4, 80) = 90.38, P < .001$. The interaction effect was significant, $F\ (12, 80) = 12.40, P < .001$.

***Table 11.*** *Analysis of variance and Post Hoc test for flexural strength.*

| Source | Type III Sum of Squares | df | Mean Square | F | Sig. |
|---|---|---|---|---|---|
| *Corrected model* | *17462.478*[a] | *19* | *919.078* | *27.891* | *.000* |
| *Intercept* | *56502.027* | *1* | *56502.027* | *1.715E3* | *.000* |
| *Fibre content* | *11912.981* | *4* | *2978.245* | *90.381* | *.000* |
| *Treatment* | *646.851* | *3* | *215.617* | *6.543* | *.001* |
| *Fibre content * Treatment* | *4902.646* | *12* | *408.554* | *12.398* | *.000* |
| *Error* | *1977.134* | *60* | *32.952* | | |
| *Total* | *75941.639* | *80* | | | |
| *Corrected total* | *19439.612* | *79* | | | |

a. R Squared = .898 (Adjusted R Squared = .866)

***Table 12.*** *Levene's test of equality of error variances: dependent variable - flexural strength.*

| F | df1 | df2 | Sig |
|---|---|---|---|
| *1.703* | *19* | *60* | *0.061* |

Test the null hypothesis that the error variance of the dependent variable is equal across groups
a.Design: intercept + Fibre content + Treatment + Fibre content*Treatment

Test of equality of error variance was conducted to investigate if the error variance of the dependent variable is equal across the groups. *Table 12* indicates equal error variance. Thus, Turkey HSD that assumes equal error variance was chosen for mean comparison to determine the factor levels with significant mean difference in the group and presented in *Table 13* & *Table 14*.

There is a significant mean difference between the flexural strength of acetylated composites and other treatments (*Table 13*). There is no significant difference among other treatments. The mean difference shows that acetylated composites has significantly lowest flexural strength among all the treatments while there is no significant difference among the flexural strength of crude, mercerization and mercerized-acetylated fibre composite. This shows that statistically, chemical modification does not significantly enhance the flexural strength of bamboo fibre composite. *Table 14* indicate significant mean differences in flexural strength among the levels of fibre content. There is no significant difference among the flexural strength of fibre contents P2, P3 and P4 while they are significantly different from P1 and P5. Thus, in order to achieve a significant increase in flexural strength, high fibre content is required.

***Table 13.*** *Turkey HSD Post Hoc multiple comparison of flexural strength among various treatments*.

| | **Crude** | **Mercerized** | **Acetylated** | **Mercerized-Acetylated** |
|---|---|---|---|---|
| **Crude** | | *-1.811* | *5.858** | *.8351* |
| **Mercerized** | *1.811* | | *7.669** | *2.646* |
| **Acetylated** | *-5.858** | *-7.669** | | *-5.023** |
| **Mercerized-Acetylated** | *-.835* | *-2.646* | *5.023** | |

***Table 14.*** *Turkey HSD Post Hoc multiple comparison of flexural strength among various levels of fibre content.*

| | **P1** | **P2** | **P3** | **P4** | **P5** |
|---|---|---|---|---|---|
| **P1** | | *-12.827** | *-14.600** | *-16.255** | *-37.838** |
| **P2** | *12.827** | | *-1.772* | *-3.427* | *-25.011** |
| **P3** | *14.600** | *1.772* | | *-1.654* | *-23.238** |
| **P4** | *16.255** | *3.427* | *1.654* | | *-21.583** |
| **P5** | *37.838** | *25.011** | *23.238** | *21.583** | |

Hence, a significant main and interaction effect of treatment and fibre content on flexural strength was observed. Mercerization and mercerized-acetylation produced better main effect on the composites than other treatments while the least effect was observed in acetylation. A general increase in flexural strength with increase in fibre content, for all treatments, was observed. The optimum parameter setting for flexural strength was found to be mercerization treatment and P5 level of fibre content which resulted to flexural strength of 62.7 MPa. The post hoc test indicated that the flexural strength of mercerized and mercerized-acetylated fibre composites is statistically significantly higher than that of other composites. However, no significant different was observed in flexural strength of mercerized and mercerized-acetylated fibre composites. The effect of P5 level of fibre content on flexural strength was significantly higher than that of all other levels of fibre content.

### *3.3. Impact Strength*

The average impact strength values measured from the experiment and their corresponding S/N ratios are listed in *Table 15*. The S/N ratios were calculated using *Eq. (3)*. *Table 16* contain the S/N ratio values of impact strength by factor level.

#### *3.3.1. Main and interaction effect of treatment and fibre content on impact strength*

The main effect of treatment and fibre contents on impact strength is shown in *Fig. 5*. In *Fig. 5a*, mercerization has the highest positive effect on the impact strength of the fibre composites. Unmodified fibre composites show the lowest impact strength.

***Table 15.*** *Factor level, mean impact strength and the corresponding signal-to-noise level of bamboo fibre polyester composites.*

| Exp. No. | Treatment | Fibre Content | Mean Impact Strength (J/cm) | S/N Ratio (dB) |
|---|---|---|---|---|
| *1* | *1* | *1* | *105.642* | *40.4535* |
| *2* | *1* | *2* | *155.599* | *43.82421* |
| *3* | *1* | *3* | *182.248* | *45.17447* |
| *4* | *1* | *4* | *132.943* | *42.47087* |
| *5* | *1* | *5* | *130.078* | *42.27101* |
| *6* | *2* | *1* | *121.658* | *41.68095* |
| *7* | *2* | *2* | *125.174* | *41.88239* |
| *8* | *2* | *3* | *158.247* | *43.79078* |
| *9* | *2* | *4* | *180.035* | *44.98056* |
| *10* | *2* | *5* | *194.488* | *45.6011* |
| *11* | *3* | *1* | *110.894* | *40.88479* |
| *12* | *3* | *2* | *171.224* | *44.57203* |
| *13* | *3* | *3* | *173.177* | *44.6705* |
| *14* | *3* | *4* | *135.981* | *42.63379* |
| *15* | *3* | *5* | *132.075* | *42.3006* |
| *16* | *4* | *1* | *126.345* | *41.89238* |
| *17* | *4* | *2* | *135.156* | *42.59417* |
| *18* | *4* | *3* | *145.660* | *43.23304* |
| *19* | *4* | *4* | *154.688* | *43.51206* |
| *20* | *4* | *5* | *192.014* | *45.61425* |

***Table 16.*** *Response table for signal to noise ratios of impact strength-larger is better.*

| Level | Treatment | Fibre Content |
|---|---|---|
| *1* | *42.84* | *41.23* |
| *2* | ***43.59*** | *43.22* |
| *3* | *43.01* | ***44.22*** |
| *4* | *43.37* | *43.40* |
| *5* | | *43.95* |
| *Delta* | *0.75* | *2.99* |
| *Rank* | *2* | *1* |

Among the modified fibre composites, acetylated fibre composites have the lowest impact strength. Acetylation probably causes agglomeration of the filler, weakening the interfacial regions and making them less resistance to crack propagation. *Fig. 5b,* shows that generally, the impact strength increases with increase in fibre content up to level 3 of fibre content, P3 after which a decline in impact strength was observed. This could be as a result of voids and imperfection which increases with increase in fibre content which results to poor interfacial adhesion and low interfacial strength.

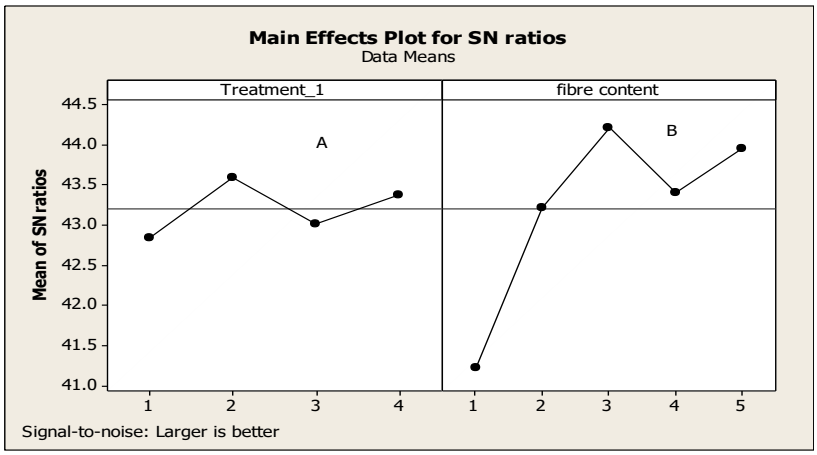


***Fig. 5.*** *Main effect plots for signal-to-noise ratio of treatment and fibre content on impact strength.*

Interaction effect was observed for treatment and fibre content on impact strength (*Fig. 6*). At the low fibre contents of P2 and P3, high impact strength was observed for crude and acetylated fibre composites but as the fibre content increases, the impact strength drastically reduced and became much lower than that of mercerized and mercerized-acetylated composite. Similar behaviour on impact strength of unmodified and acetylated fibre composites was observed by [47], they reported that the impact strength of unmodified and acetylated Piassa fibre reinforced polyestyrene composite increased with increase in fibre contend up to 4 wt% and 2.5 wt% respectively after which a steady decline was observed. They attributed the decrease in impact strength to the inability of the matrix to wet the fibres as the fibre content increased. Similar behaviour has been reported by other researchers on–sisal fibre reinforced polylactide composites, and, sisal and bamboo fibre reinforced polyester hybrid composites [34, 49]. Wiphawee et al. [50], observed a steady decline on the impact strength of untreated bamboo fibre PLA composite with increase in fibre content. They attributed it to poor interfacial adhesion between fibre and matrix.

A steady increase in the impact strength of mercerized and mercerized-acetylated composites with increase in fibre content was observed up to the maximum fibre content of P5. The highest impact strength was observed at P5 fibre content for mercerized and mercerized-acetylated fibre composites. Mercerization prior to acetylation improved the impact strength of acetylated fibre composite. Wiphawee et al. [50], reported steady increase in impact strength of treated bamboo fibre PLA composite over the untreated composite. Prasanna et al. [34], made similar observation on sisal and bamboo fibre reinforced polyester hybrid composite. They reported that alkaline treatment improved the impact strength of the composite.

Surface roughness of mercerized fibre improved relative to that of crude fibre with increase in fibre content; this resulted to improved fibre-matrix adhesion leading to higher impact strength. It also seems that acetylation reduced the protruding micro fibrils from the mercerized frayed fibres. However, increase in fibre content lead to increase in available microfribrils and rough surface in mercerized-acetylated fibre composites, to form an improved interlocking bond with the matrix. Thus, mercerized and mercerized-acetylated composites showed the highest impact strength.

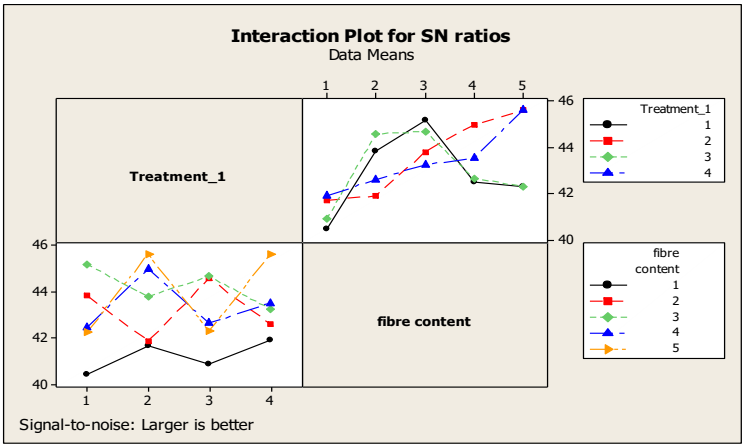


***Fig. 6.*** *Interaction plot for signal-to-noise ratio of treatment and fibre content on impact strength.*

### *3.3.2. Analysis of variance and post hoc test for impact strength*

ANOVA generated using Minitab 17 software, is reported in *Table 17*. A significant main effect of treatments on impact strength, $F\ (3, 119) = 6.97, P < .001$ and a significant main effect of fibre content on impact strength, $F\ (4, 119) = 49.98, P < .001$ was observed. The interaction effect was significant, $F\ (12, 119) = 19.27, P < .001$.

Test of equality of error variance was conducted to investigate if the error variance of the dependent variable is equal across the groups. The result of the test, shown in *Table 18*, indicates unequal error variance. Thus, a Games Howell post hoc test which assumes unequal error variance was chosen for mean comparison. The post hoc test results are reported in Tables' 19 and 20.

***Table 17.*** *Analysis of variance: dependent variable-impact strength.*

| Source | Type III Sum of Squares | df | Mean Square | F | Sig. |
|---|---|---|---|---|---|
| *Corrected Model* | *81893.782*[a] | *19* | *4310.199* | *23.791* | *.000* |
| *Intercept* | *2634387.899* | *1* | *2634387.899* | *1.454E4* | *.000* |
| *Fibre content* | *36219.386* | *4* | *9054.847* | *49.980* | *.000* |
| *Treatment* | *3787.658* | *3* | *1262.553* | *6.969* | *.061* |
| *Fibre content * Treatment* | *41886.738* | *12* | *3490.561* | *19.267* | *.000* |
| *Error* | *18116.851* | *100* | *181.169* | | |
| *Total* | *2734398.532* | *120* | | | |
| *Corrected Total* | *100010.633* | *119* | | | |

a. R Squared = .819 (Adjusted R Squared = .784)

***Table 18.*** *Levene's test of equality of error variances[a]: dependent variable - impact strength.*

| F | df1 | df2 | Sig. |
|---|---|---|---|
| *4.082* | *19* | *100* | *.000* |

Tests the null hypothesis that the error variance of the dependent variable is equal across groups.
a. Design: Intercept + Fibre content + Treatment + Fibre content * Treatment

There is no significant difference on the mean impact strength among the various treatments of bamboo-polyester composites (*Table 19*). This is in agreement with the result of the analysis of variance (*Table 17*). *Table 20* indicates significant mean differences in impact strength among the levels of fibre content. Fibre content P1, has significantly lower impact strength than fibre contents, P2-P5. The fibre content, P2 has significantly lower impact strength than P3. There is no significant difference in the impact strength among fibre contents P3, P4 and P5. This shows that increase in fibre content improves the impact strength up to P3 fibre content after which no significant improvement was observed.

***Table 19.*** *Games Howell's multiple comparison of impact strength among various treatments.*

| | Crude | Mercerized | Acetylated | Mercerized-Acetylated |
|---|---|---|---|---|
| **Crude** | | *-14.618* | *-3.368* | *-9.470* |
| **Mercerized** | *14.6* | | *11.250* | *5.147* |
| **Acetylated** | *3.36* | *-11.250* | | *-6.102* |
| **Mercerized-Acetylated** | *9.47* | *-5.147* | *6.102* | |

***Table 20.*** *Games Howell's multiple comparison of Impact strength among various levels of fibre contents*.

| | P1 | P2 | P3 | P4 | P5 |
|---|---|---|---|---|---|
| **P1** | | *-30.653** | *-48.697** | *-34.776** | *-46.028** |
| **P2** | *30.653** | | *-18.044** | *-4.123* | *-15.375* |
| **P3** | *48.697** | *18.0447** | | *13.921* | *2.669* |
| **P4** | *34.776** | *4.1233* | *-13.921* | | *-11.252* |
| **P5** | *46.028** | *15.3754* | *-2.669* | *11.252* | |

The analysis of the main and interaction effect of treatment and fibre content on impact strength shows that, the level of fibre content and the interaction between treatment and fibre content has significant effect on impact strength. However, treatment has no significant influence on impact strength of bamboo fibre polyester composites. A steady increase in the impact strength of mercerized and mercerized-acetylated composites with increase in fibre content was observed up to the maximum fibre content of P5. The optimum parameter setting for impact strength was observed at mercerization treatment and P3 fibre content with impact strength of 158.23 J/cm. The post hoc test shows that there is no significant difference among the effect of various treatments on the impact strength. The P3 level of fibre content was found to be significantly higher than that of P1 level of fibre contents. However, no significant difference among the effects of P3, P4 and P5 fibre contents on impact strength was observed.

## 4. Conclusion

This research focused on optimization of parameter settings to obtain bamboo fibre/polyester composites of improved properties. An attempt was made to obtain optimal parameter setting for Tensile strength, Flexural strength and impact strength of bamboo fibre polyester composites using Taguchi orthogonal array with focus on effect of fibre content and surface modification. Post hoc test was used to determine the parameter settings that are significantly different from others. The optimization was carried out with the goal of obtaining high performance composite and to produce a guide for composite producers and manufacturers in parameter settings selection. This research should serve as a decision guide to composite manufacturers on the choice of parameter settings based on the desired properties and the particular application of their composite product.

### Conflict of Interest

There is no conflict of interest in connection with this paper, and the material described here is not under publication or consideration for publication elsewhere.

### Funding

No funding was received to assist with the preparation of this manuscript.

## References

[1] Han-Seung, Y., Hyun-Joong, K., Jungil, S., Hee-Jum, P., Bum-Jae, L. & Tack-Sung, H. (2004). Rice-husk flour filled polypropylene composites: mechanical and morphological study. *Composite structures, 63*, 305-312.
[2] Composite World. (2010). *Natural fibres for automotive applications*. Retrieved April 21, 2016, from http://www.compositeworld.com
[3] Stewart, R. (2010). *Reinforced plastics*. Retrieved March 10, 2016, from http://www.Rplastics.com
[4] Akova, I. E. (2013). Development of natural fibre reinforced polymer composites. *Transfer Inovacii, 25*, 3-5.
[5] Grand View Research. (2016). *Natural fibre composite market analysis*. Retrieved 28 July, 2016, from www.grandviewresearch/industry-analysis/natural-fibre-composites
[6] Zheng, W., & Wenjing, G. (2007). Current status and prospects of new architectural materials from bamboo. Retrieved from https://www.inbar.int/wp-content/uploads/2020/05/1489543696.pdf
[7] Oyewole, A., Aliyu, A. A., Oladeji, A. O., & Sadiq, I. (2013). Investigation of some mechanical properties of 'Agaraba' – a native Nigerian bamboo. *AU J.T., 16*(3), 181-186.
[8] Ogunwusi, A. A., & Onwualu, A. P. (2011). Indicative inventory of bamboo availability and utilization in Nigeria. *Jornid, 9* (2), 1-9.
[9] Tran, L. Q., Fuentes, C., Verpoest, I. & Vuure, A. W. (2019). Tensile behavior of unidirectional bamboo/coir fiber hybrid composites. *Fibres, 7* (62), 1-9.
[10] Sharma, P., Dhanwantri, K., & Mehta, S. (2014). Bamboo as a building material. *International journal of civil engineering research, 3*, 249-254.
[11] Viel, Q., Esposito, A., Saiter, J. M. and Santulli, C. (2018). Interfacial characterization by pull-out test of bamboo fibres embedded in poly (Lactic Acid). *Fibres, 6*(1), 1-15.
[12] Jafari, H., & Hajikhani, A. (2016). Multi objective decision making for impregnability of needle mat using design of experiment technique and respond surface methodology. *Applied research on industrial engineering, 3* (1), 30-38.
[13] Prastyo, Y., Yatma, W. A., & Hernadewita, H. (2018). Reduction bottle cost of Milkuat LAB 70 ml using optimal parameter setting with Taguchi method. *Journal of applied research on industrial engineering, 5* (3), 223-238.
[14] John, B., & Areshankar, A. (2018). Reduction of rework in bearing end plate using six sigma methodology: a case study. *Journal of applied research on industrial engineering, 5* (1), 10-26.

[15] Phadke, M. (1989). *Quality engineering using robust design.* Englewood Cliffs: Prentice Hall.
[16] Wysk, R. A., Niebel, B. W., Cohen, P. H., & Simpson, T. W. (2000). *Manufacturing processes: integrated product and process design.* New York: McGraw Hill.
[17] Khoie, A. R., Maters, I. & Gethin, D. T. (2002). Design optimization of aluminium recycling processes using Taguchi technique. *Journal of material process technology, 127*(1), 96-106.
[18] Onyekwere, O. S., & Igboanugo, A. C. (2019). Optimal parameter setting for mercerization of bamboo fibres. *Journal of science and technology research, 1* (1), 12-22.
[19] Onyekwere, O. S., Igboanugo, A. C., & Adeleke, T. B. (2019). Optimisation of acetylation parameters for reduced moisture absorption of bamboo fibre using Taguchi experimental design and genetic algorithm optimisation tools. *Nigerian journal of technology, 38* (1), 104 – 111.
[20] Shehu, U., Isa, M. T., Aderemi, B. O. & Bello, T. K. (2017). Effects of NaOH modification on the mechanical properties of baobab pod fibre reinforced LDPE composites. *Nigerian journal of technology, 36* (1), 87 - 95.
[21] Hassan, M. A., Onyekwere, O. S., Yami, A., & Raji, A. (2014). Effects of Chemical modification on physical and mechanical properties of rice husk - stripped oil palm fruit bunch fibre polypropylene hybrid composite. *IOSR journal of mechanical and civil engineering (IOSR-JMCE), 11* (4), 1-5.
[22] Edeerozey, A. M., Akil, H. M., Azhar, A. B., & Ariffin, M. Z. (2007). Chemical modification of kenaf fibres. *Materials letters, 61*(10), 2023-2025.
[23] Hassan, M. Z., Roslan, S. A., Sapuan, S. M., Rasid, Z. A., Nor, A. F., Daud, M. Y., et al. (2020). Mercerisation optimization of bamboo (Bambusa vulgaris) fibre reinforced epoxy composite structures using Box-Behnken design. *Polymers, 12* (1367), 1-19.
[24] Wang, H., Memon, H., Hassan, E. A., Miah, M. S. & Ali, M. A. (2019). Effect of jute fibre modification on mechanical properties of jute fibre composites. *Materials, 12* (1226), 1-11
[25] Herrera-Estrada, L., Pillay, S., & Vaidya, U. (2008). Banana fiber composites for automotive and transportation applications. *8th annual automotive composites conference and exhibition (ACCE)* (pp. 16-18). United States
[26] Pradeep, K., Kushwaha, & Rakesh, K. (2010). Effect of silanes on mechanical properties of bamboo fibre-epoxy composites. *Journal of reinforced plastics and composites, 29* (5), 718 - 724.
[27] Krishnaraj, C., Balamurugan, M., Samuel, P. S., & Ayyasamy, C. (2013). Analysing the characterisation of alkali treated coir fibre composites. *International journal of innovative research in science engineering and technology, 2* (10), 5403-5412.
[28] Salisu, A. A., Musa, H., Yakasai, M. Y., & Aujara, K. M. (2015). Effects of chemical surface treatment on mechanical properties of sisal fiber unsaturated polyester reinforced composites. *ChemSearch journal, 6*(2), 8-13.
[29] Rashed, H. M. M. A., Islam, M. A., & Rizvi, F. B. (2006). Effects of process parameters on tensile strength of jute fiber reinforced thermoplastic composites. *Journal of naval architecture and marine engineering, 3*(1), 1-6.
[30] Girisha, C., Sanjeevamurthy, Gunti, & Rangasrinivas. (2012). Tensile properties of natural fibre-reinforced epoxy-hybrid composites. *International journal of modern engineering research (IJMER), 2* (2), 471-474.
[31] Wambua, P., Ivens, J., & Verpoest, I. (2003). Natural fibres: can they replace glass in fibre reinforced plastics? *Composites science and technology, 63* (9), 1259-1264.
[32] Jayaraman, K. (2003). Manufacturing sisal-polypropylene composites with minimum fibre degradation. *Composites science and technology, 63* (3), 367-374.
[33] Khoathane, M. C., Vorster, O. C. & Sadiku, E. R. (2008). Hemp fibre-reinforced 1-pentene/polypropylene copolymer: the effect of fibre loading on the mechanical and thermal characteristics of the composites. *Journal of reinforced plastics and composites, 27* (14), 1533 - 1544.
[34] Prasanna, V. R., Ramanathan, K. & Srinivasa, R. V. (2016). Tensile, flexual, impact and water absorption properties of natural fibre reinforced polyester hybrid composites. *Fibres & textiles in Eastern Europe, 24* (3), 90-94.
[35] Hussain, S. A., Pandurangadu, V. & Palanikuamar, K. (2012). Mechanical properties of short bamboo fibre polyester composite filled with alumina particles. *IRACST - engineering science and technology: an international journal, 2* (3), 449 - 453.
[36] Neslihan, O., Murat, O. and Abdullah, M. (2014). Comparison of mechanical characteristics of chopped bamboo and chopped coconut shell reinforced epoxy matrix composite. *European international journal of science and technology, 3*(8), 15-20.
[37] Shito, T., Okubo, K., & Fujii, T. (2002). Development of eco-composites using natural bamboo fibers and their mechanical properties. *WIT transactions on the built environment, 59*.

[38] Chukwudi, A. D., Uzoma, O. T., Azuka, U. A. A., & Sunday, E. C. (2015). Comparison of acetylation and alkali treatments on the physical and morphological properties of raffia palm fibre reinforced composite. *Science*, *3*(4), 72-77.

[39] Shah, H., Srinivasulu, B., & Shit, S. C. (2013). Influence of banana fibre chemical modification on the mechanical and morphological properties of woven banana fabric/unsaturated polyester resin composites. *Polymers from renewable resources*, *4*(2), 61-84.

[40] Aziz, S. H. & Ansell, M. P. (2004). The effect of alkalization and fibre alignment on the mechanical and thermal properties of kenaf and hemp bast fibre composites. *Composite science technology*, *64* (9), 1219–1230.

[41] Kallakas, H., Shamim, M., Olutubo, T., Poltimäe, T., Süld, T. & Krumme, A. (2015). Effect of chemical modification of wood flour on the mechanical properties of wood-plastic composites. *Agronomy research*, *13* (3), 639–653.

[42] Jayabal, S., Sathiyamurthy, S., Loganathan, K. T. & Kalyanasundaram, S. (2012). Effect of soaking time and concentration of NaOH solution on mechanical properties of coir–polyester composites. *Bulletin of material science*, *35* (4), 567-574.

[43] Yousif, B. F., Shalwan, A., Chin, C. W., & Ming, K. C. (2012). Flexural properties of treated and untreated kenaf/epoxy composites. *Materials and design*, *40*, 378-385.

[44] Krishnan, M. R., Santhoskumar, A., & Srinivasulu, B. (2015). Effect of Isora fibres and Nanoclay reinforced with polypropylene. *International journal of latest research in science and technology*, *4* (1), 2278-5299.

[45] Singha, A. S., & Thakur, V. K. (2009). Fabrication and characterization of H. sabdariffa fiber-reinforced green polymer composites. *Polymer-plastics technology and engineering*, *48*(4), 482-487.

[46] Singha, A. S., & Vijay, K. T. (2009b). Mechanical, Thermal and morphological properties of Grewia Optiva Fibre/Polymer matrix composite. *Plastic technology and engineering*, *48* (2), 201- 208.

[47] Obasi, H. C., Nwanonenyi, S. C., Chiemenem, L. I., & Nwosu-Obieogu, K. (2018). Effects of fibre acetylation and fibre content on the properties of piassava fibre reinforced polystyrene. *Futo journal series*, *4* (1), 475-491.

[48] Sabinesh, S., Thomas, R. C., & Sathish, S. (2014). Investigation on tensile and flexural properties of cotton fibre reinforced Isophthallic polyester composites. *International journal of current engineering and technology*, 482-487. https://doi.org/10.1080/03602550902725498

[49] Zhaoqian, L., Xiaodong, Z., & Chonghua, P. (2011). Effect of sisal fiber surface treatment on properties of sisal fiber reinforced polylactide composites. *International journal of polymer science*, 1-7. https://doi.org/10.1155/2011/803428

[50] Wiphawee, N., Putinun, U., Weraporn, P. A. & Hiroyuki, H. (2013). Impact property of flexible epoxy treated natural fiber reinforced PLA composite. *Energy procedia*, *34*, 839-847. https://doi.org/10.1016/j.egypro.2013.06.820

J. Appl. Res. Ind. Eng. Vol. 7, No. 4 (2020) 365–394

Journal of Applied Research on Industrial Engineering
www.journal-aprie.com

# The Transmission Dynamics of HPV, HIV/ADS and HSV-II Co-Infection Model

***Eshetu Dadi Gurmu*, Boka Kumsa Bole, Purnachandra Rao Koya***
*Department of Mathematics, College of Natural and Computational Science, Wollega University, Nekemte, Ethiopia.*

**PAPER INFO**

**Chronicle:**
*Received: 25 July 2020*
*Reviewed:19 August 2020*
*Revised: 07 October 2020*
*Accepted: 30 October 2020*

**Keywords:**
*Mathematical Model.*
*Co-Infection. Reproduction Number.*

**ABSTRACT**

The aim of study is to formulate and analyze a mathematical model for coinfection of sexually transmitted diseases HPV, HIV, and HSV-II. The well possedness of the developed model equations was proved and the equilibrium points of the model have been identified. Qualitative analysis of the formulated model equations was proved and the equilibrium points of the model have been identified. Qualitative analysis of the formulated model was established using basic reproduction number. The results show that the disease free equilibrium is locally asymptotically stable if the basic reproduction is less than one. The endemic states are considered to exist when the basic reproduction number for each disease is greater than one. Finally, numerical simulations of the model equations are carried out using the software MATLAB R2015b with ODE45 solver. Numerical simulations illustrated that all infection solutions converge to zero when the basic reproduction number is less than unity.

## 1. Introduction

Sexually Transmitted Diseases (STDs) can be transmitted through genital-genital, orogenital, or anogenital contacts and remain to be a public health concern worldwide. In the world, around one million people are believed to be newly infected with each day. Numerous causative agents including bacteria, viruses, protozoa, yeast, and fungi are responsible for sexually transmitted infections. However, viruses exhibit more serious risks, probabilities and outcomes of STDs than other organisms. The most lethal viral STIs are Human Immunodeficiency Virus-1 (HIV), Herpes Simplex viruses 1 and 2 (HSV-1 and HSV-2), and Human Papillomavirus (HPV), which are responsible for major sexually transmitted viral infections including AIDS, herpes simplex, and genital warts, respectively. Despite the fact that several prevention strategies such as vaccination, abstinence from sex, limiting sex partners,

Gurmu, E. D., Bole, B. K., & Koya, P. R. (2020). The transmission dynamics of HPV, HIV/ADS and HSV-II co-infection model. *Journal of applied research on industrial engineering, 7*(4), 365-394.

* Corresponding author
E-mail address: eshetudadi1@gmail.com

10.22105/jarie.2020.253001.1200

the use of condoms and a range of therapeutic drugs have drastically reduced the risk of contracting STIs, these three infections continue to spread at an alarming rate [1].

Human Papillomaviruses (HPVs) named for warts (papillomas) are the most common sexually transmitted infectious agents both in men and women across the world. HPV is a small, nonenveloped, and double-stranded DNA virus [1]. Most of the HPV infections are asymptomatic and can feed away without treatment over the course of a few years. About 70% of HPV infections fed away with in a year and 90% within two years. However, in some people infection can persist for many years and can cause warts or low risk genotype of HPV, while other types lead to different kinds of cancers or high risk genotype of HPV, including cervical cancer [2-3]. Statistics show that there are 18.1 million new cases, 9.6 million cancer related deaths, and 43.8 million people living with cancer in 2018. The number of new cases is expected to rise from 18 million to 22 million by 2030 and the number of global cancer deaths is projected to increase by 45% by 2030 [4].

Human Immunodeficiency Viruses (HIV) are an RNA retrovirus. That is, to enter a cell, HIV translates its RNA to DNA with a viral enzyme called reverse transcriptase [5]. The target cell of HIV is CD4 T cells. A healthy human body has about $1000/mm^3$ of CD4 T cells. When the CD4 T cells of a patient decline to $200/mm^3$ or below, then that person is classified as having AIDS [6]. In the world, new HIV infections among young women aged 15–24 years were reduced by 25% between 2010 and 2018. The annual number of deaths from AIDS-related illness among people living with HIV globally has fallen from a peak of 1.7 million in 2004 to 770 000 in 2018. The global decline in deaths has largely been driven by progress in eastern and southern Africa, which is home to 54% of the world's people living with HIV. AIDS-related mortality in the region declined by 44% from 2010 to 2018.The annual number of new infections since 2010 has declined from 2.1 million to 1.7 million in 2018 [7].

Herpes Simplex Virus Type II (HSV-II) infections are the primary cause of genital herpes. Genital herpes is a chronic, life-long viral infection caused by Herpes Simplex Virus-I (HSV-I) and Herpes Simplex Virus-II (HSV-II). HSV-II can be transmitted during sexual contact with someone who has a genital HSV-II infection [8]. Worldwide, an estimated 19.2 million new HSV-II infections occurred among adults and adolescents aged 15-49 years in 2012 with the highest rates among younger age groups. HSV-II is a lifelong infection and the estimated global HSV-II prevalence of 11.3% translates into an estimated 417 million people with the infection in 2012. The prevalence of HSV-II is highest in the WHO African Region (31.5%), followed by the Region of the Americas (14.4%) [9].

Co-infection is more than one disease co-existing within a single host. HPV, HIV and HSV-II are among the diseases that contaminate a large number of individuals worldwide. People with a weakened immune system such as those with HIV/AIDS are susceptible to diseases such as HPV, HSV-II. HPV-HIV-HSV-II is the co-infection of three of diseases responsible for loss of many lives. When an individual is co-infected with HPV-HIV, HPV-HSV-II, HIV-HSV-II and HPV-HIV-HSV-II at acute and clinical latency stages is called the initial stage. The final stage of the co-infection of HPV-HIV, HPV-HSV-II, HIV-HSV-II and HPV-HIV-HSV-II involves AIDS with Cervical cancer, cervical cancer with Herpes Simplex Virus-II, AIDS with HSV-II and Cervical Cancer-AIDS-HSV-II. This paper develops and analyses the mathematical model of HPV-HIV-HSV-II co-infection.

Mathematical modelling plays an important role in increasing our understanding of the dynamics of co-infectious diseases and also to investigate the optimal use of intervention strategies to control the spread of infectious diseases. Old and recent studies such as [10-12] developed a mathematical model of Human Papillomavirus to understand the transmission dynamics of the disease. A lot of scholars [13,

15] developed a mathematical model of HIV to describe the dynamics of the disease that helped them to propose disease control mechanism and also described the transmission dynamics of the diseases. Some of them are [16, 24] developed and analyzed a deterministic model for the transmission dynamics of Herpes Simplex Virus-II. Mhlanga et al. [17] proposed and analyzed a mathematical model for the spread of HSV-2 by incorporating all the relevant biological details and poor treatment adherence.

Furthermore, a lot of scholars developed a mathematical model to illustrate the dynamics of the co-infection with other infectious diseases and to suggest disease control mechanism. Some of them are [18, 19] the co-dynamics of HPV and HIV Disease. In their study, it was found that if the basic reproduction number of HPV becomes very small approaching zero, there is no new HPV infection which reduces the rate of AIDS progression. There are also some findings on coinfection of HPV and HSV-II by authors [20, 21]. The analysis of their study showed that HPV infection increases the risk of HSV-II similarly; HSV-II infection increases the risk for HPV. Moreover, Mhlanga [22] proposed a deterministic mathematical model for the co-interaction of HIV and HSV-II in a community, with all the relevant biological detail and poor HSV-II treatment adherence. In this study threshold parameters of the model are determined and stabilities are analyzed. Results from their simulation suggests that more effort should be devoted to monitoring and counseling of individuals dually infected with HIV and HSV-II as compared to those infected with HSV-II only.

So far, several mathematical studies have been undertaken to understand the transmission dynamics HPV, HIV, HSV-II, but they did not considered the coinfection of three disease i.e. coinfection of HPV-HIV-HSV-II in their studies.

## 2. Model Description and Formulation

The total human population $N$ is subdivided into 22 subclasses, namely susceptible individuals, which are capable of becoming infected $S(t)$, individuals who are exposed to HPV$E_p(t)$, individuals who are exposed to HIV $E_h(t)$, individuals who are exposed to HSV-II $E_s(t)$, individuals who are exposed to both HPV and HIV $E_{ph}(t)$, individuals who are exposed to both HPV and HSV-II $E_{ps}(t)$, individuals who are exposed to both HIV and HSV-II $E_{hs}(t)$, individuals who are infected with HPV$I_p(t)$, individuals who are infected with HIV $I_h(t)$, individuals who are infected with HSV-II $E_s(t)$, individuals who are coinfected with both HPV and HIV $I_{ph}(t)$, individuals who are coinfected with both HPV and HSV-II $I_{ps}(t)$, individuals who are coinfected with both HIV and HSV-II $I_{hs}(t)$, individuals having cervical cancer $C(t)$, individuals having AIDS $A(t)$, individuals having HSV-II $H(t)$, individuals having both cervical cancer and AIDS $CA(t)$, individuals having both cervical cancer and HSV-II $CH(t)$, individuals having both AIDS and HSV-II $AH(t)$, individuals having cervical cancer AIDS and HSV-II $CAH(t)$, individuals recovered from HPV infection $R_p$, and individuals recovered from HSV infection $R_s$ are considered.

The whole population is susceptible to human papillomavirus, HIV and HSV-II. It is assumed that individuals enter to the susceptible subclass through birth at a rate Π and the number of susceptible increases by those individuals that lost their temporary immunity from subclass of recovered $R_p$ and $R_s$ with rate $\chi_p$ and $\chi_s$ respectively. Susceptible individuals may acquire HPV infection, HIV infection, HSV-II infection, HPV-HIV coinfection, HPV-HSV-II coinfection and HIV-HSV-II coinfection with force of infection $\lambda_p = \frac{\beta_p I_p}{N_p}$, $\lambda_h = \frac{\beta_h I_h}{N_h}$, $\lambda_s = \frac{\beta_s I_s}{N_s}$, $\lambda_{ph} = \frac{\beta_{ph} I_{ph}}{N_{ph}}$, $\lambda_{ps} = \frac{\beta_{ps} I_{ps}}{N_{ps}}$ and $\lambda_{hs} = \frac{\beta_{hs} I_{hs}}{N_{hs}}$ respectively. Here $\beta_p$, $\beta_h$, $\beta_s$, $\beta_{ph}$, $\beta_{ps}$ and $\beta_{hs}$ are transmission coefficient of HPV, HIV, HSV-II, HPV-

HIV coinfection, HPV-HSV-II coinfection and HIV-HSV-II coinfection. Individuals in $E_p$ and $E_h$ subclass move to $E_{ph}$ with rate $\nu_1$ and $\nu_2$. Individuals in $E_p$ and $E_s$ subclass are also move to $E_{ps}$ with rate $\nu_{19}$ and $\nu_{20}$. Similarly, individuals in $E_h$ and $E_s$ subclass move to $E_{hs}$ with rate $\nu_3$ and $\nu_4$. Furthermore, individuals in $E_p, E_{ph}, E_{ps}, E_h, E_{hs}$ and $E_s$ sub-class progress to $I_p, I_{ph}, I_{ps}, I_h, I_{hs}$ and $I_s$ sub-class with per capita rate of $\eta_p, \eta_{ph}, \eta_{ps}, \eta_h, \eta_{hs}$ and $\eta_s$ respectively. Addition to this, individuals in $I_p$ and $I_h$ subclass move to $I_{ph}$ with rate $\nu_6$ and $\nu_7$. Also, Individuals in $I_p$ and $I_s$ subclass are move to $I_{ps}$ with rate $\nu_{15}$ and $\nu_{16}$. Similarly, individuals in $I_h$ and $I_s$ subclass move to $I_{hs}$ with rate $\nu_8$ and $\nu_9$. Moreover, individuals in subclass $I_p, I_{ph}, I_{ps}, I_h, I_{hs}$ and $I_s$ may develop cervical cancer, cervical cancer-AIDS coinfection, cervical cancer-HSV-II coinfection, AIDS, AIDS-HSV-II coinfection and HSV-II with progression rates $\alpha_p, \alpha_{ph}, \alpha_{ps}, \alpha_h, \alpha_{hs}$ and $\alpha_s$ respectively. Finally, individuals in $C$, $CA$, $CH$, $A$, $AH$ and $H$ may developed coinfection of HPV-HIV-HSV-II with rate $\varphi$, $\theta$, $\pi$, $\psi$, $\delta$ and $\gamma$, respectively. All individuals suffer natural mortality at a rate $\mu$ and sick, die of cervical cancer, AIDS, HSV-II, cervical cancer-AIDS coinfection, AIDS-HSV-II coinfection, cervical cancer-HSV-II infection and cervical cancer-AIDS-HSV-II coinfection at rate $\xi$. The schematic diagram that describes the flow of the model is given below in *Fig. 1*.

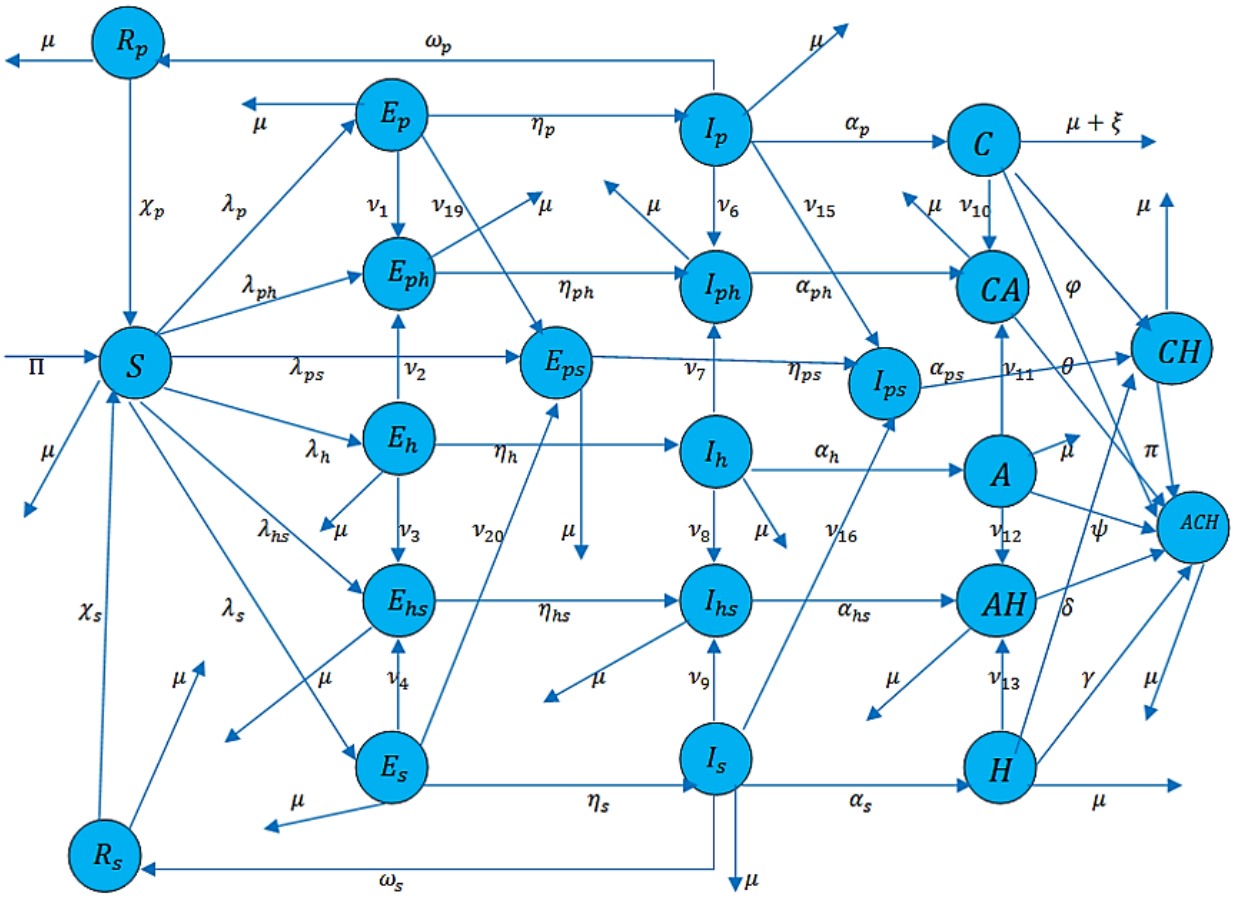


***Fig. 1.*** *Schematic diagram for HPV-HIV-HSV-II coinfection model.*

Based on model assumption and *Fig. 1* we obtain the following system of linear differential equation

$$\frac{dS}{dt} = \Pi + \chi_p R_p + \chi_s R_s - (\lambda_p + \lambda_{ph} + \lambda_h + \lambda_{ps} + \lambda_{hs} + \lambda_s + \mu)S, \quad (1)$$

$$\frac{dE_p}{dt} = \lambda_p S - (\eta_p + \nu_{19} + \nu_1 + \mu)E_p,$$

$$\frac{dE_{ph}}{dt} = \lambda_{ph} S + \nu_1 E_p + \nu_2 E_h - (\eta_{ph} + \mu)E_{ph},$$

$$\frac{dE_{ps}}{dt} = \lambda_{ps} S + \nu_{19} E_p + \nu_{20} E_s - (\eta_{ps} + \mu)E_{ps},$$

$$\frac{dE_h}{dt} = \lambda_h S - (\eta_h + \nu_2 + \nu_3 + \mu)E_h,$$

$$\frac{dE_{hs}}{dt} = \lambda_{hs} S + \nu_3 E_h + \nu_4 E_s - (\eta_{hs} + \mu)E_{hs},$$

$$\frac{dE_s}{dt} = \lambda_s S - (\eta_s + \nu_4 + \nu_{20} + \mu)E_s,$$

$$\frac{dI_p}{dt} = \eta_p E_p - (\alpha_p + \nu_{15} + \nu_6 + \omega_p + \mu)I_p,$$

$$\frac{dI_{ph}}{dt} = \eta_{ph} E_{ph} + \nu_6 I_p + \nu_7 I_h - (\alpha_{ph} + \mu)I_{ph},$$

$$\frac{dI_{ps}}{dt} = \eta_{ps} E_{ps} + \nu_{15} I_p + \nu_{16} I_s - (\alpha_{ps} + \mu)I_{ps},$$

$$\frac{dI_h}{dt} = \eta_h E_h - (\alpha_h + \nu_7 + \nu_8 + \mu)I_h,$$

$$\frac{dI_{hs}}{dt} = \eta_{hs} E_{hs} + \nu_8 I_h + \nu_9 I_s - (\alpha_{hs} + \mu)I_{hs},$$

$$\frac{dI_s}{dt} = \eta_s E_s - (\omega_s + \nu_9 + \nu_{16} + \mu)I_s,$$

$$\frac{dC}{dt} = \alpha_p I_p - (\nu_{10} + \nu_{17} + \varphi + \mu + \xi)C,$$

$$\frac{dCA}{dt} = \alpha_{ph} I_{ph} + \nu_{10} C + \nu_{11} A - (\theta + \mu + \xi)CA,$$

$$\frac{dCH}{dt} = \alpha_{ps} I_{ps} + \nu_{17} C + \nu_{18} H - (\pi + \mu + \xi)CH,$$

$$\frac{dA}{dt} = \alpha_h I_h - (\nu_{11} + \nu_{12} + \psi + \mu + \xi)A,$$

$$\frac{dAH}{dt} = \alpha_{hs} I_{hs} + \nu_{12} A + \nu_{13} H - (\delta + \mu + \xi)AH,$$

$$\frac{dH}{dt} = \alpha_s I_s - (\nu_{13} + \nu_{18} + \gamma + \mu + \xi)H,$$

$$\frac{dACH}{dt} = \varphi C + \theta CA + \pi CH + \psi A + \delta AH + \gamma H - (\mu + \xi)ACH,$$

$$\frac{dR_p}{dt} = \omega_p I_p - (\chi_p + \mu)R_p,$$

$$\frac{dR_s}{dt} = \omega_s I_s - (\chi_s + \mu)R_s.$$

With initial condition

$S(0) = S_0,\ E_p(0) = E_{p0},\ E_{ph}(0) = E_{ph0},\ E_{ps}(0) = E_{ps0}, E_h(0) = E_{h0},\ E_{hs}(0) = E_{hs0},\ E_s(0) = E_{s0},\ I_p(0) = I_{p0},\ I_{ph}(0) = I_{ph0},\ I_{ps}(0) = I_{ps0}, I_h(0) = I_{h0},\ I_{hs}(0) = I_{hs0}, I_s(0) = I_{s0},\ A(0) = A_0,\ C(0) = C_0,\ CA(0) = CA_0,\ AH(0) = AH_0,\ CH(0) = CH_0,\ H(0) = H_0\ , ACH(0) = ACH_0, R_p = R_{p0}, R_s = R_{s0}.$

## 3. Analysis HPV only Model

Here analysis of HVP only model is considered and model equation obtained from *Eq. (1)*. This is

$$\begin{aligned}
\frac{dS}{dt} &= \Pi + \chi_p R_p - (\lambda_p + \mu)S, \qquad (2)\\
\frac{dE_p}{dt} &= \lambda_p S - (\eta_p + \mu)E_p,\\
\frac{dI_p}{dt} &= \eta_p E_p - (\alpha_p + \omega_p + \mu)I_p,\\
\frac{dC}{dt} &= \alpha_p I_p - (\mu + \xi)C,\\
\frac{dR_p}{dt} &= \omega_p I_p - (\chi_p + \mu)R_p.
\end{aligned}$$

### *3.1. Invariant Region*

In this section, we get a region in which the solution of *Eq. (2)* is bounded. To obtain this, first we considered the total population $(N_p)$, where $(N_p) = S + E_p + I_p + C + R_p$. Then, differentiating $(N_p)$ both sides with respect to $t$ leads

$$\frac{dN_p}{dt} = \frac{dS}{dt} + \frac{dE_p}{dt} + \frac{dI_p}{dt} + \frac{dC}{dt} + \frac{dR_p}{dt}. \qquad (3)$$

Substituting *Eq. (2)* into *Eq. (3)*, we can get

$$\frac{dN_p}{dt} = \Pi - \mu N_p - \xi C,$$

$$\Rightarrow \frac{dN_p}{dt} \leq \Pi - \mu N_p,$$

where $(\xi = 0)$ i.e., in the absence of mortality

$$\int \frac{dN_p}{\Pi - \mu N_p} \leq \int dt,$$

$$\Leftrightarrow \frac{-1}{\mu}\ln(\Pi - \mu N_p) \leq t + c_1,$$

where $c_1$ is integration constant

$$\Rightarrow (\Pi - \mu N_p) \geq ce^{-\mu t},$$

where $c = e^{-c_1}$.

Then, applying initial condition $N_p(0) = N_{p0}$, we obtain

$$\Rightarrow \mathrm{N_p} \leq \frac{\Pi}{\mu} - [\frac{\Pi - \mu \mathrm{N_p}}{\mu}]\mathrm{e}^{-\mu \mathrm{t}}. \quad (4)$$

Further, it can be observed that $N_p(t) \to (\Pi/\mu)$ as $t \to \infty$. That is, the total population size $N_p(t)$ takes off from the value $N_p(0)$ at the initial time $t = 0$ and ends up with the bounded value $(\Pi/\mu)$ as the time $t$ grows to infinity. Thus, it can be concluded that $N_p(t)$ is bounded as $0 \leq N_p(t) \leq (\Pi/\mu)$. Thus, the feasible solution set of the system equation of the model enters and remains in the region:

$$\Omega_{\mathrm{p}} = \{(\mathrm{S}, \quad \mathrm{E_p}, \quad \mathrm{I_p}, \quad \mathrm{C}, \quad \mathrm{R_p}) \in \Re_+^5 \ : \ \mathrm{N_p} \leq \Pi/\mu\}.$$

Therefore, the *Eq. (2)* is well posed epidemiologically and mathematically. Hence, it is sufficient to study the dynamics of the basic model in the region $\Omega_p$.

### *3.2. Existence of Solution*

*Lemma 1.* Solutions of the model *Eq. (2)* together with the initial conditions $S(0) > 0, S, E_p(0) > 0, I_p(0) >), C(0) > 0, \quad R_p(0) > 0$ exist in $\mathbb{R}_+^5$ i.e., the model variables $S(t), E_p(t), I_p(t), C(t)$ and $R_p(t)$ exist for all $t$ and will remain in $\mathbb{R}_+^5$.

*Proof.* The right hand sides of the system of *Eq. (2)* can be expressed as follows:

$$\mathrm{f_1(S, E_p, I_p, C, R_p)} = \Pi + \chi_{\mathrm{p}}\mathrm{R_p} - (\lambda_{\mathrm{p}} + \mu)\mathrm{S},$$

$$\mathrm{f_2(S, E_p, I_p, C, R_p)} = \lambda_{\mathrm{p}}\mathrm{S} - (\eta_{\mathrm{p}} + \mu)\mathrm{E_p},$$

$$\mathrm{f_3(S, E_p, I_p, C, R_p)} = \eta_{\mathrm{p}}\mathrm{E_p} - (\alpha_{\mathrm{p}} + \omega_{\mathrm{p}} + \mu)\mathrm{I_p},$$

$$\mathrm{f_4(S, E_p, I_p, C, R_p)} = \alpha_{\mathrm{p}}\mathrm{I_p} - (\mu + \xi)\mathrm{C},$$

$$\mathrm{f_5(S, E_p, I_p, C, R_p)} = \omega_{\mathrm{p}}\mathrm{I_p} - (\chi_{\mathrm{p}} + \mu)\mathrm{R_p}.$$

According to Derrick and Groosman theorem, let $\Omega_p$ denote the region $\Omega_p = \{(S, E_p, I_p, C, \quad R_p) \in \Re_+^5 \ : N_p \leq \Pi/\mu\}$. Then *Eq. (1)* have a unique solution if $(\partial f_i)/(\partial x_j)$, $i, j = 1, 2, 3, 4, 5$ are continuous and bounded in $\Omega_p$. Here, $x_1 = S, \ x_2 = E_p, \ x_3 = I_p, \ x_4 = C$ and $x_6 = R_p$. The continuity and the boundedness are verified as here under in *Table 1*.

***Table 1***. *Continuity and boundedness of the model solution.*

| | | |
|---|---|---|
| $\lvert(\partial f_1)/(\partial S)\rvert = \lvert-(\lambda_p+\mu)\rvert < \infty$ | $\lvert(\partial f_2)/(\partial S)\rvert = \lvert\lambda_p\rvert < \infty.$ | $\lvert(\partial f_3)/(\partial S)\rvert = 0 < \infty.$ |
| $\lvert(\partial f_1)/(\partial I_p)\rvert = \lvert-(\beta_1 S/N_p)\rvert < \infty.$ | $\lvert(\partial f_2)/(\partial E_p)\rvert = \lvert-(\eta_p+\mu)\rvert < \infty.$ | $\lvert(\partial f_3)/(\partial E_p)\rvert = \lvert\eta_p\rvert < \infty.$ |
| $\lvert(\partial f_1)/(\partial R_p)\rvert = \lvert\eta\rvert < \infty.$ | $\lvert(\partial f_2)/(\partial I_p)\rvert = \lvert\beta_1 S/N_p\rvert < \infty.$ | $\lvert(\partial f_3)/(\partial I_p)\rvert = \lvert-(\alpha_p+\omega_p+\mu)\rvert < \infty.$ |
| $\lvert(\partial f_1)/(\partial E_p)\rvert = \lvert(\partial f_1)/(\partial C)\rvert = 0 < \infty.$ | $\lvert(\partial f_2)/(\partial C)\rvert = \lvert(\partial f_2)/(\partial R_p)\rvert = 0 < \infty.$ | $\lvert(\partial f_3)/(\partial C)\rvert = \lvert(\partial f_2)/(\partial R_p)\rvert = 0 < \infty.$ |
| $\lvert(\partial f_4)/(\partial S)\rvert = \lvert(\partial f_4)/(\partial E_p)\rvert = 0 < \infty.$ | $\lvert(\partial f_4)/(\partial R_p)\rvert = 0 < \infty.$ | $\lvert(\partial f_5)/(\partial C)\rvert = 0 < \infty.$ |
| $\lvert(\partial f_4)/(\partial I_p)\rvert = \lvert\alpha_p\rvert < \infty.$ | $\lvert(\partial f_5)/(\partial S)\rvert = \lvert(\partial f_5)/(\partial E_p)\rvert = 0 < \infty.$ | $\lvert(\partial f_5)/(\partial R_p)\rvert = \lvert-(\chi_p+\mu)\rvert < \infty.$ |
| $\lvert(\partial f_4)/(\partial C)\rvert = \lvert-(\mu+\xi)\rvert < \infty.$ | $\lvert(\partial f_5)/(\partial I_p)\rvert = \lvert\omega_p\rvert < \infty.$ | |

Thus, all the partial derivatives $(\partial f_i)/(\partial x_j), i,j = 1,2,3,4,5$ exist, continuous and bounded in $\Omega_p$. Hence, by Derrick and Groosman theorem, a solution for the *Model (2)* exists and is unique.

### *3.3. Positivity of Solution*

The solution of the system remains positive at any point in time *t*, if the initial values of all the variables are positive.

*Lemma 2.* Let $\Omega_{\mathrm{p}} = \{(S,\ E_p,\ I_p,\ C,\quad R_p) \in \mathbb{R}^5_+;\ S_0(0) > 0,\ E_{p0}(0) > 0,\ I_{p0}(0) >),\ C_0(0) > 0,\quad R_{p0}(0) > 0\}$; then the solutions of $\{S,\ E_p,\ I_p,\ C,\ R_p\}$ are positive for all $t \geq 0$.

Proof: Positivity is verified separately for each of the model $S(t),\ E_p(t),\ I_p(t),\ C(t)$ and $R_p(t)$.

Positivity of$S(t)$: From *Eq. (2)* we have:

$\frac{dS}{dt} = \Pi + \chi_p R_p - (\lambda_p+\mu)S$, eliminating the positive terms $(\Pi + \chi_p R_p)$ we get,

$\Leftrightarrow \frac{dS}{dt} \geq -(\lambda_p+\mu)S$, using variables separable method we get,

$$\Rightarrow \int \frac{\mathrm{dS}}{\mathrm{S}} \geq -\int (\lambda_{\mathrm{p}}+\mu)\,\mathrm{dt},$$

$$\Rightarrow \ln \mathrm{S} \geq -(\lambda_{\mathrm{p}}+\mu)\mathrm{t} + \mathrm{c}_3,$$

where $c_3$ is integration constant.

$\Rightarrow S(t) \geq S_0 \mathrm{e}^{-(\lambda_p+\mu)t}$,$S_0 = \mathrm{e}^{\mathrm{c}_3}$ and $\mathrm{e}^{-(\lambda_p+\mu)t} \geq 0$, for all $t \geq 0$.

Hence, it can be concluded that $S(t) \geq 0$.

Positivity of $E_p(t)$: From *Eq. (2)* we have:

$\frac{dE_p}{dt} = \lambda_p S - (\eta_p+\mu)E_p$, eliminating the positive terms $(\lambda_p S)$ we get,

$\Leftrightarrow \frac{dE_p}{dt} \geq -(\eta_p+\mu)E_p$, using variables separable method we get,

$\Rightarrow \frac{dE_p}{E_p} \geq -(\eta_p + \mu)dt$, integrating both side we can get,

$$\Rightarrow \int \frac{dE_p}{E_p} \geq -\int (\eta_p + \mu)\, dt,$$

$$\Rightarrow \ln E_p \geq -(\eta_p + \mu)t + c_4,$$

where $c_4$ is integration constant

$\Rightarrow E_p(t) \geq E_{p_0} e^{-(\eta_p+\mu)t}$, $S_0 = e^{c_4}$and $e^{-(\eta_p+\mu)t} \geq 0$, for all $t \geq 0$.

Hence, it can be concluded that $E_p(t) \geq 0$.

Positivity of $I_p(t)$: From *Eq. (2)* we have:

$\frac{dI_p}{dt} = \eta_p E_p - (\alpha_p + \omega_p + \mu)I_p$, eliminating the positive terms $(\eta_p E_p)$we get,

$\Leftrightarrow \frac{dI_p}{dt} \geq -(\alpha_p + \omega_p + \mu)I_p$, using variables separable method we get,

$\Rightarrow \frac{dI_p}{I_p} \geq -(\alpha_p + \omega_p + \mu)dt$, integrating both side we can get,

$$\Rightarrow \int \frac{dI_p}{I_p} \geq -\int (\alpha_p + \omega_p + \mu)\, dt,$$

$$\Rightarrow \ln I_p \geq -(\alpha_p + \omega_p + \mu)t + c_5,$$

where $c_5$ is integration constant

$\Rightarrow I_p(t) \geq I_{p0} e^{-(\alpha_p+\omega_p+\mu)t}$, $I_{p0} = e^{c_5}$and $e^{-(\alpha_p+\omega_p+\mu)t} \geq 0$,for all $t \geq 0$.

Hence, it can be concluded that $I_p(t) \geq 0$.

Positivity of $C(t)$: From *Eq. (2)* we have:

$\frac{dC}{dt} = \alpha_p I_p - (\mu + \xi)C$, eliminating the positive terms $(\alpha_p I_p)$we get,

$\Leftrightarrow \frac{dC}{dt} \geq -(\mu + \xi)C$, using variables separable method we get,

$\Rightarrow \frac{dC}{C} \geq -(\mu + \xi)dt$, integrating both side we can get,

$$\Rightarrow \int \frac{dC}{C} \geq -\int (\mu + \xi)\, dt,$$

$$\Rightarrow \ln C \geq -(\mu + \xi)t + c_6,$$

where $c_6$ is integration constant

$\Rightarrow C(t) \geq C_0 e^{-(\mu+\xi)t}$, $C_0 = e^{c_6}$ and $e^{-(\mu+\xi)t} \geq 0$, for all $t \geq 0$.

Hence, it can be concluded that $C(t) \geq 0$.

Positivity of $R_p(t)$: From *Eq. (2)* we have:

$\frac{dR_p}{dt} = \omega_p I_p - (\chi_p + \mu)R_p$, eliminating the positive terms $(\omega_p I_p)$ we get,

$\Leftrightarrow \frac{dR_p}{dt} \geq -(\chi_p + \mu)R_p$, using variables separable method we get,

$\Rightarrow c_7 \frac{dR_p}{R_p} \geq -(\chi_p + \mu)dt$, integrating both side we can get,

$$\Rightarrow \int \frac{dR_p}{R_p} \geq -\int (\chi_p + \mu)\, dt,$$

$$\Rightarrow \ln R_p \geq -(\chi_p + \mu)t + c_7,$$

where is integration constant

$\Rightarrow R_p(t) \geq R_{p0} e^{-(\chi_p+\mu)t}$, $R_{p0} = e^{c_7}$ and $e^{-(\chi_p+\mu)t} \geq 0$, for all $t \geq 0$.

Hence, it can be concluded that $R_p(t) \geq 0$.

Therefore, the model variables $S(t)$, $E_p(t)$, $I_p(t)$, $C(t)$ and $R_p(t)$representing population sizes of various types of cells are positive quantities and will remain in $\mathbb{R}_+^5$ for all $t$.

### *3.4. Local Stability of the Disease-Free Equilibrium (DFE)*

The disease free equilibrium of *Eq. (2)* is obtained by equating all equations of the model equation to zero and then letting $E_p = I_p = C = R_p = 0$. Then we obtain

$$E_1 = \left\{\left(\frac{\Pi}{\mu}\right), \quad 0, \quad 0, \quad 0, \quad 0\right\}.$$

The linear stability of the DFE, $E_1$, can be established using the next generation operator method in Van den Driessche and Watmouth [23] on the *System (2)*. The matrice $F$ s (for the new infection terms) and $V$ (of the transition terms) are given, respectively by,

$$F = \begin{bmatrix} 0 & \beta_p & 0 \\ 0 & 0 & 0 \\ 0 & 0 & 0 \end{bmatrix} \text{ and } V = \begin{bmatrix} \eta_p & 0 & 0 \\ -\eta_p & (\alpha_p + \omega_p + \mu) & 0 \\ 0 & -\alpha_p & \mu + \xi \end{bmatrix}.$$

The associated reproduction number, denoted by $\Re_p$ is then given by,

$$\Re_p = \frac{(\beta_p \eta_p)}{(\alpha_p + \omega_p + \mu)(\mu + \xi)}.$$

Further using theorem in Van den Driessche and Watmouth [23], the following result is established. The DFE is locally asymptotically stable if $\Re_p < 1$ and unstable is $\Re_p > 1$.

### *3.5. Stability Analysis of Endemic Equilibrium*

*Lemma 3.* The HPV only model has a unique endemic equilibrium if and only if $\Re_p > 1$.

*Proof.* Let the endemic equilibrium point of the *Eq. (2)* be denoted by,

$$E_1^* = (S^*, \quad E_p^*, \quad I_p^*, \quad C^*, \quad R_p^*),$$

and consider the force of infection

$$\lambda_p^* = [\beta_p I^*]/[N]. \tag{5}$$

Solving the equations in *System (5)* by setting the right hand sides of equations equal to zero, gives,

$$S^* = [\Pi + \chi_p R_p^*]/[\lambda_p^* + \mu], \tag{6}$$

$$E_p^* = [\lambda_p^*(\Pi + \chi_p R_p^*)]/[(\lambda_p^* + \mu)(\eta_p + \mu)],$$

$$I_p^* = [\lambda_p^* \eta_p (\Pi + \chi_p R_p^*)]/[(\lambda_p^* + \mu)(\eta_p + \mu)(\alpha_p + \omega_p + \mu)],$$

$$C^* = [\lambda_p^* \eta_p \alpha_p (\Pi + \chi_p R_p^*)]/[(\lambda_p^* + \mu)(\eta_p + \mu)(\alpha_p + \omega_p + \mu)(\mu + \xi)]\, R_p^*$$
$$= [\omega_p \eta_p \Pi \lambda_p^*]/[(\lambda_p^* + \mu)(\eta_p^* + \mu)(\alpha_p + \omega_p + \mu)(\chi_p + \mu) - \omega_p \eta_p \lambda_p^* \chi_p].$$

Substituting *Eq. (6)* in *Eq. (5)* gives

$$(\eta_p + \mu)(\lambda_p^*)^2 + \lambda_p^* \mu \left[1 - \Re_p \left(\frac{\Pi + \chi_p + R_p^*}{\Pi}\right)\right] = 0. \tag{7}$$

This shows that the non-zero (positive endemic) equilibrium point of the model equation satisfy

$$D_1 \lambda_p^* + D_2 = 0. \tag{8}$$

Where $D_1 = (\eta_p + \mu)$and $D_2 = \mu \left[1 - \Re_p \left(\frac{\Pi + \chi_p + R_p^*}{\Pi}\right)\right]$.

It is clear that $D_1 > 0$ and $D_2 < 0$ when $\Re_p \left(\frac{\Pi+\chi_p+R_p^*}{\Pi}\right) > 1$. Thus the *Linear System (8)* has a unique positive solution, given by $\lambda_p^* = \frac{-D_2}{D_1}$ whenever $\Re_p > 1$.

Now, to show its local stability analysis, *Eq. (7)* gives a fixed point problem of the form

$$f(\lambda_p^*) = (\eta_p + \mu)(\lambda_p^*)^2 + \lambda_p^* \mu \left[1 - \Re_p \left(\frac{\Pi+\chi_p+R_p^*}{\Pi}\right)\right] = 0.$$

Then, derivatives of $f(\lambda_p^*)$ become

$$f'(\lambda_p^*) = \left[2(\eta_p + \mu)\lambda_p^*\right] + \mu \left[1 - \Re_p \left(\frac{\Pi + \chi_p + R_p^*}{\Pi}\right)\right].$$

Evaluating $f'(\lambda_p^*)$ at $\lambda_p^* = -D_2/D_1$ gives

$$f'(-D_2/D_1) = 3\mu \left[1 - \Re_p \left(\frac{\Pi + \chi_p + R_p^*}{\Pi}\right)\right],$$

$\Rightarrow |f'(\lambda_p^*)| < 1$ at $\lambda_p^* = -D_2/D_1$, whenever $\Re_p \left(\frac{\Pi+\chi_p+R_p^*}{\Pi}\right) > 1$.

Therefore, the unique endemic equilibrium is locally asymptotically stable if $\Re_p > 1$.

## 4. Analysis HIV only Model

Here analysis of HIV only model is considered and model equation obtained from *Eq. (1)*. This is

$$\begin{aligned}
\frac{dS}{dt} &= \Pi - (\lambda_h + \mu)S, \qquad (9)\\
\frac{dE_h}{dt} &= \lambda_h S - (\eta_h + \mu)E_h,\\
\frac{dI_h}{dt} &= \eta_h E_h - (\alpha_h + \mu)I_h,\\
\frac{dA}{dt} &= \alpha_h I_h - (\mu + \xi)A.
\end{aligned}$$

The invariant region, existence of solution and uniqueness of solution is can be determined similar to Section 3.1, 3.2, and 3.3.

### *4.1. Local Stability of the Disease-Free Equilibrium (DFE)*

The disease free equilibrium of *Eq. (9)* is obtained by setting the system of equations in *Model (9)* to zero. At disease free equilibrium there are no infection and recovery. Then we obtain

$$E_2 = \left\{\left(\frac{\Pi}{\mu}\right), \quad 0, \quad 0, \quad 0\right\}.$$

The stability analysis of the DFE, $E_2$, can be established using basic reproduction number. The concept of the next generation matrix would be employed in computing the basic reproduction number. Using theorem 2 in Van den Driessche and Watmouth [23] on the HIV model in *Eq. (9)*, the basic reproduction number of the HIV only model, denoted by $\Re_h$ is then given by

$$\Re_h = \frac{(\beta_h \eta_h)}{(\alpha_h + \mu)(\mu + \xi)}.$$

Further using theorem 2 in Van den Driessche and Watmouth [23], the following result is established. The DFE is locally asymptotically stable if $\Re_h < 1$ and unstable is $\Re_h > 1$.

### *4.2. Stability Analysis of Endemic Equilibrium*

The endemic equilibrium points are computed by setting the system of differential equations in the HIV only *Model (9)* to zero. The endemic equilibrium points are as follows:

$$S^* = [\Pi]/[\lambda_h^* + \mu], \tag{10}$$

$$E_h^* = [\lambda_h^* \Pi]/[(\lambda_h^* + \mu)(\eta_h + \mu)],$$

$$I_h^* = [\lambda_h^* \eta_h \Pi]/[(\lambda_h^* + \mu)(\eta_h + \mu)(\alpha_h + \mu)],$$

$$A^* = [\lambda_h^* \eta_h \alpha_h \Pi]/[(\lambda_h^* + \mu)(\eta_h + \mu)(\alpha_h + \mu)(\mu + \xi)].$$

*Lemma 4.* The HIV only model has a unique endemic equilibrium if and only if $\Re_h > 1$.

*Proof.* Substituting *Eq. (10)* into force of infection, we can get

$$(\eta_h + \mu)(\lambda_h^*)^2 + \lambda_h^* \mu[1 - \Re_h] = 0. \tag{11}$$

This shows that the non-zero (positive endemic) equilibrium point of the model equation satisfy

$$D_1 \lambda_h^* + D_2 = 0. \tag{12}$$

Where $D_1 = (\eta_h + \mu)$ and $D_2 = \mu[1 - \Re_h]$.

It is clear that $D_1 > 0$ and $D_2 < 0$ when $\Re_h > 1$. Thus the *Linear System (12)* has a unique positive solution, given by $\lambda_h^* = \frac{-D_2}{D_1}$ whenever $\Re_h > 1$.

Now, to show its local stability analysis, *Eq. (11)* gives a fixed point problem of the form

$$f(\lambda_h^*) = (\eta_h + \mu)(\lambda_h^*)^2 + \lambda_h^* \mu[1 - \Re_h] = 0.$$

Then, derivatives of $f(\lambda_h^*)$ become

$$f'(\lambda_h^*) = [2(\eta_h + \mu)\lambda_h^*] + \mu[1 - \Re_h]].$$

Evaluating $f'(\lambda_h^*)$ at $\lambda_h^* = -D_2/D_1$ gives

$$f'(-D_2/D_1) = 3\mu[1 - \Re_h]],$$

$\Rightarrow |f'(\lambda_h^*)| < 1$ at $\lambda_h^* = -D_2/D_1$ , whenever $\Re_h > 1$.

Therefore, the unique endemic equilibrium is locally asymptotically stable if $\Re_h > 1$.

## 5. Analysis HSV-II only Model

Here analysis of HSV-II only model is considered and model equation obtained from *Eq. (1)*. This is

$$\begin{aligned}
\frac{dS}{dt} &= \Pi + \chi_s R_s - (\lambda_s + \mu)S, \\
\frac{dE_s}{dt} &= \lambda_s S - (\eta_s + \mu)E_s, \\
\frac{dI_s}{dt} &= \eta_s E_h - (\alpha_s + \omega_s + \mu)I_s, \\
\frac{dH}{dt} &= \alpha_s I_s - (\mu + \xi)H, \\
\frac{dR_s}{dt} &= \omega_s I_s - (\chi_s + \mu)R_s.
\end{aligned} \tag{13}$$

The invariant region, existence of solution and uniqueness of solution is can be determined similar to Section 3.1, 3.2, and 3.3.

### *5.1. Local Stability of the Disease-Free Equilibrium (DFE)*

The disease free equilibrium of *Eq. (13)* is obtained by setting the system of equations in *Model (13)* to zero. At disease free equilibrium there are no infection and recovery. Then we obtain;

$$E_3 = \left\{\left(\frac{\Pi}{\mu}\right), \quad 0, \quad 0, \quad 0, \quad 0\right\}.$$

The stability analysis of the DFE, $E_3$, can be established using basic reproduction number. The concept of the next generation matrix would be employed in computing the basic reproduction number. Using theorem 2 in Van den Driessche and Watmouth [23] on the HSV-II model in *Eq. (13)*, the basic reproduction number of the HSV-II only model, denoted by $\Re_s$ is then given by

$$\Re_s = \frac{(\beta_s \eta_s)}{(\alpha_s + \omega_s + \mu)(\mu + \xi)}.$$

Further using theorem 2 in Van den Driessche and Watmouth [23], the following result is established. The DFE is locally asymptotically stable if $\Re_s < 1$ and unstable is $\Re_s > 1$.

### *5.2. Stability Analysis of Endemic Equilibrium*

The endemic equilibrium points are computed by setting the system of differential equations in the HSV-II only *Model (13)* to zero. The endemic equilibrium points are as follows

$$S^* = [\Pi + \chi_s R_s^*]/[\lambda_s^* + \mu], \tag{14}$$

$$E_s^* = [\lambda_s^*(\Pi + \chi_s R_s^*)]/[(\lambda_s^* + \mu)(\eta_s + \mu)],$$

$$I_s^* = [\lambda_s^* \eta_s(\Pi + \chi_s R_s^*)]/[(\lambda_s^* + \mu)(\eta_s + \mu)(\alpha_s + \omega_s + \mu)],$$

$$H^* = [\lambda_s^* \eta_s \alpha_s(\Pi + \chi_s R_s^*)]/[(\lambda_s^* + \mu)(\eta_s + \mu)(\alpha_s + \omega_s + \mu)(\mu + \xi)]\, R_s^*$$
$$= [\omega_s \eta_s \Pi \lambda_s^*]/[(\lambda_s^* + \mu)(\eta_s^* + \mu)(\alpha_s + \omega_s + \mu)(\chi_s + \mu) - \omega_s \eta_s \lambda_s^* \chi_s].$$

*Lemma 5.* The HSV-II only model has a unique endemic equilibrium if and only if $\Re_s > 1$.

*Proof.* Substituting *Eq. (10)* into force of infection, we can get

$$(\eta_s + \mu)(\lambda_s^*)^2 + \lambda_s^* \mu \left[1 - \Re_s \left(\frac{\Pi + \chi_s + R_s^*}{\Pi}\right)\right] = 0. \tag{15}$$

This shows that the non-zero (positive endemic) equilibrium point of the model equation satisfy

$$D_1 \lambda_s^* + D_2 = 0. \tag{16}$$

Where $D_1 = (\eta_s + \mu)$and $D_2 = \mu \left[1 - \Re_s \left(\frac{\Pi + \chi_s + R_s^*}{\Pi}\right)\right]$.

It is clear that $D_1 > 0$ and $D_2 < 0$ when $\Re_s \left(\frac{\Pi + \chi_s + R_s^*}{\Pi}\right) > 1$. Thus the *Linear System (16)* has a unique positive solution, given by $\lambda_s^* = \frac{-D_2}{D_1}$ whenever $\Re_s > 1$.

Now, to show its local stability analysis, *Eq. (15)* gives a fixed point problem of the form

$$f(\lambda_s^*) = (\eta_s + \mu)(\lambda_s^*)^2 + \lambda_s^*\mu\left[1 - \Re_s\left(\frac{\Pi + \chi_s + R_s^*}{\Pi}\right)\right] = 0.$$

Then, derivatives of $f(\lambda_s^*)$ become

$$f'(\lambda_s^*) = [2(\eta_s + \mu)\lambda_s^*] + \mu\left[1 - \Re_s\left(\frac{\Pi + \chi_s + R_s^*}{\Pi}\right)\right].$$

Evaluating $f'(\lambda_s^*)$ at $\lambda_s^* = -D_2/D_1$ gives

$$f'(-D_2/D_1) = 3\mu\left[1 - \Re_s\left(\frac{\Pi + \chi_s + R_s^*}{\Pi}\right)\right].$$

$\Rightarrow |f'(\lambda_s^*)| < 1$ at $\lambda_s^* = -D_2/D_1$ , whenever $\Re_s\left(\frac{\Pi+\chi_s+R_s^*}{\Pi}\right) > 1$.

Therefore, the unique endemic equilibrium is locally asymptotically stable if $\Re_s > 1$.

## 6. Analysis HPV-HIV only Coinfection Model

Here analysis of HPV-HIV only coinfection model is considered and model equation obtained from *Eq. (1)*. This is

$$\frac{dS}{dt} = \Pi - (\lambda_{ph} + \mu)S, \tag{17}$$

$$\frac{dE_{ph}}{dt} = \lambda_{ph}S - (\eta_{ph} + \mu)E_{ph},$$

$$\frac{dI_{ph}}{dt} = \eta_{ph}E_{ph} - (\alpha_{ph} + \mu)I_{ph},$$

$$\frac{dCA}{dt} = \alpha_{ph}I_{ph} - (\mu + \xi)CA.$$

The invariant region, existence of solution and uniqueness of solution is can be determined similar to section 3.1, 3.2, and 3.3.

### *6.1. Local Stability of the Disease-Free Equilibrium (DFE)*

The disease free equilibrium of *Eq. (17)* is obtained by setting the system of equations in *Model (17)* to zero. At disease free equilibrium there are no infection and recovery. Then we obtain

$$E_4 = \left\{\left(\frac{\Pi}{\mu}\right), \quad 0, \quad 0, \quad 0\right\}.$$

The stability analysis of the DFE, $E_4$, can be established using basic reproduction number. The concept of the next generation matrix would be employed in computing the basic reproduction number. Using theorem 2 in Van den Driessche and Watmouth [23] on the HPV-HIV coinfection model in *Eq. (17)*,

the basic reproduction number of the HPV-HIV only coinfection model, denoted by $\mathfrak{R}_{ph}$ is then given by

$$\mathfrak{R}_{\mathrm{ph}} = \frac{(\beta_{\mathrm{ph}}\eta_{\mathrm{ph}})}{(\alpha_{\mathrm{ph}} + \mu)(\mu + \xi)}.$$

Further using theorem 2 in Van den Driessche and Watmouth [23], the following result is established. The DFE is locally asymptotically stable if $\mathfrak{R}_{ph} < 1$ and unstable is $\mathfrak{R}_{ph} > 1$.

### *6.2. Stability Analysis of Endemic Equilibrium*

The endemic equilibrium points are computed by setting the system of differential equations in the HPV-HIV only *Coinfection Model (17)* to zero. The endemic equilibrium points are as follows;

$$S^* = [\Pi]/[\lambda_{ph}^* + \mu], \tag{18}$$

$$E_{ph}^* = [\lambda_{ph}^*\Pi]/[(\lambda_{ph}^* + \mu)(\eta_{ph} + \mu)],$$

$$I_{ph}^* = [\lambda_{ph}^*\eta_{ph}\Pi]/[(\lambda_{ph}^* + \mu)(\eta_{ph} + \mu)(\alpha_{ph} + \mu)],$$

$$CA^* = [\lambda_{ph}^*\eta_{ph}\alpha_{ph}\Pi]/[(\lambda_{ph}^* + \mu)(\eta_{ph} + \mu)(\alpha_{ph} + \mu)(\mu + \xi)].$$

*Lemma 6.* The HPV-HIV only coinfection model has a unique endemic equilibrium if and only if $\mathfrak{R}_{ph} > 1$.

*Proof.* Substituting *Eq. (18)* into force of infection, we can get

$$(\eta_{\mathrm{ph}} + \mu)(\lambda_{\mathrm{ph}}^*)^2 + \lambda_{\mathrm{ph}}^*\mu[1 - \mathfrak{R}_{\mathrm{ph}}] = 0. \tag{19}$$

This shows that the non-zero (positive endemic) equilibrium point of the model equation satisfy

$$\mathrm{D}_1\lambda_{\mathrm{ph}}^* + \mathrm{D}_2 = 0. \tag{20}$$

Where $D_1 = (\eta_{ph} + \mu)$ eand $D_2 = \mu[1 - \mathfrak{R}_{ph}]$.

It is clear that $D_1 > 0$ and $D_2 < 0$ when $\mathfrak{R}_{ph} > 1$. Thus the *Linear System (20)* has a unique positive solution, given by $\lambda_{ph}^* = \frac{-D_2}{D_1}$ whenever $\mathfrak{R}_{ph} > 1$.

Now, to show its local stability analysis, *Eq. (19)* gives a fixed point problem of the form

$$f(\lambda_{ph}^*) = (\eta_{ph} + \mu)(\lambda_{ph}^*)^2 + \lambda_{ph}^* \mu[1 - \Re_{ph}] = 0.$$

Then, derivatives of $f(\lambda_{ph}^*)$ become

$$f'(\lambda_{ph}^*) = [2(\eta_{ph} + \mu)\lambda_{ph}^*] + \mu[1 - \Re_{ph}].$$

Evaluating $f'(\lambda_{ph}^*)$ at $\lambda_{ph}^* = -D_2/D_1$ gives

$f'(-D_2/D_1) = 3\,\mu[1 - \Re_{ph}] \Rightarrow |f'(\lambda_{ph}^*)| < 1$ at $\lambda_{ph}^* = -D_2/D_1$ , whenever $\Re_{ph} > 1$.

Therefore, the unique endemic equilibrium is locally asymptotically stable if $\Re_{ph} > 1$.

## 7. Analysis HPV-HSV-II only Coinfection Model

Here analysis of HPV-HSV-II only coinfection model is considered and model equation obtained from *Eq. (1)*. This is

$$\frac{dS}{dt} = \Pi - (\lambda_{ps} + \mu)S, \tag{21}$$

$$\frac{dE_{ps}}{dt} = \lambda_{ps}S - (\eta_{ps} + \mu)E_{ps},$$

$$\frac{dI_{ps}}{dt} = \eta_{ps}E_{ps} - (\alpha_{ps} + \mu)I_{ps},$$

$$\frac{dCH}{dt} = \alpha_{ps}I_{ps} - (\mu + \xi)CH.$$

The invariant region, existence of solution and uniqueness of solution is can be determined similar to Section 3.1, 3.2, and 3.3.

### *7.1. Local Stability of the Disease-Free Equilibrium (DFE)*

The disease free equilibrium of *Eq. (21)* is obtained by setting the system of equations in *Model (21)* to zero. At disease free equilibrium there are no infection and recovery. Then we obtain;

$$E_5 = \left\{\left(\frac{\Pi}{\mu}\right), \quad 0, \quad 0, \quad 0\right\}.$$

The stability analysis of the DFE, $E_5$, can be established using basic reproduction number. The concept of the next generation matrix would be employed in computing the basic reproduction number. Using theorem 2 in Van den Driessche and Watmouth [23] on the HPV-HSV-II coinfection model in *Eq. (21)*, the basic reproduction number of the HPV-HSV-II only coinfection model, denoted by $\Re_{ps}$ is then given by

$$\Re_{ps} = \frac{(\beta_{ps}\eta_{ps})}{(\alpha_{ps} + \mu)(\mu + \xi)}.$$

Further using theorem 2 in Van den Driessche and Watmouth [23], the following result is established. The DFE is locally asymptotically stable if $\Re_{ps} < 1$ and unstable is $\Re_{ps} > 1$.

### *7.2. Stability Analysis of Endemic Equilibrium*

The endemic equilibrium points are computed by setting the system of differential equations in the HPV-HSV-II only *Coinfection Model (21)* to zero. The endemic equilibrium points are as follows;

$$S^* = [\Pi]/[\lambda_{ps}^* + \mu], \tag{22}$$

$$E_{ps}^* = [\lambda_{ps}^* \Pi]/[(\lambda_{ps}^* + \mu)(\eta_{ps} + \mu)],$$

$$I_{ps}^* = [\lambda_{ps}^* \eta_{ps} \Pi]/[(\lambda_{ps}^* + \mu)(\eta_{ps} + \mu)(\alpha_{ps} + \mu)],$$

$$CH^* = [\lambda_{ps}^* \eta_{ps} \alpha_{ps} \Pi]/[(\lambda_{ps}^* + \mu)(\eta_{ps} + \mu)(\alpha_{ps} + \mu)(\mu + \xi)].$$

*Lemma 7.* The HPV-HSV-II only coinfection model has a unique endemic equilibrium if and only if $\Re_{ps} > 1$.

*Proof.* Substituting *Eq. (22)* into force of infection, we can get

$$(\eta_{ps} + \mu)(\lambda_{ps}^*)^2 + \lambda_{ps}^* \mu[1 - \Re_{ps}] = 0. \tag{23}$$

This shows that the non-zero (positive endemic) equilibrium point of the model equation satisfy

$$D_1 \lambda_{ps}^* + D_2 = 0. \tag{24}$$

Where $D_1 = (\eta_{ps} + \mu)$ and $D_2 = \mu[1 - \Re_{ps}]$.

It is clear that $D_1 > 0$ and $D_2 < 0$ when $\Re_{ps} > 1$. Thus the *Linear System (24)* has a unique positive solution, given by $\lambda_{ps}^* = \frac{-D_2}{D_1}$ whenever $\Re_{ps} > 1$.

Now, to show its local stability analysis, *Eq. (23)* gives a fixed point problem of the form

$$f(\lambda_{ps}^*) = (\eta_{ps} + \mu)(\lambda_{ps}^*)^2 + \lambda_{ps}^* \mu[1 - \Re_{ps}] = 0.$$

Then, derivatives of $f(\lambda_{ps}^*)$ become

$$f'(\lambda_{ps}^*) = [2(\eta_{ps} + \mu)\lambda_{ps}^*] + \mu[1 - \Re_{ps}]].$$

Evaluating $f'(\lambda_{ps}^*)$ at $\lambda_{ps}^* = -D_2/D_1$ gives

$$f'(-D_2/D_1) = 3\mu[1 - \Re_{ps}]],$$

$\Rightarrow |f'(\lambda_{ps}^*)| < 1$ at $\lambda_{ps}^* = -D_2/D_1$ , whenever $\Re_{ps} > 1$.

Therefore, the unique endemic equilibrium is locally asymptotically stable if $\Re_{ps} > 1$.

## 8. Analysis HIV-HSV-II only Coinfection Model

Here analysis of HIV-HSV-II only coinfection model is considered and model equation obtained from *Eq. (1)*. This is

$$\frac{dS}{dt} = \Pi - (\lambda_{hs} + \mu)S, \tag{25}$$

$$\frac{dE_{hs}}{dt} = \lambda_{hs}S - (\eta_{hs} + \mu)E_{hs},$$

$$\frac{dI_{hs}}{dt} = \eta_{hs}E_{hs} - (\alpha_{hs} + \mu)I_{hs},$$

$$\frac{dAH}{dt} = \alpha_{hs}I_{hs} - (\mu + \xi)AH.$$

The invariant region, existence of solution and uniqueness of solution is can be determined similar to Section 3.1, 3.2, and 3.3.

### *8.1. Local Stability of the Disease-Free Equilibrium (DFE)*

The disease free equilibrium of *Eq. (25)* is obtained by setting the system of equations in *Model (25)* to zero. At disease free equilibrium there are no infection and recovery. Then we obtain

$$E_6 = \left\{\left(\frac{\Pi}{\mu}\right), \quad 0, \quad 0, \quad 0\right\}.$$

The stability analysis of the DFE, $E_6$, can be established using basic reproduction number. The concept of the next generation matrix would be employed in computing the basic reproduction number. Using theorem 2 in Van den Driessche and Watmouth [23] on the HIV-HSV-II coinfection model in *Eq. (25)*, the basic reproduction number of the HIV-HSV-II only coinfection model, denoted by $\Re_{hs}$ is then given by

$$\Re_{hs} = \frac{(\beta_{hs}\eta_{hs})}{(\alpha_{hs} + \mu)(\mu + \xi)}.$$

Further using theorem 2 in Van den Driessche and Watmouth [23], the following result is established. The DFE is locally asymptotically stable if $\Re_{hs} < 1$ and unstable is $\Re_{hs} > 1$.

### *8.2. Stability Analysis of Endemic Equilibrium*

The endemic equilibrium points are computed by setting the system of differential equations in the HIV-HSV-II only *Coinfection Model (25)* to zero. The endemic equilibrium points are as follows

$$S^* = [\Pi]/[\lambda_{hs}^* + \mu], \tag{26}$$

$$E_{hs}^* = [\lambda_{hs}^* \Pi]/[(\lambda_{hs}^* + \mu)(\eta_{hs} + \mu)],$$

$$I_{hs}^* = [\lambda_{hs}^* \eta_{hs} \Pi]/[(\lambda_{hs}^* + \mu)(\eta_{hs} + \mu)(\alpha_{hs} + \mu)],$$

$$AH^* = [\lambda_{hs}^* \eta_{hs} \alpha_{hs} \Pi]/[(\lambda_{hs}^* + \mu)(\eta_{hs} + \mu)(\alpha_{hs} + \mu)(\mu + \xi)].$$

*Lemma 7.* The HIV-HSV-II only coinfection model has a unique endemic equilibrium if and only if $\Re_{hs} > 1$.

*Proof.* Substituting *Eq. (26)* into force of infection, we can get

$$(\eta_{hs} + \mu)(\lambda_{hs}^*)^2 + \lambda_{hs}^* \mu[1 - \Re_{hs}] = 0. \tag{27}$$

This shows that the non-zero (positive endemic) equilibrium point of the model equation satisfy

$$D_1 \lambda_{hs}^* + D_2 = 0. \tag{28}$$

Where $D_1 = (\eta_{hs} + \mu)$ and $D_2 = \mu[1 - \Re_{hs}]$.

It is clear that $D_1 > 0$ and $D_2 < 0$ when $\Re_{hs} > 1$. Thus the *Linear System (28)* has a unique positive solution, given by $\lambda_{hs}^* = \frac{-D_2}{D_1}$ whenever $\Re_{hs} > 1$.

Now, to show its local stability analysis, *Eq. (27)* gives a fixed point problem of the form

$$f(\lambda_{hs}^*) = (\eta_{hs} + \mu)(\lambda_{hs}^*)^2 + \lambda_{hs}^* \mu[1 - \Re_{hs}] = 0.$$

Then, derivatives of $f(\lambda_{hs}^*)$ become

$$f'(\lambda_{hs}^*) = [2(\eta_{hs} + \mu)\lambda_{hs}^*] + \mu[1 - \Re_{hs}]].$$

Evaluating $f'(\lambda_{hs}^*)$ at $\lambda_{hs}^* = -D_2/D_1$ gives

$$f'(-D_2/D_1) = 3\mu[1 - \Re_{hs}]],$$

$\Rightarrow |f'(\lambda_{hs}^*)| < 1$ at $\lambda_{hs}^* = -D_2/D_1$ , whenever $\Re_{hs} > 1$.

Therefore, the unique endemic equilibrium is locally asymptotically stable if $\Re_{hs} > 1$.

## 9. Analysis HPV-HIV-HSV-II only Coinfection Model

Here analysis of HPV-HIV-HSV-II *Coinfection Model (1)* is considered. The invariant region, existence of solution and uniqueness of solution is can be determined similar to Section 3.1, 3.2, and 3.3.

### *9.1. Local Stability of the Disease-Free Equilibrium (DFE)*

The disease free equilibrium of *Eq. (1)* is obtained by setting the system of equations in *Model (1)* to zero. At disease free equilibrium there are no infection and recovery. Then we obtain;

$$\mathrm{E}_7 = \left\{\left(\frac{\Pi}{\mu}\right), 0, 0, 0, 0, 0, 0, 0, 0, 0, 0, 0, 0, 0, 0, 0, 0, 0, 0, 0, 0, 0, 0\right\}.$$

The stability analysis of the DFE, $E_7$, can be established using basic reproduction number. The concept of the next generation matrix would be employed in computing the basic reproduction number. Using theorem 2 in Van den Driessche and Watmouth [23] on the HPV-HIV-HSV-II coinfection model in *Eq. (1)*, the basic reproduction number of the HPV-HIV-HSV-II only coinfection model, denoted by $\Re_{phs}$ is then given by

$$\Re_{\mathrm{phs}} = \max\{\Re_{\mathrm{p}}, \Re_{\mathrm{h}}, \Re_{\mathrm{s}}, \Re_{\mathrm{ph}}, \Re_{\mathrm{ps}}, \Re_{\mathrm{hs}}\}.$$

Where

$$\Re_{\mathrm{p}} = \frac{(\beta_{\mathrm{p}}\eta_{\mathrm{p}})}{(\alpha_{\mathrm{p}}+\omega_{\mathrm{p}}+\mu)(\mu+\xi)}, \qquad \Re_{\mathrm{ph}} = \frac{(\beta_{\mathrm{ph}}\eta_{\mathrm{ph}})}{(\alpha_{\mathrm{ph}}+\mu)(\mu+\xi)},$$

$$\Re_{\mathrm{h}} = \frac{(\beta_{\mathrm{h}}\eta_{\mathrm{h}})}{(\alpha_{\mathrm{h}}+\mu)(\mu+\xi)}, \qquad \Re_{\mathrm{ps}} = \frac{(\beta_{\mathrm{ps}}\eta_{\mathrm{ps}})}{(\alpha_{\mathrm{ps}}+\mu)(\mu+\xi)},$$

$$\Re_{\mathrm{s}} = \frac{(\beta_{\mathrm{s}}\eta_{\mathrm{s}})}{(\alpha_{\mathrm{s}}+\omega_{\mathrm{s}}+\mu)(\mu+\xi)}, \qquad \Re_{\mathrm{hs}} = \frac{(\beta_{\mathrm{hs}}\eta_{\mathrm{hs}})}{(\alpha_{\mathrm{hs}}+\mu)(\mu+\xi)}.$$

Further using theorem 2 in Van den Driessche and Watmouth [23], the following result is established. The DFE is locally asymptotically stable if $\Re_{phs} < 1$ and unstable is $\Re_{phs} > 1$.

## 10. Numerical Simulation

In this section, numerical simulation study of model *Eqs. (1), (2), (9), (13), (17), (21)* and *(25)* are carried out using the software MATLAB R 2015b with ODE45 solver. To conduct the study, a set of physically meaningful values are assigned to the model parameters. These values are either taken from literature or assumed on the basis of reality. Using the parameter values given in *Table 2* and the initial conditions $S(0) = 600,\ E_p(0) = 170,\ E_{ph}(0) = 250,\ E_{ps}(0) = 200, E_h(0) = 200,\ E_{hs}(0) = 240,\ E_s(0) = 250,\ I_p(0) = 140,\ I_{ph}(0) = 140,\ I_{ps}(0) = 140,\ I_h(0) = 160,\ I_{hs}(0) = 180, I_s(0) = 160,\ A(0) = 40,\ C(0) = 60,\ CA(0) = 40,\ AH(0) = 50,\ CH(0) = 50,\ H(0) = 50\ , ACH(0) = 30, R_p = 120, R_s = 130$ in the model

*Eqs. (1), (2), (9), (13), (17), (21)* and *(25)* a simulation study is conducted and the results are given in the following Figures.

***Table 2.*** *Parameter values used in simulations.*

| Parameter | Value | Source | Parameter | Value | Source |
|---|---|---|---|---|---|
| $\Pi$ | *0.004* | *[18]* | $\pi$ | *0.01* | *assumed* |
| $\beta_s$ | *0.0018* | *assumed* | $\psi$ | *0.3* | *assumed* |
| $\beta_h$ | *0.042* | *assumed* | $\delta$ | *0.12* | *assumed* |
| $\beta_p$ | *0.042* | *assumed* | $\gamma$ | *0.14* | *assumed* |
| $\beta_{ph}$ | *0.019* | *assumed* | $\nu_{19}$ | *0.02* | *assumed* |
| $\beta_{ps}$ | *0.03* | *assumed* | $\nu_1$ | *0.04* | *assumed* |
| $\beta_{hs}$ | *0.02* | *assumed* | $\nu_2$ | *0.02* | *assumed* |
| $\chi_p$ | *0.045* | *assumed* | $\nu_{20}$ | *0.03* | *assumed* |
| $\chi_s$ | *0.045* | *assumed* | $\nu_3$ | *0.04* | *assumed* |
| $\eta_s$ | *0.02* | *assumed* | $\nu_4$ | *0.05* | *assumed* |
| $\eta_h$ | *0.02* | *assumed* | $\nu_{15}$ | *0.02* | *assumed* |
| $\eta_p$ | *0.02* | *assumed* | $\nu_6$ | *0.03* | *assumed* |
| $\eta_{ph}$ | *0.02* | *assumed* | $\nu_7$ | *0.04* | *assumed* |
| $\eta_{ps}$ | *0.02* | *assumed* | $\nu_{16}$ | *0.03* | *assumed* |
| $\eta_{hs}$ | *0.02* | *assumed* | $\nu_8$ | *0.02* | *assumed* |
| $\alpha_s$ | *0.03* | *assumed* | $\nu_9$ | *0.02* | *assumed* |
| $\alpha_h$ | *0.03* | *assumed* | $\nu_{10}$ | *0.03* | *assumed* |
| $\alpha_p$ | *0.03* | *assumed* | $\nu_{17}$ | *0.04* | *assumed* |
| $\alpha_{ph}$ | *0.03* | *assumed* | $\nu_{11}$ | *0.05* | *assumed* |
| $\alpha_{ps}$ | *0.03* | *assumed* | $\nu_{18}$ | *0.02* | *assumed* |
| $\alpha_{hs}$ | *0.03* | *assumed* | $\nu_{12}$ | *0.03* | *assumed* |
| $\omega_p$ | *0.035* | *assumed* | $\nu_{13}$ | *0.04* | *assumed* |
| $\omega_s$ | *0.045* | *assumed* | $\varphi$ | *0.1* | *assumed* |
| $\xi$ | *0.0001* | *[18]* | $\theta$ | *0.2* | *assumed* |

In *Fig. 2* we observe that all the solutions converge towards the equilibrium point. This was obtained when $\Re_p < 1$. At disease free equilibrium point, all infection solutions converge to zero while the susceptible individuals decreases and then remains constant. Cervical cancer cannot be cured that is why susceptible individuals remain constant. This indicates that the disease free equilibrium point is locally asymptotically stable.

*Fig. 3* illustrate that all the solutions converge towards the equilibrium point. This was obtained when $\Re_h < 1$. At disease free equilibrium point, all infection solutions converge to zero while the susceptible individuals decreases and then remains constant. AID cannot be cured that is why susceptible individuals remain constant. This indicates that the disease free equilibrium point is locally asymptotically stable. *Fig. 4* show that all the solutions converge towards the equilibrium point. This was obtained when $\Re_s < 1$. At disease free equilibrium point, all infection solutions converge to zero while the susceptible individuals decreases and then remains constant. This indicates that the disease free equilibrium point is locally asymptotically stable.

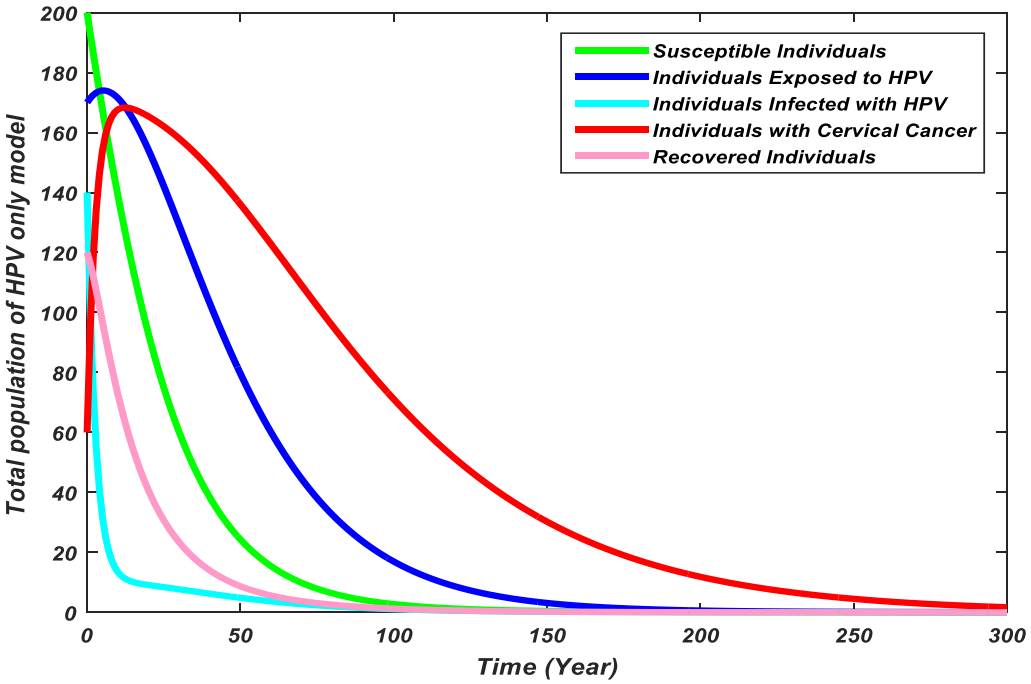


***Fig. 2.*** *Dynamics of HPV model.*

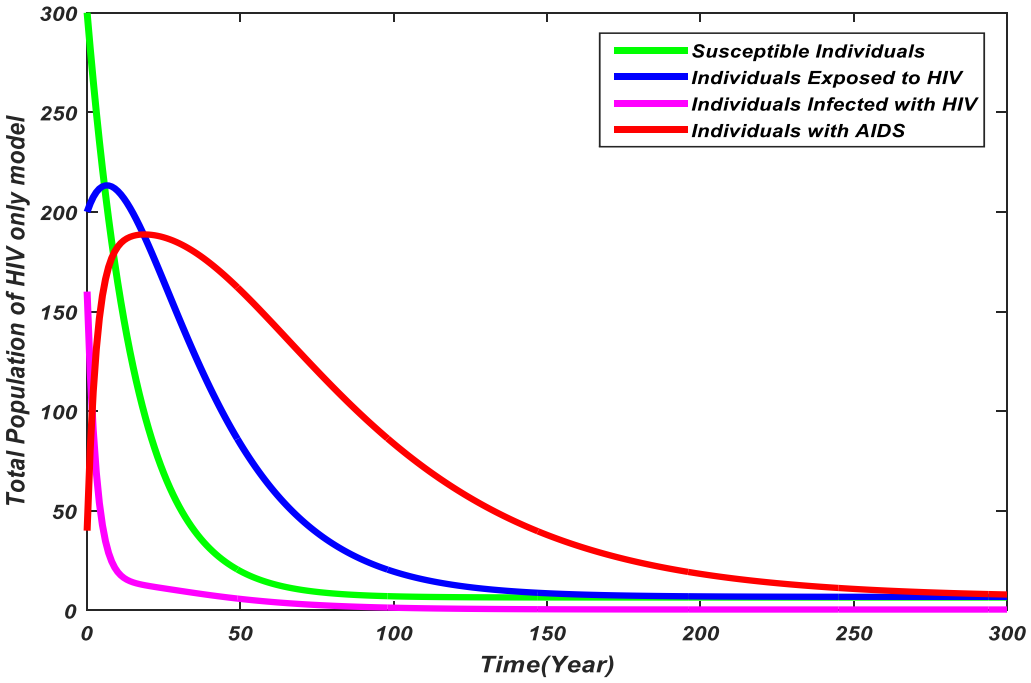


***Fig. 3.*** *Dynamics of HIV model.*

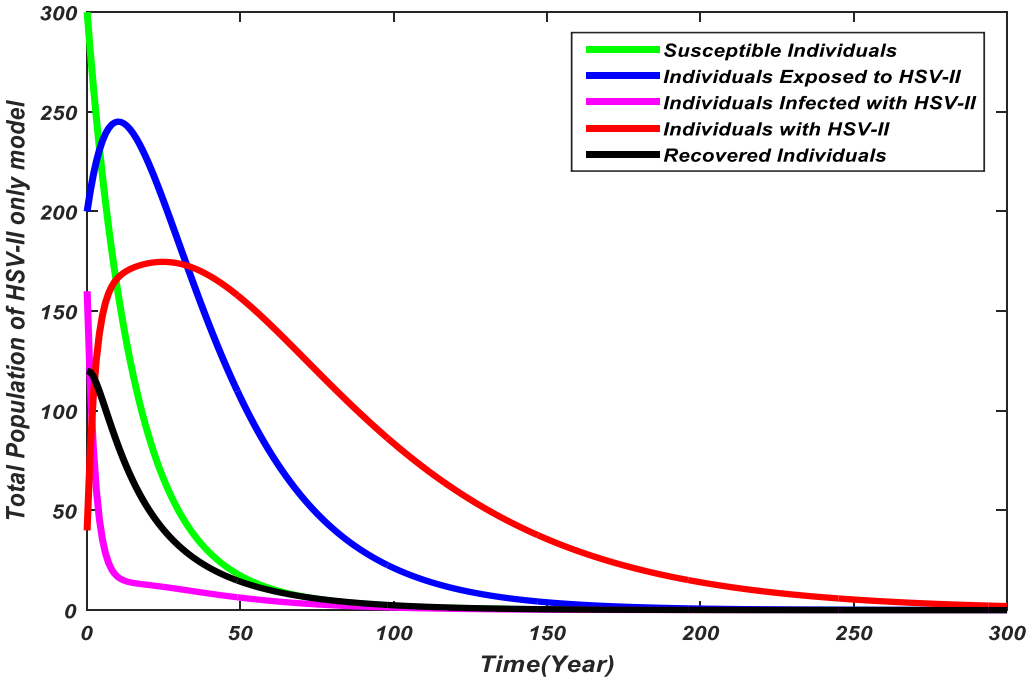


***Fig. 4.*** *Dynamics of HSV-II.*

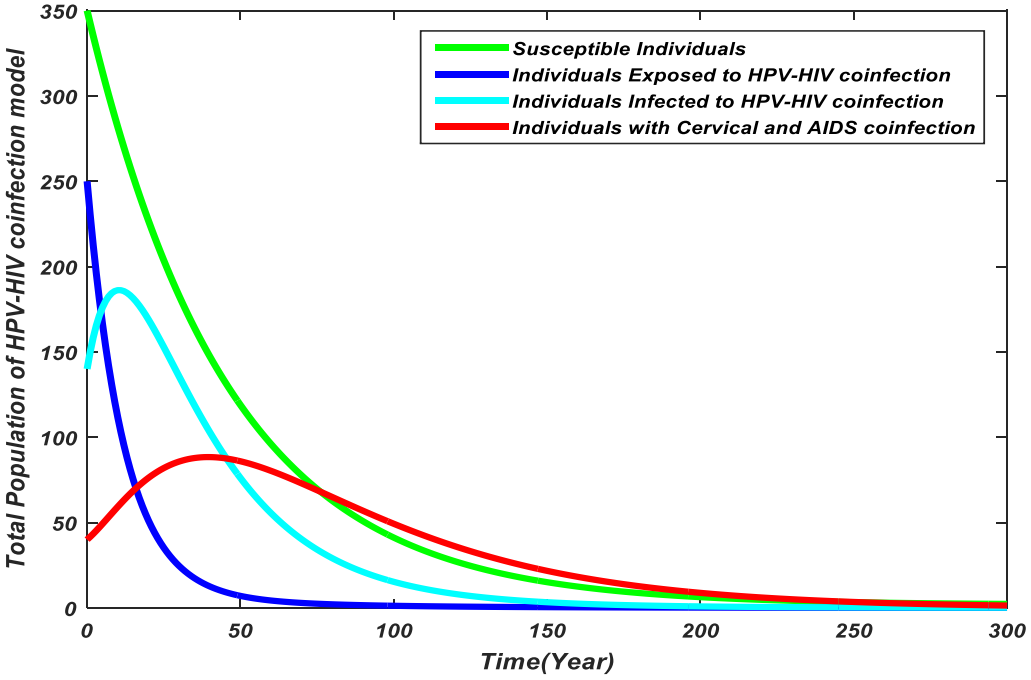


***Fig. 5.*** *Dynamics of HPV-HIV coinfection.*

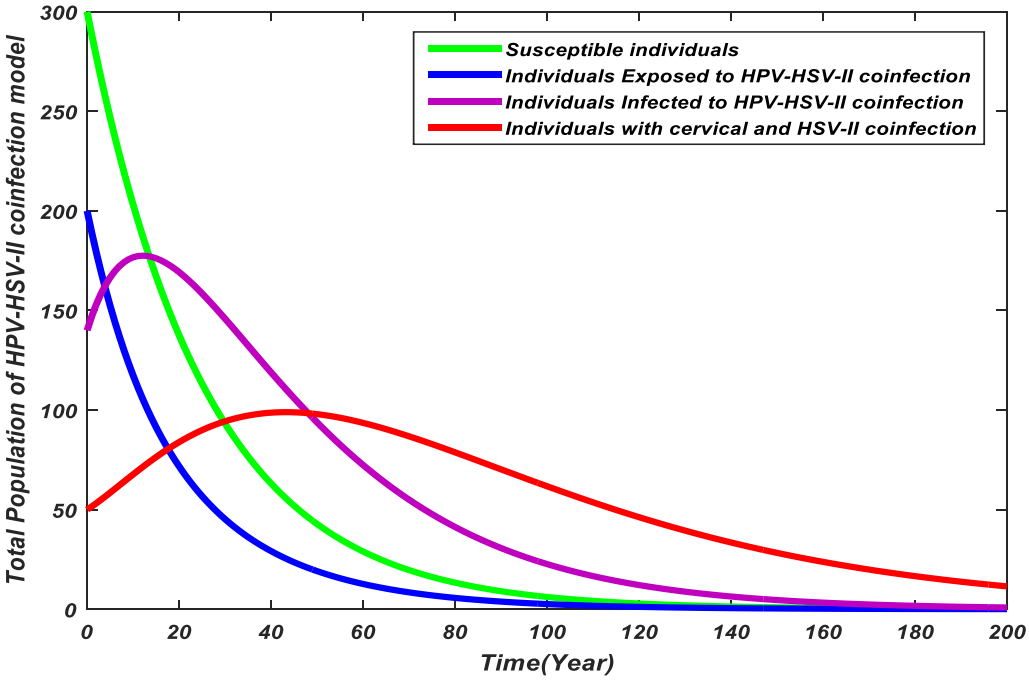


***Fig. 6.*** *Dynamics of HPV-HSV-II coinfection.*

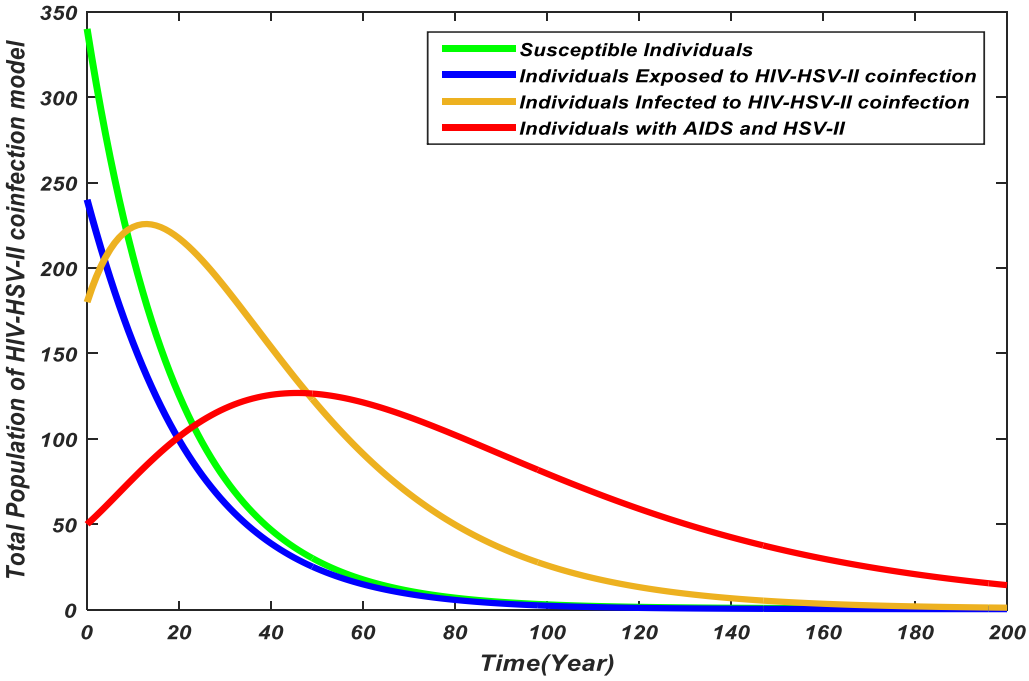


***Fig. 7.*** *Dynamics of HIV-HSV-II coinfection.*

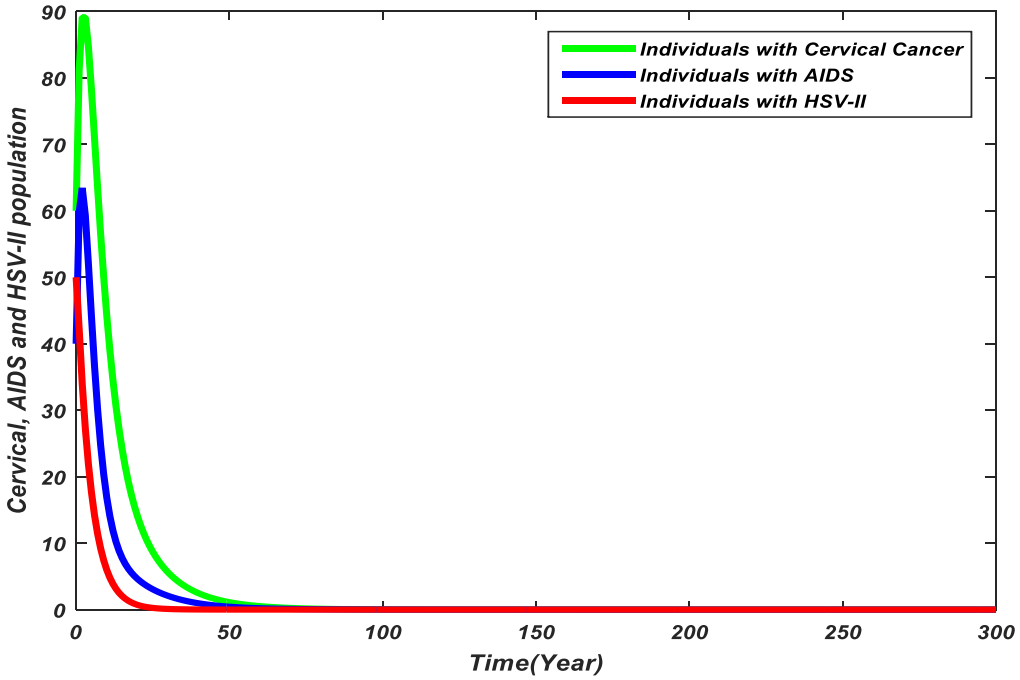


***Fig. 8.*** *Dynamics of cervical cancer, AIDS and HSV-II.*

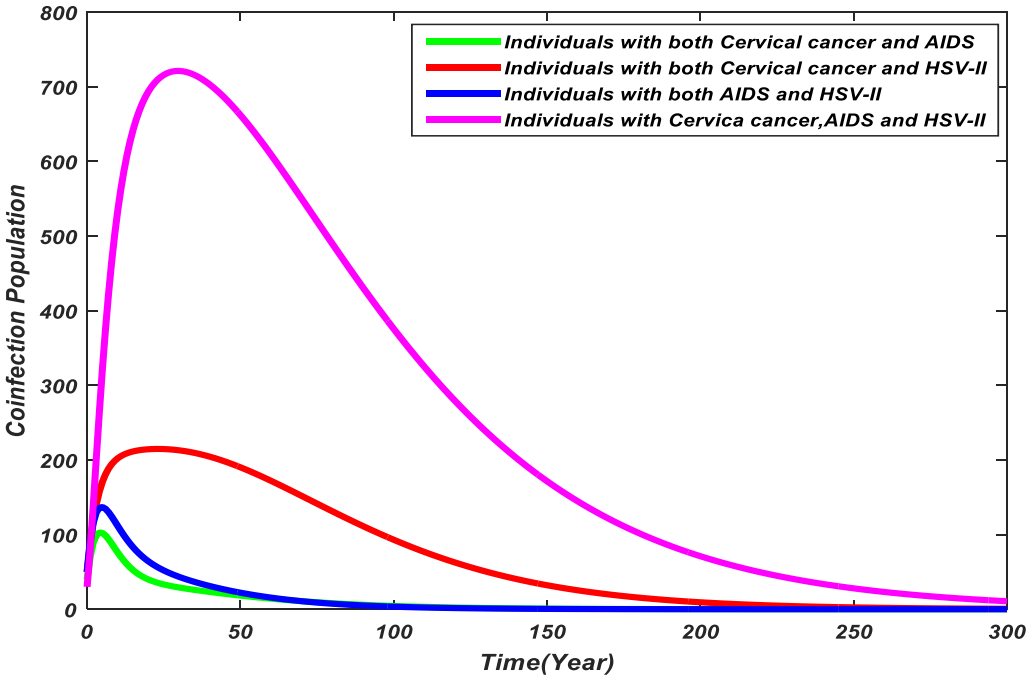


***Fig. 9.*** *Dynamics of co-infectious.*

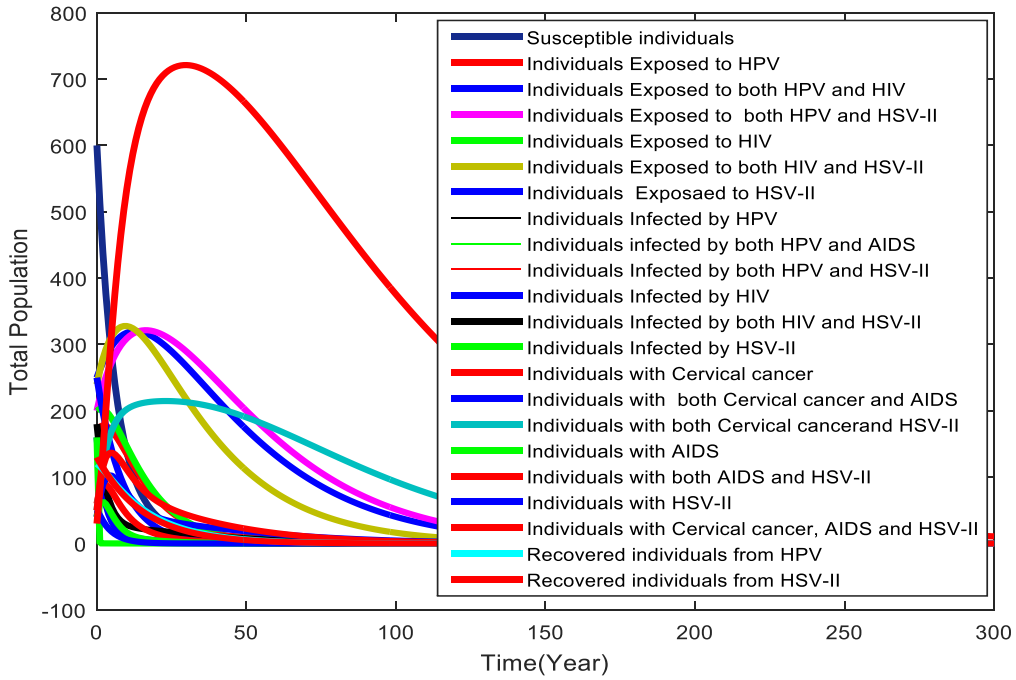


***Fig. 10.*** *Dynamics of total population*.

Furthermore, *Fig. 5* describe that all the solutions converge towards the equilibrium point. At disease free equilibrium point, all infection solutions converge to zero while the susceptible individuals decreases and then remains constant. AIDS with Cervical cancer cannot be cured that is why susceptible individuals remain constant. This indicates that the disease free equilibrium point is locally asymptotically stable. Also, in *Fig. 6* we observe that all the solutions converge towards the equilibrium point. At disease free equilibrium point, all infection solutions converge to zero while the susceptible individuals decreases and then remains constant. Cervical cancer with HSV-II cannot be cured that is why susceptible individuals remain constant. This indicates that the disease free equilibrium point is locally asymptotically stable. Similarly *Fig. 7* show that all solution converges to disease free equilibrium.

Moreover, *Fig. 8* illustrate that cervical cancer affects people more than AIDS and HSV-II, but AIDS affects people more than HSV-II. Also, *Fig. 9* describe that the coinfection of three diseases (i.e. Cervical cancer, AIDS and HSV-II) affects people more than coinfection of two diseases (i.e. Cervical cancer-AIDS, Cervical cancer-HSV-II, AIDS-HSV-II coinfection). Finally, *Fig. 10* show that at disease free equilibrium all solution converges to zero. This indicates that the disease free equilibrium point is locally asymptotically stable.

## 11. Discussions and Conclusions

In this paper, we developed a deterministic model for the transmission dynamics of HPV, HIV and HSV-II coinfection. The qualitative analysis of the model shows that there exists a domain where the model is epidemiologically and mathematically well-posed. The stability analysis of the model was investigated using the basic reproduction number that governs the disease transmission. The HPV only model, HIV only model, HSV-II only model, HPV-HIV only coinfection model, HPV-HSV-II only coinfection model, HIV-HSV-II only coinfection model, and HPV-HIV-HSV-II only coinfection model, has a locally stable disease free equilibrium whenever the associated reproduction number is

less than unity. Also, the model has a unique endemic equilibrium whenever the basic reproduction number is less great unity. Furthermore, numerical simulation shows that at disease free equilibrium point, all infection solutions converge to zero. This was obtained when the associated reproduction number is less than unity. This indicates that the disease free equilibrium point is locally asymptotically stable.

## Data Availability

The data used in this paper is freely accessible for the user.

## Conflicts of Interest

The authors state that there are no conflicts of interest concerning to the publication of this article.

## Reference

[1] Shahzad, N., Farooq, R., Aslam, B., & Umer, M. (2017). Microbicides for the Prevention of HPV, HIV-1, and HSV-2: Sexually Transmitted Viral Infections. In *Fundamentals of sexually transmitted infections*. DOI: 10.5772/intechopen.68927

[2] Bergot, A. S., Kassianos, A., Frazer, I. H., & Mittal, D. (2011). New approaches to immunotherapy for HPV associated cancers. *Cancers*, *3*(3), 3461-3495.

[3] Lowy, D. R., & Schiller, J. T. (2006). Prophylactic human papillomavirus vaccines. *The journal of clinical investigation*, *116*(5), 1167-1173.

[4] World Health Organization. (2017). *WHO list of priority medical devices for cancer management*. World Health Organization.

[5] Wodarz, D. (2007). *Killer cell dynamics mathematical and computational approaches to immunology*. Springer.

[6] Nowak, M., & May, R. M. (2000). *Virus dynamics: mathematical principles of immunology and virology: mathematical principles of immunology and virology*. Oxford University Press, UK.

[7] UNAIDS data 2019. (2019). Retrieved from https://www.unaids.org/en/resources/documents/2019/2019-UNAIDS-data

[8] CDC. (2001). *Genital herpes information*. Retrieved July 15, 2020, from www.cdc.gov/std/Herpes/default.htm

[9] *WHO guidelines for the treatment of genital herpes simplex virus*. (2016). World Health Organization. Retrieved from file:///C:/Users/jpour/Downloads/9789241549875-eng.pdf

[10] Taira, A. V., Neukermans, C. P., & Sanders, G. D. (2004). Evaluating human papillomavirus vaccination programs. *Emerging infectious diseases*, *10*(11), 1915-1923.

[11] Ribassin-Majed, L., Lounes, R., & Clémençon, S. (2012). Efficacy of vaccination against HPV infections to prevent cervical cancer in France: present assessment and pathways to improve vaccination policies. *PloS one*, *7*(3), e32251.

[12] Gurmu, E. D., & Koya, P. R. (2019). Sensitivity analysis and modeling the impact of screening on the transmission dynamics of human papilloma virus (HPV). *American journal of applied mathematics*, *7*(3), 70-79. Doi: 10.11648/j.ajam.20190703.11

[13] Okosun, K. O., Makinde, O. D., & Takaidza, I. (2013). Impact of optimal control on the treatment of HIV/AIDS and screening of unaware infectives. *Applied mathematical modelling*, *37*(6), 3802-3820.

[14] Silva, C. J., & Torres, D. F. (2017). Modeling and optimal control of HIV/AIDS prevention through PrEP. *Discrete and continuous dynamical systems series S*, *11*(9), 119-141. 10.3934/dcdss.2018008

[15] Gurmu, E. D., Bole, B. K., & Koya, P. R. (2020). Mathematical Modelling of HIV/AIDS Transmission Dynamics with Drug Resistance Compartment. *American journal of applied mathematics*, *8*(1), 34-45.

[16] Schiffer, J. T., Swan, D. A., Magaret, A., Schacker, T. W., Wald, A., & Corey, L. (2016). Mathematical modeling predicts that increased HSV-2 shedding in HIV-1 infected persons is due to poor immunologic control in ganglia and genital mucosa. *PloS one*, *11*(6), e0155124. Doi:10.1371/journal.pone.0155124

[17] Mhlanga, A., Bhunu, C. P., & Mushayabasa, S. (2015, November). A computational study of HSV-2 with poor treatment adherence. *Abstract and applied analysis* (Vol. 2015). https://doi.org/10.1155/2015/850670

[18] Gurmu, E. D., Bole, B. K., & Koya, P. R. (2020). Mathematical model for co-infection of HPV with cervical cancer and HIV with AIDS diseases. *Int. J. Sci. Res. in mathematical and statistical sciences*, *7*(2), 107-121.

[19] Sanga, G. G., Makinde, O. D., Massawe, E. S., & Namkinga, L. (2017). Modeling co-dynamics of Cervical cancer and HIV diseases. *Global journal of pure and applied mathematics*, *13*(6), 2057-2078.

[20] Gurmu, E. D., Bole, B. K., & Koya, P. R. (2020). A Mathematical model for co-infection of HPV and HSV-II with drug resistance compartment. *Int. J. Sci. Res. in mathematical and statistical sciences*, *7*(2), 34-46.

[21] Hühns, M., Simm, G., Erbersdobler, A., & Zimpfer, A. (2015). HPV infection, but not EBV or HHV-8 infection, is associated with salivary gland tumours. *BioMed research international*. https://doi.org/10.1155/2015/829349

[22] Mhlanga, A. (2018). A theoretical model for the transmission dynamics of HIV/HSV-2 co-infection in the presence of poor HSV-2 treatment adherence. *Applied mathematics and nonlinear sciences*, *3*(2), 603-626.

[23] Van den Driessche, P., & Watmough, J. (2002). Reproduction numbers and sub-threshold endemic equilibria for compartmental models of disease transmission. *Mathematical biosciences*, *180*(1-2), 29-48.

[24] Weinstein, S. J., Holland, M. S., Rogers, K. E., & Barlow, N. S. (2020). Analytic solution of the SEIR epidemic model via asymptotic approximant. *Physica D: nonlinear phenomena*, *411*, 132633. https://doi.org/10.1016/j.physd.2020.132633

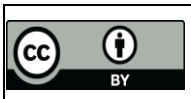

Journal of Applied Research on Industrial Engineering
www.journal-aprie.com

# A Multi-Objective Optimization Approach for a Nurse Scheduling Problem Considering the Fatigue Factor (Case Study: Labbafinejad Hospital)

***Niloofar Khalili*[1], *Parisa Shahnazari Shahrezaei*[2,*], *Amir Gholm Abri*[3]**
[1]*Department of Industrial Management, Firoozkooh Branch, Islamic Azad University, Firoozkooh, Iran.*
[2]*Department of Industrial Engineering, Firoozkooh Branch, Islamic Azad University, Firoozkooh, Iran.*
[3]*Department of Mathematics, Firoozkooh Branch, Islamic Azad University, Firoozkooh, Iran.*

**PAPER INFO**

**Chronicle:**
*Received: 02 July 2020*
*Reviewed: 08 August 2020*
*Revised: 21 October 2020*
*Accepted: 11 November 2020*

**Keywords:**
*Combined Optimization.*
*Nurses' Scheduling.*
*Ergonomic.*
*Fatigue.*
*Meta-Heuristic Algorithm.*

**ABSTRACT**

The current study, according to ergonomic factors, aims to model the nurses' work shift scheduling problem. Considering the urgent needs of the hospitals in providing better services to patients, it seems significant to take the preferences of nurses in scheduling shifts into account. Therefore, in this paper, a multi-objective model of nurses' scheduling with emphasis on reducing their fatigue during the career shift is presented. To evaluate the outputs of the model, two numerical instances in small and large sizes with real data of Labbafinejad Hospital were designed in 18-person and 90-person wards. To solve a small size problem, a comprehensive standard decision method is employed, the results of which showed that nurses take their most rest during the night shift and in the middle of their working hours to reduce fatigue. Furthermore, due to the NP-Hard nature of the nurses' scheduling problem, in the problem of the 90-person ward, MOPSO and NSGA II algorithms are applied based on the design of a new chromosome. Using the TOPSIS method and entropy weighting method shows that the designed NSGA II algorithm can solve the nurses' scheduling problem of Labbafinejad Hospital faster and better.

## 1. Introduction

In recent years, presenting the scientific approaches to make appropriate decisions in various fields of scheduling, where time is an important factor, has attracted the attention of many researchers. The issue of nurses' scheduling, as one of the important issues related to decision-making in hospitals, has received a lot of attention due to health care and the difficulty of nurses' work. In hospitals, the head nurse of each ward usually develops a monthly time schedule and tries to make sure that this schedule is

Khalili, N., Shahnazari Shahrezaei, P., & Abri, A. Gh. (2020). A multi-objective optimization approach for a nurse scheduling problem considering the fatigue factor (case study: Labbafinejad hospital). *Journal of applied research on industrial engineering, 7*(4), 396-423.

* Corresponding author
E-mail address: parisa_shahnazari@yahoo.com

10.22105/jarie.2020.259483.1215

compatible with all the restrictions and demands of the nurses and other staff of the [25]. The work schedule should meet the needs of the required number of skilled people in each shift. On the other hand, the program has other restrictions such as people's preferences for days off, the presence of people with special situations such as breastfeeding mothers, or people who are on leave due to illness or other accidents [26]. Mostly, for the nurses working in turning shifts, night shifts can have unpleasant consequences on their normal lives, many of which are out of control. Night shift has negative physical, psychological, and social effects on nurses' personal lives and consequently, these effects can also affect their families and long working hours endanger their health and safety [27]. Nurses are always prone to health threats in various dimensions due to long work shifts and the consequent resulting fatigue. Cardiovascular disease and heart attacks are more common among shift-work nurses than day-work ones. These different work shifts such as working night shifts, on weekdays and at different hours of the day and overtime can be a serious threat to the physical and mental health of nurses. These different work shifts such as working night shifts, on all weekdays and at different hours of a day as well as overtime work can lead to a serious threat to the physical and mental health of nurses [8]. Those nurses, who are not in good general health, will not be able to provide good care such as physical and psychological support to patients. As a result, the risk of mistakes and accidents at work will be increased, and ultimately the consequences of which affect the patient and the nurse [29].

In most developing countries, 5 to 10% of government costs are allocated to the health sector, and among the various components of the health system, hospital services are the major driver of costsgrowth. Hospitals, as the largest center for providing health services, occupy the major part of the resources and credits of the health sector of a country, for instance, in Iran, about 40% of government health expenditures are related to hospital care. However, among the operating costs of the hospital, the costs related to human resources account for the largest share of total hospital costs, and in Iran, on average, the cost of humanpower is estimated about 55-60% of the total costs of the hospital operations. According to research, lack of nursing staff or its inappropriate distribution is usually one of the main problems of hospitals. Therefore, standardizing the number and distribution of nursing staff in clinical wards is necessary to improve the efficiency and quality of services provided to patients, to make the best use of available facilities and improve productivity in hospitals. Nowadays, hospital managers decide to increase their job satisfaction by providing appropriate scheduling by assigning optimal work shifts to nurses leading to improving the quality of services provided to patients [30]. Nowadays, hospital managers decide to increase their job satisfaction by providing appropriate scheduling by assigning optimal work shifts to nurses leading to improving the quality of services provided to patients [30]. In fact, the more the schedule assigned to each nurse is consistent with that nurse's preferences for his/her preferred work shifts, the more patients the nurse will treat with a higher spirit. As a result, the services provided to patients will be of better quality. From this point of view, the issue of scheduling nurses in hospitals has been considered by many researchers in recent years. Considering nurses' scheduling, the number of nurses required to meet the demand for location-shifts is available during the scheduling period, and the purpose of solving the problem is to assign nurses to shifts. So that the demand for shifts is met [31]. Finally, a table presenting the time shifts assigned to nurses is provided and nurses are required to serve them in the assigned work shifts. Meanwhile, even by considering the optimal allocation of work shifts to nurses and taking their preferences into account, nurses can't provide services continuously in each work shift because with each passing hour, nurses' fatigue increases. Therefore, short-term rest in each work shift can lead to rehabilitation in the workforce of nurses so that they can provide services with a higher spirit. As a result, in addition to assigning work shifts to nurses, the fatigue caused by the continuous activity of nurses on each working day should also be considered. Accordingly, in this paper, a mathematical model of nurses' work shift scheduling is presented by considering ergonomic factors. One of the main goals of this paper is presenting the optimal allocation

of work shifts according to nurses' preferences and government laws besides the hospital policies, as well as reducing nurses' daily fatigue by taking short breaks to retrieve nurses. Due to the NP-Hard nature of the nurses' scheduling problem, the Multi-Objective Particle Swarm Optimization (MOPSO) and the Nondominated Sorting Genetic Algorithm II (NSGA-II) as metaheuristic algorithms have been used to solve the model in a case study.

## 2. Literature Review

The importance of nurses' shift scheduling issues has led to many researchers modeling such issues and offering different methods to solve the problem in recent years. Various features in nursing shift scheduling issues such as cost reduction, social, ergonomics, etc. have been considered by researchers, the most important of which are discussed in this section. A mathematical model for cyclic and non-cyclic planning of 12-hour shift nurses was introduced, and a concept called stint was introduced, a pattern that is characterized by start date, length, cost, and work shifts. Using stints as nodes in a network, a rotation diagram was created on which nurse programs could be defined. The models are shown on data samples from a local hospital [3]. A branch and price algorithm is employed to solve the problem of nurses' shift scheduling. The objectives of the model in this study include the optimal allocation of nurses to work shifts in a way that minimizes the cost of deviations from nurses' work in their non-specialized field [22].

Considering recent studies, the Cplex method has been used to maximize nurses' flexibility in a single-objective problem in which the model shows the optimal allocation of nurses in each work shift [16]. Genetic algorithms have been used to improve nurses' scheduling problem solving time with the aim of minimizing the cost of assigning nurses to lower skill levels and the results show the high efficiency of this algorithm [17]. Refrigeration simulation algorithm has been used to solve the nurses' scheduling model by considering work rules and regulations, hospital policy and with the aim of maximizing nurses' preferences for work shifts and weekends. The results showed that the refrigeration simulation algorithm offers far better solutions than the programs provided by the head nurses [18].

The mathematical model of nurses' work shift scheduling is presented with the aim of maximizing nurses' preferences for work shifts and weekends. In this model, the last days of the previous planning horizon are considered to determine the shift of nurses in the early days of the current planning horizon. Additionally, leave days requested by nurses are not fully considered [19]. A two-step innovative algorithm is proposed to achieve the goals of fairness and flexibility in determining the nurse shift. The first step identifies a combination of shift types, and the second step creates nurse lists that allocate weekend shifts as evenly as possible. The proposed model is based on a case study using data from a US hospital to demonstrate the applicability of the method. It was found that the cost savings and fairness can be achieved through proper shift design [14]. A study has examined the factors that lead to or prevent nurses' fatigue. Interviews were conducted using a qualitative content analysis method by the Patient Safety System Engineering Initiative (SEIPS) model and analyzed. The findings show what nurses perceive as a cause of fatigue and the factors that are beneficial and harmful to coping with fatigue in their work system [12].

A nurse-balanced scheduling model was also developed where the case study was used at a local hospital in Ratchaburi Province to test the model. The aim of this study is to balance the load of each shift for all nurses. Objective constraints were applied to determine positive and negative deviations from the mean load of each shift. The proposed model was solved by Premium Solver in Microsoft Excel and it was found that the balanced load was improved [8]. In the study of a new strategy, a hybrid

approach based on the experimental model of fuzzy regular weight average has been used to identify the best solution to the problem of nurses' scheduling regeneration. This strategy has been used on the nurses' scheduling model at the Vojvodina Oncology Institute in Serbia [21].

In one study, a traditional algorithm was proposed to solve the nurse scheduling problem in which the results of the return algorithm and other innovative algorithms including genetic algorithm and refrigeration simulation were compared. Experimental results showed that the recursive algorithm produces an optimal solution with small applications compared to traditional innovative algorithms [11]. In one study, a proposed mathematical model for the nurses' scheduling problem was proposed, which is based on the idea of a multi-product network flow model. The proposed model was validated by hypothetical cases as well as standard cases, and then it was applied to a real case study in an Egyptian hospital. The results showed the advantage of using the proposed model in producing the program needed to solve the problem [7].

An innovative solution to the nurses' scheduling problem has been proposed. This solution is based on the practice of changing shifts performed by nurses who receive an unfavorable program. Constraints are arranged in order of importance. First, a program is created that meets all the strict constraints and ensures fairness. The second level is trying to meet as many soft constraints as possible while maintaining hard constraints [20]. Using the Gurobi optimizer in Python 3.7, a comparative analysis was presented to examine nurses' scheduling models in terms of target performance and their time complexity. A case study was also presented to analyze the performance of the model. Techniques based on bee colony optimization, simulated annealing and memetic algorithm were studied. Finally, the results were confirmed using statistical analysis [31]. A dual objective model was presented with the aims of minimizing the cost of allocating staff to the skill level and balancing the burden of each shift for all nurses in a nurses' scheduling problem. To form the Pareto Front, the constraint planning technique in Python has been used to solve the problem [13].

A mathematical programming model was presented to maximize nurses' preferences for shift work, and then the Werner fuzzy operator-based fuzzy modeling approach was used, and several randomized test problems were generated and solved using the fuzzy model. In addition, a sensitivity analysis was performed to investigate the effects of parameter changes on the results [9]. To improve productivity, a two-step approach to planning treatment for new patients, planning the nurse needs, and assigning the patient's daily composition to existing nurses was proposed, using a mathematical formula to use the waiting list to use last minute cancellations. In the first step, at the end of each day, an appointment with new patients is made, the nurses' daily needs are estimated, and a waiting list is generated. The second stage assigns patients to nurses while minimizing the number of nurses required [10].

A genetic algorithm was used to solve the nursing scheduling problem at the Bringkoning Community Health Center. It is found that the value of the genetic algorithm parameter affects the optimization results. The small parameter makes the search area in the genetic algorithm more limited, while if the parameter size is too large, it requires more computational time and does not guarantee that for some of those variables it will lead to a desirable value. Therefore, achieving the optimal result of the nursing care program in the emergency room depends on the number of admission days [6].

A two-step strategy is proposed to solve the nurses' scheduling problem. In the first stage, three innovative algorithms - HRA1 (allocation of human resources based on hospital size), HRA2 (allocation of human resources based on average allocation) and HRA3 (allocation of human resources based on the severity of fines) - were proposed for allocating mailboxes. In the second stage, the improved

Particle Swarm Optimization (PSO) algorithm was used to schedule the nursing staff in a reasonable time. The findings of this study help hospital managers make decisions about the allocation and planning of nursing staff [4]. The issue of integrated nursing planning and rescheduling was considered under demand uncertainty. This problem was set and solved as a correct two-step random program. The value of the random solution was estimated using real problem cases on a monthly planning horizon based on data provided by a private health care provider in Ankara [5].

*Table 1* examines the most important papers and the differences between the solution methods and the defined goals of nurses' shift work scheduling models. According to the literature and the research background, there is no comprehensive multi-objective model including ergonomic factors such as staff fatigue in a nurses' scheduling problem. Therefore, in the following, a multi-objective problem of nurses' work shift scheduling is modeled by considering ergonomic factors.

## 3. Problem Definition and Modeling

In this case, there is nurse staff with the skills of nurse, practical nurse, and assistant nurse who must be present in the morning, evening, and night shifts according to the predefined schedule in the hospital. Due to the limited number of nurses and the urgent need for any skills in each shift, there is a need for proper staff scheduling. There are various limitations and assumptions regarding nurses' shift work scheduling, imposing of which has led to the complexity of the problem and its proximity to the real world. On the other hand, ergonomic factors are considered in this issue and the designed model seeks to reduce nurses' fatigue and in fact balance their working hours to reduce fatigue during work shifts. Dawson and Fletcher [1, 2] hypothesized that employee fatigue follows a specific rhythm during their working hours, which can be prevented by excessive rest during work. Therefore, along with other aspects of hospital staff work shift scheduling, the goal is to reduce their fatigue

The limitations and assumptions of the nurses' shift scheduling model studied in this article are as follows:

- The number of nurses (nurse, practical nurse, and assistant nurse) in each work shift (morning, evening, and night) is determined in advance daily.
- Each nurse can work at a lower skill level than his real skill.
- Each nurse in each shift of each day can not work at more than one skill level.
- The minimum and maximum working hours of nurses are known every day and every month and this range of working hours must be observed for each nurse.
- Each nurse can not work more than 12 hours in a day or 12 hours in a row (morning and night shifts or evening and night shifts in one day and also night shifts in one day and morning shifts in the next day are not allowed).
- Morning and evening shifts are 6 working hours and night shifts are 12 working hours.
- If a nurse works in the morning and evening shifts of one day or in the night shift, she/he should rest the next day and there is no need for her/him to be in the hospital.
- Nurses' fatigue in each work shift is considered as a sinusoidal function.
- The number of night shifts that a nurse can work during the monthly planning period is limited.
- Each nurse can not rest for more than 4 sequent days and not present in the hospital.
- There should be at least one nurse with the highest level of skills in each shift of each day.
- Every nurse tends not to be assigned to work on pre-arranged days and shifts.
- The lower and upper limit on the total number of hours worked by each nurse during a week is clear that should be observed as much as possible.

***Table 1.*** *Literature review and the comparison of the studies done in the field of nurses' shift work schedule.*

| Reference | Multi-Objective | The Objective Function | Ergonomic Factors | Model Type | Solution Method |
|---|---|---|---|---|---|
| *Tsai and Li [23]* | - | *Maximizing nurses' preferences for work shifts and weekends.* | - | *MILP* | *Genetic Algorithm* |
| *Maenhout and Vanhoucke [22]* | - | *Minimizing the cost of allocating staff to the skill level.* | - | *MILP* | *Branch & Price* |
| *Maenhout and Vanhoucke [24]* | * | *1- Balancing the load of each shift for all nurses.*<br>*2- Maximizing nurses' preferences for work shifts.* | - | *MILP* | *Epsilon Constraint* |
| *Kumar et al. [16]* | - | *Maximizing staff work flexibility.* | * | *MILP* | *Cplex* |
| *Kim et al. [17]* | - | *Minimizing the cost of allocating staff to low skill levels.* | - | *MILP* | *Genetic Algorithm* |
| *Jafari and Salmasi [18]* | - | *Maximizing nurses' preferences for work shifts and weekends.* | - | *MILP* | *Simulated Annealing* |
| *Thongsanit et al. [8]* | - | *Balancing the load of each shift for all nurses.* | - | *MILP* | *Premium Solver* |
| *Jafari et al. [19]* | - | *Maximizing nurses' preferences for work shifts and weekends.* | - | *MILP* | *Fuzzy Mathematical Model* |
| *Ko et al. [11]* | - | *Maximizing nurses' preferences for work shifts and weekends.* | - | *MILP* | *BackTrack Algorithm* |
| *Youssef and Senbel [20]* | - | *Minimizing the cost of allocating staff to lower skill levels.* | - | *MILP* | *Simulated Annealing* |
| *Alade and Amusat [13]* | * | *1- Minimizing the cost of allocating personnel to a lower skill level.*<br>*2- Balancing the load of each shift for all nurses.* | - | *MILP* | *Constraint Programming Technique* |
| *Jafari [9]* | - | *Maximizing nurses' preferences.* | - | *MILP* | *Fuzzy Mathematical Model* |
| *Mala Sari Rochman et al. [6]* | - | *Maximizing nurses' preferences.* | - | *MILP* | *Genetic Algorithm* |
| *Chen et al. [4]* | - | *Maximizing nurses' preferences.* | - | *MILP* | *Particle Swarm Optimization* |
| *The Present Study* | * | *1- Minimizing the cost of allocating personnel to the skill level.*<br>*2- Minimizing the total deviations from the shifts that personnel tend not to be assigned to work.*<br>*3- Minimizing the amount of morning and evening shifts that personnel are assigned to work continuously.*<br>*4- Minimizing the total deviations from the lower and upper limits on the total number of hours worked.*<br>*5- Minimizing the total fatigue of nurses.* | * | *MINLP* | *LP-Metrics - MOPSO – NSGA II* |

The aims of this issue are divided into two types, the objectives of employers and the preferences of nurses. If nurses of any skill level are assigned to work at a lower skill level than their actual skills, employers will have to pay a fine. Therefore, employers tend to pay the minimum penalty for assigning nurses at lower skill levels than their actual skills. Nurses also tend to work as many hours as they choose during the planning period and not be assigned to work on the days or shifts that they themselves have announced at the beginning of the planning period. Therefore, 5 different objective functions have been considered for the problem, which include minimizing (1) the cost of assigning a nurse to a skill level lower than their actual skill level, (2) the total deviations from the days and shifts that nurses tend not to assign to work, (3) the amount of morning and evening shifts that nurses are assigned to work continuously, (4) the sum of deviations from the lower and upper limits on the total number of hours worked by nurses during a week, and (5) the sum of maximum total fatigue of nurses every day and in every work shift.

According to the assumptions, limitations, and explanations of the problem, the nurses' work shift scheduling model will be as follows:

### *3.1. Sets*

| | |
|---|---|
| $I$ | Set of nurses ($i = 1,2,\dots,I$); |
| $J$ | Shift set ($j = 1,2,\dots,J$); |
| $K$ | Set of working days ($k = 1,2,\dots,K$); |
| $LK$ | Set of working weeks ($lk = 1,2,\dots,LK$); |
| $S$ | Set of skill levels ($s = 1,2,\dots,S$). |

As mention previously in this section, three work shifts and three different skill levels are considered. The work shifts are presented as morning shift ($j = 1$), evening shift ($j = 2$) and night shift ($j = 3$). Besides, the level of nursing skills is indicated by $s = 1$, the level of practical nursing skills is shown by $s = 2$, and the level of assistant nursing skills is represented by $s = 3$.

### *3.2. Parameters*

| | |
|---|---|
| $h_{kj}$ | Shift length $j$ per day $k$; |
| $Dh_{max}$ | Maximum working hours of nurses per day; |
| $Wh_{min}$ | Minimum working hours of nurses per week; |
| $Wh_{max}$ | Maximum working hours of nurses per week; |
| $Mh_{min}$ | Minimum working hours of nurses per month; |
| $Mh_{max}$ | Maximum working hours of nurses per month; |
| $RN_{kjs}$ | Total number of nurses required at skill level $s$ in shift $j$ from day $k$; |
| $Max_{night}$ | The maximum number of night shifts that a nurse can work during a one-month planning period; |
| $\alpha_{kj}^{i}$ | The amount of penalty for assigning nurse $i$ to work at a lower skill level in shift $j$ from day $k$; |
| $k_i$ | The set of days that the nurse $i$ tends not to be assigned to work in some or all of the shifts; |
| $j_{k_i}$ | The set of shifts from day $k_i$ that nurse $i$ tends not to be assigned to work; |
| $T_{j-half}$ | The set of half-hour intervals in each shift $j$; |
| $RSL_{kjs}^{i}$ | Parameter (0 and 1) that takes 1 if nurse $i$ can be assigned to work at her actual skill level or any lower skill level $s$ in shift $j$ from day $k$; otherwise it takes the value 0. |

### *3.3. Decision variables*

$d_{kj}^{1i}$ Deviation from days or shifts that the nurse $i$ does not want to be assigned to work;
$d_{k_1}^{2i}$ Deviation from the lower limit on the total number of hours worked by nurse $i$ during a week;
$d_{k_1}^{3i}$ Deviation from the upper limit on the total number of hours worked by nurse $i$ during a week;
$d_{kjs}^{4i}$ The rest rate of the nurse $i$ with skill level $s$ while working in shift $j$ from day $k$;
$r_{kjts}^{i}$ The fatigue score of the nurse $i$ with skill level $s$ while working in shift $j$ from day $k$ at the hour $t$;
$f_{kjts}^{i}$ The fatigue score of the nurse $i$ with skill level $s$ while working in shift $j$ from day $k$ at the end of hour $t$;
$x_{kjs}^{i}$ Takes 1 if nurse $i$ is assigned to work at skill level $s$ in shift $j$ from day $k$, otherwise it takes the value 0;
$O_{k}^{i}$ Takes 1 if nurse $i$ is assigned to work continuously in the morning and evening shifts from day $k$, otherwise it takes the value 0;
$F_{k}^{i}$ Takes 1 if nurse $i$ is assigned to work in night shift from day $k$, otherwise it takes the value 0;
$\omega_{kjts}^{i}$ Takes 1 if nurse $i$ is assigned to work at skill level $s$ in shift $j$ from day $k$ in half an hour $t$, Otherwise it takes the value 0.

### *3.4. Modeling of the Multi-Objective Problem of Nurses' Work Shift Scheduling*

$$Z_1 = \text{Min} \sum_{i} \sum_{k} \sum_{j} \sum_{s} \left[\alpha_{kj}^{i}.\left(s - RSL_{kjs}^{i}\right).X_{kjs}^{i}\right], \quad (1)$$

$$Z_2 = \text{Min} \sum_{i} \sum_{k\in k_i} \sum_{j\in j_{k_i}} d_{kj}^{1i}, \quad (2)$$

$$Z_3 = \text{Min} \sum_{i} \sum_{k}^{|LK|} O_{k}^{i}, \quad (3)$$

$$Z_4 = \text{Min} \sum_{i} \sum_{k_1=1} \left(d_{k_1}^{2i} + d_{k_1}^{3i}\right), \quad (4)$$

$$Z_5 = \text{Min}\left(\sum_{i} \max_{k,j,t,s} f_{kjts}^{i}\right), \quad (5)$$

s. t.

$$\sum_{j} \sum_{s} h_{kj}\, x_{kjs}^{i} \le Dh_{\max}, \quad \forall i, k \quad (6)$$

$$\sum_{k} \sum_{j} \sum_{s} h_{kj} x_{kjs}^{i} \ge Mh_{\min}, \quad \forall\, i \quad (7)$$

$$\sum_{k} \sum_{j} \sum_{s} h_{kj} x_{kjs}^{i} \le Mh_{\max}, \quad \forall\, i \quad (8)$$

$$\sum_{i} x_{kjs}^{i} = RN_{kjs}, \quad \forall\, k, j, s \quad (9)$$

$$\sum_{s} x_{kjs}^{i} \le 1, \quad \forall\, i, j, k \quad (10)$$

$$x_{kjs}^{i} \le RSL_{kjs}^{i}, \quad \forall i, k, j, s \quad (11)$$

$$\sum_{k=k_1}^{k_1+1} \sum_{s} x_{k(j\in 3)s}^{i} \le 1, \quad \forall\, i, k_1 < K \quad (12)$$

$$\sum_{k}\sum_{s} x^{i}_{k(j\in 3)s} \le \max_{night}, \quad \forall\, i \tag{13}$$

$$\sum_{s} x^{i}_{k(j\in 1)s} + \sum_{s} x^{i}_{k(j\in 3)s} \le 1, \quad \forall\, i,k \tag{14}$$

$$\sum_{s} x^{i}_{k(j\in 2)s} + \sum_{s} x^{i}_{k(j\in 3)s} \le 1, \quad \forall\, i,k \tag{15}$$

$$\sum_{s} x^{i}_{k(j\in 3)s} + \sum_{s} x^{i}_{(k+1)(j\in 1)s} \le 1, \quad \forall\, i,k < K \tag{16}$$

$$\sum_{j}\sum_{s} x^{i}_{kjs} \le 2, \quad \forall\, i,k \tag{17}$$

$$O^{i}_{k} - \sum_{s} x^{i}_{k(j\in 1)s} \le 0, \quad \forall\, i,k \tag{18}$$

$$O^{i}_{k} - \sum_{s} x^{i}_{k(j\in 2)s} \le 0, \quad \forall\, i,k \tag{19}$$

$$O^{i}_{k} - \sum_{s} x^{i}_{k(j\in 1)s} - \sum_{s} x^{i}_{k(j\in 2)s} \ge -1, \quad \forall\, i,k \tag{20}$$

$$\sum_{s} x^{i}_{k(j\in 1)s} + \sum_{s} x^{i}_{k(j\in 2)s} + \sum_{j}\sum_{s} x^{i}_{(k+1)js} + O^{i}_{k} \le 3, \quad \forall\, i,k < K \tag{21}$$

$$F^{i}_{k} - \sum_{s} x^{i}_{k(j\in 3)s} = 0, \quad \forall\, i,k \tag{22}$$

$$\sum_{s} x^{i}_{k(j\in 3)s} + \sum_{j}\sum_{s} x^{i}_{(k+1)js} + F^{i}_{k} \le 2, \quad \forall\, i,k < K \tag{23}$$

$$\sum_{k=l}^{l+4}\sum_{j}\sum_{s} x^{i}_{ljs} \ge 1, \quad \forall\, i,k \le K-4 \tag{24}$$

$$\sum_{i} x^{i}_{kj(s\in 1)} \ge 1, \quad \forall\, j,k \tag{25}$$

$$\sum_{s} x^{i}_{kjs} - d^{1i}_{kj} = 0\,, \quad \forall i, k \in k_i, j \in j_{k_i} \tag{26}$$

$$\sum_{k=7k_1-6}^{7k_1}\sum_{j}\sum_{s} h_{kj} x^{i}_{kjs} + d^{2i}_{k_1} \ge Wh_{min}, \quad \forall i, k_1 \in LK \tag{27}$$

$$\sum_{k=7k_1-6}^{7k_1}\sum_{j}\sum_{s} h_{kj} x^{i}_{kjs} - d^{3i}_{k_1} \le Wh_{max}, \quad \forall i, k_1 \in LK \tag{28}$$

$$r^{i}_{kjts} = \frac{1}{2}\sin\left(\frac{2\pi}{24}(t+1)\right) + 1.5, \quad \forall i,j,k,t \le T_{j-half}, s \tag{29}$$

$$f^{i}_{kjts} = f^{i}_{kj(t-1)s} + \omega^{i}_{kjts}.\, r^{i}_{kjts} - 2\left(1-\omega^{i}_{kjts}\right).\, r^{i}_{kjts}, \quad \forall i,j,k,t \le T_{j-half}, s \tag{30}$$

$$\sum_{t=1}^{T_{j-half}} 0.5(\omega^{i}_{kjts}) + d^{4i}_{kjs} = h_{kj} x^{i}_{kjs}, \quad \forall i,j,k,s \tag{31}$$

$$d^{4i}_{kjs} \le \frac{T_{j-half}}{12}, \quad \forall i,j,k,t,s \tag{32}$$

$$d^{1i}_{kj}, d^{2i}_{k_1}, d^{3i}_{k_1}, d^{4i}_{kjs}, r^{i}_{kjts}, f^{i}_{kjts} \ge 0, \tag{33}$$

$$x^{i}_{kjs}, O^{i}_{k}, F^{i}_{k}, \omega^{i}_{kjts} \in \{0,1\}. \tag{34}$$

In this modeling, *Eq. (1)* minimizes the cost of assigning nurses to the skill level below their actual skill level. *Eq. (2)* shows the minimization of the total deviations from the days and shifts that nurses tend not to assign to work. *Eq. (3)* minimizes the number of morning and evening shifts that nurses are assigned to work continuously. *Eq. (4)* describes the fourth objective function of the problem and involves minimizing the sum of deviations from the lower and upper bounds on the total number of hours worked by nurses during a week. *Eq. (5)* sums the total maximum fatigue score of all nurses in each skill level in each shift of each day. This objective function actually reduces nurses' fatigue during work shifts. *Eq. (6)* illustrates the maximum number of working hours that each nurse can work in a day. *Relationships (7)* and *(8)* show the minimum and maximum number of working hours that each nurse can work in a one-month planning period, respectively. *Eq. (9)* also shows the total number of case nurses at each skill level in each shift of each day. *Eq. (10)* ensures that each nurse in each shift of each day can not work at more than one skill level. *Eq. (11)* ensures that each nurse can work at their actual skill level or at a lower skill level. *Eq. (12)* indicates that night shifts are not permitted. *Eq. (13)* presents the maximum number of night shifts that each nurse can work in a one-month planning period. *Relationships (14)* - *(17)* show that morning and night shifts or evening and night shifts on one day as well as night shifts on one day and morning shifts on the next day are not allowed, meaning that each nurse cannot work more than 12 hours a day or 12 hours in a row. *Relationships (18)* - *(23)* express that if a nurse works one day in the morning and evening shift or night shift, the next day should not be working. *Eq. (24)* ensures that each nurse can not rest more than 4 days in a row and not be assigned to any shifts. *Eq. (25)* ensures that there should be at least one nurse with the highest level of skill in each shift of each day. *Eq. (26)* shows that every nurse tends not to be assigned to work on pre-determined days and shifts. *Eqs. (27)* and *(28)* show the upper and lower bounds on the total number of hours worked by each nurse during a week. *Eq. (29)* shows the nurse's fatigue score every half hour of her shift. *Eq. (30)* also shows the nurse's fatigue score at the end of each half hour of work, taking into account her rest. *Eq. (31)* indicates the total amount of nurse rest hours in each shift of each working day. *Eq. (32)* presents the maximum number of half-hour breaks for a nurse in each work shift of each day. *Relationships (33)* and *(34)* show the type and gender of decision variables.

## 4. Solution Methods and Comparison Indicators

After presenting the mathematical model of the multi-objective problem of nurses' work shift scheduling, in this section, the solution methods, as well as the comparison indicators of the solution methods used in the article are presented. Due to the multi-objective nature of the developed mathematical model, different methods should be used to find the Pareto front and efficient solutions. Therefore, to solve the developed multi-objective problem, comprehensive standard decision methods, as well as NSGA II and MOPSO meta-heuristic algorithms, have been used. In the following, each of the solution methods as well as the primary chromosomes of the meta-heuristic algorithms are described.

### *4.1. LP-Metrics Method*

In LP-Metrics, it is necessary to obtain the best value of each objective function by individual optimization method. That is, the value of each objective function must first be obtained without considering the other objective function to be used in the calculations. *Eq. (35)* shows the multi-objective decision-making method named LP-Metrics.

$$L_p = \left\{ \sum_{i=1}^{n} w_i \left[ \frac{(f_i - f_i^*)}{(f_i^*)} \right]^p \right\}^{\frac{1}{p}} \quad , p \geq 1 \tag{35}$$

In the above relation $w_i$ is the weight assigned to each objective function, $f_i$ is the objective function of the problem and $f_i^*$ is the optimal value of each objective function obtained from the individual optimal method. Also, the soft $p$ (norm) of the problem indicates that in this paper the linear norm, ie ($p = 1$) has been used to solve the multi-objective problem.

### *4.2. MOPSO Algorithm*

Eberhart and Kennedy [15] first proposed a method called particle motion by modeling the movement of birds in the air and discovering the logical relationship between the change of direction and speed of birds and using the knowledge of physics. The scientists later discovered in their research that these movements were interdependent and found that a bird's movement was due to information it received from birds around it, so they completed the proposed method and named it a swarm movement. In general, the cumulative particle motion algorithm has many similarities with algorithms such as ants or genetics, but there are serious differences with them that make this algorithm different and simple. For example, this algorithm does not use operators such as crossover and mutation, so the algorithm does not require the use of number strings and the decryption step, so it is much simpler than algorithms such as genetics. This algorithm divides the solution space into several paths using a quasi-probabilistic function, which are formed by the movement of individual particles in space. The motion of a group of particles consists of two main components (definite and probable). Each particle is interested in moving in the direction of the best current answer $x^*$ or the best answer obtained so far $g^*$. *Eqs. (36)* and *(37)* show the speed and motion functions of birds in each iteration of the MOPSO algorithm.

$$\mathrm{V_i^{t+1}} = \mathrm{wV_i^t} + \mathrm{C_1 rand(pbest_i - X_i^t)} + \mathrm{C_2 rand(gbest_i - X_i^t)}, \tag{36}$$

$$\mathrm{X_i^{t+1}} = \mathrm{X_i^t} + \mathrm{V_i^{t+1}}. \tag{37}$$

In the above relations, $V_i^{t+1}$ is the velocity of the particle $i$ in the new iteration $t$. $V_i^t$is the velocity of the particle $i$ in the current iteration $t$. $X_i^{t+1}$ is the current position of the particle $t + 1$. $X_i^t$is the position of the particle in the new iteration, $pbest_i$ is the best position has ever taken by the particle $i$. $rand$ is the best position of the best particle (the best position that all particles have ever taken). The rand is a random number between zero and one that is used to maintain group diversity. $C_1$ and $C_2$ are cognitive and social parameters, respectively. Selecting the appropriate value for these parameters leads to accelerating the convergence of the algorithm and preventing premature convergence in local optimizations. Recent research shows that choosing a larger value for the cognitive parameter $C_1$ is more appropriate than the social parameter $C_2$. The parameter $w$ is called weight inertia, which is used to ensure convergence in the particle group. Gravitational inertia is used to control the effect of previous velocity records on current velocities.

### *4.3. NSGA II Algorithm*

Genetic algorithms start by randomly generating an initial population of chromosomes, while satisfying the boundaries or limitations of the problem. In other words, chromosomes are strings of proposed values for problem-solving variables, and each represents a possible answer to the problem. Chromosomes are inferred from consecutive repeats called generations. During each generation, these

chromosomes are evaluated according to the goal of optimization, and the chromosomes that are the better answer to the problem are more likely to reproduce the answers to the problem. It is important to formulate the chromosome evaluation function to help speed up the convergence of calculations toward the general optimal answer. Because in the genetic algorithm, the value of the evaluation function must be calculated for each chromosome, and because we usually have a significant number of chromosomes in many problems, the time consuming calculation of the evaluation function can make it practically impossible to use the genetic algorithm in some problems. Therefore, based on the obtained values of the objective function in the population of strings, a fit number is assigned to each string. This fitness number will determine the probability of selection for each discipline. Based on this selection probability, a set of strings is selected first. To produce the next generation, new chromosomes called offspring are created by linking two chromosomes from the current generation using a combination operator or by modifying the chromosome using a mutation operator. Therefore, new strings replace strings from the original population so that the number of strings in the various computational iterations is constant. The random mechanisms that act on the selection and removal of strings are such that strings that are more fitting are more likely to combine and produce new strings and are more resilient than other strings in the replacement phase. Thus, the population of sequences in a competition based on the objective function is completed over different generations and increases by the value of the objective function in the population of the strings, so that after several years, the algorithm converges to the best chromosome, which hopefully indicates optimal or suboptimal solution. In general, in this algorithm, while in each computational iteration, new points of the response space are searched by genetic operators, by the selection mechanism, it explores the space in which the statistical average of the objective function is higher. Usually the new population that replaces the previous population is more appropriate. This means that the population is improving from generation to generation. The search will be fruitful when we have reached the maximum possible generation, or if convergence has been achieved, or the cessation criteria have been met, and as a result, the best chromosome obtained from the last generation will be selected as the optimal solution or optimal solution to the problem.

#### *4.3.1. Initial chromosome design*

The most important part in designing and using algorithms in problem solving is how to define problem variables called problem chromosomes. In this section, the primary chromosome design of the nursing shift work schedule in the hospital is discussed. According to the model assumptions, in this article, three types of personnel (nurse A, practical nurse B and assistant nurse C) are considered who should be present in the work shifts according to the predefined schedule. Therefore, to define the primary chromosome as well as its decoding, a schedule with four type **A** personnel, three type **B** personnel and two type **C** personnel is considered for 3 working days. *Fig. 1* shows the basic information and the initial chromosome of the nurses' shift work schedule.

| Day | Personnel allocation | A1 | A2 | A3 | A4 | B1 | B2 | B3 | C1 | C2 |
|---|---|---|---|---|---|---|---|---|---|---|
| *first day* | *Personnel* | *2* | *4* | *3* | *1* | *-* | *-* | *-* | *-* | *-* |
| *second day* | *type A* | *4* | *1* | *3* | *2* | *-* | *-* | *-* | *-* | *-* |
| *third day* | | *1* | *3* | *2* | *4* | *-* | *-* | *-* | *-* | *-* |
| *first day* | *Personnel* | *3* | *1* | *4* | *5* | *2* | *6* | *7* | *-* | *-* |
| *second day* | *type A and B* | *5* | *2* | *7* | *3* | *6* | *4* | *1* | *-* | *-* |
| *third day* | | *3* | *2* | *1* | *4* | *5* | *4* | *2* | *-* | *-* |
| *first day* | *Personnel* | *2* | *3* | *1* | *8* | *9* | *4* | *6* | *7* | *5* |
| *second day* | *type A and B* | *4* | *3* | *5* | *7* | *9* | *1* | *8* | *6* | *2* |
| *third day* | *and C* | *5* | *7* | *6* | *2* | *9* | *4* | *3* | *8* | *1* |

| | The first shift | | | The second shift | | | The third shift | | |
|---|---|---|---|---|---|---|---|---|---|
| *first day* | *1 C* | *1 B* | *-* | *1 C* | *-* | *1 A* | *-* | *2 B* | *1 A* |
| *second day* | *1 C* | *-* | *1 A* | *-* | *1 B* | *-* | *1 C* | *-* | *1 A* |
| *third day* | *-* | *-* | *1 A* | *1 C* | *1 B* | *1 A* | *1 C* | *1 B* | *-* |

***Fig. 1.*** *Initial chromosome for the nurses' work shift scheduling problem.*

According to *Fig. 1*, the primary chromosome is the replacement for number of personnel of type A, B and C per day. *Fig. 1* also shows the number of personnel required per day and per shift. The following are the steps for decoding the primary chromosome.

*Step 1.* To decipher the problem, first the assignment of type A personnel and from the third shift is done. Therefore, according to the assumptions of the problem, the highest priority of the primary chromosome is selected on the first day and the personnel is assigned to the third shift. According to the random priority created in *Fig. 1*, personnel A2 are assigned as the first personnel to the first day and the third shift. In this case, due to the non-assignment of personnel A2 on the second day (according to the assumptions of the problem), the priorities related to personnel A2 on the second day will be reduced to zero. After assigning personnel in the third shift, type A personnel will be assigned in the second and first shifts. *Fig. 2* shows the allocation of type A personnel according to the assumptions of the problem based on chromosome in *Fig. 1*.

| Personnel allocation | A1 | A2 | A3 | A4 | The third shift |
|---|---|---|---|---|---|
| *first day* | *2* | *4* | *3* | *1* | *A2* |
| *second day* | *4* | *0* | *3* | *2* | *A1* |
| *third day* | *0* | *3* | *2* | *4* | - |

| Personnel allocation | A1 | A2 | A3 | A4 | The second shift |
|---|---|---|---|---|---|
| *first day* | *2* | *0* | *3* | *1* | *A3* |
| *second day* | *0* | *0* | *3* | *2* | - |
| *third day* | *0* | *3* | *2* | *4* | *A4* |

| Personnel allocation | A1 | A2 | A3 | A4 | The first shift |
|---|---|---|---|---|---|
| *first day* | *2* | *0* | *0* | *1* | *-* |
| *second day* | *0* | *0* | *3* | *2* | *A3* |
| *third day* | *0* | *3* | *2* | *0* | *A2* |

| | The first shift | The second shift | The third shift |
|---|---|---|---|
| *first day* | *-* | *A3* | *A2* |
| *second day* | *A3* | *-* | *A1* |
| *third day* | *A2* | *A4* | *-* |

***Fig. 2.*** *Assignment of type A personnel based on initial chromosome decoding*.

*Step 2.* After assigning type A personnel in each shift and every day, type B personnel will be assigned from the third shift. Given that type A personnel have the ability to perform the activities of type B personnel, so the chromosome of the second part is a combination of type A and B personnel. For example, personnel A1 and A4 along with personnel B1, B2 and B3 can be assigned as Type B personnel. *Fig. 3* shows the allocation of Type B personnel according to the assumptions of the problem based on the chromosome of *Fig. 1* and the modified *Fig. 2*.

| Personnel allocation | A1 | A2 | A3 | A4 | B1 | B2 | B3 | The third shift |
|---|---|---|---|---|---|---|---|---|
| *first day* | *3* | *0* | *0* | *5* | *2* | *6* | *7* | *B2-B3* |
| *second day* | *0* | *0* | *0* | *3* | *6* | *0* | *0* | *-* |
| *third day* | *0* | *0* | *1* | *0* | *5* | *4* | *2* | *B1* |

| Personnel allocation | A1 | A2 | A3 | A4 | B1 | B2 | B3 | The second shift |
|---|---|---|---|---|---|---|---|---|
| *first day* | *3* | *0* | *0* | *5* | *2* | *0* | *0* | *-* |
| *second day* | *0* | *0* | *0* | *3* | *6* | *0* | *0* | *B1* |
| *third day* | *0* | *0* | *1* | *0* | *0* | *4* | *2* | *B2* |

| Personnel allocation | A1 | A2 | A3 | A4 | B1 | B2 | B3 | The first shift |
|---|---|---|---|---|---|---|---|---|
| first day | 3 | 0 | 0 | 5 | 2 | 0 | 0 | A4 |
| second day | 0 | 0 | 0 | 3 | 0 | 0 | 0 | - |
| third day | 0 | 0 | 1 | 0 | 0 | 4 | 2 | - |

| | The first shift | | The second shift | | The third shift | |
|---|---|---|---|---|---|---|
| first day | A4 | - | - | A3 | B2-B3 | A2 |
| second day | - | A3 | B1 | - | - | A1 |
| third day | - | A2 | - | A4 | B1 | - |

***Fig. 3.*** *Assignment of type A and B personnel based on initial chromosome decoding.*

<u>*Step 3.*</u> After assigning type A and B personnel in each shift and every day, type C personnel will be assigned from the third shift. Given that type A personnel have the ability to perform the activities of type B and C personnel and also type B personnel have the ability to perform the activities of type C personnel, so the chromosome of the third part is a combination of type A, B and C personnel. *Fig. 4* shows the allocation of Type C personnel according to the problem assumptions based on chromosomes in *Fig. 1* and the modified *Fig. 2* and *Fig. 3*.

| Personnel allocation | A1 | A2 | A3 | A4 | B1 | B2 | B3 | C1 | C2 | The third shift |
|---|---|---|---|---|---|---|---|---|---|---|
| first day | 0 | 0 | 0 | 0 | 9 | 0 | 0 | 7 | 5 | - |
| second day | 0 | 0 | 0 | 0 | 0 | 0 | 0 | 6 | 2 | C1 |
| third day | 0 | 0 | 6 | 0 | 0 | 4 | 3 | 0 | 1 | A3 |

| Personnel allocation | A1 | A2 | A3 | A4 | B1 | B2 | B3 | C1 | C2 | The second shift |
|---|---|---|---|---|---|---|---|---|---|---|
| first day | 2 | 0 | 0 | 0 | 9 | 0 | 0 | 7 | 5 | B1 |
| second day | 0 | 0 | 0 | 7 | 0 | 1 | 8 | 0 | 2 | - |
| third day | 0 | 7 | 0 | 0 | 0 | 4 | 3 | 0 | 1 | A2 |

| Personnel allocation | A1 | A2 | A3 | A4 | B1 | B2 | B3 | C1 | C2 | The first shift |
|---|---|---|---|---|---|---|---|---|---|---|
| *first day* | *2* | *3* | *0* | *0* | *0* | *0* | *0* | *7* | *5* | *C1* |
| *second day* | *0* | *0* | *0* | *7* | *0* | *0* | *0* | *0* | *2* | *A4* |
| *third day* | *0* | *0* | *0* | *2* | *0* | *4* | *3* | *0* | *1* | *-* |

| | The first shift | | | The second shift | | | The third shift | | |
|---|---|---|---|---|---|---|---|---|---|
| *first day* | *C1* | *A4* | *-* | *B1* | *-* | *A3* | *-* | *B2-B3* | *A2* |
| *second day* | *A4* | *-* | *A3* | *-* | *B1* | *-* | *C1* | *-* | *A1* |
| *third day* | *-* | *-* | *A2* | *A2* | *-* | *A4* | *A3* | *B1* | *-* |

***Fig. 4.*** *Assignment of type A, B and C of personnel based on the initial chromosome decoding*.

The above decoding should be updated and modified based on the following assumptions at each stage:

- If the staff is working in the third shift, they should not be working the next day.
- There is a limit to the number of third shifts for staff.
- Should not be assigned to any other shift if each staff member's working hours are exceeded.
- Every day, each staff member can be employed in only one skill.
- If the staff is working in the first and second shifts, they are exempted from working in the third shift and the next day.

### *4.3.2. Combining operators*

The Combining operators is one of the operators of the NSGA II algorithm, which is modeled by changing the genes of the parents to create new children and improve fitness. In this paper, a single point combination is used to combine chromosomes. *Fig. 5* shows the combination on one of the problem chromosomes.

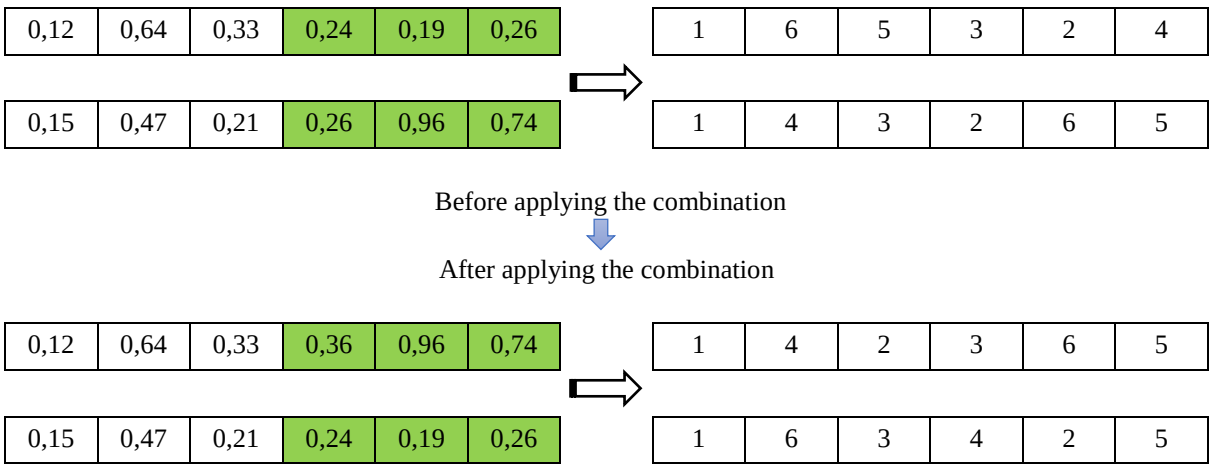


***Fig. 5.*** *Performing a single point combination.*

*4.3.3. Mutation operator*

Mutation is another operator that produces other possible answers. In a genetic algorithm, after a member is created in a new population, each of its genes mutates with a certain probability of mutation. In mutation, a gene may be removed from a population of genes or a gene that did not previously exist in the population may be added. In this paper, the transfer mutation is used for the mutation operator between the problem chromosomes. *Fig. 6* shows how this chromosome is applied and converted into a valid answer.

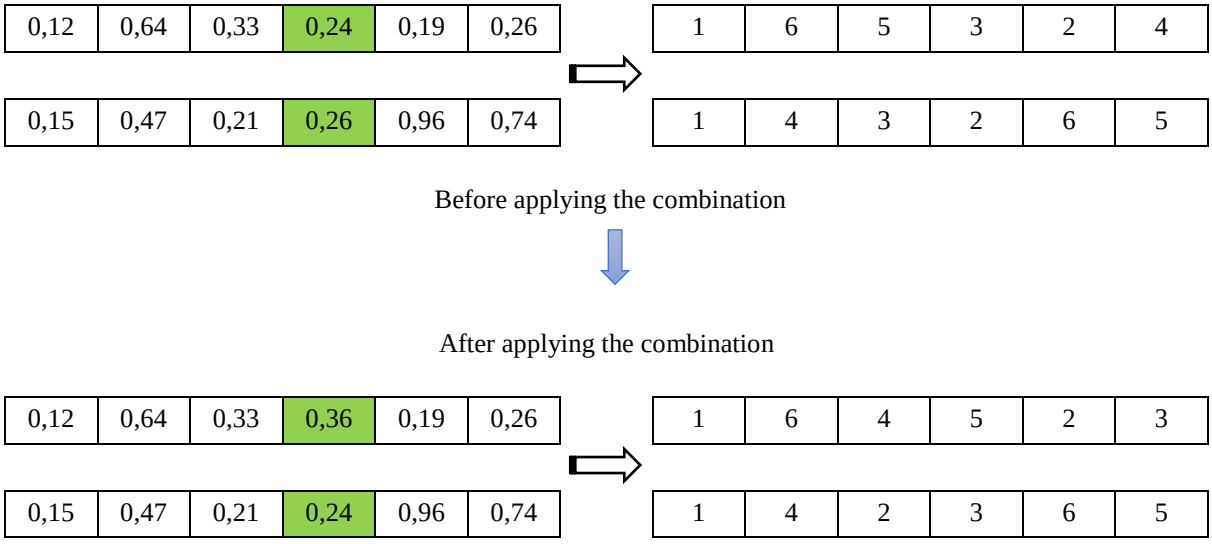


***Fig. 6.*** *How the mutation operator works.*

Due to the continuous space of NSGA II and MOPSO algorithms, as well as the discrete space of the primary chromosome response space, it is possible to create an impossible answer at any stage of the algorithm repetition. Therefore, using the following mechanism, the continuous answers generated in each iteration of the algorithm are converted to discrete answers. *Fig. 7* shows how to convert continuous space to discrete space. In this mechanism, the largest continuous number is identified and the corresponding house number becomes the highest priority of discrete space. Then the next largest number in continuous space is selected and the highest priority of discrete space is assigned to that house number. This operation continues until the last continuous number is converted to discrete.

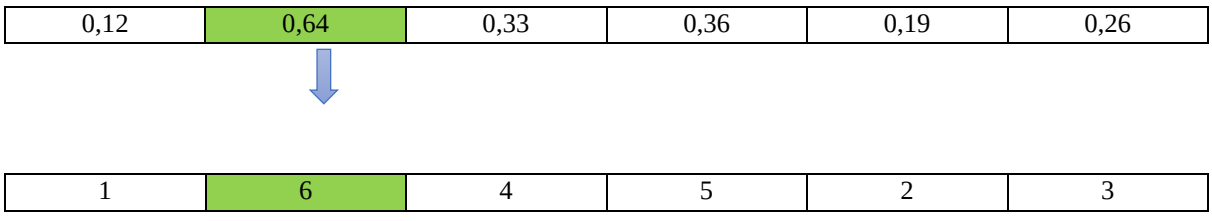


***Fig. 7.*** *Mechanism of conversion for continuous to discrete space.*

### *4.4. Comparative Indicators of Metaheuristic Algorithms*

One of the problems in solving multi-objective problems is how to evaluate the quality of the final solutions, which can sometimes be complicated due to the conflicting used goals. For this purpose, in the early 1990s, visual (observational) methods were used to compare Pareto collections. Convergence to Pareto optimal solutions and providing density and variability among the obtained set of solutions are the two main goals of any multi-objective evolutionary algorithm. But since these two goals are somewhat at odds with each other, there is no standard by which to make an absolute decision about the performance of algorithms. Therefore, to evaluate the performance of the proposed algorithms, the following criteria are used:

- Computational time: An algorithm that has less computational time will be more desirable.
- Number of answers in Pareto: Shows the number of unsuccessful answers in the Pareto set obtained for each problem.
- Maximum expansion: This criterion shows how many of the answers of a Pareto set are distributed in the answer space, which is calculated from *Fig. 38*. The larger the value of this criterion, the better the variety of Pareto set answers.

$$\mathrm{MSI} = \sqrt{\sum_{m=1}^{M} \left(\max_{i=1:|Q|} f_m^i - \max_{i=1:|Q|} f_m^i\right)^2}. \tag{38}$$

- Distance: Indicates the uniformity of the answers, which is calculated using *Eq. (39)*.

$$\mathrm{SM} = \sqrt{\frac{1}{|Q|}\sum_{i=1}^{|Q|} \left(d_i - \bar{d}\right)^2}. \tag{39}$$

In the above relation, $|Q|$ represents the size of the Pareto archive, and the values $d_i$ and $\bar{d}$ can be calculated from *Eqs. (40)* and *(41)*, respectively. An algorithm with less of this criterion would be more desirable.

$$d_i = \min_{k \in Q \cap k \neq i} \sum_{m=1}^{M} \left|f_m^i - f_m^k\right|. \tag{40}$$

$$\bar{d} = \sum_{i=1}^{|Q|} \frac{d_i}{|Q|}. \tag{41}$$

- Distance from the ideal point: This criterion is used to measure the degree of proximity to the optimal level of the real Pareto, which is calculated from *Eq. (42)*:

$$\mathrm{MID} = \frac{\sum_{i=1}^{n} c_i}{n}. \tag{42}$$

In this relation $n$ is the number of answers in the Pareto optimal set and $c_i$ is the Euclidean distance of each member of the Pareto set from the ideal point which is calculated from *Eq. (43)*:

$$c_i = \sqrt{(f_{1i} - f_1^*)^2 + (f_{2i} - f_2^*)^2 + \cdots + (f_{mi} - f_m^*)^2}. \quad (43)$$

### *4.5. Parameter Setting of Metaheuristic Algorithms*

In this section, the basic parameters of MOPSO and NSGA II meta-heuristic algorithms are set by Taguchi method. In Taguchi method, first the appropriate factors should be identified and then the levels of each factor should be selected and then the appropriate test design for these control factors should be determined. Once the test design is determined, the experiments are performed and the experiments are analyzed in order to find the best combination of parameters. In this study, for each factor, 3 levels are considered according to *Table 2*. For each algorithm, according to the number of factors and the number of their levels, the design of the experiment and their execution are determined. Given the multi-objective nature of the proposed model, the value of each experiment must first be calculated from *Eq. (44)*. This relation is used in case of subtraction of the indicators used in comparison of meta-heuristic algorithms including indicators (number of answers in Pareto, maximum expansion, distance, distance from the ideal point and computational time). After determining the value of each experiment, the scaled value of each experiment, RPD, is calculated from *Eq. (45)* to analyze the design of the Taguchi experiment.

$$S_i = \left|\frac{NPF + MSI + SM + MID + CPU\_time}{5}\right|. \quad (44)$$

$$RPD = \frac{S_i - S_i^*}{S_i^*}. \quad (45)$$

In *Relation (45)*, $S_i$ is the index value obtained from each Taguchi experiment and $S_i^*$ is the best index value among all Taguchi experiments.

***Table 2.*** *Levels of proposed parameters for parameterization of meta-heuristic algorithms by Taguchi method.*

| Algorithm | Parameter | Symbol | Level 1 | Level 2 | Level 3 |
|---|---|---|---|---|---|
| **NSGA II** | *Maximum number of repetitions* | *Max it* | *50* | *100* | *200* |
| | *Number of population* | *Npop* | *50* | *100* | *200* |
| | *Combination rate* | *Pc* | *0,3* | *0,5* | *0,7* |
| | *Mutation rate* | *Pm* | *0,3* | *0,5* | *0,7* |
| **MOPSO** | *Maximum number of repetitions* | *Max it* | *50* | *100* | *200* |
| | *Number of particles* | *N particle* | *50* | *100* | *200* |
| | *Individual learning coefficient* | *C1* | *1* | *1,5* | *2* |
| | *Collective learning coefficient* | *C2* | *1* | *1,5* | *2* |
| | *Gravity coefficient* | *w* | *0,7* | *0,8* | *1* |

By comparing the difference between the maximum and minimum values obtained in the NSGA II algorithm for the SN index, the significant effect of the Max it parameter (maximum number of repetitions) in improving the solution process of the NSGA II algorithm is evident. The parameters Pm (Mutation rate), Npop (population size) and Pc (combination rate) are in the next influential ranks, respectively (*Table 3*).

***Table 3.*** *Results of parameter analysis of NSGA II algorithm.*

| Level | Maximum number of Repetitions | Number of Population | Combination Rate | Mutation Rate |
|---|---|---|---|---|
| *1* | *0,14794* | *0,15478* | *0,09527* | *0,08686* |
| *2* | *0,19249* | *0,11135* | *0,16801* | *0,11512* |
| *3* | *0,01125* | *0,08556* | *0,08840* | *0,14970* |
| *Delta* | *0,18146* | *0,06922* | *0,07961* | *0,06284* |
| *Rank* | *1* | *3* | *2* | *4* |

*Fig. 8* shows the mean S / N ratio and the mean for the NSGA II algorithm. As stated, the maximum value of the SN criterion is the criterion for selecting the values of the parameters.

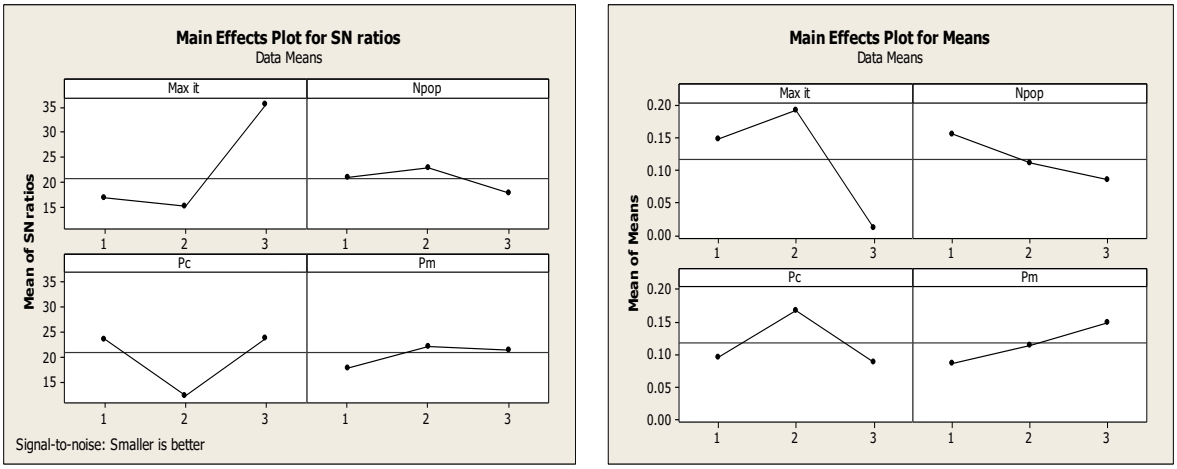


***Fig. 8.*** *Average graph of S / N ratio and average of averages in NSGA II algorithm*.

According to the results shown in *Fig. 8*, the NSGA II algorithm will be most effective if the maximum number of iterations is at level 3, the population at level 2, the combination rate at level 3, and the mutation rate at level 2. By comparing the difference between the maximum and minimum values obtained in the MOPSO algorithm for the SN index, the significant effect of the Max it parameter (maximum number of iterations) in improving the solution process of the MOPSO algorithm is evident. The parameters w (gravity coefficient), c1 (individual learning coefficient), Nparticle (number of particles) and c2 (collective learning coefficient) are in the next ranks of influence (*Table 4*).

***Table 4.*** *Results of parameter setting analysis of MOPSO algorithm.*

| Level | Maximum Number of Repetitions | Number of Particles | Gravity Coefficient | Individual Learning Coefficient | Collective Learning Coefficient |
|---|---|---|---|---|---|
| *1* | *0,13846* | *0,11466* | *0,08044* | *0,10832* | *0,13885* |
| *2* | *0,19160* | *0,14906* | *0,10510* | *0,12855* | *0,13836* |
| *3* | *0,06227* | *0,12861* | *0.20678* | *0,15546* | *0,11511* |
| *Delta* | *0,12933* | *0,03440* | *0,12634* | *0,04713* | *0,02374* |
| *Rank* | *1* | *4* | *2* | *3* | *5* |

*Fig. 9* shows the mean S / N ratio and the mean for the MOPSO algorithm. As stated, the maximum value of the SN criterion is the criterion for selecting the values of the parameters.

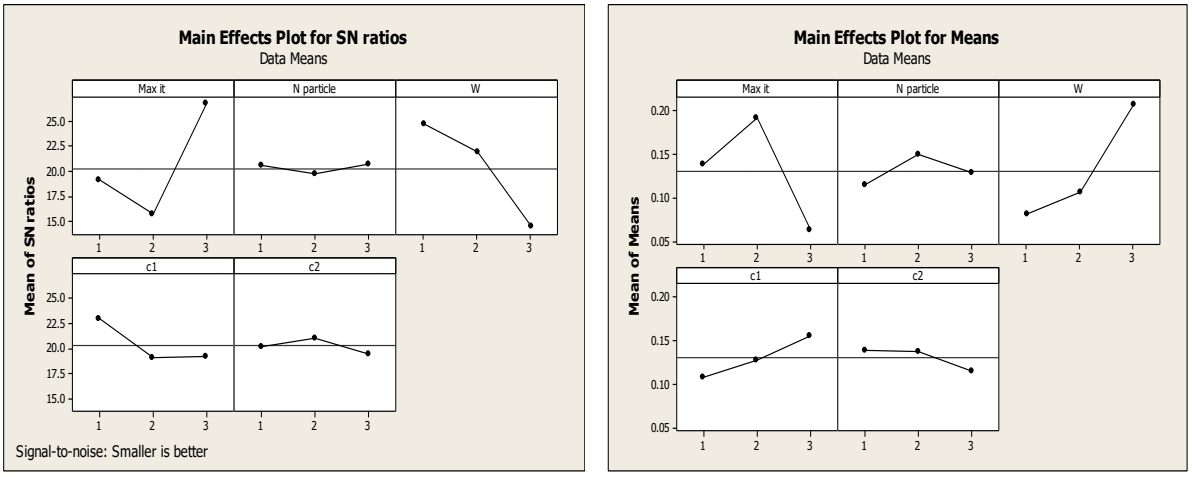


***Fig. 9.*** *Average graph of S / N ratio and average of averages in MOPSO algorithm*.

According to the observable results of *Fig. 9*, if the maximum number of repetitions is at level 3, the number of particles at level 2, the gravity coefficient at level 3, the individual learning coefficient at level 3, and the collective learning coefficient at level 1, the MOPSO algorithm will be most efficient.

## 5. Results Analysis

In this section, in order to investigate the issue of multi-objective scheduling of nurses' work shifts by considering ergonomics, a small example is considered for Shahid Labbafinejad Hospital in Iran. Dr. Labbafinejad Hospital started operating in 1981 and gradually continued its growth trend with the provision of facilities and equipment and began its serious activities by attracting committed, and specialized medical personnel. Simultaneously with the establishment of the hospital, preparations were made for its incorporation into the educational system. At present, this center is one of the hospitals of the Social Security Organization, but it is under the supervision of Shahid Beheshti University of Medical Sciences. All wards of the hospital have been approved by the Secretariat of the Medical and Specialized Council, and specialized and sub-specialized assistants, postgraduate students, interns and interns, in other words, all-inclusive categories are engaged in training in this center. The total number of nurses (including nurses, practical nurses and assistant nurses) in the study ward of Shahid Labbafinejad Hospital is 18 people who work in three shifts during 24 hours. The length of the morning and evening shifts is 6 hours and the length of the night shifts is 12 hours. All nurses are divided into 3 skill levels: nurse, practical nurse and assistant nurse. The nurse skill level is the highest skill level and the nurse assistant skill level is the lowest skill level. In this study, all these 3 skill levels are called nurse (according to the hospital custom). When necessary, the skill level is precisely specified. The characteristics of the whole problem are presented in *Table 5* and the characteristics of the staff and the required number of each nurse at different skill levels in an 18-person ward in *Tables 6* and *7* for Shahid Labbafinejad Hospital.

***Table 5.*** *Required data for the small size problem.*

| **Planning horizon** | **30 days** |
|---|---|
| *The length of each shift.* | *(Morning and noon shift 6 hours and night shift 12 hours)* |
| *Maximum working hours per workforce per day.* | *12 hours* |
| *Minimum working hours required for each workforce per week.* | *35 hours* |
| *Maximum working hours per workforce per week.* | *42 hours* |
| *Minimum working hours required for each workforce during the month.* | *100 hours* |
| *Maximum working hours allowed for each workforce during the month.* | *180 hours* |
| *Penalty coefficient for allocating each workforce at a lower skill level.* | *15 to 20 currencies* |
| *Maximum allowed night shifts in a planning period.* | *15 shifts* |

***Table 6.*** *Characteristics of employees in 18 people department.*

| **Employees Number** | **Real Skill Level** | **Preferred Days for Leave** | **Employees Number** | **Real Skill Level** | **Preferred Days for Leave** |
|---|---|---|---|---|---|
| *1* | *Nurse* | *-* | *10* | *Nurse* | *-* |
| *2* | *Nurse* | *29* | *11* | *Nurse* | *7,14* |
| *3* | *Nurse* | *28,29* | *12* | *Practical Nurse* | *1,2,3,4* |
| *4* | *Nurse* | *-* | *13* | *Practical Nurse* | *22* |
| *5* | *Nurse* | *-* | *14* | *Practical Nurse* | *19,20,21,22* |
| *6* | *Nurse* | *24,25,26* | *15* | *Practical Nurse* | *-* |
| *7* | *Nurse* | *9,10,11,12* | *16* | *Practical Nurse* | *-* |
| *8* | *Nurse* | *26* | *17* | *Assistant Nurse* | *-* |
| *9* | *Nurse* | *16,17,18* | *18* | *Assistant Nurse* | *-* |

***Table 7.*** *The required number of each skill level of employees in each shift of each day in the planning period in 18 people department.*

| **Day** | **Shift** | **Nurse** | **Practical Nurse** | **Assistant Nurse** |
|---|---|---|---|---|
| *1,2,15,28* | Morning | 3 | 0 | 1 |
| | *Noon* | *2* | *1* | *1* |
| | *Night* | *2* | *1* | *0* |
| *6,10,13,20,22,27* | *Morning* | *2* | *1* | *0* |
| | *Noon* | *2* | *1* | *0* |
| | *Night* | *2* | *1* | *0* |
| *3,4,5,7,8,9,11,12* | *Morning* | *4* | *0* | *1* |
| *14,16,17,18,19,21* | *Noon* | *2* | *1* | *1* |
| *23,24,25,26,29,30* | *Night* | *2* | *1* | *0* |

According to the Lp metrics method in *Relation (35)*, to obtain an efficient answer, it is necessary to obtain a receiving table. Therefore, by solving the problem by individual optimization method, the value of the first objective function 1867, the second and third objective functions 0, the fourth objective function 181 and the fifth objective function 573.117 are obtained.

Based on the comprehensive criterion method, the obtained efficient solution optimizes all objective functions simultaneously. Therefore, the shift schedule of the problem under study can be shown in *Table 8*.

***Table 8.*** *Scheduling problem for the small sample.*

| Day | Morning Shift | | | Noon shift | | | Night Shift | | |
|---|---|---|---|---|---|---|---|---|---|
| | **Nurse** | **P- nurse[1]** | **A- nurse[2]** | **Nurse** | **P-nurse** | **A- nurse** | **Nurse** | **P-nurse** | **A-nurse** |
| *1* | *2-3-4* | | *17* | *5-7* | *16* | *18* | *1-9* | *12* | |
| *2* | *4-5-11* | | *17* | *6-7* | *15* | *18* | *2-10* | *13* | |
| *3* | *1-3-4-9* | | *18* | *5-7* | *14* | *16* | *8-11* | *15* | |
| *4* | *1-5-7-10* | | *18* | *2-3* | *1* | *17* | *4-6* | *12* | |
| *5* | *3-5-7-10* | | *17* | *9-11* | *13* | *16* | *2-8* | *14* | |
| *6* | *9-10* | *16* | | *1-6* | *13* | | *3-11* | *15* | |
| *7* | *4-5-7-10* | | *13* | *1-9* | *12* | *17* | *6-8* | *14* | |
| *8* | *1-2-3-4* | | *18* | *5-10* | *13* | *17* | *7-9* | *15* | |
| *9* | *3-4-5-6* | | *17* | *2-8* | *12* | *13* | *10-10* | *14* | |
| *10* | *6-9* | *15* | | *1-2* | *16* | | *5-7* | *12* | |
| *11* | *1-3-4-8* | | *16* | *6-10* | *14* | *18* | *2-11* | *15* | |
| *12* | *1-4-5-6* | | *18* | *7-8* | *13* | *17* | *3-9* | *16* | |
| *13* | *4-11* | *13* | | *2-8* | *14* | | *6-10* | *12* | |
| *14* | *3-7-9-11* | | *17* | *4-5* | *13* | *14* | *1-8* | *16* | |
| *15* | *2-10-11* | | *17* | *3-7* | *12* | *18* | *6-9* | *15* | |
| *16* | *1-2-4-10* | | *12* | *5-11* | *16* | *17* | *3-8* | *14* | |
| *17* | *2-4-5-11* | | *17* | *6-9* | *13* | *18* | *7-10* | *16* | |
| *18* | *3-4-8-11* | | *18* | *2-6* | *12-13* | | *1-5* | *15* | |
| *19* | *2-3-4-9* | | *18* | *7-8* | *16* | *17* | *6-10* | *13* | |
| *20* | *1-8* | *16* | | *4-5* | *15* | | *7-9* | *12* | |
| *21* | *2-4-5-8* | | *17* | *3-6* | *13* | *18* | *1-11* | *14* | |
| *22* | *2-9* | *12* | | *5-10* | *13* | | *3-8* | *15* | |
| *23* | *1-2-5-7* | | *17* | *4-10* | *12* | *18* | *9-11* | *13* | |
| *24* | *3-4-5-7* | | *16* | *1-8* | *14* | | *6-10* | *15* | *12* |
| *25* | *2-3-4-11* | | *18* | *1-7* | *16* | *17* | *8-9* | *14* | |
| *26* | *2-3-7-10* | | *18* | *4-5* | *16* | *1* | *6-11* | *12* | |
| *27* | *1-7* | *14* | | *3-10* | *13* | | *2-5* | *15* | |
| *28* | *1-7-8* | | *18* | *9-11* | *13* | *17* | *4-6* | *16* | |
| *29* | *1-5-9-11* | | *18* | *2-3* | *12* | *7* | *8-10* | *15* | |
| *30* | *1-2-4-9* | | *13* | *6-11* | *14* | *3* | *5-7* | *12* | |

*[1]Practical nurse*
*[2]Asistant nurse*

Ergonomic factor in this study isconsidered in the form of short breaks in each work shift for staff. Personnel can take a short break in each shift to avoid excessive fatigue and rehabilitate their work force. *Table 9* shows the number of rest times of each staff in each work shift to answer the workload.

***Table 9.*** *Number of rest times of each staff in each shift for small sample problem.*

| Day | Morning Shift | | | Noon Shift | | | Night Shift | | |
|---|---|---|---|---|---|---|---|---|---|
| | Nurse | P- nurse[1] | A- nurse[2] | Nurse | P-nurse | A- nurse | Nurse | P-nurse | A-nurse |
| *1* | - | - | *(2) 17* | - | - | *(2) 18* | - | *(1) 12* | - |
| *2* | - | - | *(2) 17* | - | *(1) 15* | *(2) 18* | - | - | - |
| *3* | - | - | - | - | - | - | - | - | - |
| *4* | - | - | *(2) 18* | - | - | - | - | - | - |
| *5* | - | - | *(2) 17* | - | - | *(1) 16* | - | *(1) 14* | - |
| *6* | - | - | - | - | - | - | - | - | - |
| *7* | - | - | - | - | - | - | - | - | - |
| *8* | - | - | *(2) 18* | - | *(1) 13* | *(2) 17* | - | - | - |
| *9* | - | - | - | - | *(1) 12* | *(1) 13* | - | - | - |
| *10* | - | - | - | - | - | - | - | - | - |
| *11* | - | - | *(2) 16* | - | *(1) 14* | *(2) 18* | - | - | - |
| *12* | - | - | *(2) 18* | - | - | - | - | - | - |
| *13* | - | - | - | - | *(2) 14* | - | - | - | - |
| *14* | - | - | *(2) 17* | - | - | *(1) 14* | - | - | - |
| *15* | - | - | - | - | *(1) 12* | - | - | - | - |
| *16* | - | - | *(2) 12* | - | - | - | - | | - |
| *17* | - | - | *(2) 17* | - | - | *(2) 18* | - | *(3) 16* | - |
| *18* | - | - | *(2) 18* | - | - | - | - | - | - |
| *19* | - | - | *(2) 18* | - | *(2) 16* | *(2) 17* | - | - | - |
| *20* | - | - | - | - | *(1) 15* | - | - | - | - |
| *21* | - | - | - | - | - | - | - | *(4) 14* | - |
| *22* | - | - | - | - | *(2) 13* | - | - | - | - |
| *23* | - | - | - | - | *(1) 12* | *(2) 18* | - | - | - |
| *24* | - | - | - | - | - | - | - | *(1) 15* | - |
| *25* | - | - | *(2) 18* | - | *(2) 16* | *(2) 17* | - | *(1) 14* | - |
| *26* | - | - | *(2) 18* | - | - | - | - | - | - |
| *27* | - | - | | - | *(2) 13* | - | - | *(4) 15* | - |
| *28* | - | - | *(2) 18* | - | - | - | - | - | - |
| *29* | - | - | *(2) 18* | - | *12* | *(2) 7* | - | - | - |
| *30* | - | - | *(23) 13* | - | - | - | - | - | - |

[1]*Practical nurse*
[2]*Asistant nurse*

As can be seen from *Table 9*, the highest number of breaks occurred during one shift is in the night shift, which is due to the 12-hour night shift. Therefore, some personnel in the night shift during their service need 4 short breaks to rehabilitate their workforce. Based on the results, it is observed that most of the break time occurs in the middle of staff working hours, which continue to operate after a short break. It is also observed that a person's behavior every day is almost predictable and his rest period is also estimated. Therefore, by obtaining information before the schedule, a more detailed and accurate schedule regarding the shift schedule and also the working hours of nurses in the hospital can be provided.

In the following, a large sample size problem in Labbafinejad Hospital is solved by considering 90 staff and the information of *Table 5* with NSGA II and MOPSO algorithms. The number of personnel required in different shifts is as described in *Table 10*.

***Table 10.*** *The required number of each skill level of nurses in each shift of each day in the planning period in a 90-person department.*

| Day | Shift | Nurse | Practical nurse | Asistant nurse |
|---|---|---|---|---|
| | morning | 15 | 0 | 5 |
| *1,2,15,28* | *noon* | *10* | *5* | *5* |
| | *night* | *10* | *5* | *0* |
| | *morning* | *10* | *5* | *0* |
| *3,10,13,20,22,27* | *noon* | *10* | *5* | *0* |
| | *night* | *10* | *5* | *0* |
| *3,4,5,7,8,9,11,12* | *morning* | *20* | *0* | *5* |
| *14,16,17,18,19,21* | *noon* | *10* | *5* | *5* |
| *23,24,25,26,29,30* | *night* | *10* | *5* | *0* |

Due to the inefficiency of the comprehensive standard method in solving the nurses' scheduling problem, the large size model has been solved by NSGA II and MOPSO algorithms and the efficient response comparison indices are obtained as described in *Table 11*. Furthermore, *Fig. 10* demonstrates the Pareto front resulting from problem solving by two algorithms.

***Table 11.*** *Comparison indicators of meta-heuristic algorithms.*

| Algorithm | NSGA II | MOPSO |
|---|---|---|
| *The average of the first objective function.* | *3411,89* | *3407,17* |
| *The average of the second objective function.* | *46,02* | *50,70* |
| *The average of the third objective function.* | *0,45* | *0,62* |
| *The average of the forth objective function.* | *5379,43* | *5379,43* |
| *The average of the fifth objective function.* | *2710,77* | *2732,09* |
| *Number of answers in Pareto* | *64* | *24* |
| *The most spread.* | *466,94* | *325,98* |
| *Distance.* | *0,36* | *0,38* |
| *Distance from the ideal point.* | *225,89* | *158,49* |
| *Computational time.* | *2641,35* | *2248,63* |

According to the results of *Table 11*, it can be seen that NSGA II algorithm has obtained 64 efficient answers in 2641.35 seconds and MOPSO algorithm has obtained 24 efficient answers in 2248.63 seconds. Moreover, NSGA II algorithm has worked better than MOPSO algorithm in reducing nurses' shift scheduling.

## 6. Conclusion

In this paper, the nurses' work shift scheduling problem is modeled by considering ergonomic factors. Given the urgent need of hospitals to provide better staff services to patients, it is necessary to consider the preferences of nurses in scheduling shifts. Therefore, a multi-objective model of scheduling nurses meeting different objectives as well as reducing nurses' fatigue during their day-to-day activities is presented in this article. The main objectives of the article include minimizing 1- the cost of allocating personnel to the skill level, 2- the total deviations from the shifts that personnel tend not to be assigned to work 3- the amount of morning and evening shifts that personnel allocate to work continuously 4- The sum of deviations from the lower and upper limits on the total number of hours worked and 5- fatigue is the sum of nurses. Moreover, all government regulations and hospital policies are included in the modeling. To solve the developed model, two algorithms, NSGA II and MOPSO, have been used by presenting a new chromosome. The designed chromosome first programs the hard limits of the problem and then tries to improve the soft limits of the problem. Therefore, to evaluate the outputs of

the model, two numerical examples in small and large size with real data of Labbafinejad Hospital were designed. In the first example, the schedule of an 18-person ward of Labbafinejad Hospital was analyzed and the results showed that nurses take the most breaks during the night shift and in the middle of their working hours to reduce fatigue. Then, due to the inability of the comprehensive standard method to solve large size problems, a problem with 90 staff was designed for Labbafinejad Hospital and the problem was solved with MOPSO and NSGA II algorithms. The output of the problem showed that the MOPSO algorithm was more efficient than the NSGA II algorithm in obtaining distance point indices from the ideal point as well as computational time. While the NSGA II algorithm performed well in obtaining Pareto response rate indices, the maximum expansion and metric distance. Therefore, the TOPSIS method and the use of entropy weighting method showed that the designed NSGA II algorithm has the ability to solve the problem of scheduling the nurses of Labbafinejad Hospital faster and better.

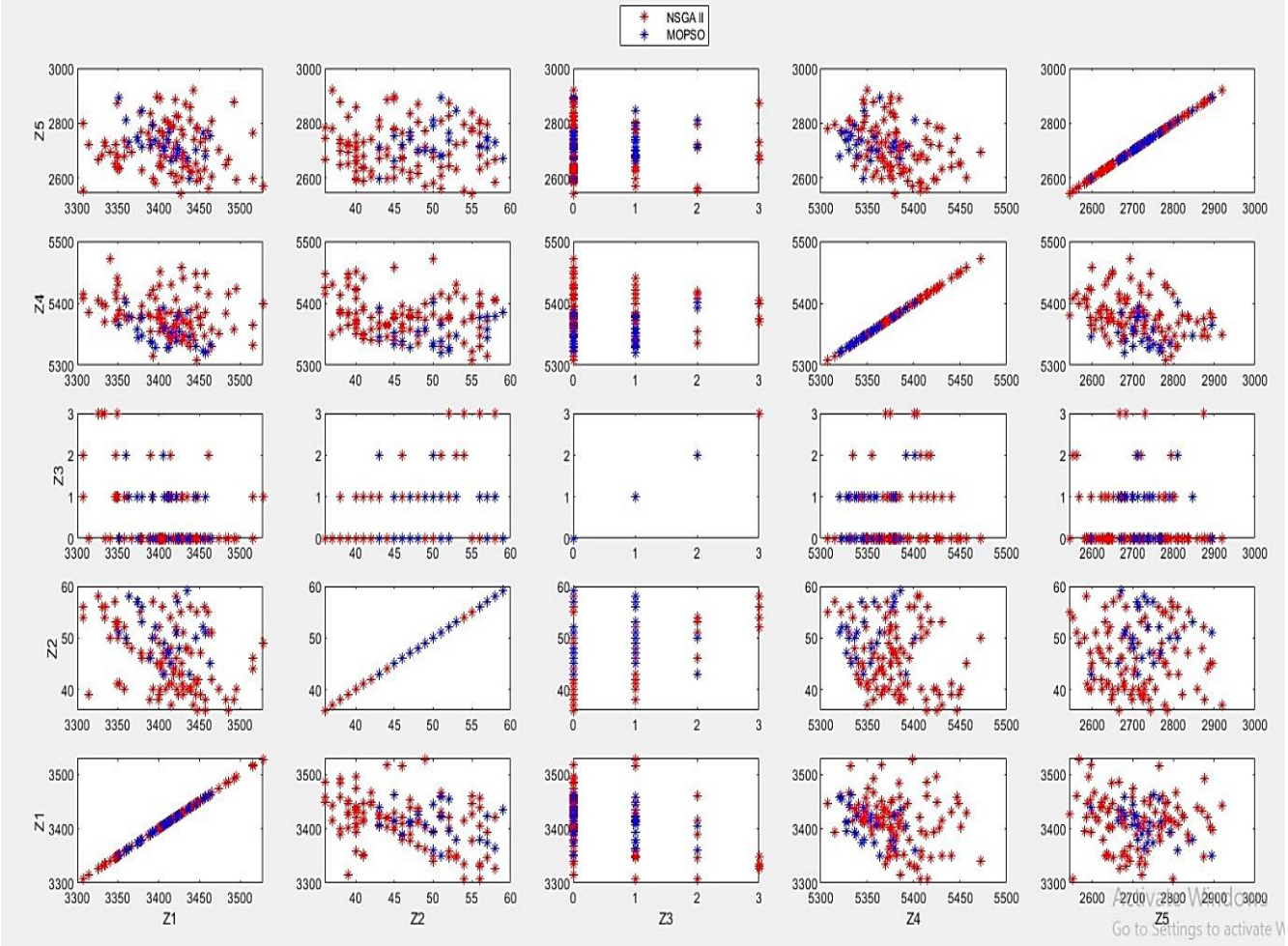


***Fig. 10.*** *Pareto front resulting from large-scale problem solving.*

## References

[1] Dawson, D., & Fletcher, A. (2001). A quantitative model of work-related fatigue: background and definition. *Ergonomics*, *44*(2), 144-163.

[2] Lin, R. C., Sir, M. Y., Sisikoglu, E., Pasupathy, K., & Steege, L. M. (2013). Optimal nurse scheduling based on quantitative models of work-related fatigue. *IIE transactions on healthcare systems engineering*, *3*(1), 23-38.

[3] Millar, H. H., & Kiragu, M. (1998). Cyclic and non-cyclic scheduling of 12 h shift nurses by network programming. *European journal of operational research*, *104*(3), 582-592.

[4] Chen, P. S., Huang, W. T., Chiang, T. H., & Chen, G. Y. H. (2020). Applying heuristic algorithms to solve inter-hospital hierarchical allocation and scheduling problems of medical staff. *International Journal of computational intelligence systems*, *13*(1), 318-331.

[5] Batun, S., & Karpuz, E. (2020). Nurse scheduling and rescgeduling under uncertainty. *Hacettepe University Journal of Economics & Administrative Sciences/Hacettepe Üniversitesi Iktisadi ve Idari Bilimler Fakültesi Dergisi*, *38*(1).

[6] Mala Sari Rochman, E., Rachmad, A., & Santosa, I. (2020). The application of genetic algorithms as an optimization step in the case of nurse scheduling at the Bringkoning Community health center. *JPhCS*, *1477*(2), 022026.

[7] El Adoly, A. A., Gheith, M., & Fors, M. N. (2018). A new formulation and solution for the nurse scheduling problem: A case study in Egypt. *Alexandria engineering journal*, *57*(4), 2289-2298.

[8] Thongsanit, K., Kantangkul, K., & Nithimethirot, T. (2016). Nurse's shift balancing in nurse scheduling problem. *Science, engineering and health studies (former name: Silpakorn University science and technology journal)*, 43-48. https://doi.org/10.14456/sustj.2016.6

[9] Jafari, H. (2020). Developing a fuzzy model for the nurse scheduling problem. *Journal of operational research in its applications (applied mathematics)-Lahijan Azad University*, *17*(2), 93-107.

[10] Benzaid, M., Lahrichi, N., & Rousseau, L. M. (2020). Chemotherapy appointment scheduling and daily outpatient–nurse assignment. *Health care management science*, *23*(1), 34-50.

[11] Ko, Y. W., Kim, D. H., Uhmn, S., & Kim, J. (2017). Nurse scheduling problem using backtracking. *Advanced science letters*, *23*(4), 3792-3795.

[12] Steege, L. M., & Dykstra, J. G. (2016). A macroergonomic perspective on fatigue and coping in the hospital nurse work system. *Applied ergonomics*, *54*, 19-26.

[13] Alade, O. M., & Amusat, A. O. (2019). Solving nurse scheduling problem using constraint programming technique. arXiv preprint arXiv:1902.01193.

[14] Zhong, X., Zhang, J., & Zhang, X. (2017). A two-stage heuristic algorithm for the nurse scheduling problem with fairness objective on weekend workload under different shift designs. *IISE transactions on healthcare systems engineering*, *7*(4), 224-235.

[15] Eberhart, R., & Kennedy, J. (1995, October). A new optimizer using particle swarm theory. *MHS'95 proceedings of the sixth international symposium on micro machine and human science* (pp. 39-43). IEEE.

[16] Kumar, B. S., Nagalakshmi, G., & Kumaraguru, S. (2014). A shift sequence for nurse scheduling using linear programming problem. *Journal of nursing and health science*, *3*(6), 24-28.

[17] Kim, S. J., Ko, Y. W., Uhmn, S., & Kim, J. (2014). A strategy to improve performance of genetic algorithm for nurse scheduling problem. *International journal of software engineering and its applications*, *8*(1), 53-62.

[18] Jafari, H., & Salmasi, N. (2015). Maximizing the nurses' preferences in nurse scheduling problem: mathematical modeling and a meta-heuristic algorithm. *Journal of industrial engineering international*, *11*(3), 439-458.

[19] Jafari, H., Bateni, S., Daneshvar, P., Bateni, S., & Mahdioun, H. (2016). Fuzzy mathematical modeling approach for the nurse scheduling problem: a case study. *International journal of fuzzy systems*, *18*(2), 320-332.

[20] Youssef, A., & Senbel, S. (2018, January). A bi-level heuristic solution for the nurse scheduling problem based on shift-swapping. *2018 IEEE 8th annual computing and communication workshop and conference (CCWC)* (pp. 72-78). IEEE.

[21] Simić, S., Simić, D., Milutinović, D., Đorđević, J., & Simić, S. D. (2017, September). A fuzzy ordered weighted averaging approach to rerostering in nurse scheduling problem. *International joint conference SOCO'17-CISIS'17-ICEUTE'17 León, Spain, September 6–8, 2017, proceeding* (pp. 79-88). Springer. Cham. https://doi.org/10.1007/978-3-319-67180-2_8

[22] Maenhout, B., & Vanhoucke, M. (2010). Branching strategies in a branch-and-price approach for a multiple objective nurse scheduling problem. *Journal of scheduling*, *13*(1), 77-93.
[23] Tsai, C. C., & Li, S. H. (2009). A two-stage modeling with genetic algorithms for the nurse scheduling problem. *Expert systems with applications*, *36*(5), 9506-9512.
[24] Maenhout, B., & Vanhoucke, M. (2011). Reactive personnel scheduling: insights and policy decisions. *25th annual conference of the Belgian operations research society (ORBEL 25)* (pp. 29-30). http://hdl.handle.net/1854/LU-1147910
[25] Ikeda, K., Nakamura, Y., & Humble, T. S. (2019). Application of quantum annealing to nurse scheduling problem. *Scientific reports*, *9*(1), 1-10.
[26] Hamid, M., Tavakkoli-Moghaddam, R., Golpaygani, F., & Vahedi-Nouri, B. (2020). A multi-objective model for a nurse scheduling problem by emphasizing human factors. *Proceedings of the institution of mechanical engineers, Part H: journal of engineering in medicine*, *234*(2), 179-199.
[27] Bagheri, M., Devin, A. G., & Izanloo, A. (2016). An application of stochastic programming method for nurse scheduling problem in real word hospital. *Computers & industrial engineering*, *96*, 192-200.
[28] Thongsanit, K., Kantangkul, K., & Nithimethirot, T. (2016). Nurse's shift balancing in nurse scheduling problem. *Science, Engineering and Health Studies (Former name: Silpakorn University Science and Technology Journal)*, 43-48.
[29] Nasiri, M. M., & Rahvar, M. (2017). A two-step multi-objective mathematical model for nurse scheduling problem considering nurse preferences and consecutive shifts. *International journal of services and operations management*, *27*(1), 83-101.
[30] Sangai, J., & Bellabdaoui, A. (2017, April). Workload balancing in nurse scheduling problem models and discussion. *2017 international colloquium on logistics and supply chain management (LOGISTIQUA)* (pp. 82-87). IEEE.
[31] Svirsko, A. C., Norman, B. A., Rausch, D., & Woodring, J. (2019). Using mathematical modeling to improve the emergency department nurse-scheduling process. *Journal of emergency nursing*, *45*(4), 425-432.

Journal of Applied Research on Industrial Engineering
www.journal-aprie.com

# Robust Control for Variable Order Time Fractional Butterfly-Shaped Chaotic Attractor System

***Anis Shabani*[1], *Amir Hossein Refahi Sheikhani*[1,*], *Hossein Aminikhah*[2]**
[1]*Department of Applied Mathematics, Faculty of Mathematical Sciences, Lahijan Branch, Islamic Azad University, Lahijan, Iran.*
[2]*Department of Applied Mathematics, Faculty of Mathematical Sciences, University of Guilan, Rasht, Iran.*

**PAPER INFO**

**Chronicle:**
*Received: 02 June 2020*
*Reviewed: 18 July 2020*
*Revised: 22 September 2020*
*Accepted: 13 November 2020*

**Keywords:**
*Variable-Order Fractional Derivatives.*
*Adams Numerical Scheme.*
*Butterfly- Shaped Chaotic Attractor System.*
*Robust Control.*

**ABSTRACT**

In this article, we investigated the robust control approach for variable-order fractional time fractional butterfly- shaped chaotic attractor system that the fractional derivative is considered in Atangana-Baleanu-Caputo sense. We show the computational algorithm with high accuracy for solving the proposed systems. For the suggested system, Adams-Bashforth-Moulton approach applied for converting the system of the equations into a system of linear or nonlinear algebraic equations. The existence and uniqueness of the solution are shown and also asymptotically stable is investigated in this article. At the end, a number of statistical indicators were presented in order efficiency, accuracy and simple applicability of the proposed method.

## 1. Introduction

By means of Fractional Calculus (FC), the integration operators and differentiation operators achieve fractional order. In recent decades, the study of FC has absorbed growing attention as hot research topic on a global scale [1-14]. Samko extended the constant order FC in an outstanding manner [15].

In this research work, fractional operators in which order is considered to be a function of time, space or a few other variables are proposed. Noticeable applications of such fractional variable-order operators are introduced in [16-18]. Due to the fact that finding the exact solutions of variable-order fractional differential equations is impossible, devising numerical schemes in order to solve these equations is an important research topic. Adams-Bashforth's method is known to, from a conventional

Shabani, A., Refahi Sheikhani, A. H., & Aminikhah, H. (2020). Robust control for variable order time fractional butterfly- shaped chaotic attractor system. *Journal of applied research on industrial engineering, 7*(4), 435-449.

* Corresponding author
E-mail address: ah_refahi@yahoo.com
10.22105/jarie.2020.253993.1203

point of view, as powerful and excellent numerical method that can present a numerical solution of fractional differential equations [19-22].

Recently the authors have developed a constant-order numerical scheme- in [23]– that is able to combine the fundamental theorem of fractional calculus and the two-step Lagrange polynomial. Drawing on this method, the present paper generalizes the numerical schemes that were introduced in [23] to simulate variable-order fractional differential operators with power-law, exponential-law and Mittag-Leffler kernel. Stability analysis, dynamical properties and simulation of some fractional differential equations are dealt with in [24-27].

Nonlinear systems, form a holistic point of view, are not in line with the superposition principle. Mathematically speaking, a nonlinear system is a problem, in which the variables that are supposed to be solved are not writable as an independent component linear combination. In case the equation involves a nonlinear function (power or cross product), the system is also considered nonlinear. Moreover, if the system is characterized with a nonlinear transfer, for instance a diode current-voltage characteristic, it is then regarded as nonlinear. Most importantly, we must refer to typical nonlinearity. Moreover, the system is nonlinear provided that a typical amount of nonlinearity like saturation, hysteresis, etc exists. Characteristics like this are the fundamental attributes of a nonlinear system. As the majority of real physical systems are, in essence, nonlinear, nonlinear systems have fascinated engineers, physicists and mathematicians. Solving non-linear equations by means of analytical methods would prove difficult and arise remarkable phenomena such as chaos and bifurcation. Even simple nonlinear (or piecewise linear) dynamical systems may behave entirely unpredictably, referred to as deterministic chaos. Owing to the fact that trivial systems can also involve chaos, chaos theory has become highly important. It is noteworthy, at this point, no unique definition is given for chaos. Chaotic dynamics are most commonly the ones originating from regular dynamical equations that do not include stochastic coefficients, yet simultaneously have trajectories the same as or indistinguishable from a number of stochastic processes. Some definitions are given for chaotic dynamics, e.g., (i) system characterized with minimum one positive Lyapunov exponent is called chaotic, (ii) a system characterized with positive entropy is called chaotic, and (iii) a system that is equivalent to hyperbolic or Anosov system is called chaotic, and so on. What all these definitions have in common is that local instability and divergence of initially close trajectories exist there. Nonetheless, the definitions are not entirely similar in their sense.

This paper mainly handles robust control. This issue is then briefly discussed here. Sectors like car production industry, mining, and other hardware make widespread use of feedback control systems. To meet the ever-growing demands for higher reliability and better efficiency levels, such control systems are constantly obliged to accomplish more accurate and desirable general performance in response to the ever-changing and challenging operating circumstances. For designing control systems to achieve more desirable robustness and efficiency while monitoring complex procedures, control engineers need novel designing apparatus and a more effective control theory. A standard technique of enhancing a control system performance is adding more sensors and actuators. As a result, a Multi-Input Multi-Output (MIMO) control system will necessarily be obtained. Therefore, each methodology related to designing modern feedback control systems must be capable of managing the issue of multiple actuators and sensors. A control system is also robust when: (1) its sensitivity level is low, (2) over a range of parameter variations, it remains stable, and (3) the performance invariably meets the specifications in the presence of a set of system parameter variations [28-32].

The present paper is outlined as follows: Some required preliminaries in the sequel are presented in Section 2. Section 3 deals with the existence and uniqueness of solutions. Section 4 deals with the numerical approach procedure. Robust control for variable order time fractional butterfly- shaped chaotic attractor system is discussed in Section 5. Section 6 presents simulation results. Finally, the method and the generated results are briefly discussed in Section 7.

## 2. Preliminaries

Some basic tools that will be needed in future are given in this section. The Atangana-Baleanu fractional derivative with variable- $\alpha(t)$ order in Liouville-Caputo sense (ABC) is defined [33] as

$$ {}^{ABC}_{0}D_t^{\alpha(t)} f(t) = \frac{B(\alpha(t))}{1-\alpha(t)} \int_0^t E_{\alpha(t)}\left[ -\alpha(t) \frac{(t-\tau)^{\alpha(t)}}{1-\alpha(t)} \right] f'(\tau) d\tau, n-1 < \alpha(t) \le n, \quad (1) $$

Where $B(\alpha(t)) = 1-\alpha(t) + \frac{\alpha(t)}{\Gamma(\alpha(t))}$ is a normalization function. Related integral Atangana-Baleanu can be formulated as

$$ {}^{ABC}_{0}I_t^{\alpha(t)} f(t) = \frac{1-\alpha(t)}{B(\alpha(t))} f(t) + \frac{\alpha(t)}{B(\alpha(t))\Gamma(\alpha(t))} \int_0^t f(\tau)(t-\tau)^{\alpha(t)-1} d\tau, \; n-1 < \alpha(t) \le n. \quad (2) $$

Consider $n^{th}$ an -order fractional differential equation of the form

$$ {}^{ABC}_{0}D_t^{\alpha(t)} f(t) = G(t, f(t)), \quad f^{(k)}(0) = f_0^k, k = 0,1,\ldots,n-1. \quad (3) $$

This equation can be rewritten as

$$ f(t) = f_0 + \frac{1-\alpha(t)}{B(\alpha(t))} G(t, f(t)) + \frac{\alpha(t)}{B(\alpha(t))\Gamma(\alpha(t))} \int_0^t G(\tau, f(\tau))(t-\tau)^{\alpha(t)-1} d\tau. \quad (4) $$

The Adams method can be extended for this equation as follows:

$$ f_{i+1}^{P} = f_0 + \frac{1-\alpha(t_i)}{B(\alpha(t_i))} G(t_i, f_i) + \frac{\alpha(t_i)}{B(\alpha(t_i))\Gamma(\alpha(t_i))} \sum_{j=0}^{i} b_{j,i+1} G(t_i + f_i), \quad (5) $$

$$ f_{i+1} = f_0 + \frac{1-\alpha(t_{i+1})}{B(\alpha(t_{i+1}))} G\left(t_i + 1, f_{i+1}^{p}\right) + \frac{\alpha(t_{i+1}) h^{\alpha(t_i+1)}}{B(\alpha(t_{i+1}))\Gamma(\alpha(t_{i+1})+2)} \times $$

$$\left[G\left(t_{i+1}, f_{i+1}^{p}\right)+\sum_{j=0}^{i} a_{j,i+1} G\left(t_j + f_j\right)\right],$$

where

$$b_{j,i+1}=\frac{h^{\alpha(t_{i+1})}}{\alpha(t_{i+1})}\left((i-j+1)^{\alpha(t_{i+1})}-(i-j)^{\alpha(t_{i+1})}\right), \quad j=0,1,..i, \tag{6}$$

and

$$a_{j,i+1}\begin{cases} i^{\alpha(t_{i+1})+1}-\left(i-\alpha\left(t_i+1\right)\right)(i+1)^{\alpha(t_{i+1})}, & j=0. \\ (i-j+2)^{\alpha(t_{i+1})+1}+(i-j)^{\alpha(t_{i+1})+1}-2(i-j+1)^{\alpha(t_{i+1})+1}, & 1\le j\le i. \end{cases} \tag{7}$$

## 3. Existence and Uniqueness of Solutions under Atangana Baleanu Fractional Derivative with Variable-Order $\alpha(t)$

In this section, we use well-known fixed point technique for the existence of solutions of ***Eq. (3)***. Thus, by taking AB-fractional integral operator of variable-order $\alpha(t)$ which is given in ***Eq. (2)***, we obtain

$$\mathrm{f}(t)-\mathrm{f}(0)=\frac{1-\alpha(t)}{\mathrm{B}(\alpha(t))}\mathrm{G}(t,\mathrm{f}(t))+\frac{\alpha(t)}{\mathrm{B}(\alpha(t))\Gamma(\alpha(t))}\int_0^t (t-\theta)^{\alpha(t)-1}\mathrm{G}(\theta,\mathrm{f}(\theta))\,\mathrm{d}\theta. \tag{8}$$

We assume that, for continuous functions $G$ and $f_1 \in L[0,1]$, there exist a constant $\lambda_1$ such that the following hold true

$$\left\|\mathrm{G}(t,\mathrm{f})-\mathrm{G}(t,\mathrm{f}_1)\right\|\le\lambda_1\left\|\mathrm{f}-\mathrm{f}_1\right\|. \tag{9}$$

From ***Eq. (8)***, we define the following recursive relation

$$\mathrm{f}_n(t)-\mathrm{f}(0)=\frac{1-\alpha(t)}{\mathrm{B}(\alpha(t))}\mathrm{G}(t,\mathrm{f}_{n-1}(t))+\frac{\alpha(t)}{\mathrm{B}(\alpha(t))\Gamma(\alpha(t))}\int_0^t (t-\theta)^{\alpha(t)-1}\mathrm{G}(\theta,\mathrm{f}_{n-1}(\theta))\,\mathrm{d}\theta. \tag{10}$$

With initial condition $f_0(t)=f(0)$, we consider the following differences

$$\begin{aligned}\psi^{n+1}(t)=(\mathrm{f}_{n+1}-\mathrm{f}_n)(t)&=\frac{1-\alpha(t)}{\mathrm{B}(\alpha(t))}(\mathrm{G}(t,\mathrm{f}_n(t))-\mathrm{G}(t,\mathrm{f}_{n-1}(t)) \\ &+\frac{\alpha(t)}{\mathrm{B}(\alpha(t))\Gamma(\alpha(t))}\int_0^t (t-\theta)^{\alpha(t)-1}(\mathrm{G}(\theta,\mathrm{f}_n(\theta))-\mathrm{G}(\theta,\mathrm{f}_{n-1}(\theta))\,\mathrm{d}\theta.\end{aligned} \tag{10}$$

Take the norm of ***Eq. (11)***, then we have

$$\begin{aligned}\left\|\psi^{n+1}(t)\right\| &= \left\|(f_{n+1}-f_n)(t)\right\| = \left\|\frac{1-\alpha(t)}{B(\alpha(t))}(G(t,f_n(t))-G(t,f_{n-1}(t))\right.\\ &\left.+\frac{\alpha(t)}{B(\alpha(t))\Gamma(\alpha(t))}\int_0^t (t-\theta)^{\alpha(t)-1}(G(\theta,f_n(\theta))-G(\theta,f_{n-1}(\theta))\,d\theta\right\|\\ &\le \frac{1-\alpha(t)}{B(\alpha(t))}\left\|(G(t,f_n(t))-G(t,f_{n-1}(t))\right\|\\ &+\frac{\alpha(t)}{B(\alpha(t))\Gamma(\alpha(t))}\left\|\int_0^t (t-\theta)^{\alpha(t)-1}(G(\theta,f_n(\theta))-G(\theta,f_{n-1}(\theta))\,d\theta\right\|\\ &\le \frac{1-\alpha(t)}{B(\alpha(t))}\left\|(G(t,f_n(t))-G(t,f_{n-1}(t))\right\|\\ &+\frac{\alpha(t)}{B(\alpha(t))\Gamma(\alpha(t))}\int_0^t (t-\theta)^{\alpha(t)-1}\left\|G(\theta,f_n(\theta))-G(\theta,f_{n-1}(\theta)\right\|d\theta.\end{aligned} \tag{11}$$

Applying ***Eq. (12)*** and we prove the existence of solution for ***Eq. (3)***. For this aim, we define the function $\phi_n(t)=(f_{n+1}-f)(t)+f(0)$. Then, using ***Eq. (12)***, we obtain

$$\begin{aligned}\left\|\phi_n(t)\right\| &= \left\|\frac{1-\alpha(t)}{B(\alpha(t))}(G(t,f_n(t))-G(t,f(t))\right.\\ &\left.+\frac{\alpha(t)}{B(\alpha(t))\Gamma(\alpha(t))}\int_0^t (t-\theta)^{\alpha(t)-1}(G(\theta,f_n(\theta))-G(\theta,f(\theta))\,d\theta\right\|\\ &\le \frac{1-\alpha(t)}{B(\alpha(t))}\left\|(G(t,f_n(t))-G(t,f(t))\right\|\\ &+\frac{\alpha(t)}{B(\alpha(t))\Gamma(\alpha(t))}\left\|\int_0^t (t-\theta)^{\alpha(t)-1}(G(\theta,f_n(\theta))-G(\theta,f(\theta))\,d\theta\right\|\\ &\le \frac{1-\alpha(t)}{B(\alpha(t))}\left\|(G(t,f_n(t))-G(t,f(t))\right\|\\ &+\frac{\alpha(t)}{B(\alpha(t))\Gamma(\alpha(t))}\int_0^t (t-\theta)^{\alpha(t)-1}\left\|G(\theta,f_n(\theta))-G(\theta,f(\theta)\right\|d\theta\\ &\le \frac{1-\alpha(t)}{B(\alpha(t))}\lambda_1\left\|f_n(t)-f(t)\right\|+\frac{1}{B(\alpha(t))\Gamma(\alpha(t))}\lambda_1\left\|f_n(t)-f(t)\right\|\\ &\le \left[\frac{1-\alpha(t)}{B(\alpha(t))}+\frac{1}{B(\alpha(t))\Gamma(\alpha(t))}\right]^n\left\|f(t)-f_1(t)\right\|\lambda_1{}^n.\end{aligned} \tag{13}$$

Then ***Eq. (13)***, shows that the function $lim_{n\to\infty}\phi_n(t)=0$ for $\frac{1-\alpha(t)}{B(\alpha(t))}+\frac{1}{B(\alpha(t))\Gamma(\alpha(t))}<1$ and $\lambda_1<1$ which further shows that $lim_{n\to\infty} f_{n+1}(t)=f(t)$. Thus, solutions of the ***Eq. (3)*** exist.

For analysis of the uniqueness of solutions of the model ***Eq. (3)***, we consider the contrary path for the proof. That is, let there exist another pair of solutions $(f_1,f_2)$ of ***Eq. (3)*** satisfying the integral system given as

$$f_1(t)-f_1(0)=\frac{1-\alpha(t)}{B(\alpha(t))}G(t,f_1(t))+\frac{\alpha(t)}{B(\alpha(t))\Gamma(\alpha(t))}\int_0^t (t-\theta)^{\alpha(t)-1}G(\theta,f_1(\theta))\,d\theta. \quad (14)$$

For the model ***Eq. (3)***, we consider $f_1(0)=0$, then we have

$$\begin{aligned}\|(f-f_1)(t)\| &= \left\|\frac{1-\alpha(t)}{B(\alpha(t))}(G(t,f(t))-G(t,f_1(t))\right.\\ &\left.+\frac{\alpha(t)}{B(\alpha(t))\Gamma(\alpha(t))}\int_0^t (t-\theta)^{\alpha(t)-1}(G(\theta,f(\theta))-G(\theta,f_1(\theta))\,d\theta\right\|\\ &\le \frac{1-\alpha(t)}{B(\alpha(t))}\|(G(t,f(t))-G(t,f_1(t))\|\\ &+\frac{\alpha(t)}{B(\alpha(t))\Gamma(\alpha(t))}\left\|\int_0^t (t-\theta)^{\alpha(t)-1}(G(\theta,f(\theta))-G(\theta,f_1(\theta))\,d\theta\right\| \quad (15)\\ &\le \frac{1-\alpha(t)}{B(\alpha(t))}\lambda_1\|f-f_1\|\\ &+\frac{1}{B(\alpha(t))\Gamma(\alpha(t))}\lambda_1\|f-f_1\|\\ &=[\frac{1-\alpha(t)}{B(\alpha(t))}+\frac{1}{B(\alpha(t))\Gamma(\alpha(t))}]\lambda_1\|f-f_1\|.\end{aligned}$$

Which implies

$$\|(f-f_1)(t)\|(1-[\frac{1-\alpha(t)}{B(\alpha(t))}+\frac{1}{B(\alpha(t))\Gamma(\alpha(t))}]\lambda_1)\le 0. \quad (16)$$

Using ***Eq. (16)***, we obtain $\|(f-f_1)(t)\|\to 0$. Consequently, the solution of ABC-fractional order which is given by ***Eq. (3)***, is unique.

## 4. Numerical Approach

This paper discusses a recently presented butterfly-shaped chaotic attractor system with six terms such as three multipliers for presenting the necessary nonlinearity for the folding trajectories [34, 35]. The numerical simulation and theoretical analysis demonstrate vividly that the new system is similar to Lorenz and other chaotic attractors. However, its topological structure differs from any chaotic attractors that exist. Adams method for the butterfly-shaped chaotic attractor system is developed here

$$\begin{cases} {}^{ABC}_{0}D_t^{\alpha(t)}x(t)=G_1(t_i,x_i,y_i,z_i)=a(y-x)(t),\\ {}^{ABC}_{0}D_t^{\alpha(t)}y(t)=G_2(t_i,x_i,y_i,z_i)=x(t)z(t)+by(t),\\ {}^{ABC}_{0}D_t^{\alpha(t)}z(t)=G_3(t_i,x_i,y_i,z_i)=-x^2(t)-cz(t),\end{cases} \quad (17)$$

The same as the previous section, we have

$$\begin{cases} x_{i+1}^{p} = x_0 + \dfrac{1-\alpha(t_i)}{B(\alpha(t_i))} G_1(t_i, x_i, y_i, z_i) + \dfrac{\alpha(t_i)}{B(\alpha(t_i))\Gamma(\alpha(t_i))} \sum_{j=0}^{i} b_{j.i+1} G_1(t_j, x_j, y_j, z_j) \\ y_{i+1}^{p} = y_0 + \dfrac{1-\alpha(t_i)}{B(\alpha(t_i))} G_2(t_i, x_i, y_i, z_i) + \dfrac{\alpha(t_i)}{B(\alpha(t_i))\Gamma(\alpha(t_i))} \sum_{j=0}^{i} b_{j.i+1} G_2(t_j, x_j, y_j, z_j) \\ z_{i+1}^{p} = z_0 + \dfrac{1-\alpha(t_i)}{B(\alpha(t_i))} G_3(t_i, x_i, y_i, z_i) + \dfrac{\alpha(t_i)}{B(\alpha(t_i))\Gamma(\alpha(t_i))} \sum_{j=0}^{i} b_{j.i+1} G_3(t_j, x_j, y_j, z_j). \end{cases} \quad (18)$$

And

$$\begin{cases} x_{i+1} = x_0 + \dfrac{1-\alpha(t_{i+1})}{B(\alpha(t_{i+1}))} G_1(t_{i+1}, x_{i+1}^{p}, y_{i+1}^{p}, z_{i+1}^{p}) + \dfrac{\alpha(t_{i+1}) h^{ti+1}}{B(\alpha(t_{i+1}))\Gamma(\alpha(t_{i+1})+2)} \times \\ \left[ G_1(t_{i+1}, x_{i+1}^{p}, y_{i+1}^{p}, z_{i+1}^{p}) + \sum_{j=0}^{i} a_{j.i+1} G_1(t_j, x_j, y_j, z_j) \right], \\ y_{i+1} = y_0 + \dfrac{1-\alpha(t_{i+1})}{B(\alpha(t_{i+1}))} G_2(t_{i+1}, x_{i+1}^{p}, y_{i+1}^{p}, z_{i+1}^{p}) + \dfrac{\alpha(t_{i+1}) h^{ti+1}}{B(\alpha(t_{i+1}))\Gamma(\alpha(t_{i+1})+2)} \times \\ \left[ G_2(t_{i+1}, x_{i+1}^{p}, y_{i+1}^{p}, z_{i+1}^{p}) + \sum_{j=0}^{i} a_{j.i+1} G_2(t_j, x_j, y_j, z_j) \right], \\ z_{i+1} = z_0 + \dfrac{1-\alpha(t_{i+1})}{B(\alpha(t_{i+1}))} G_3(t_{i+1}, x_{i+1}^{p}, y_{i+1}^{p}, z_{i+1}^{p}) + \dfrac{\alpha(t_{i+1}) h^{ti+1}}{B(\alpha(t_{i+1}))\Gamma(\alpha(t_{i+1})+2)} \times \\ \left[ G_3(t_{i+1}, x_{i+1}^{p}, y_{i+1}^{p}, z_{i+1}^{p}) + \sum_{j=0}^{i} a_{j.i+1} G_3(t_j, x_j, y_j, z_j) \right], \end{cases} \quad (19)$$

that is an iterative technique to obtain a solution for this fractional problem.

## 5. Robust Control for Variable Order Time Fractional Butterfly- Shaped Chaotic Attractor System

If two exactly similar copies of a chaotic system start in similar initial conditions, they will not have the same motions for a long period of time. The exponential divergence of orbits will amplify all of the initial minor errors. Apparently, it will firstly prove very difficult to keep the two chaotic system copies synchronized. Since then, chaotic dynamical system synchronization has been under extensive scientific examination. Identical synchronization is, in principle, to take two copies of a fixed chaotic system and to make one of them take control of the other. The master or drive system creates a signal to feed the slave or response system subsequently.

The signal is normally one of the applied coordinates in explaining the chaotic system. Synchronization can be considered as a form of chaos control and the simplicity of the coupling mechanism would make multiple applications possible.

Let us consider the system [36-42]

$$\begin{cases} {}^{ABC}_{0}D_{t}^{\alpha(t)} x(t) = a(y-x)(t), \\ {}^{ABC}_{0}D_{t}^{\alpha(t)} y(t) = x(t)z(t) + by(t), \\ {}^{ABC}_{0}D_{t}^{\alpha(t)} z(t) = -x^{2}(t) - cz(t). \end{cases} \quad (20)$$

Where the variable x, y, z denotes the states, and a, b, c are positive parameters.

$$\begin{cases} ABC_0D_t^{\alpha(t)}x(t) = a(y-x)(t) + u_x, \\ ABC_0D_t^{\alpha(t)}y(t) = x(t)z(t) + by(t) + u_y, \\ ABC_0D_t^{\alpha(t)}z(t) = -x^2(t) - cz(t) + u_z. \end{cases} \quad (21)$$

Robust control is aimed at suppressing the chaotic behavior in the systems. $\bar{x},\bar{y}$ and $\bar{z}$ are defined as the auxiliary system equilibrium points.

$$\begin{cases} ABC_0D_t^{\alpha(t)}\bar{x}(t) = a(\bar{y}-\bar{x})(t), \\ ABC_0D_t^{\alpha(t)}\bar{y}(t) = \bar{x}(t)\bar{z}(t) + b\bar{y}(t), \\ ABC_0D_t^{\alpha(t)}\bar{z}(t) = -\bar{x}^2(t) - c\bar{z}(t). \end{cases} \quad (22)$$

Now, the control errors are defined as

$$\begin{cases} e_x(t) = x(t) - \bar{x}(t), \\ e_y(t) = y(t) - \bar{y}(t), \\ e_z(t) = z(t) - \bar{z}(t), \end{cases} \quad (23)$$

then

$$\begin{cases} {}^{ABC}_{0}D_t^{\alpha(t)}e_x(t) = a(e_y - e_x) + u_x, \\ {}^{ABC}_{0}D_t^{\alpha(t)}e_y(t) = e_x(e_z + \bar{z}) + be_y + u_y, \\ {}^{ABC}_{0}D_t^{\alpha(t)}e_z(t) = -e_x(e_x + \bar{x}) - ce_z + u_z. \end{cases} \quad (24)$$

As mentioned in the previous section, the systems' chaos behavior will be suppressed. The equilibrium points are then defined as equal to zero *i.e* $\bar{x} = \bar{y} = \bar{z} = 0$. ***Eq. (24)***,

$$\begin{cases} {}^{ABC}_{0}D_t^{\alpha(t)}e_x(t) = -ae_y - ae_x + u_x, \\ {}^{ABC}_{0}D_t^{\alpha(t)}e_y(t) = e_xe_z + be_y + u_y, \\ {}^{ABC}_{0}D_t^{\alpha(t)}e_z(t) = -e_x^2 - ce_z + u_z. \end{cases} \quad (25)$$

From ***Eq. (25)***, the control law is defined as

$$\begin{cases} u_x = -ae_y + xe_x - k_xe_x, \\ u_y = -e_xe_z - be_y - k_ye_y, \\ u_z = +e_x^2 + ce_z - k_ze_z. \end{cases} \quad (26)$$

Where $k_x,k_y,k_z > 0$.

*Theorem 1.* On condition that the control is defined as ***Eq. (26)***, the ***system (20)*** is asymptotically stable.

*Proof.* The controller ***stability (26)*** will be provable through the following Lyapanov function

$$V(t)=\frac{1}{2}\left(e_x^2+e_y^2+e_z^2\right)$$

Then the derivative of the Lyapanov function is given by

$$^{ABC}_{0}D_t^{\alpha(t)}V(t)=e_x\,{}^{ABC}_{0}D_t^{\alpha(t)}e_x+e_y\,{}^{ABC}_{0}D_t^{\alpha(t)}e_y+e_z\,{}^{ABC}_{0}D_t^{\alpha(t)}e_z. \quad (27)$$

From ***Eqs. (25)*** and ***(26)***, the dynamic of each control error can be defined as

$$\begin{cases} {}^{ABC}_{0}D_t^{\alpha(t)}e_x(t)=ae_y-ae_x-ae_y+ae_x-k_xe_x, \\ {}^{ABC}_{0}D_t^{\alpha(t)}e_y(t)=e_xe_z+be_y-e_xe_z-be_y-k_ye_y, \\ {}^{ABC}_{0}D_t^{\alpha(t)}e_z(t)=-e_x^2-ce_z+e_x^2+ce_z-k_ze_z, \end{cases} \quad (28)$$

Therefore

$$\begin{cases} {}^{ABC}_{0}D_t^{\alpha(t)}e_x(t)=-k_xe_x, \\ {}^{ABC}_{0}D_t^{\alpha(t)}e_y(t)=-k_ye_y, \\ {}^{ABC}_{0}D_t^{\alpha(t)}e_z(t)=-k_ze_z, \end{cases} \quad (29)$$

Substituting ***Eq. (29)*** into ***Eq. (28)*** we have

$$^{ABC}_{0}D_t^{\alpha(t)}V(t)=-k_xe_x^2-k_ye_y^2-k_ze_z^2\le 0. \quad (30)$$

The fact that $k_x,k_y,k_z>0$ guarantees that the derivative of the Lyapunov function will always be negative or equal to zero causing asymptomatic stability.

## 6. Simulation Results

This section is to generalize the numerical scheme for the fractional butterfly- shaped chaotic attractor system in Atangana-Baleanu-Caputo fractional derivatives with variable order $\alpha(t)$ i. One of the initial motivations of the fractional control presented here is to promote the performance adjustment flexibility.

After implementing the robust controller proposed with $k_y$, ***system (20)*** changes to

$$\begin{cases} {}^{ABC}_{0}\mathrm{D}_t^{\alpha(t)}\mathrm{x}(t)=\mathrm{a}(\mathrm{y}-\mathrm{x})(t), \\ {}^{ABC}_{0}\mathrm{D}_t^{\alpha(t)}\mathrm{y}(t)=\mathrm{x}(t)\mathrm{z}(t)+\mathrm{b}_y(t)-\mathrm{k}_y\mathrm{y}(t), \\ {}^{ABC}_{0}\mathrm{D}_t^{\alpha(t)}\mathrm{z}(t)=-\mathrm{x}^2(t)-\mathrm{cz}(t). \end{cases}$$

The numerical results are here obtained assuming $x_0 = 1$, $y_0 = 2$ and $z_0 = 10$. The problem parameters are $a$ = 30, $b$ =15, $c$ = 11. In Fig. 1, the phase diagram is drawn for the fixed differential order $\alpha(t)=1$ and robust controller with similar derivative order is drawn in ***Fig. 2*** $Ky=5$. The system simulation was performed over 200 seconds.

The phase diagram and robust controller with $Ky=5$ are drawn assuming $\alpha(t)=\tanh(\frac{\pi}{2}+t)$ in ***Figs. 3*** and ***4***, respectively. From the figure, it is obvious that the Adams-Bashforth-Moulton method is capable of solving the variable-order fractional differential equation simply and effectively. Furthermore, compared to ***Figs. 1*** and ***2***, it is observed that the derivative order has profound effects on the system results.

The analysis given above implies that designers could reach the suitable dynamic behavior of turbofan and expenses through determining the proper fractional control.

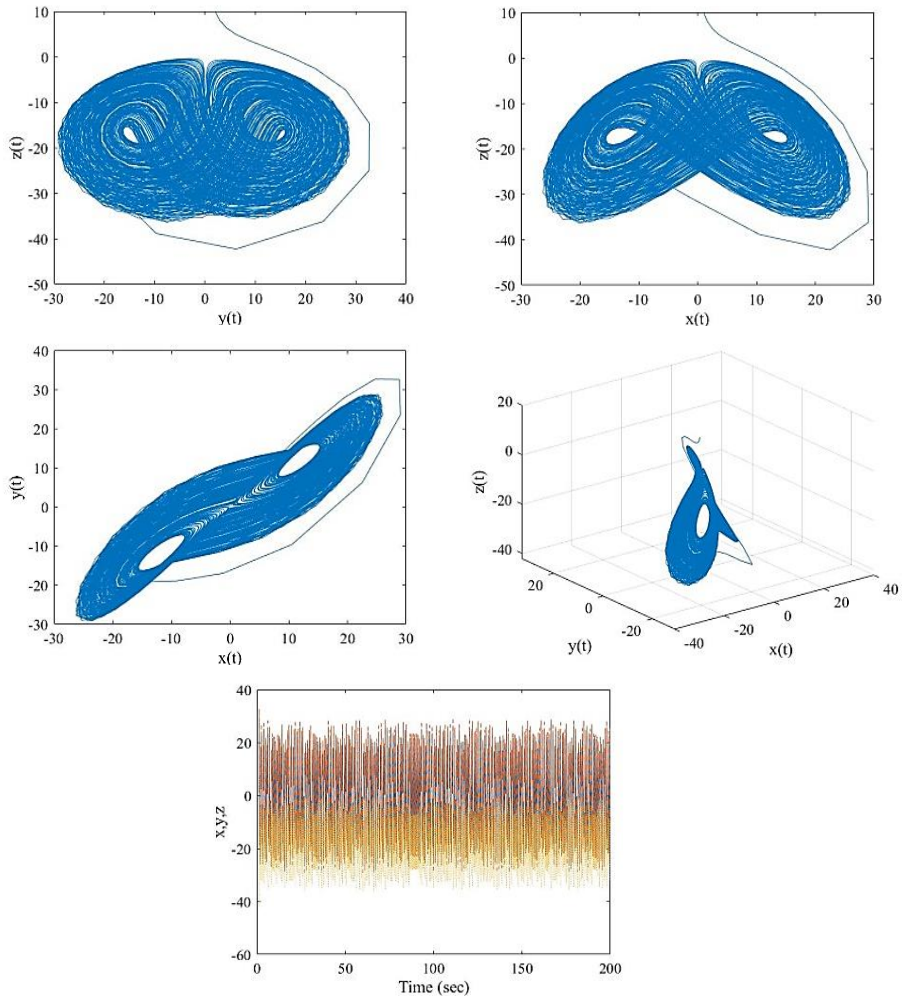


***Fig. 1.*** *The system's phase diagram for the order* $\alpha(t)=1$ .

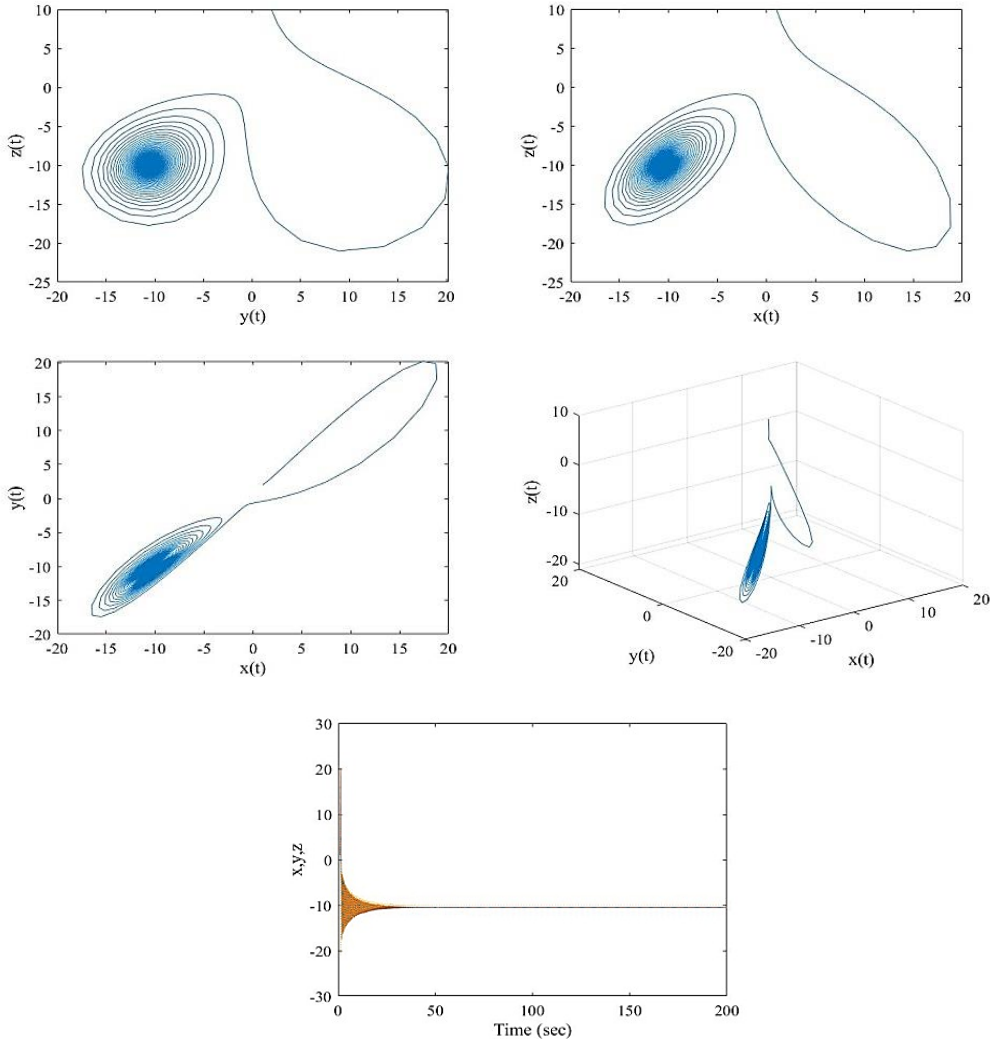


***Fig. 2.*** *The proposed system's robust controller for the order* $\alpha(t)=1$ .

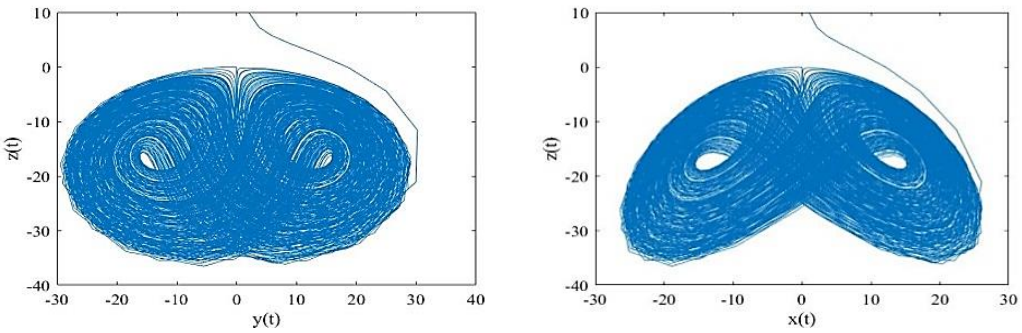

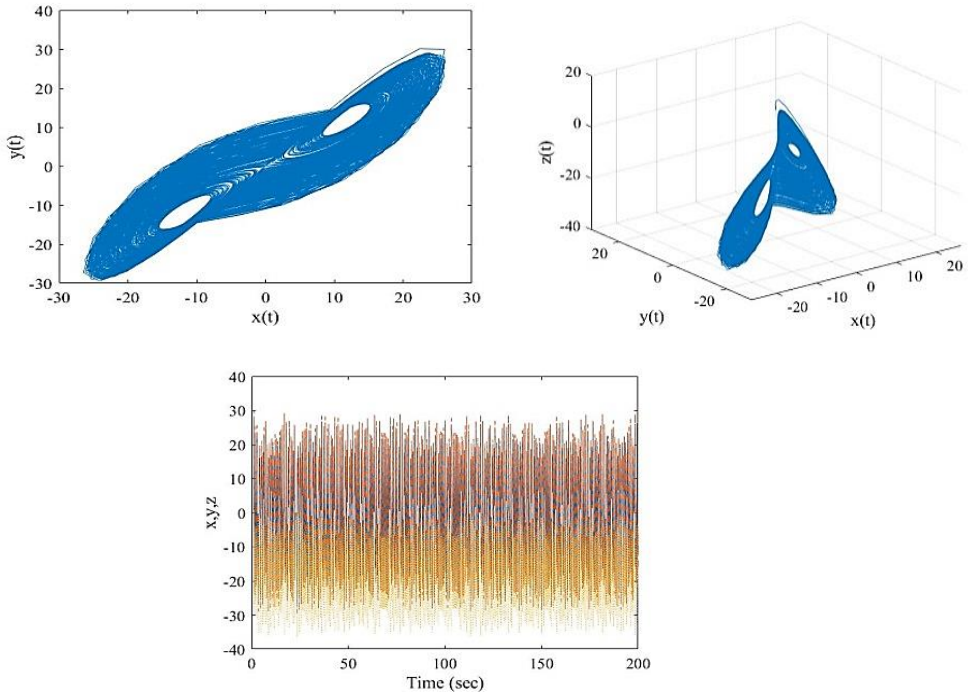


***Fig. 3.*** *The system's phase diagram for the order* $\alpha(t) = \tanh(\frac{\pi}{2} + t)$ .

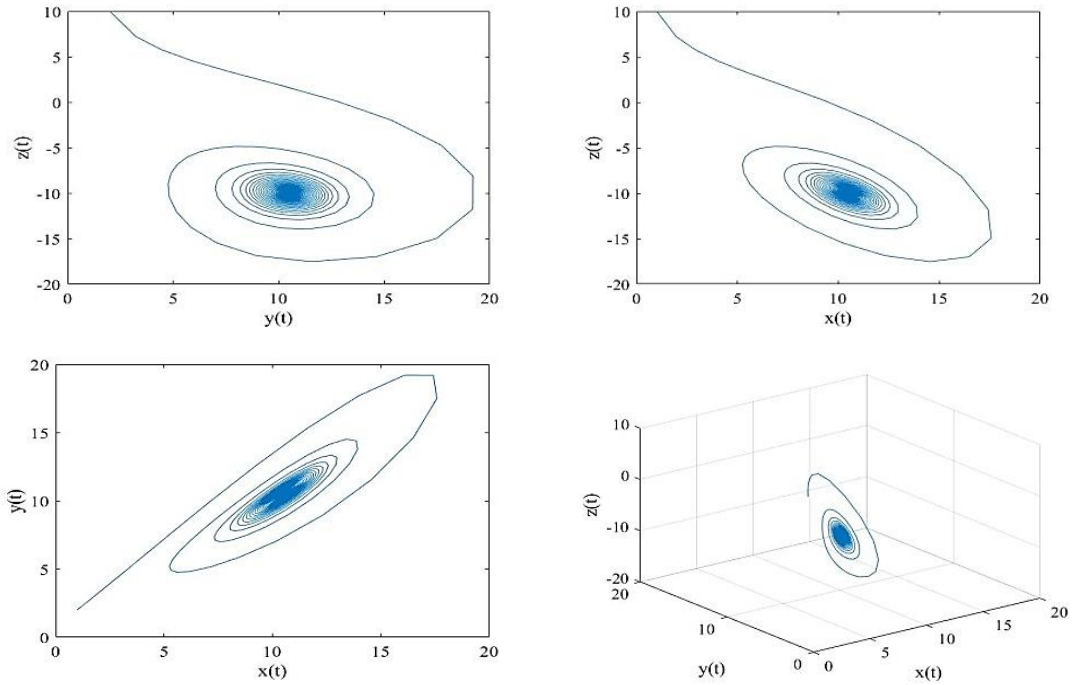

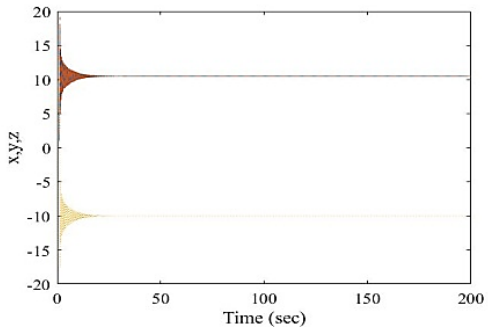


***Fig. 4.*** *Proposed robust controller of the system for the order* $\alpha(t) = \tanh(\frac{\pi}{2} + t)$ .

## 7. Conclusion

A variable order butterfly- shaped chaotic attractor fractional chaotic system is considered by a numerical solution based on the Adams method. Numerical solutions are successfully obtained and the method is demonstrated to operate accurately and powerfully. Numerical examples with different Atangana-Baleanu-Caputo variable- order were given to prove that the method is effective. The robust control of this system is investigated and it is stated that the control has a more flexible and general structure which was one of the motivations of work presented here.

## References

[1] Wolf, A., Swift, J. B., Swinney, H. L., & Vastano, J. A. (1985). Determining Lyapunov exponents from a time series. *Physica D: nonlinear phenomena*, *16*(3), 285-317.

[2] Guo, Y. M., Zhao, Y., Zhou, Y. M., Xiao, Z. B., & Yang, X. J. (2017). On the local fractional LWR model in fractal traffic flows in the entropy condition. *Mathematical methods in the applied sciences*, *40*(17), 6127-6132.

[3] Atangana, A. (2018). Non validity of index law in fractional calculus: a fractional differential operator with Markovian and non-Markovian properties. *Physica A: statistical mechanics and its applications*, *505*, 688-706.

[4] Hristov, J. (2017). The non-linear Dodson diffusion equation: Approximate solutions and beyond with formalistic fractionalization. *Math. Nat. Sci*, *1*(1), 1-17.

[5] Singh, J., Kumar, D., Hammouch, Z., & Atangana, A. (2018). A fractional epidemiological model for computer viruses pertaining to a new fractional derivative. *Applied mathematics and computation*, *316*, 504-515.

[6] Khalil, H. K. (2001). *Nonlinear systems*. Prentice-Hall..

[7] Zhang, J., Yang, H., Li, M., & Wang, Q. (2019). Robust model predictive control for uncertain positive time-delay systems. *International journal of control, automation and systems*, *17*(2), 307-318.

[8] Holzfuss, J., & Parlitz, U. (1991). Lyapunov exponents from time series. In *Lyapunov exponents* (pp. 263-270). Berlin, Heidelberg: Springer.

[9] Mashoof, M., Sheikhani, A. R., & Najafi, H. S. (2018). Stability analysis of distributed-order Hilfer–Prabhakar systems based on Inertia theory. *Mathematical notes*, *104*(1), 74-85.

[10] Aminikhah, H., Sheikhani, A. R., & Rezazadeh, H. (2015). Stability analysis of linear distributed order system with multiple time delays. *UPB scientific bulletin-series a-applied mathematics and Physics*, *77*, 207-218.

[11] Mashoof, M., & Sheikhani, A. R. (2017). Simulating the solution of the distributed order fractional differential equations by block-pulse wavelets. *UPB Sci. Bull., Ser. A: Appl. Math. Phys*, *79*, 193-206.

[12] Aminikhah, H., Sheikhani, A. H. R., & Rezazadeh, H. (2018). Approximate analytical solutions of distributed order fractional Riccati differential equation. *Ain shams engineering journal*, *9*(4), 581-588.

[13] Mehrdoust, F., Sheikhani, A. H. R., Mashoof, M., & Hasanzadeh, S. (2017). Block-pulse operational matrix method for solving fractional Black-Scholes equation. *Journal of economic studies*, *44*(3), 489-502.
[14] Gholamin, P., & Sheikhani, A. R. (2019). Dynamical analysis of a new three-dimensional fractional chaotic system. *Pramana*, *92*(6). https://doi.org/10.1007/s12043-019-1738-y
[15] Samko, S. (2013). Fractional integration and differentiation of variable order: an overview. *Nonlinear dynamics*, *71*(4), 653-662.
[16] Atangana, A. (2015). On the stability and convergence of the time-fractional variable order telegraph equation. *Journal of computational physics*, *293*, 104-114.
[17] Sun, H., Chen, W., Li, C., & Chen, Y. (2010). Fractional differential models for anomalous diffusion. *Physica A: statistical mechanics and its applications*, *389*(14), 2719-2724.
[18] Atangana, A., & Botha, J. F. (2013). A generalized groundwater flow equation using the concept of variable-order derivative. *Boundary value problems*, *2013*(1), 1-11.
[19] Wang, F., & Zheng, Z. (2019). Quasi-projective synchronization of fractional order chaotic systems under input saturation. *Physica A: statistical mechanics and its applications*, *534*, 122132.
[20] Rabah, K., & Ladaci, S. (2020). A fractional adaptive sliding mode control configuration for synchronizing disturbed fractional-order chaotic systems. *Circuits, systems, and signal processing*, *39*(3), 1244-1264.
[21] Nadjette, D., Okba, Z., & Sihem, Z. (2019). Dynamics of fractional-order chaotic and hyper-chaotic systems. *Nonlinear studies*, *26*(2).
[22] Li, G., & Sun, C. (2019). Adaptive neural network backstepping control of fractional-order Chua–Hartley chaotic system. *Advances in difference equations*, *2019*(1), 1-14.
[23] Toufik, M., & Atangana, A. (2017). New numerical approximation of fractional derivative with non-local and non-singular kernel: application to chaotic models. *The european physical journal plus*, *132*(10), 1-16.
[24] Kim, D., & Chang, P. H. (2013). A new butterfly-shaped chaotic attractor. *Results in physics*, *3*, 14-19.
[25] Gholamin, P., & Sheikhani, A. R. (2017). A new three-dimensional chaotic system: dynamical properties and simulation. *Chinese journal of physics*, *55*(4), 1300-1309.
[26] Aminikhah, H., Sheikhani, A. H. R., Houlari, T., & Rezazadeh, H. (2017). Numerical solution of the distributed-order fractional Bagley-Torvik equation. *IEEE/CAA journal of automatica Sinica*, *6*(3), 760-765.
[27] Sheikhani, A. H. R., & Mashoof, M. (2018). Numerical solution of fractional differential equation by wavelets and hybrid functions. *Boletim da sociedade paranaense de matemática*, *36*(2), 231-244.
[28] ur Rehman, A., Khan, O., Ali, N., & Pervaiz, M. (2018, February). Nonlinear robust control of a variable speed-wind turbine. *2018 international conference on engineering and emerging technologies (ICEET)* (pp. 1-6). IEEE.
[29] Sun, H., Zhao, H., Huang, K., Qiu, M., Zhen, S., & Chen, Y. H. (2017). A fuzzy approach for optimal robust control design of an automotive electronic throttle system. *IEEE transactions on fuzzy systems*, *26*(2), 694-704.
[30] Navabi, M., Davoodi, A., & Reyhanoglu, M. (2020). Optimum fuzzy sliding mode control of fuel sloshing in a spacecraft using PSO algorithm. *Acta astronautica*, *167*, 331-342.
[31] Soorki, M. N., & Tavazoei, M. S. (2018). Adaptive robust control of fractional-order swarm systems in the presence of model uncertainties and external disturbances. *IET control theory & applications*, *12*(7), 961-969.
[32] Behinfaraz, R., Ghaemi, S., & Khanmohammadi, S. (2019). Adaptive synchronization of new fractional-order chaotic systems with fractional adaption laws based on risk analysis. *Mathematical methods in the applied sciences*, *42*(6), 1772-1785.
[33] Atangana, A., & Baleanu, D. (2016). New fractional derivatives with nonlocal and non-singular kernel: theory and application to heat transfer model. *arXiv preprint arXiv:1602.03408*.
[34] Zuñiga-Aguilar, C. J., Gómez-Aguilar, J. F., Escobar-Jiménez, R. F., & Romero-Ugalde, H. M. (2018). Robust control for fractional variable-order chaotic systems with non-singular kernel. *The European physical journal plus*, *133*(1), 1-13.
[35] Atangana, A., & Qureshi, S. (2019). Modeling attractors of chaotic dynamical systems with fractal–fractional operators. *Chaos, solitons & fractals*, *123*, 320-337.
[36] Mainieri, R., & Rehacek, J. (1999). Projective synchronization in three-dimensional chaotic systems. *Physical review letters*, *82*(15), 3042.
[37] Wen, G., Zhai, X., Peng, Z., & Rahmani, A. (2020). Fault-tolerant secure consensus tracking of delayed nonlinear multi-agent systems with deception attacks and uncertain parameters via impulsive control. *Communications in nonlinear science and numerical simulation*, *82*, 105043. https://doi.org/10.1016/j.cnsns.2019.105043

[38] An, L., & Yang, G. H. (2018). LQ secure control for cyber-physical systems against sparse sensor and actuator attacks. *IEEE transactions on control of network systems*, *6*(2), 833-841.

[39] Kingni, S. T., Jafari, S., Pham, V. T., & Woafo, P. (2017). Constructing and analyzing of a unique three-dimensional chaotic autonomous system exhibiting three families of hidden attractors. *Mathematics and computers in simulation*, *132*, 172-182.

[40] Eshaghi, S., Ghaziani, R. K., & Ansari, A. (2020). Hopf bifurcation, chaos control and synchronization of a chaotic fractional-order system with chaos entanglement function. *Mathematics and computers in simulation*, *172*, 321-340.

[41] Ourahou, M., Ayrir, W., Hassouni, B. E., & Haddi, A. (2020). Review on smart grid control and reliability in presence of renewable energies: Challenges and prospects. *Mathematics and computers in simulation*, *167*, 19-31.

[42] Ghasemi, P., & Khalili-Damghani, K. (2021). A robust simulation-optimization approach for pre-disaster multi-period location–allocation–inventory planning. *Mathematics and computers in simulation*, *179*, 69-95.

# JARIE

Publisher: Ayandegan Institute of Higher Education, Iran.
Director- in-Charge: Seyyed Esmaeil Najafi
Editor-in-Chief: Nachiappan Subramanian
Sientific & Executive Manager: Seyyed Ahmad Edalatpanah

Journal of Applied Research on Industrial Engineering is an international scholarly open access, peer-reviewed, interdisciplinary and fully refereed journal. The mission of this journal is to provide a forum for industrial engineering educators, researchers, and practitioners to advance the practice and understanding of applied and theoretical aspects of industrial engineering and related areas.